National Library of Canada
Bibliothèque nationale du Canada

Canadian Theses Service
Service des thèses canadiennes

Ottawa, Canada
K1A 0N4

NOTICE

The quality of this microform is heavily dependent upon the quality of the original thesis submitted for microfilming. Every effort has been made to ensure the highest quality of reproduction possible.

If pages are missing, contact the university which granted the degree.

Some pages may have indistinct print especially if the original pages were typed with a poor typewriter ribbon or if the university sent us an inferior photocopy.

Reproduction in full or in part of this microform is governed by the Canadian Copyright Act, R.S.C. 1970, c. C-30, and subsequent amendments.

AVIS

La qualité de cette microforme dépend grandement de la qualité de la thèse soumise au microfilmage. Nous avons tout fait pour assurer une qualité supérieure de reproduction.

S'il manque des pages, veuillez communiquer avec l'université qui a conféré le grade.

La qualité d'impression de certaines pages peut laisser à désirer, surtout si les pages originales ont été dactylographiées à l'aide d'un ruban usé ou si l'université nous a fait parvenir une photocopie de qualité inférieure.

La reproduction, même partielle, de cette microforme est soumise à la Loi canadienne sur le droit d'auteur, SRC 1970, c. C-30, et ses amendements subséquents.

NL-339 (r. 88/04) c

Canada

UNIVERSITY OF ALBERTA

DEVELOPMENT OF A LARGE-ANIMAL HUMAN GLIOMA XENOGRAFT MODEL

By

BOHDAN WALTER KRUSHELNYCKY

A THESIS

SUBMITTED TO THE FACULTY OF GRADUATE STUDIES AND RESEARCH IN PARTIAL FULFILLMENT OF THE REQUIREMENTS FOR THE DEGREE OF

DOCTOR OF PHILOSOPHY

IN EXPERIMENTAL SURGERY

DEPARTMENT OF SURGERY

EDMONTON, ALBERTA

SPRING 1991

National Library of Canada
Bibliothèque nationale du Canada

Canadian Theses Service
Service des thèses canadiennes

Ottawa, Canada
K1A 0N4

The author has granted an irrevocable non-exclusive licence allowing the National Library of Canada to reproduce, loan, distribute or sell copies of his/her thesis by any means and in any form or format, making this thesis available to interested persons.

L'auteur a accordé une licence irrévocable et non exclusive permettant à la Bibliothèque nationale du Canada de reproduire, prêter, distribuer ou vendre des copies de sa thèse de quelque manière et sous quelque forme que ce soit pour mettre des exemplaires de cette thèse à la disposition des personnes intéressées.

The author retains ownership of the copyright in his/her thesis. Neither the thesis nor substantial extracts from it may be printed or otherwise reproduced without his/her permission.

L'auteur conserve la propriété du droit d'auteur qui protège sa thèse. Ni la thèse ni des extraits substantiels de celle-ci ne doivent être imprimés ou autrement reproduits sans son autorisation.

ISBN 0-315-66799-0

Canada

UNIVERSITY OF ALBERTA

RELEASE FORM

NAME OF AUTHOR:	Bohdan Walter Krushelnycky
TITLE OF THESIS:	Development of a Large-Animal Human Glioma Model
DEGREE:	Doctor of Philosophy
YEAR THIS DEGREE GRANTED:	1991

Permission is hereby granted to the UNIVERSITY OF ALBERTA LIBRARY to reproduce single copies of this thesis and to lend or sell such copies for private, scholarly or scientific research purposes only.
The author reserves other publication rights, and neither the thesis nor extensive extracts from it may be printed or otherwise reproduced without the author's written permission.

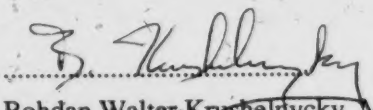

Bohdan Walter Krushelnycky, M.D.
11135 - 83 Ave.
Edmonton, Alberta
T6G 2C6

Dec. 11, 1990

UNIVERSITY OF ALBERTA

FACULTY OF GRADUATE STUDIES AND RESEARCH

The undersigned certify that they have read, and recommend to the Faculty of Graduate Studies and Research for acceptance, a thesis entitled DEVELOPMENT OF A LARGE-ANIMAL HUMAN GLIOMA XENOGRAFT MODEL submitted by BOHDAN WALTER KRUSHELNYCKY in partial fulfillment of the requirements for the degree of DOCTOR OF PHILOSOPHY in EXPERIMENTAL SURGERY (BIOPHYSICS)

J.D.S. McKean, M.D., co-supervisor

P.S.Allen, Ph.D., co-supervisor

K.C.Petruk, M.D., Ph.D.

A. Franko, Ph.D.

A. Noujaim, Ph.D.

M.G.A. Grace, Ph.D.

H.B. Coakham, M.D., M.R.C.P.
External Examiner

Sept. 4, 1990

This thesis is dedicated to my parents, Wolodymyr and Joanne

without whose patience and loving devotion

nothing would have taken place

ABSTRACT

A large-animal model was developed to facilitate the non-invasive investigation of the response of human glioma-derived D-54MG (glioblastoma multiforme) continuous cell line to therapeutic regimens. A total of 17 random-bred male cats were implanted intracerebrally with D-54 MG human glioblastoma cells grown in monolayer culture, after being placed into one of three groups :

1) Low-dose Cyclosporin A (80 mg/day) in 7 cats PO, weighing 4-5 kg., starting 24 hours pre-implant.

2) High-dose Cyclosporin A (120 mg/day) starting 24 hours pre-implant - 4 cats.

3) High-dose Cyclosporin A (120 mg/day) starting 10n days pre-implant - 6 cats.

An additional 3 cats were given placebo (carrier solution). Reproducible success of D-54 MG xenotransplantation (100% - 6/6cats) was achieved only after pre-treatment with 120 mg. CyA daily for ≥ 10 days prior to implantation. HPLC-derived whole blood CyA 12-hour trough levels of ≥ 640 ng/ml. were seen in successful implants. Lesions ranging from 2 to 20 mm. in diameter were seen in cats sacrificed 27-44 days after implantation.

An in-vitro study was performed to determine the relative cell kill efficiencies of Methylprednisolone, BCNU and Daunomycin on the D-54 MG cell line. HPLC and ^{1}H-NMR analyses were also performed on incubation media at various times post-drug administration to determine the presence of changes in lactate and amino acid levels, possibly reflecting transport fluxes of these compounds in D-54 MG cells. Daunomycin was found to have an IC_{50} = 0.5mM using a colony-formation assay - a factor of 10 times more efficacious than BCNU (IC_{50} = 11.7 mM) in cell kill. Analysis of metabolite levels by HPLC revealed that daunomycin produced

significant elevations in media glutamate and taurine concentrations as well as a significant decrease in media lactate levels - an effect which did not occur with administration of BCNU or with untreated cells. Elevation of glutamate levels was also demonstrated with ^{1}H NMR media analysis although significance could not be achieved due to greater variability in the data.

A combined in-vitro and in-vivo immunohistochemical study was performed to determine the presence of GM2, a ganglioside cell surface antigen, on the membranes of D-54 MG cells grown in cell culture and as intracerebral tumours xenografted into cat brain. The presence of GM2 in-vitro was confirmed using an anti-GM2 MAb (10-11), which also revealed a much greater abundance of GM2 in intracerebral D-54 MG tumours than in the normal host brain surrounding them. Preliminary radioimmunoscintigraphic studies using ^{131}I-labelled 10-11 and ^{125}I-labelled control MAb (MOPC-21) were also performed.

Key Words: Human glioma, xenotransplantation, Cyclosporin A, large-animal model, glutamate, taurine, lactate, HPLC, ^{1}H-NMR analysis, BCNU, daunomycin, ganglioside antigen, immunohistochemistry, radioimmunoscintigraphy

PREFACE

This thesis reports a series of three studies on the D-54 MG human glioblastoma-derived continuous cell line. The behaviour of this cell line is used to represent the behaviour of in-situ gliomas found clinically.

The introductory chapter of this work details our current understanding of the biology of brain tumours. Specifically, this includes a review of the incidence of gliomas, their histopathological features, metabolism of key substrates such as glucose and glutamine, and their antigen expression. Gangliosides - key components of the cell surface antigen array in gliomas, are also reviewed. A major part of this chapter is devoted to the methods found to-date that model the biological characteristics of in-situ gliomas. These include the development of a wide variety of animal models, some with autochthonous and others with implanted tumours.

Chapter II details a study that was performed to ascertain whether Cyclosporin A could lead to the induction of the growth, in large animals, of implanted D-54 MG human glioma-derived cells. The next chapter reports on an in-vitro analysis of chemosensitiivity of the D-54 MG cell line to 3 drugs - methylprednisolone, BCNU and daunomycin, as well as giving a preliminary indication of metabolite flux aberrancies that may be induced by the latter two drugs. Chapter IV outlines a combined in-vitro and in-vivo investigation to detremine the presence and distribution of the GM2 ganglioside cell surface antigen in D-54 MG cells grown in culture as well as in the form of xenografted tumours grown in cat brain. Preliminary in-vivo radioimmunoscintigraphic studies using the large-animal human glioma xenograft model are also discussed. The final chapter summarizes the results and attempts to provide some directions that future research into this problem could follow.

ACKNOWLEDGEMENTS

This thesis and the work detailed between its covers could never have been performed without the consistent and dedicated support of a valuable and cherished group of individuals.

I wish to thank my co-supervisors, Dr. John McKean and Dr. Peter S. Allen for their timely guidance and valued criticisms during the entire extent of this work. I would also like to extend my gratitude to the chairman of the Department of Surgery, Dr. Bryce Weir for his benevolent guidance at critical stages of this project's development. I am deeply indebted to the chairman of my supervisory committee, Dr. Kenneth Petruk, whose unswerving dedication, moral , physical and financial support, as well as patient intelligence, was, in many ways, responsible for the existence of the brain tumour laboratory and our project within it.

The planning and execution of the experiments as well as much of this thesis could never have been carried out without the devoted and caring work of our invaluable research assistants, Maxine Farr-Jones and Audrey Speelman. The following pages are a testimony to the workings of a harmonious lab group that regularly strove to accomplishments above and beyond the call of duty.

A very special debt of gratitude goes to my mother, Mrs. Joanne Krushelnycky for her unparalleled scientific typing and editing skills; she is responsible for the legible production of each text page within these covers, frequently deciphered from almost illegible script.

I wish to acknowledge the efforts and support of a Dr. Bruce Mielke whose clear interpretations and wise counsel helped to resolve many dilemmas. I would also like to thank members of Biomira, Inc., specifically Dr. A. Noujaim, Dr. M. Suresh, Dr. T. Sykes and T. Woo for their invaluable assistance with the intricacies of MAb technology, as well as their timely and successful collaborative efforts.

Dr. Keith Walker as well as selected members of the Dept. of Laboratory Medicine, specifically L. Yakymyshyn and J. Dakin deserve special mention in recognition of our collaborations, resulting in a major portion of the data collected in metabolic studies. Dr. D. Neil and the staff of HSLAS provided a consistently high quality of animal care and should be commended for their ingenuity and innovativeness in solving some very difficult management problems.

I would also like to acknowledge the efforts of D. Doran at the In-Vivo Animal NMR Unit and Dr. B. Sykes at the In-Vitro NMR Analytical Facility in the Dept. of Biochemistry for their cheerful assistance. Dr. R. Urtasun, Dr. A. Franko and Dr. M. Grace deserve special thanks for timely critique and patient answers to many trying questions.

This project received support from the Alberta Cancer Board and I am personally grateful to the Alberta Heritage Foundation for Medical Research for fellowship funding, as well as to Dr. G. Murphy of Sandoz, Inc. for wise and intuitive suggestions as well as the provision of Cyclosporin A, without which the majority of this work could not have been performed.

TABLE OF CONTENTS

CHAPTER		PAGE
I	**Introduction**.....	1
	Overview of biology of malignant gliomas.....	2
	Incidence.....	3
	Institutional - based surveys.....	3
	Regional - based surveys.....	4
	Population - based studies.....	5
	Histopathological Features.....	7
	Associated conditions.....	10
	Associated factors.....	11
	Glioma - associated antigens.....	12
	Molecular biology of gliomas.....	17
	Metabolism of malignant gliomas.....	20
	Glucose metabolism in gliomas.....	20
	Metabolism of glutamate.....	27
	In-situ assays of metabolite levels...	32
	Gangliosides in the central nervous system	41
	Structure and nomenclature.....	41
	Ganglioside distribution.....	46
	Animal models of human gliomas.....	51
	Murine ependymoblastoma.....	53
	ASV - induced astrocytoma.....	55
	Nitrosourea - induced tumours.....	58
	Human tumour xenografts.....	62

TABLE OF CONTENTS - II

CHAPTER		PAGE
I (cont'd)		
	Therapy of malignant gliomas.....	67
	Surgical treatment.....	67
	Radiotherapy.....	68
	Chemotherapy.....	70
	Immunotherapy.....	71
	The application of monoclonal antibodies to tumour management	72
	In-vivo localization of MAb's to antigens associated with intracranial tumours.....	77
	Bibliography.....	80
II	**Development of a large-animal model of human glioma in immunosuppressed cats.....**	132
	Introduction.....	132
	Methods and Materials.....	133
	Results.....	137
	Discussion.....	140
	Bibliography.....	144
	Tables and Figures.....	147
III	**Regulation of extracellular substrate levels by D-54 MG human glioblastoma cell line.....**	155
	Introduction.....	155
	Methods and Materials.....	157
	Results.....	161

TABLE OF CONTENTS - III

CHAPTER		PAGE
III (cont'd)		
	Discussion.....	164
	Bibliography.....	168
IV	**In-vitro and in-vivo localization of GM2 ganglioside to D-54 MG human glioma-derived cells using immunohistochemical technique.....**	181
	Introduction.....	181
	Methods and materials.....	183
	Results.....	186
	Discussion.....	188
	Bibliography.....	192
	Tables and figures.....	196
V	**Conclusions and recommendations for future research.....**	204
	Appendix 1 - In-vivo NMR spectroscopy.....	208
	Introduction.....	208
	Methods and materials.....	210
	Results.....	213
	Discussion.....	213
	Tables and figures.....	220

LIST OF TABLES

Table		Page
I - 1	Glioma-associated Antigens.....	13
I - 2	Alterations in Activity of Glucose-Metabolizing Enzymes in Human Gliomas.....	23
II - 1.	An analysis of the 6 cats receiving 120 mg/d CyA, starting ≥ 10 days pre-implant.....	147
III - 1	Amino acid levels seen at t=24 hours, in medium incubating D-54 MG cells, as determined by HPLC and ^{1}H-NMR.....	180
IV - 1	Comparative tissue uptakes of ^{131}I-10-11 and ^{125}I-MOPC-21 labelled MAbs 24 hours after intrathecal injection.....	203

LIST OF FIGURES

Figure		Page
I - 1	Cellular Metabolic Pathways of Glucose.....	21
I - 2	Cellular Metabolic Pathways of Glutamate.....	28
I - 3	System of Ganglioside Nomenclature proposed by Svennerholm[346].....	44
I - 4	General Pathways involved in Ganglioside Biosynthesis.	48
II - 1	Karyotype Distribution of 50 metaphases from the D-54 MG cell line (passage 66).....	147
II - 2	Marker chromosomes found in a representative D-54 MG cell (grown in tissue culture).....	149
II - 3	Representative time course of blood [CyA] values after administration of 60 mg. of CyA dissolved in olive-oil carrier solution.....	150
II - 4	Six coronal NMR images of cat brain (B-116).....	151
II - 5	Four coronal NMR images of cat brain (B-116).....	152
II - 6	Photomicrograph of D-54 MG glioblastoma multiforme implanted into cat brain showing interface between tumour and brain.....	153
II - 7	High-power photomicrograph of Figure II - 6.....	153
II - 8	Whole-mount coronal section of cat brain taken 70 days after being implanted with D-54 MG and 13 days after TE671 implantation	154
III - 1	Colony-formation chemosensitivity assay of D-54 MG human glioma-derived cells after treatment with Methylprednisolone and BCNU.....	172

LIST OF FIGURES (cont'd)

Figure		Page
III - 2	Colony-formation chemosensitivity assay of D-54 MG human glioma-derived cells after treatment with Daunomycin.....	173
III - 3	Representation of Media Concentration of lactate (mM) vs. time (hrs.).....	173
III - 4	Representation of Protein levels (mg/plate) vs. time.....	174
III - 5	Aspartate, serine and taurine levels in the incubation medium of untreated D-54 MG cells with time.....	174
III - 6	Threonine, glycine and glutamine levels in the incubation medium of untreated D-54 MG cells with time.	175
III - 7	Glutamate, alanine and isoleucine levels in the incubation medium of untreated D-54 MG cells with time.	175
III - 8	Aspartate levels in incubation medium of untreated, BCNU- and Daunomycin-treated D-54 MG cells with time.....	176
III - 9	Glutamate levels in incubation medium of untreated, BCNU- and Daunomycin-treated D-54 MG cells with time, as determined by HPLC.....	176
III - 10	Valine levels in incubation medium of untreated, BCNU- and Daunomycin-treated D-54 MG cells with time, as determined by HPLC.....	177

LIST OF FIGURES (cont'd - III)

Figure		Page
III - 11	Glutamine levels in incubation medium of untreated, BCNU- and Daunomycin-treated D-54 MG cells with time, as determined by HPLC.....	177
III - 12	Glutamate levels in incubation medium of untreated, BCNU- and Daunomycin-treated D-54 MG cells with time, as determined by integration of peak areas in ^{1}H-NMR spectra.....	178
III - 13	Typical representation of ^{1}H-NMR Spectrum taken of medium incubating untreated D-54 MG cells.....	179
IV - 1	Composite images of in-vitro immunoreactivity of 10-11 (anti-GM2) MAb to D-54 MG cells.....	196
IV - 2	Photomicrograph of a Tissue Section of D-54 MG human glioma cells grown as a xenograft in cat brain.....	197
IV - 3	High-power photomicrograph of a Tissue Section of D-54 MG human glioma cells grown as a xenograft in cat brain.....	197
IV - 4	Photomicrograph of a Tissue Section of D-54 MG human glioma cells grown as a xenograft in cat brain.....	198
IV - 5	Photomicrograph of a Tissue Section of D-54MG human glioma cells grown as a xenograft in cat brain. This section is stained immunohistochemically (ABC) with MOPC-21 MAb (control).....	198

LIST OF FIGURES (cont'd - IV)

Figure		Page
IV - 6	Radioimmunoscintigraphic image obtained by injection of ^{131}I-10-11 (α-GM2) MAb into the intrathecal space of a D-54 MG human glioma-bearing cat (intracerebral tumour). Head image taken at 1 hour post-injection of a right lateral view.....	199
IV - 7	Radioimmunoscintigraphic image obtained by injection of ^{131}I-10-11 (α-GM2) MAb into the intrathecal space of a D-54 MG human glioma-bearing cat (intracerebral tumour). Head image taken at 20 hours.....	199
IV - 8	Radioimmunoscintigraphic image obtained by injection of ^{131}I-10-11 (α-GM2) MAb into the intrathecal space of a non-tumour bearing cat. Head image taken at 1 hour of a right lateral view.....	200
IV - 9	Radioimmunoscintigraphic image obtained by injection of ^{131}I-10-11 (α-GM2) MAb into the intrathecal space of a non-tumour bearing cat. Head image taken at 24 hours of a right lateral view.....	200

LIST OF FIGURES (cont'd - V)

Figure		Page
IV - 10	Radioimmunoscintigraphic image obtained by injection of ^{131}I-10-11 (α-GM2) MAb into the intrathecal space of a D-54 MG human glioma-bearing cat (intracerebral tumour). Body image taken at 1 hour of an antero-posterior view.....	201
IV - 11	Radioimmunoscintigraphic image obtained by injection of ^{131}I-10-11 (α-GM2) MAb into the intrathecal space of a D-54 MG human glioma-bearing cat (intracerebral tumour). Body image atken at 24 hours of an antero-posterior view.....	201
IV - 12	Gd-EDTA enhanced coronal NMR image of the D-54 MG tumour- bearing cat 21 days post-tumour implantation.....	201
Appendix I - NMR		
Figure 1	Animal constraint device, front plate.....	220
Figure 2	Animal constraint device, rear plate.....	221
Figure 3.	Animal constraint device, cross-section through head restraint.....	222
Figure 4.	Animal constraint device, lateral view.....	223
Figure 5.	Animal constraint device, top view.....	224
Figure 6.	^{1}H-NMR localized spectrum acquisition sequence.....	226
Figure 7.	Three overlapping spectra (^{1}H) of a glass phantom.....	225
Figure 8.	Representative ^{1}H-NMR spectrum from a 2.25cc volume of interest enclosing a 1cc D-54 MG human glioma grown in cat brain.....	227

CHAPTER 1 - INTRODUCTION

Primary central nervous system neoplasms constitute approximately 10% of all cancer-related admissions to hospital and are responsible for about 1% of all human mortality in North America[1] . Eighty per cent of these tumours involve the brain with one-half of this sum falling into the category of malignant gliomas[2]. Malignant glioma and its worst case (glioblastoma multiforme) produces a 50% mortality within 6 months, increasing to 90% within 18 months after tumour diagnosis[3].

Traditionally, treatment of malignant brain tumours consisted of surgical extirpation which rarely, if ever, resulted in prolonged cures[1]. Commencing in the late 1970's mainly as a result of clinical trials performed by the Brain Tumour Study Group (BTSG) in San Francisco[4,5], therapeutic X-ray irradiation was added to the therapeutic regime in an effort to improve clinical outcome. Despite this combined therapy however, the median survival rates increased from a natural history survival of 6 months to a treatment survival of only 14 months. Chemotherapeutic agents, the third pillar on which CNS tumour treatment rests, have resulted in only marginal improvements in overall mortality rates. Although newer compounds continue to be developed and different chemotherapeutic strategies (ie. multiple drug regimens) applied, little progress with respect to increased cure rates has resulted. This disappointing historical setting has fostered new and creative approaches to meet the challenge of tumour therapy.

To determine both the potential therapeutic efficacy and the incidence of undesirable effects produced by chemotherapeutic agents prior to their incorporation in clinical studies, experimental tumour models grown both in the culture dish and

in various anatomical locations in experimental animals, have been utilized. Many of these tumour models, however, bear little resemblance in morphology or growth characteristics to the naturally-occurring tumour. Predictions of treatment efficacy using such models, therefore, may contain serious flaws. In addition, only a few parameters e.g. tumour dimensions and blood flow, can be accurately determined in-vivo. An animal model of malignant gliomas that would faithfully reproduce treatment responses and have the flexibility to accomodate testing of recently-developed therapeutic innovations could have an important bearing on the synthesis of an effective therapeutic strategy.

The main purpose of this project is to devise a multiparameter testbed suited for the study of human brain tumours in-vivo. This testbed is based on the development of a large- animal human glioma xenograft model which potentially has a high fidelity to gliomas found in-situ. This model is specifically designed for use with non-invasive methodologies and also capable of accomodating a variety of novel administration routes, hitherto underutilized because of the size constraints found in small animal models.

OVERVIEW OF BIOLOGY OF MALIGNANT GLIOMAS

INCIDENCE OF HUMAN GLIOMAS

Worldwide, the incidence of gliomas varies considerably from 1/100,000[6,7] to 15/100,000[8,9]. The variability in this figure is in part artifactual, possibly reflecting availability of diagnostic technology (e.g. computerized-axial tomography - CAT), type of study performed , availability of accurate data, size and stability of the population base and the time course over which the study was carried out.

Studies of the incidence of brain tumours can be divided into 3 general classes of database selection :1) Patients with brain tumours seen in a particular institution; 2) Patients with brain tumours seen by several institutions in a particular region and 3) General population studies.

Institutional-based surveys

The first class encompasses studies done by individuals or departments based either on a) admissions with clinical diagnoses (chart surveys) and/or b) autopsies with pathological diagnoses. Examples of chart surveys of brain tumour incidence are numerous, including those done by Gudmundssen[10] (Mean annual incidence = 3.02 gliomas/100,000 population - Iceland), Mancuso et al.[11] (4.26 gliomas/100,000 population - Ohio), Odeku et al.[6,7] (1 glioma/100,000 population - Nigeria - low rate probably due to underreporting) and a large survey by Walker et al.[12] (4.49 gliomas/100,000 population - U.S.A.)., A common feature, however, of all studies performed within this sub-class was the substantial percentage of brain tumours diagnosed without pathological confirmation, in one case, being as high as 80%[13].

Compilation of data from patients referred to a sub-specialty are also numerous. Analyses in this group include Zimmerman's classic comparative survey of data[14] derived from several studies including a personal dataset (gliomas representing 31 - 43% of all intracranial tumours) as well as studies done by Green et al.[15] (gliomas = 38% of intracranial tumours - Barrow) and others. While useful because of the high proportion of pathologically documented cases, it becomes extremely difficult in this type of survey to determine true tumour incidence due to a population base that cannot be precisely quantitated. This is especially difficult in

the light of what Zimmerman describes as a "funnelling" effect of tumour referrals, sent to the various authors for consultation due to their well-known interest in the field. This also results in a maldistribution of proportions of different intracranial neoplasms in a population-based registry.

Alternatively, studies of autopsied cases, as part of a compilation of general pathology seen in an institution, have the advantage of discovering incidental CNS tumours[16-18]. Unfortunately, these have suffered from lack of specificity in pathological diagnosis as well as a selection bias for autopsy patients that may not accurately represent tumour incidences in the general population. Most autopsy series in the recent past may, however, actually be classified into the following class of studies - regional based surveys.

Regional-based surveys

Regional-based studies can be divided into data derived from a) General Autopsies or b) Regional Brain Tumour Registries.

General autopsy data, when used as a basis for a regional-based study, suffers from the same deficiencies that were mentioned previously with institutional-based studies. One advantage, however, is the much larger, although perhaps more mobile population base from which data is collected, which partially corrects for biases incurred with individual institutions. Studies such as those done by Weil[17], where a total of 62,142 autopsy results collected from 4 cities, in some cases over an 80 year period, showed that gliomas were found in 0.7% of general cases and 49% of intracranial tumour cases. Courville, in a study of 40,000 necropsies[18] found that 0.74% of general cases were accounted for by primary brain tumours, with gliomas accounting for 61% of intracranial tumours found.

Regional brain tumour registries serve as the basis for the data used by the majority of brain-tumour incidence studies performed recently. Discrepancies from true epidemiological incidences result from underreporting and lack of information on incidental tumours, such as that found in general autopsy series. Heshmat et al.[19] reports an age-adjusted annual glioma incidence of 4.37 gliomas/100,000 population for Caucasian males with 2.25/100,000 population for Black males; 2.52/100,000 population for Caucasian females with 1.45/100,000 population for Black females in Washington, D.C.. Cohen et al.[20] determined the rate for Israelis born in Asia to be 2.8 gliomas/100,000 population (age-adjusted) whereas Israelis born in Europe incurred a rate of 5.5/100,000 population - the male to female ratio being 1.4 : 1. Barker et al.[21] surveyed Southern England and derived a rate of 3.94 gliomas/100,000 population, gliomas representing 57.5% of all intracranial neoplasms. The only Canadian regional-based incidence study[22] gave an age-adjusted rate for astrocytomas as 4.2/100,000 population for males and 2.7/100,000 population for females (Manitoba), with this tumour type accounting for 41% of all intracranial tumours.

Population-based studies

As Russell and Rubinstein point out in their monograph entitled "Pathology of Tumours of the Nervous System"[23], population-based studies, ie. the prospective analysis of a small, select, stable population for a long period of time (from 30 to 50 years) are "the only ones which exemplify a consistent statistical approach to the problem and which attempt a comprehensive epidemiological analysis".

There have not been many population-based studies performed, possibly due to the amount of accurate data ie. the number of accurate autopsies, needed in a

surveyed population for the calculation of a true incidence of a pathology. The higher the proportion of deaths autopsied in a selected population, the closer one comes to the true incidence in that population. Notable contributions to this group of studies include Percy et al.[24] (70%-overall autopsy rate - Rochester, Minnesota), Schoenberg et al.[25] (38% autopsy rate - Connecticut), Codd et al.[26] (56% autopsy rate - Boston) and Fogelholm et al.[27] (82% autopsy rate - Finland).

On the basis of these studies, supported by the work mentioned in previous sections, one can form some basic conclusions on the incidence of gliomas :

1) The median age adjusted annual incidence of gliomas varies between 2.5 and 5.5 cases per 100,000 population per year - this subset representing between 30 and 60% of all intracranial tumours;

2) There is, in general, a higher incidence in males than in females, which is on the order of 1.5 : 1;

3) In most cases, a bimodal age distribution in incidence occurs with an early peak at between 0 - 5 years and a later peak at between 60 - 69 years of age.

4) Evidence exists for a lower incidence of gliomas among peoples of African origin.

5) Population-based studies based on a dataset with a high proportion of autopsies reveals many asymptomatic primary intracranial tumours growing in older patients, first diagnosed at autopsy, that result in underestimates of glioma incidence by antemortem-based studies.

6) In general, the greater the ease of access to specialized medical care, the higher the incidence of malignant gliomas, revealing underreporting as an important confounding variable[13].

HISTOPATHOLOGICAL FEATURES

Eighty percent of malignant gliomas belong to the sub-group of fibrillary astrocytomas, the remainder forming a group including astrocytomas of the cerebellum, optic nerve and hypothalamus (pilocytic astrocytomas).

There are two main classifications of fibrillary astrocytomas in general use today - the four-tiered Kernohan classification and the three-tiered system adopted by the World Health Organization in 1979[28]. The Kernohan method[29] divides astrocytomas into Astrocytomas Grade 1-4, Grade 1 representing the least malignant and Grade 4 harbouring the greatest malignant potential. Grades 3 and 4 represent two different grades of glioblastoma multiforme - Grade 3 being less malignant than Grade 4. The WHO system[30] removed Grade 1 Kernohan tumours and classed the remaining three groups on the basis of increasing malignant potential - astrocytoma, anaplastic astrocytoma and glioblastoma multiforme. This eliminated the moot issue of attempting to differentiate between glioblastomas of greater or lesser degrees of anaplasia. There seems to be a trend at present of referring to tumour class using the WHO system. It should be noted, however, that there are no well-defined histopathological criteria for differentiating any of the three WHO classes, thereby requiring a reliance on the experience and judgement of the neuropathologist to establish a pathological diagnosis.

Features that are commonly focussed upon by neuropathologists in establishing the malignant potential of a biopsied tumour include :

1) Heterogeneity of cell populations
2) Presence of a hypercellular appearance
3) Variability in tumour cell size and shape
4) Presence of mitotic figures
5) Presence of clumped nuclear chromatin

6) Presence of necrotic foci

7) Morphological alterations in vascular and other adjacent structures.

The primary rationale for biopsy procurement is to prove the existence of gliomatous pathology. The boundary conditions needed to establish such a diagnosis would be most evident in the differentiation of "benign" astrocytoma from reactive gliosis. In this case, absence of other cell populations ie. microglia, oligodendrocytes, satellitosis of astrocytes into cortical layers and/or areas of proliferation of astrocytes with mild morphological variability would lead one to suspect "benign" astrocytoma, although the bigger the biopsy, the greater the diagnostic certainty.

Differentiation between "benign" astrocytomas and astrocytomas is subtle and not well characterized. Astrocytomas have a greater degree of variation in the size and shape of tumour cells as well as more hypercellular appearance.

Upon establishment of a diagnosis of astrocytoma, there are also features, which when present, can modify estimates of survival. Pathological confirmation, criteria reviewed in detail in Russell and Rubinstein[31], of the following astrocytoma sub-types : subependymal giant-cell, pleomorphic xanthoastrocytoma, juvenile pilocytic astrocytoma as well as the magnocellular subgroup of the gemistocytic astrocytomas, usually results in survival estimates longer than that generally seen with astrocytomas.

Anaplastic astrocytomas can be differentiated from astrocytomas by several features. There is even more variation in cellular morphology and a greater degree of astrocytic proliferation than that found in astrocytomas. In addition, scattered mitotic figures as well as the presence of clumped nuclear chromatin can for the first time be discerned. Hypertrophic and hyperplastic changes in both the endothelial and

adventitial components of local vascular structures seen in tumours with this degree of anaplasia further strengthen the evidence on which to base this diagnosis.

There is considerable debate regarding whether glioblastoma multiforme represents a tumour which has evolved from a state of limited proliferative potential (ie. astrocytoma) or an entity with an entirely unique pathological history[32]. It can be localized, on gross examination, most frequently to the parietal, temporal and/or frontal lobes (rarely to the occipital lobes) just like the astrocytomas. However, there is a multiplicity of distinguishing features that cannot be observed in other tumours of glial origin. Glioblastomas frequently contain foci of necrosis, which are surrounded by hyperchromatic astroglial cells, themselves arranged in rows with tapered process all pointing towards the central necrotic area in a pattern described as "pallisading"[33]. The tumour cells show a wide range of morphology including giant and multinucleated cells with frequent mitoses indicating a high degree of anaplasia. The existence and especially the degree of the vascular endothelial proliferation is almost pathognomonic for this condition. The neovascular structures contain endothelial components that are markedly hypertrophic and hyperplastic in appearance, sometimes to the extent of forming "glomeruloid" structures of tangled capillaries[33]. The growth and invasiveness of glioblastomas is profound. Even with the best available treatment, the median survival is only 9.25 months[34]. Glioblastomas may take on a "butterfly"[33] appearance, resulting from their spread along the white matter tracts in the corpus callosum to the contralateral hemisphere. There is also a great deal of anecdotal evidence documenting a "total" resection of small glioblastomas only to have tumour recurrence in a different lobe,
frequently on the contralateral side[33]. Whether this represents tumour spread or an underlying genetic abnormality in all cells of astrocytic origin in both hemispheres of such patients, remains a mystery.

Associated Conditions

There are four defined genetic conditions which have been associated with malignant gliomas :

1) Turcot's syndrome - autosomal recessive (though possibly autosomal dominant with incomplete penetrance)[214]. Findings include colonic polyps associated with colon adenocarcinoma as well as with the formation of medulloblastoma or glioma of different grades.

2) Multiple nevoid basal cell carcinoma syndrome - autosomal dominant. Associated with cerebellar astrocytomas[215].

3) Tuberous sclerosis - autosomal dominant. Findings include "ash-leaf" locus of depigmented skin, along with adenoma sebaceum, subepidermal fibrosis, subungual angiofibromas, retinal hamartomas as well as periventricular calcifications with, in some cases, gliomatosis cerebri and subependymal astrocytomas[216].

4) Neurofibromatosis - autosomal dominant. Findings include multiple cafe´-au-lait coloured areas of cutaneous hyperpigmentation, along with neurofibromas, Lesch nodules of the iris, bilateral acoustic neuromas, meningiomas, optic gliomas as well as an increased incidence of cerebral gliomas[212,213]. Recent studies have presented strong evidence that a large gene of unknown length, labelled NF1LT, mapped to chromosome 17q11.2 plays the predominant causative role in producing Neurofibromatosis Type 1[217]. Neurofibromatosis Type 2 (bilateral acoustic neuromas) is still thought to be caused by an abnormal gene located on chromosome 22[218].

In addition, there are now nine documented cases of focal nodular hyperplasia associated with CNS abnormalities - 3 with astrocytomas and 3 with meningiomas[219].There have also been sporadic reports of families in which clusters

of gliomas have been discovered. Van der Weil[220] noted a 4-fold higher incidence of gliomas among family members of glioma patients. Furthermore, there have been case reports of monozygotic twins, both of whom were harbouring astrocytomas, mixed gliomas, or oligodendrogliomas in addition to the more commonly observed medulloblastomas[220].

Associated Factors

There has been considerable controversy surrounding the role of environmentally-derived factors in the development of malignant gliomas. However, despite the many studies performed to clarify this issue, no factor has yet been identified that can be conclusively linked to a statistically-significant replicable increase in the incidence of these tumours.

There are a number of variables reported to be risk factors for glioma development. These include ionizing irradiation[221,222], lead exposure[223], exposure to vinyl chloride[231], exposure to farm animals[225], barbiturate exposure in children[226], multiple sclerosis[227], diabetes mellitus[228](inverse relationship), blood group A[229], work in rubber manufacturing[224], airline pilots[230] (exposure to gamma-irradiation), employment in the petrochemical industry[232] and exposure to low-frequency electromagnetic fields[233].

A number of factors have also been found, within the factors covered by the surveys, not to affect brain tumour incidence. These include head injuries, smoking, alcohol consumption, oral contraceptives, birth order, birth weight, family of cancer or congenital disease, exposure of parents to aromatic hydrocarbons.

Glioma-associated Antigens

Surface antigens common to gliomatous tumours (and not to normal CNS tissues)have the potential utility of enabling the differentiation of tumourous from non-tumourous tissues.Application of monoclonal antibody (MAb) technology to the selective expression of tumour-associated antigens can assist diagnostically in tumour localization - in-vitro and in-vivo. In addition, therapeutic strategies have evolved by selective tumour targetting. The first study to determine the existence of glioma-associated antigens was performed by Coakham in 1974[389]. Human astrocytoma-associated antigen(s) was detected with an assay using dye-exclusion to determine the cytotoxicity of rabbit-derived anti-astrocytoma serum to the same immunizing astrocytoma cells grown in culture. Since that time, a number of antigens common to gliomatous tumours have been isolated.

Glioma-associated antigens can be classified according to their specificity as well as their histological location. The specificity of glioma-associated antigens can be categorized into three general classes : 1) antigens present in gliomas, but also present in a variety of neuroectodermally-derived tumours as well as in normal CNS tissues; 2) antigens present in gliomas as well as other neuroectodermally-derived tumours, but not present in the normal CNS; 3) antigens present exclusively in gliomas. The histological localization of these antigens can be classified into:
1) intracellular; useful only in in-vitro diagnostic tests using fixed or frozen tissue sections and tissue-cultured cells ; 2) cell surface antigens; useful for in-vitro diagnostic assessments as well as having potential utility as in-vivo receptors for immunolocalization and/or immunotherapy. Table I - 1 presents a current summary of the antigens found in association with gliomas.

1) Normal and Malignant Neuroectodermal Tissue

Location	Antigen	Normal Expression	CNS Tumour Expression	Antibody
Intracellular	GFAP	Astrocytes	A, M	anti - GFAP (many)
	S100	Neurons, Glia	A, M, S, O, E, AN	anti - S100 (many)
	Vimentin	Mesenchymal	A, ML, E, S	anti - Vimentin (many)
	Creatine Kinase - BB fraction	Neurons, Glia	A,ML, MN, MD, S	anti - Creatine (many)
	Glutamine Synthetase	Neurons, Glia	A	anti - Glutamine synthetase (many)
	Cytokeratin	Most normal cells	Most tumours	174H.1 MAb
Cell Surface	Gq	Many CNS tissues	A, MN, N, MD	A2B5
	Leu-7	Glia	A, O, S	HNK-1
	Acidic Glycolipid	Normal Neuroectoderm	A, MD, N, MN	UJ13A
	Thy-1	Fetal brain	A, N	anti-Thy-1
	unknown Ag	Fetal brain	A, N	PI 15313
	EGFR	Glia	A	anti-EGFR

Table I - 1. Glioma - asscciated Antigens.
Abbreviations: A - Astrocytomas; AN - Acoustic Neuromas; E - Ependymomas; MD - Medulloblastoma; ML - Melanoma; MN - Meningioma; N - Neuroblastoma; S - Schwannoma.

2) Malignant Neuroectodermal Tissue

Intracellular	BrdU	------	----------	anti-BrdU
	Nuclear Ag	------	----------	Ki -67
Cell surface	Tenascin	------	A	81C6
	Chondroitin sulfate	------	A,ML	Mel-14
	p97 Glycoprotein	?	A, N, ML	P96.5
	GM2	trace	A, ML	10-11, 5-3
	GD2	trace	A, N, ML	3F8, 2F7, 3G6, 3A7
	GD3	trace	A, ML	MB3.6, R24, 4-2

3) Malignant Gliomas

Intracellular	-------	--------	-------	-----
Cell surface	3'-iso-LM1	--------	A	C50

Table I - 1b. Continuation of Table I - 1a.

Glial fibrillary protein (GFAP), S100 and vimentin are the most commonly-used antigens for determination of a neuroectodermal origin for a given tumour tissue sample. GFAP is a 49 kD protein[35], with a high proportion of acidic amino acid residues eg. aspartate, glutamate and arginine. It is localized in normal CNS tissues to fibrillary astrocytes but is also present in non-myelinating Schwann cells, cells lining Rathke's cleft, lens epithelium as well as Kupffer cells of the liver among other non-CNS tissues. GFAP expression in gliomas is variable, but a correlation does exist with malignant potential. The higher the glioma grade, the lower the GFAP expression within the tumour[39].

The soluble S100 protein is 21 kD in size and takes a dimeric form. It is localized to both glial cells and neurons, where function has been hypothesized to have a bearing on microtubule assembly and stability[36]. The S100 protein may in fact be several different proteins[37]. This may account for its low specificity with value only as an adjunct to more specific antibodies such as GFAP and HNK-1 (α-Leu-7 MAb). In non-CNS tissues, it can also be seen in chondrocytes, melanocytes, Langerhans and T cells[38].

Vimentin (57kD in molecular weight) is an intermediate filament protein, much like GFAP, and is associated with GFAP in immature astrocytes[40]. It is also seen in virtually all cell types, associated with a variety of other intermediate filament proteins[41]. Due to its perinuclear location, in contrast to GFAP which favours cell processes, it has been hypothesized that vimentin may represent part of a second, non-GFAP cytoskeletal network[42]. However, its ubiquity lowers its value as a marker for human gliomas.

Enzymes such as creatine kinase-BB fraction[43] and glutamine synthetase have been found in normal glial cells[44] but their expression in gliomas is both

heterogeneous and low. Some reporters have found glutamine synthetase to be useful in confirming astrocytic derivation of GFAP-negative glioblastomas.

There are many cytokeratins in CNS tissue, with increased concentrations in gliomas. A 200kD cytokeratin is the glioma-associated antigen recognized by the 174H.1MAb[45]. It was first detected in adenocarcinoma of colon. Reactivity of 174H.1MAb to normal CNS tissues is unknown.

Both A2B5 and UJ13A MAb's recognize acidic glycolipid antigens on the cell surface[46]. The antigen specificity of the A2B5 MAb seems restricted to a ganglioside (Gq)[46]. The UJ13A MAb was elicited after immunization of mice with human fetal brain, but the specific antigen has not been characterized[46].

HNK-1 MAb recognizes the Leu-7 glycoprotein on the cell surface of astrocytomas, although it was initially raised against human T-lymphoblastoid cells[47]. It can also bind to myelin sheath components in both normal (Schwann, oligodendrocytes) and pathological (schwannoma, oligodendroglioma) tissue.

Anti-bromodeoxyuridine (BrdU) MAb's are useful in estimating growth fractions of gliomas, after in-situ instillation of BrdU, a thymidine analog taken up by S-phase DNA[48]. There is probably a minor staining component due to reactive astrocytes undergoing S-phase. Ki-67 MAb can also be used for the same purpose[49]. This MAb recognizes a nuclear antigen seen only in dividing and proliferating cells. Other MAb's seen in Table 1 will be discussed in a later section in greater detail. As yet, there is no known intracellular antigen restricted exclusively to gliomas. The cell surface ganglioside - 3'-iso-LM1 has been postulated to have just such a restricted expression[50] but further tissue characterization needs to be performed to confirm this distribution.

Molecular Biology of Gliomas

Genetic abnormalities in gliomas were first investigated, in the late 1970's, using analysis of cellular karyotypes. Basic investigations of chromosomal number revealed a marked heterogeneity between cells in a given tumour, ranging from near diploid to tetraploid and greater. One of the few trends that came to light was the following - the greater the number of chromosomes in a cell, the greater its sensitivity to chemotherapy[51]. Analysis of single clone-derived cell populations also revealed heterogeneity in chromosome counts indicating that a mechanism existed whereby near-diploid cells could also produce cells of great diversity in chromosome number.

In recent years, karyotypic analysis of gliomas has revealed a pattern of non-random chromosomal abnormalities that seems to be restricted to tumours of glial origin. General studies have shown that the basic pattern consists of : 1) gains of chromosome 7; 2) loss of chromosomes 10 and 22; 3) major alterations in chromosomes 6, 9p, 17q, and 19q and 4) the presence of double minutes (DM)[52].

Additional chromosome 7's have been found in other tumour types including adenocarcinoma of the colon[52,53], and malignant melanoma[54]. Chromosome 10 deletions are rarely found in non-glial tumours. However, chromosome 22 loss, either in whole or in part, is seen in a variety of neurogenic tumours including neurofibromas[55], acoustic neuromas[56] and meningiomas[57,58]. Double minutes are found in approximately 50% of gliomas[59]. They represent chromosome fragments that usually contain multiple copies of one particular genetic sequence. DM's in tumours were first noted as the location of multiple copies of the dihydrofolate reductase (DHFR) gene, whose product produced the resistance seen, in some tumours, to methotrexate[60]. If a DM is seen in a glioma karyotype, there is a 70% probability that an overexpression of epidermal growth factor receptor (EGFR)

molecules will also be observed[61].

The c-erb-B2 gene, coding for the epidermal growth factor receptor protein (EGFR)[62,63] is only one of a number of genes found to be amplified in human gliomas. Among the protooncogenes studied to-date, the most commonly overexpressed is c-erb-B2 (80% of gliomas), followed by c-sis, with c-gli, c-myc and N-myc also amplified in human gliomas[64]. N-myc is also found in overabundance in developing human brain[65]. The first two genes (c-erb-B2; c-sis) code for a growth factor receptor (EGFR) and a growth factor (platelet-derived growth factor (PDGF) - B-chain). The last three oncogenes code for nuclear proteins of unknown function.

The EGF receptor is a transmembrane protein that acts as a tyrosine kinase[66,67]. Addition of a phosphate group to tyrosine residues seems to be crucial to cell growth and differentiation. EGF receptor binds both EGF and transforming growth factor (TGFα)[68]. The EGFR gene is normally located on the short arm of chromosome 7[69]. In gliomas, it can be altered as well as amplified - the alteration producing a protein similar to only the intracellular portion of the EGFR molecule[70]. TGFα is expressed only in tumours and during normal fetal development[71]. If an overexpression of normal EGFR protein were taking place, TGFα could be postulated to have an increased effect on cell growth.

Platelet-derived growth factor (PDGF) is a protein originally isolated from intracellular granules in platelets[72]. PDGF usually takes one of three forms - a heterodimer, composed of an A and a B chain or one of two homodimers - A-A or B-B[73]. Carbohydrate moieties can also attach onto the molecule, resulting in a complex of 28-30 kilodaltons in size. The normal cellular location for the c-sis gene is chromosome 22 (with the PDGF-A chain gene located on chromosome 7)[74]. The

normal function for PDGF is thought to be wound healing and tissue repair[161]. In the CNS, its mitogenic activity is suspected of preventing differentiation and sustaining proliferation of astrocytic progenitor cells[76]. Overexpression of PDGF and its receptor, may assist in driving glioma cells to increasing rates of growth.

Other growth factors or their receptors found in enhanced amounts in gliomas include the insulin-like growth factor receptor (IGF-II receptor) as well as IGF-II, setting up the possibility of another autocrine, growth factor-related loop that could possibly increase glioma growth rates[77].

Underexpression or absence of a tumour suppressor factor can be just as potent a mitogenic stimulus as overexpression of an oncogene product. One putative tumour suppressor gene, the p53 gene, has been found to be mutated in several glioma biopsies (and resultant cell lines)[78]. This gene maps to chromosome 17p[79]. In the four glioma samples tested, there was loss of heterozygosity seen in 100% of cases, with mutations observed in all the remaining alleles. In 3 of the 4 cases, these mutations were in "hot spots" in the gene that seem to mutate more frequently than elsewhere in the sequence. This results in an underexpressed, mutated p53 gene product that may be totally ineffective in tumour suppression[78].

Although a systematic alteration in a few genes and/or their products has been uncovered in most human gliomas, the role they play in the intricate pattern of gene expression in these tumours remains unknown. An entire network of connections between many genes and many gene products needs to be elucidated before the mechanism of tumourigenesis and its control can be established.

METABOLISM OF MALIGNANT GLIOMAS

The metabolism of malignant gliomas is complex and remains a poorly-understood subject.. The following review is restricted to an analysis of the more salient features of the metabolism of two of the substrates fundamental to the synthetic and replicative functions of glioma cells - glucose and glutamate, because these substrates or the metabolites produced during their degradation may potentially acquire diagnostic or therapeutic significance. The last subsection of this review describes the methodologies that can potentially monitor substrates and/or metabolites generated by these two pathways under conditions of minimal technique-related tissue destruction, ie. techniques that can be performed in-situ.

Glucose Metabolism in Gliomas

There are four main pathways through which glucose is processed upon entering a normal cell. Figure I - 1 outlines the metabolic intermediates involved in each process. The endpoints are the synthesis of 1) glycogen (glycogenesis), 2) CO_2 and H_2O (cytochrome chain / Kreb's cycle), 3) lactic acid (glycolysis), and 4) DNA/RNA (hexose monophosphate shunt).

In normal brain (both white and grey matter) , there is minimal glycogen present, implying a low total rate of glycogenesis as well as a known dependence on a continuous supply of glucose[237]. Furthermore, although normal glial cells derive >95% of their energy-containing substrates (ATP, NAD, NADP) from oxidative pathways[238], recent investigations have shown that, on average, glioma cells have an energy-producing strategy balanced almost equally between glycolytic and oxidative contributions[239], similar to embryonic CNS tissue[240], with the degree of dependence on glycolysis increasing in proportion to the aggressiveness of the tumour[241,242].

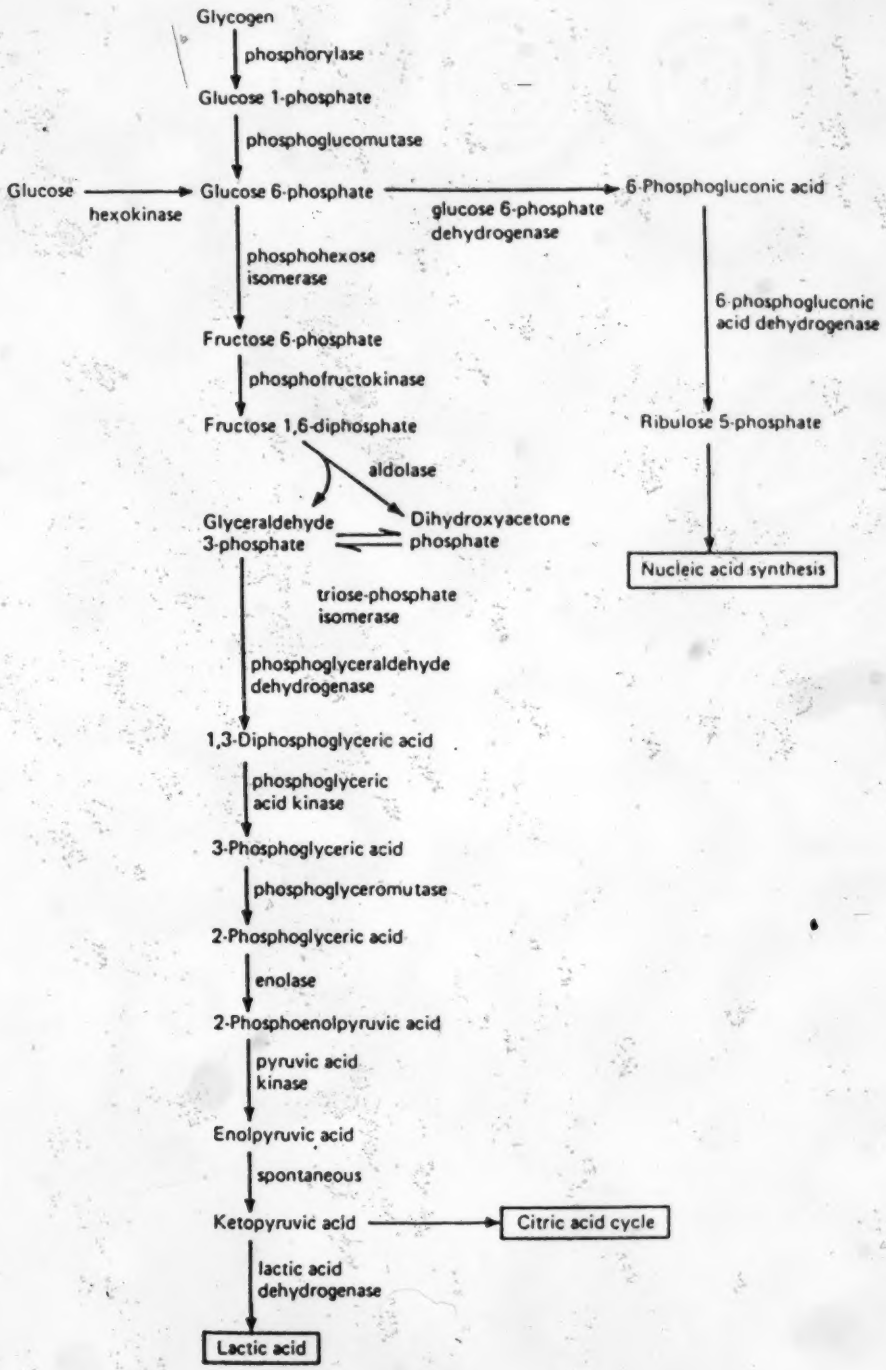

Figure I - 1. Cellular Metabolic Pathways of Glucose. Adapted from Timperley et al. (ref. 237).

It is now generally accepted that aerobic glycolysis is an important mechanism through which energy is produced from hexose substrates in gliomas. The term "aerobic glycolysis", first introduced by O. Warburg in 1930[243], refers to the phenomenon, seen in many tumour types, of high lactate production even in the presence of normal tissue oxygenation. This, implies a high rate of glycolytic processing of hexose substrates, mainly glucose, and/or a low rate of substrate flux through O_2-dependent pathways such as the cytochrome enzyme chain..

How do gliomas achieve this change in substrate balance? The complete answer is not yet known, but there are a number of leads. In general, the level of activity of enzymes in both the respiratory chain, principally cytochrome oxidase[244] as well as enzymes such as malate dehydrogenase[245] and citrate synthetase in the citric acid cycle[246,247], is much reduced in these tumours. In addition, the level of activity of some of the enzymes involved in glycolysis is increased[237]. Enzyme activity levels can be altered in one of two ways - a change in the intracellular enzyme concentration or a change in enzyme structure that affects its catalytic and/or its cofactor rate dependence. Gliomas use both strategies, depending on the enzyme, to effect this change. Table I - 2 gives a summary of the alterations in glycolytic enzyme activity arranged with regard to enzyme concentration and structural alteration due to isoenzyme shifts.

There are certain enzymes in any metabolic pathway that control the rate at which substrates progress through the entire process. In glycolysis, these enzymes are hexokinase, phosphofructokinose and pyruvate kinase[248]. In the absence of glucose, glycogen phosphorylase plays an important role (until the minimal glycogen reserves are depleted)[249]. Hexokinase catalyzes the phosphorylation of glucose to glucose-6-phosphate, itself the branchpoint origin for the hexose monophosphate

Enzyme	Activity	Isoenzyme Pattern		Comments
		Normal	Glioma	
Glycolytic Pathway				
Hexokinase	↓	1 >> 2	1 = 2	Type 2 = fetal enzyme after 36 weeks
Phosphogluco-isomerase	↓	13 types	N.D.	
Phosphofructo-kinase	↓	2, 3	2, 3, 4	
Aldolase	↑	A, C	A, C	
3-Phosphoglycerate dehydrogenase	↑	several	N.D.	
Pyruate kinase	↔	M1 > M2	M2 > M1	Fetal isoenzyme pattern
Pyruvate dehydro-genase	N.D.	N.D.	N.D.	
Pyruvate Carboxylase	N.D.	N.D.	N.D.	
Lactate dehydro-genase	↔	LDH1-LDH4	LDH4, LDH5	Type 5 = increased responsiveness to pyruvate
Hexose Monophos-phate Shunt				
Glucose -6-Phosphate dehydrogenase	↑	several	N.D.	Altered form in gliomas - less sensitive [NADPH]
6-Phospho-glycerate dehydrogenase	↑	several	N.D.	

Table I-2 Alterations in Activity of Glucose-Metabolizing Enzymes in Human Gliomas.

shunt[250]. It is decreased in its activity[251], which may be accounted for both by a decrease in concentration and a change in enzyme conformation. Four different isoenzymes of hexokinase have been found[252]. The vast majority of hexokinase in normal brain is of type 1, with a small amount of the type 2 isoenzyme[253]. Human gliomas contain a greater proportion of the type 2 isoenzyme, which can also be found in fetal brain after 36 weeks gestation[254].

Phosphofructokinase is the rate-limiting enzyme for the glycolytic pathway with its function being the phosphorylation of fructose-6-phosphate to fructose-1,6-disphosphate[248]. Its activity is also decreased (30 - 60%) in gliomatous tissue[247]. Isoenzyme determinations on this enzyme have been hampered by its instability[255]. Nevertheless, four isoenzyme variants have been isolated, with normal brain, both grey and white matter, producing both type 2 and 3[256]. Gliomas tend to produce type 4 as well, an isoenzyme usually seen only in the liver[256]. The more undifferentiated the glioma, the more type 4 phosphofructokinase produced[256]. Although activity of this enzyme is lower on average, it does increase with increasing proliferative potential. This may be due to the increase in the type 4 component of this enzyme[257].

Pyruvate kinase, converting phosphoenolpyruvate into pyruvate, seems to be present at an activity level approximating that of normal glial cells. The enzyme is made up of four subunits, each of which can exist in one of three forms - K, M_1 and M_2[258]. Whereas the M_1 type subunit forms the vast majority of subunits found in adult glia, the M_2 type subunit is present in equal proportion to the M_1 subunit in gliomas, similar to the distribution seen in fetal brain[256].

Pyruvate is a critical metabolite of glucose - the one that is converted to Acetyl CoA which serves as the first substrate of the Kreb's cycle, or transformed into lactate thereby completing glycolysis. To be able to enter Kreb's cycle, pyruvate must be transported from the cytosol into the mitochondrial matrix, where it encounters the pyruvate dehydrogenase complex[259]. This complex consists of multiple copies of three enzymes - pyruvate dehydrogenase, dihydrolipoyl transacetylase, dehydrolipoyl dehydrogenase, along with five cofactors and two regulatory proteins (protein kinase and a protein phosphatase)[259]. It is known that its activity in other tissues is modulated by extracellular oxygen levels[259]. Although this enzyme complex represents the main link between glycolysis and oxidative phosphorylation through the Kreb's cycle, the flux of substrate through this enzyme complex has never been measured, to the author's knowledge, in either normal glia or in gliomas.

The activity of pyruvate carboxylase, the other enzyme linking pyruvate to the Kreb's cycle (through oxaloacetate) is high in astrocytes (1.8 nmol/min/mg protein)[260], relative to other cells, and nonexistent in neurons. The activity of this enzyme in malignant gliomas also remains unexplored.

Lactate dehydrogenase has been demonstrated to exist with higher activity levels than are seen in normal brain[261]. It is also found in an isoenzyme form (type 5) that is normally detected in tissues that have low metabolic rates and undergo periods of hypoxia (eg. skeletal muscle)[262]. There is also strong evidence that there is a high rate of substrate flux through the hexose monophosphate shunt[238,263,264]. One of the possible explanations for this observation is the diversion of substrates into the production of nucleic acids needed for replication with the accrual of some energy-rich metabolites (NADPH) in the process. Specifically, the activity of glucose-6-phosphate dehydrogenase, the rate-controlling enzyme for

the pathway is increased 2.8 fold in glioblastomas[246,247]. This may be due to an altered form of the enzyme which is only 70% inhibited by an NADPH / $NADP^+$ ratio of 20:1 whereas the normal form is 100% inhibited by a ratio of only 7:1[265]. There is also a marked increase in the activity of 6-phosphogluconate dehydgrogenase as well. None of the other enzymes involved in this pathway, which seems to shunt away a large portion of energy-rich substrates (approx. 3-5% in normal glia) have been studied.

In summary, glucose in glioma cells is metabolized through two main pathways (although others do contribute some metabolic activity) : i) Glycolytic Pathway and ii) Hexose Monophosphate Shunt.

The exact mechanism by which metabolism is shifted away from aerobic metabolism is unclear but it may intracellularly be due to a number of factors, including :

1) Reduction of the activity of several key enzymes in both the Kreb's cycle and cytochrome chain;
2) Increased activity of some glycolytic enzymes - lactate dehydrogenase and possibly pyruvate kinase, resulting in increased glycolytic flux, and increased levels of pyruvate as well as lactate;
3) Increased flux through the hexose monophosphate shunt due, at least in part, to markedly increased G6PD and 6-PGD activity.

The role of enzymes linking the glycolytic pathway to the Kreb's cycle remain unclear as is the role of other enzymes in the shunt pathway. Extracellular factors (tumour vasculature, tumour cell position relative to nutrient supply, tumour necrosis,

extracellular growth factors) that may alter availability of O_2 and other nutrients must also be considered in any solution that attempts to clarify metabolic pathway choices made by tumours.

Metabolism of Glutamate and Related Amino Acids

Glutamate, along with glutamine, are the two most abundant amino acids in the mammalian CNS. Glutamate itself has two main roles. It is used as a supplementary substrate in the Kreb's cycle for both glia and neurons as well as serving as the major amino acid neurotransmitter in the brain. Its presence and level exert a direct influence on the metabolic fluxes of amino acids such as glutamine, aspartate, branched-chain amino acids (valine, leucine and isoleucine) as well as non-amino acid substrates such as γ-aminobutyric acid (GABA) and α-ketoglutarate[266]. Figure I - 3 describes the metabolic pathways involved in the metabolism of glutamate and the other amino acids whose metabolic fluxes it influences.

There are 3 stages of interaction between a glutamate molecule and an astrocyte - uptake, metabolic processing and release. In general, under normal conditions, the glutamate taken up by astrocytes is derived from that released as a neurotransmitter from surrounding glutamatergic neurons. Glial cells, therefore, act as the main scavengers of glutamate and, as a result, represent the major intracellular store of this amino acid in the CNS[267]. Glutamate is taken up via an active transport carrier molecule[268] whose uptake kinetics are dependent on both sodium[269] and potassium[270] concentration as well as on extracellular levels of glutamate and glutamine[271]. This uptake is highest around pathways having a high proportion of

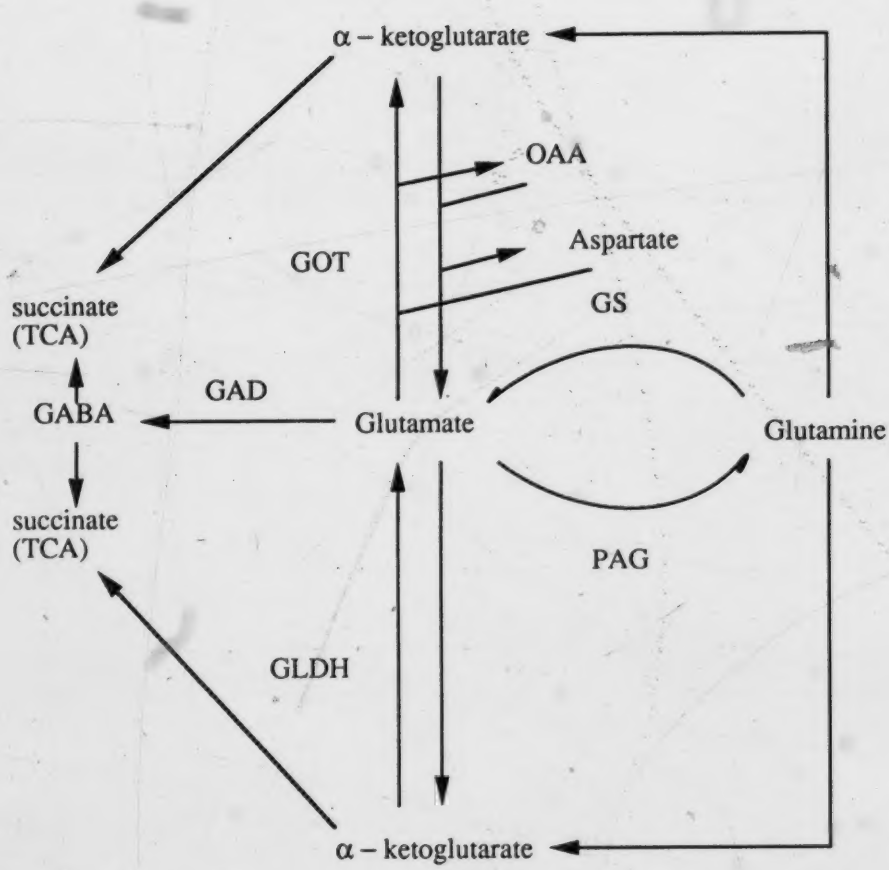

Figure I - 2. Cellular Metabolic Pathways of Glutamate.

glutamatergic neurons[272]. It has also been shown in-vitro that the rate of glial cell uptake of glutamate is dependent upon the type of neuron that is co-cultured along with it.

The carrier molecule for glutamate uptake in glioma cells is different from that found in normal glia. This is evidenced by slightly different substrate specificities when exposed to D-aspartate-4-hydroxamate. The L-isomer inhibits carrier-mediated uptake in both cultured glia and glioma cells whereas the D-form inhibits the glioma cells alone[271]. A similar effect is encountered with the use of L-glutamate-5-hydroxamate271. This, perhaps, may partially explain an L-glutamate uptake in glioma cells, less than that of astrocytes (K_m : 21.8 vs. 67.0 mM; V_{max} : 11.6 vs. 14.3 nmol/mg/min)[271]. However, the rate of L-glutamate uptake and sequestration in gliomas still exceeds uptake rates for all amino acids except glutamine[274].

Under ischemic stress, astrocytes fail to increase the influx through their potassium-dependent glutamate pump, thereby contributing in part to the excess of extracellular glutamate seen under these conditions[275]. No equivalent studies have been performed on brain tumours.

Glutumate, on entering the cell, is metabolized to 2 main metabolites - α-ketoglutarate and glutamine. The metabolism to α-ketoglutarate is achieved through either of two pathways : 1) oxidative deamination, using glutamate dehydrogenase (GLDH) or 2) transamination, catalyzed by aspartate aminotransferase (AAT). In glial cells, GLDH seems to be the predominant enzyme[276]. Glutamine is synthesized from the reaction of glutamate and ammonia, using glutamine synthetase (GS) as the catalytic enzyme[277]. This enzyme is localized only in astrocytes[277]. The

reverse reaction is also possible ie. Glutamine, going to Glutamate + NH_4^+, catalyzed by glutaminase (phosphate-activated).

Glutamine in normal astrocytes is observed to be present at a higher concentration than glutamate[278,279]. Therefore, in the case of high extracellular glutamine and uptake into the cell, the reverse reaction is dominant ie. glutamine gets metabolized into glutamate through glutaminase. This glutamate then undergoes deamination primarily via GLDH to produce α-ketoglutarate and aspartate. The α-ketoglutarate then either enters the Kreb's cycle or acts as a substrate for a reamination (which ultimately also brings greater Kreb's cycle activity) using a branched-chain amino acid (valine, isoleucine) as a co-reactant[266].

Glutamate can also be transformed into the inhibitory neurotransmitter GABA, but this occurs only in neurons, which themselves have glutamate decarboxylase (GAD)[280]. There are few studies comparing enzyme activities in normal brain and that found in gliomas. C6 glioma cells have been shown to have decreased activity of glutamine synthetase (GS) and glutamate decarboxylase (GAD) and increased activity of glutamate dehydrogenase (GLDH)[281]. 50% of six human glioma cell lines showed complete loss of immunoreactivity when exposed to an anti-glutamine synthetase (GS) antibody[282]. There are also reports of decreased aspartate aminotransferase (AAT), glutamate decarboxylase (GAD) and GABA transaminase activities in glioma biopsies whereas glutamate dehydrogenase (GLDH) activity is elevated[283,284].

One reason for this increase in GLDH activity may be an alteration in the enzyme. GLDH is a hexamer of six identical subunits of MW 56,000. A recent study has shown the existence of four distinct isoenzymes, designated - GLDH type 1, 2, 3

and 4[285]. Normal cerebellum contains all four enzymes, decreasing in relative abundance from type 1 to type 4. However, it was found that the only isoenzyme that a human glioma cell line (U-373) produced was GLDH isoenzyme 2[285]. All four isoenzymes are associated with individually distinct catalytic rates and activities.

The release of glutamate from astrocytes also occurs at a high flux (K = 0.02/min vs 0.003/min for taurine)[267]. This release can be triggered by elevated potassium concentration ($[K^+] > 20mM$), stimulating a depolarization of the astrocyte cell membrane[267]. Contrary to release mechanics in neurons, this controlled glutamate efflux is not dependent on calcium ions[275] nor is it altered by microenvironmental stresses such as anoxia, hypoglycemia or ischemia[275]. To the author's knowledge, no studies have been done to determine either the efflux of glutamate (or any other amino acid) from gliomas or any changes in those fluxes that may be incurred as a result of environmental stressors (described above) or the application of therapeutic modalities to these tumours.

In summary, under conditions of an adequate extracellular supply of glutamine, one can make the following conclusions regarding a very complex pathway :

1) Under most conditions, there is a net influx of glutamate into both astrocytes and glioma cells;

2) In general, the majority of glutamate is metabolized to produce Kreb's cycle substrates in both astrocytes and glioma cells;

3) Glioma cells tend to lack the ability to synthesize glutamine or GABA from glutamate.

4) Under hypoxic, hypoglycemic or ischemic conditions, neither influx nor efflux rates of glutamate change in astrocytes. No data is yet available on effects of these conditions or the changes produced by therapeutic stress on glutamate metabolism in gliomas

In-situ Assays of Metabolite Concentrations

In-situ assays, in principle, provide the means of obtaining accurate data concerning the concentrations, intracellular and/or extracellular (depending on the technique), of many substrates and metabolites without removing tissue from its in-vivo environment. This, therefore, should eliminate artifacts produced by the biopsying, preparation and destructive testing of studied specimens. In addition, non-destructive testing provides the unique advantage of being able to chronically resample the biochemical parameters under observation, providing a continuous measure of these levels over a period of time in the same, frequently awake, subject.

These types of assays have only been available for widespread use in the last fifteen years and new assays or variations thereof are being actively pursued. The techniques available at present can be divided into two broad classes : i) invasive and ii) non-invasive.

Invasive techniques are characterized by the constraint of having to remove tissue in order to facilitate data acquisition. There are four methods that fall into this category. They include: 1) Cortical cup fluid analysis; 2) Push-pull cannula sample acquisition; 3) Microelectrode placement and 4) Microdialysis.

The cortical cup was first used in 1953 and features the placement of a cylinder in direct, gas-tight contact with the cortical surface[286]. The cup is filled with

liquid similar to CSF in composition. This is replaced either intermittently or continuously with fresh perfusate, the replaced perfusate being taken for analysis. Although there is no damage to brain tissue, there are numerous disadvantages to this technique, including enzymatic degradation of substrates prior to analysis, a rather long period between sample acquisition (>20 min.) and the restriction of data acquisition to exclusively superficial structures.

The push-pull cannula, introduced in 1961[287], is a variation on the cortical cup method in that a cannula is inserted into the brain with fluid being injected into localized brain structures and then pulled out along with any substances that diffused into the perfusate. Although the ability to acquire samples is more refined with a greater variety of regions within the brain being accessible, there is considerable tissue damage during cannula placement. In addition, the incumbent time delay, similar to that observed with the cortical cup, can alter metabolite concentration through enzymatic degradation.

Microelectrodes have been placed intracerebrally for many years, for both electrophysiological recording as well as determination of the concentration of selected compounds. There are two types in general use depending on the substrate to be studied - a) glass ion-selective microelectrodes[288,289] and b) carbon-fiber microelectrodes[290]. Glass microelectrodes detect ions whereas those with a carbon-fiber core can detect only metabolites that can be oxidized. Both have extremely low thresholds to stress applied perpendicular to their long axis and therefore are susceptible to breakage in-situ.

Microdialysis is the technique that has most recently come to the fore. Although first developed in 1966[291], it has flourished since its marriage to the technique of analytic high-pressure liquid chromatography (HPLC). Although there is

minute tissue trauma after 48 hours of electrode introduction[292] (with a steady increase in a reactive gliosis after 7 days[293]), the blood-brain barrier does remain intact and both the local cerebral blood flow as well as the local glucose metabolism returns to normal within 24 hours[294]. Due to the dialysis membrane (the pore size in these can be varied to maximize molecular specificity) the cutoff for maximal molecular weight of diffusing substances is approximately 20,000 daltons[295]. This has the effect of eliminating enzymes from passing through the pores and degrading metabolites on the perfusate side of the membrane. This methodology has been used in both awake animals and humans with no visible after effects. Much effort has gone into developing a formula to equate the concentrations of substances seen in the perfusate with the actual concentrations in the extracellular fluid surrounding the probe. This relationship has been found to depend on the following parameters :

$C_i = \lambda^2/\alpha\ C_i\ (C_{out}\ (\lambda^2 t)/C_{out}\ (t))$, where C_i is the concentration of substrate in the extracellular space, λ = constant defining the tortuosity of the diffusion path in vivo relative to saline, α is the fraction of the total volume considered to be extracellular space, with λ^2/α usually staying between 5-20, C_i is the concentration of substrate in saline (control experiment), $C_{out}\ (\lambda^2 t)$ is the concentration of substrate in the outflow perfusate at time $(\lambda^2 t)$ and C out (t) is the concentration in the perfusate at time t[296].

There have been numerous experiments done with this technique. Most have been studies of normal, ischemic brain or brain "protected" from ischemia with drugs. These studies have centered on the concentrations of ions[297], dopamine and

its metabolites[298,299], amino acids (eg. glutamate and aspartate[300]) and glucose, along with some of its metabolites eg. lactate[301]. Several investigators have shown that the extracellular concentrations of amino acids eg. glutamate, aspartate and GABA (or their derivatives), rise in the cerebrum after ischemic stress is applied to rat brain. In the case of the first two substances, the increases are 274 and 270% respectively, and in that of GABA, by 760%, after 60 minutes[301]. It is interesting to note that these changes in concentration cannot be detected when the whole tissue content of these amino acids is determined using traditional extraction techniques in the same brain homogenates , even after 90 minutes of total vascular occlusion. Unfortunately, the cellular origin of such elevations in concentrations cannot be ascertained using this methodology due to the heterogeneity of cellular species near microdialysis placements and remain to be fully described through in-vitro studies such as those mentioned in foregoing discussions.

A team of Swedish investigators[302] implanting microdialysis probes into the infarcted regions of the brains of stroke patients not only confirmed the findings observed in animal studies but extended the observations to include rises in taurine, glycine, alanine, tyrosine, adenosine, inosine and lactate, while finding that arginine and threonine levels did not change significantly. Studies placing microdialysis probes into brain tumours have not yet been performed but may give us valuable data on steady-state CSF levels of various substances as well as any changes in those levels that may result from therapeutic intervention.

The second class of techniques that can be performed in-situ are considered non-invasive. There are three members to this group - 1) Single -photon-emission computed tomographic (SPECT) imaging; 2) NMR Spectroscopy and 3) PET Studies.

SPECT imaging is a more advanced form of gamma-camera imaging - depending on the emission of high-energy photons from gamma- emitting radionuclides having relatively short $t_{1/2}$ (days), and capable of acquiring images of thin slices of tissue. After appropriate processing, images as well as information regarding brain tumour metabolism can be derived. The most commonly used radionuclides used for brain tumour imaging include ^{99m}Tc[303], ^{201}Th[304] and ^{123}I[305]. To-date, they have been attached to a variety of substances, for the most part to determine tumour location (^{123}I-IMP[306], ^{99m}Tc-HMPAO[304]), regional cerebral blood flow (^{99m}Tc-O_4[307], ^{123}I-IMP[308], ^{123}I-HIPDM[304]), amino acid uptake (^{123}I-iodo-α-methyltyrosine[309]) and drug distribution (^{57}Co-bleomycin[310], among others). The advantages of this technique include the non-invasive acquisition of dynamic data from many regions at once, This, however, must be tempered with the disadvantages of limited study time due to radionuclide decay, the handling risk of radionuclides as well as limited spatial resolution (approx. 5mm) and temporal distribution volume. In the few studies done so far, regional cerebral blood flow (rCBF) in gliomas has been elevated relative to normal brain, as described using washout curves. Meningiomas have been found to have even higher elevations in rCBF[303].

Recently, the first radioactive tissue counts were obtained showing localization of a ^{131}I-linked monoclonal antibody that had been injected intravenously into a glioma-bearing patient[312]. The antibody had shown specificity for gliomas, compared to normal CNS tissues, in prior in-vitro and in-vivo nude mouse studies using the D-54 human glioblastoma cell line. Although preliminary in nature, the potential for better delineation of tumour seeding as well as the largely unexplored

efficacy of antibody-guided immunotherapy in the treatment of either meningeal carcinomatosis or solid tumours such as malignant gliomas using a variety of radionuclide or chemotherapeutic ligands, looks very promising.

Nuclear magnetic resonance spectroscopy, using either the ^{31}Phosphorus (^{31}P) or the proton (^{1}H) nucleus has also been used to determine metabolite levels in brain tumours. This non-invasive technique relies on the ability of certain nuclei, having quantum-mechanical spin values of = n/2, where n = odd number, to resonate with an incoming radiofrequency wave, whose frequency is determined by the natural resonant or Larmor precession frequency of the nucleus under study. Intensity of the nuclear resonance, and therefore the intensity of the received signal (echo) is, in part, dependent on the number of nuclei in the irradiated sample of tissue (eg. brain). Therefore, in principle, one can derive a value for the number of nuclei being irradiated. One can also isolate a nucleus attached to a particular molecular species, through an effect called molecular shielding, leading to an estimate of the concentration of that molecule in a solution or in-vivo. Software techniques have been developed (ISIS[313], STEAM[314]) that allow signals to be acquired from a region localized in 3-dimensional space. As a result, an estimate of the concentration of an NMR-visible substance can be determined from a localized region of tissue.

In numerous studies done with ^{31}P-containing compounds (including ATP, ADP, Phosphocreatine, phosphatidylethanolamine,phosphatidylcholine, glycerophosphorylcholine, and glycerophosphorylethanolanine), no differences have been found between levels in gliomas and those acquired from normal brain[315]. Furthermore, no consistent changes in pH values have been observed in comparing the two tissues[315].

^{1}H spectroscopy has yielded more information. Several studies have corroborated the absence of GABA in gliomas[316,317]. In addition, there is little or no N-Acety! aspartate or creatine present, in contrast to normal brain[317,319]. Lactate concentrations are elevated in gliomas (whereas alanine is increased in meningiomas)[317-319]. All of the above can serve as markers for tumour diagnosis though their specificity is yet to be determined.

The potential of this methodology is just beginning to be explored and the improvements to be made in the technique are many and varied. At present, there are limits on spatial resolution (approx. 1cc.), temporal resolution (approx. 20 min.) and spectral resolution - all determined by present-day software and hardware limits on signal gain and noise suppression. However, there are more fundamental issues that may place theoretical limits on the resolution of signal and suppression of noise. These include heterogeneity of tissue in an arbitrarily-selected tissue volume, dynamic processes occurring in-vivo systems faster than the temporal resolving ability of NMR and the multiplicity of peaks (compounds) under other signal peaks incapable of being resolved due to inherent peak-broadening caused by a large mass of tissue producing inhomogeneities in a precisely-aligned magnetic field. The most fundamental problem, however, is lack of sensitivity. At present, the solute concentration must be above 1 mM to be detected. Although introduction of labelled (^{13}C[320], ^{19}F[321]) metabolites provides a partial remedy, it may always be difficult for NMR spectroscopy to visualize signals from metabolites at much below this level.

Positron-emission tomographic (PET) imaging is another non-invasive test which is utilized for cerebral metabolic studies. Its development and use has been slowest to mature due to the high capital cost as well as high maintainence costs. Nevertheless, this technique may provide answers to scientific questions that would

be difficult to establish with any other technique. This method depends on the emission of positrons from rapidly-decaying radioactive sources (minutes to hours). Positrons travelling any distance in tissue eventually undergo an annihilation reaction on encountering an electron, producing two gamma rays which travel 180^{o} apart from each other. It is this phenomenon which enables the coincidence detectors on opposite sides of an imaging ring to localize the position of this reaction and therefore the position of the radionuclide emitter (within 2-3 mm). A variety of studies have been performed on brain tumours using a variety of nuclides including those useful for measuring regional blood volume ($C^{15}0$ - labelled red blood cells)[322], regional CBF ($C^{15}0_2$; $H_2{}^{15}0$)[322], blood-brain barrier integrity (^{68}Ga-EDTA; ^{82}Rb)[322], regional oxygen utilization and extraction ($^{15}0_2$)[322], regional glucose metabolism (^{18}F-deoxyglucose)[323] and transport (^{11}C-methylglucose)[322], regional pH (^{11}C-DMO)[324], intracellular transport of amino acids (^{11}C-methionine[325], ^{11}C-leucine[325], ^{11}C-valine[325], ^{11}C-tryptophan[325]) and drug distribution (^{11}C-BCNU, ^{18}F-5-fluorouracil, ^{57}Co-bleomycin).

It has been found that both rCBV and rCBF are increased relative to normal brain in malignant gliomas[322]. Both values, however, gradually decrease after irradiation as well as after treatment with corticosteroids[322]. Furthermore, the integrity of the blood-brain barrier has been variable in these tumors, confirming previous brain-slice data[327]. Oxygen extraction is low[328], yet there is high glucose utilization with evidence of the ratio of glucose uptake in gliomas, relative to normal brain, increasing with tumor grade[323]. This can possibly be explained by the presence of aerobic glycolysis, lending confirmation to in-vitro results, mentioned above. Tumours also seem to have a more alkalotic pH than

normal brain[324]. ^{11}C-methionine is taken up much more avidly by gliomas[329]. In fact, Tovi et al.[330] have found that tumour delineation using ^{11}C-methionine PET imaging is superior to both CT and MRI without Gd-EDTA contrast enhancement. A rough correlation has also been found between 11C-methionine uptake rate and tumour grade. It is the author's belief that scanning techniques involving positron-emission tomography hold much promise due to the variety of metabolic pathways that can be accurately studied with this technique.

GANGLIOSIDES IN THE CENTRAL NERVOUS SYSTEM

Gangliosides are a family of molecules which constitute an integral part of the membrane of most vertebrate cells. They are found in particular abundance in cells of the central nervous system, where, for example, they can represent 10 - 15% of the total lipid fraction of cellular membranes[331] with concentrations of up to 3.5 nmol sialic acid/ gm.wet weight tissue[332]. The function of these molecules within this environment is as yet unknown, but is thought to be critical to cell - cell communication[333], synaptogenesis[334] and establishment of proper links between neuronal pathways during development of the CNS[335].

Structure and Systems of Nomenclature

Gangliosides are a subclass of glycolipid molecules. The first isolation of a glycolipid (cerebroside), was performed by Thudideron in the 1880's. However, it was not until 1935-8 when Klenk performed the studies on the glycolipid that accumulates in Tay-Sach's disease (GM2), that the first definitive description and characterization of a ganglioside was achieved[336,337]. In 1941, Klenk degraded some of this "Substrate X" from bovine brains and named one of the products of this degradation as "Neurominsaure" (Neuraminic Acid), for which he proposed a molecular formula of either $C_{10}H_{19}NO_8$ or $C_{11}H_{21}NO_9$[338]. Subsequent research based on this data, using ganglioside purification (solubility difference method) as well as degradation studies (using methanolic sulfuric acid), enabled Klenk to conclude that ganglioside was composed of fatty acid, neuraminic acid, and 2 types of sugars, namely galactose and glucose[339,340].

In 1950, Blix, Svennerholm and Wernur detected galactosamine residues in brain gangliosides[341] and it was established that amine groups could be provided to gangliosides through either neuraminic acid or galactosamine. Furthermore, prior to the 1950's, ganglioside derived from brain was considered to be a single compound but in 1956, Svennerholm succeeded in the separation of gangliosides into two fractions[342]. The correct chemical structure of gangliosides was correctly defined in 1963[343], the same year that Svennerholm proposed a system of nomenclature still in wide use today[344].

Gangliosides are a family of complex acidic lipid molecules (glycosphingolipids) composed of a hydrophobic and a hydrophilic portion. The hydrophobic component consists of two molecules - a base (sphingosine) linked by an amide group to a fatty acid. Together, these two components are designated as the ceramide moiety. The hydrophilic component consists of one or more residues of neuraminic acid attached to one or more sugar molecules (usually galactose, glucose and/or N-acetyl galactosamine) themselves bound together with glycosidic linkages.

More than 40 different ganglioside structures have been defined. The variations in ganglioside structure arise from seven sources : 1) number of sugar residues; 2) substitution of glucosamine for galactosamine; 3) addition of one or more fucose groups; 4) number of neuraminic acid residues (usually between 1 and 5); 5) substitution of glycolyl for N-acetyl groups on the neuraminic acid; 6) the binding site for those neuraminic acid residues on the carbohydrate moiety and 7) attachment of O-acetyl groups to the molecule[345].

The system of nomenclature proposed by Svennerholm in 1963[346] consisted of a 3 to 4 character (2 to 3 letters, 1 number) designation of the basic ganglioside structure accounting for the number and type of sugars as well as the number and

attachment points of neuraminic acid residues. This system is illustrated in Figure I -4. Any additions of fucose, N-glycolyl and/or O-acetyl groups would be designated by a prefix using the whole word. Differences in the hydrophobic portion of the molecule, possibly due to microheterogenity and dynamic transitions between similar forms in-vivo and in-vitro were not included under this designation. The identical carbohydrate structures can also be found on two non-ganglioside classes of molecules - glycoproteins and neutral glycosphingolipids, which are glycolipid structures that do not harbour any neuraminic acid residues. This phenomenon can, in theory, confound positive identification of gangliosides when using methodologies such as monoclonal antibody localization.

The Svennerholm nomenclature assumes a maximum of four sugar residues[344]. This is designated by a number inversely proportional to the number of sugar residues (ie. GM4 has one sugar, GM1 has four). The second letter (eg. M, D, T) denotes the number of neuraminic acid residues and the G stands for the ganglioside family (see below). A further letter sometimes appears in lower case after these three characters (eg. GD1b). This designates the distribution of the neuraminic acid residues on the molecule also illustrated in Figure I - 4.

An alternate classification system was devised by the IUPAC-IPB Commission on Biochemical Nomenclature[347]. Although ensuring greater accuracy in the biochemical descriptive, it is substantially more cumbersome. The following principles were observed :

1) The number of sugars is indicated by a suffix (-base, -triose, -tetraose or -ose$_2$, -ose$_3$, -ose$_4$);

2) Each hexose sugar is given its own designation (Glu - glucose; Gal - galactose; Gal NAc - N-Acetylgalactosamine; Fuc - fucose; Lac - lactose;

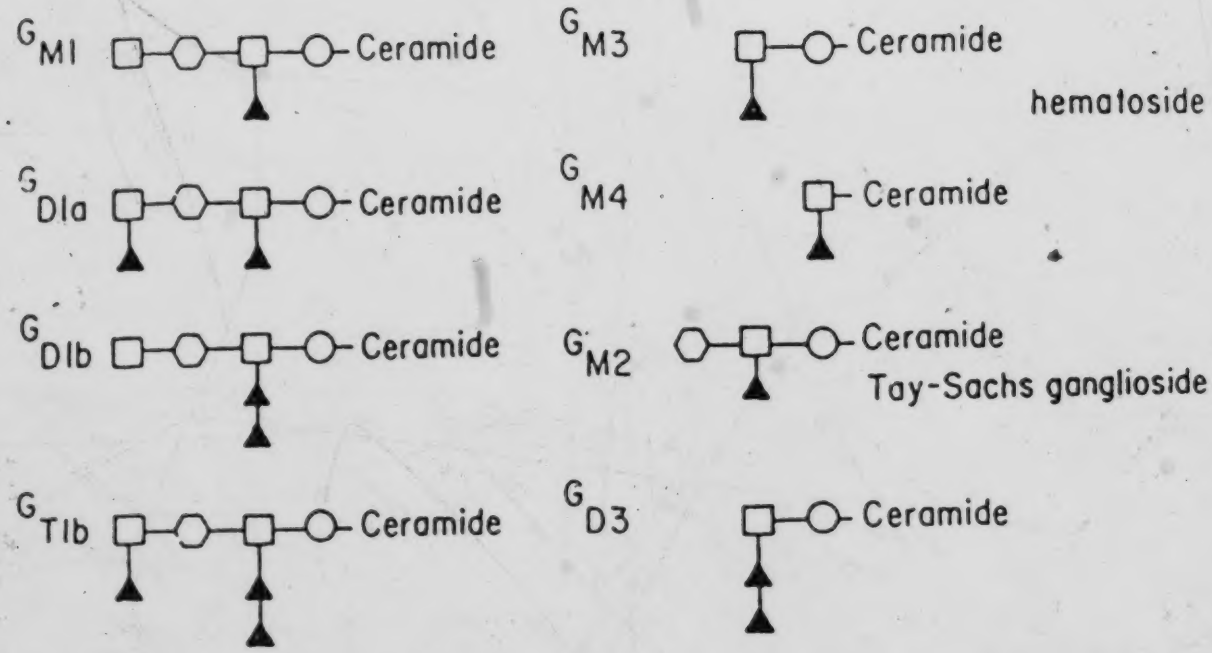

Figure I - 3. System of Ganglioside Nomenclature proposed by Svennerholm (ref. 346). According to the nomenclature of Svennerholm, M, D, and T indicate 1, 2 and 3 neuraminic acid residues (Q and P would indicate 4 and 5 such residues). Symbols: circle, glucose; square, galactose; hexagon, N-acetylgalactosamine; filled triangle, neuraminic acid.

3) Neuraminic acids are designated to be equivalent to sialic acids and the two types, N-Acetyl and N-glycolyl, are designated NeuAc and NeuGc, respectively;

4) Addition of acetyl, fucose or neuraminic acid is designated by a roman numeral indicating the sugar to which the residue is attached (counting from the ceramide end) and an arabic subscript describing the carbon within that sugar residue to which the group attaches itself. For example, AcNeu (α2-3) Gal (β1-4) Glc(β1-1) Cer (Structural Notation) = II^3-N-acetylneuraminosyllactosylceramide (IUPAC-IPB) = GM3 (Svennerholm).

Although the ceramide moiety does exhibit microheterogeneity, the main ceramide structures seen in normal human brain are eicosa-sphing - 4 -enine ($C_{20:1}$) (majority) and octadeca-sphing - 4 - enine ($C_{18:1}$)[348].

A further level of symbol reduction and grouping of gangliosides is classification into "series" or "families"[349]. A ganglioside family is defined as a linear sequence of particular sugars bound together by particular anomeric linkages. Four such families have been designated in vertebrates[349] - 1) Ganglio - (Gg) = $(GalNAc\beta\text{-}Gal\beta)_n$ - Glc -Cer; 2) Globo - (Gb) = Galβ- Gal NAcβ -Galα- Galβ- Glc- Cer; 3) Isoglobo - (iGb) = Galβ- GalNAcβ-Galβ- Galβ- Glc - Cer (Note β isomeric linkage of third sugar residue); 4) Lacto - (Lc) = $(Gal\beta\text{- Glc NAc}\beta\text{-})_n$ - Galβ- Glc - Cer

Ganglioside Distribution and Biosynthesis

The animal kingdom is phylogenetically divided into the Deuterostomia and Protostomia. Numbers of Deuterostomia include vertebrates as well as invertebrates (Echinodermata). The Insecta are amongst the most highly evolved members of the Protostomia. To-date, all glycolipids isolated from this phylum do not contain sialic acid[350]. Therefore gangliosides seem to be restricted to Deuterostomia, where members of even the phylum Echinodermata contain gangliosides, albeit of unusual form[351].

Studies of ganglioside structure and distribution in vertebrates have revealed several interesting features. All known gangliosides in vertebrates are derived from Glcβ-Cer and Galβ-Cer[352]. By far the majority of brain gangliosides in vertebrates come from the ganglio-family[353] with the exception of frog brain gangliosides which are derived from the lacto-family[349]. Although gangliosides from the other three ganglioside families are present (with globo-derived gangliosides expressed earliest during ontogenic development), they represent a minor component of vertebrate CNS ganglioside content.

The occurrence of different sialic acids is both species- and tissue-dependent. Exclusively 4-0-Acetylated sialic acids have been isolated from the horse, mule, donkey and the Australian monotreme echidna (Tachyglossus aculeatus)[354]. Although gangliosides secreted from the submandibular gland of the cow contain sialic acids of many different types, both the pig and cow contain N-glycolyl-neuraminic acid in much greater proportion to N-acetylneuraminic acid[354]. Human tissues contain the N-acetyl form of neuraminic acid almost exclusively (as well as its O-acetyl and O-lactate derivatives). However, traces of N-glycolylneuraminic acid have been revealed in patients with adenocarcinoma of the colon (Hanganutziu - Deicher antigen)[355].

Due to the predominance of ganglio-series gangliosides in vertebrate tissues, most elucidation of biosynthetic pathways has been done for this ganglioside family. Recruitment of substrates for ganglioside biosynthesis mandates a sophisticated level of functional coordination of substrate transport as well as enzymatic activity in different intracellular compartments. The overall schema of ganglioside biosynthesis is illustrated in Figure I - 5. The substrate for all carbohydrate moieties is glucose, which through glucose-6-phosphate, is transformed ultimately into galactose (via UDP-glucose) and to N-Acetylglucosamine (via fructose-6-phosphate and glutamine). Neuraminic acid is synthesized in the nucleus (linked to cytosine triphosphate (CTP)) from a glucose derivative (N-acetyl mannosamine) and cytosine monophosphate (CMP). The synthesis of sphingenine from fatty acids occurs in the cytoplasm. All three components enter the endoplasmic reticulum where they are combined into a ganglioside molecule by a series of glycosyl transferases (Gal transferase, GalNAc transferase), NeuAc transferases and acyl transferases, all having high substrate-specifity. This ganglioside is then transported from the Golgi apparatus to the plasma membrane[356].

The variations in ganglioside structure arise from use of 3 alternate biosynthetic pathways for ganglio-series products. One or more of these pathways can be used concurrently. In placental mammals and adult birds, 98% of the gangliosides are synthesized using pathway I or II. Adult fish and other lower vertebrates seem to favour pathway III[357,358].

Several trends have been noted in an analysis of gangliosides in 150 vertebrate species[331]. In general, the higher the level of organization of the CNS, the greater is the concentration of gangliosides within the brain, although much variability does occur. In cold-blooded vertebrates, the ganglioside concentration varies between

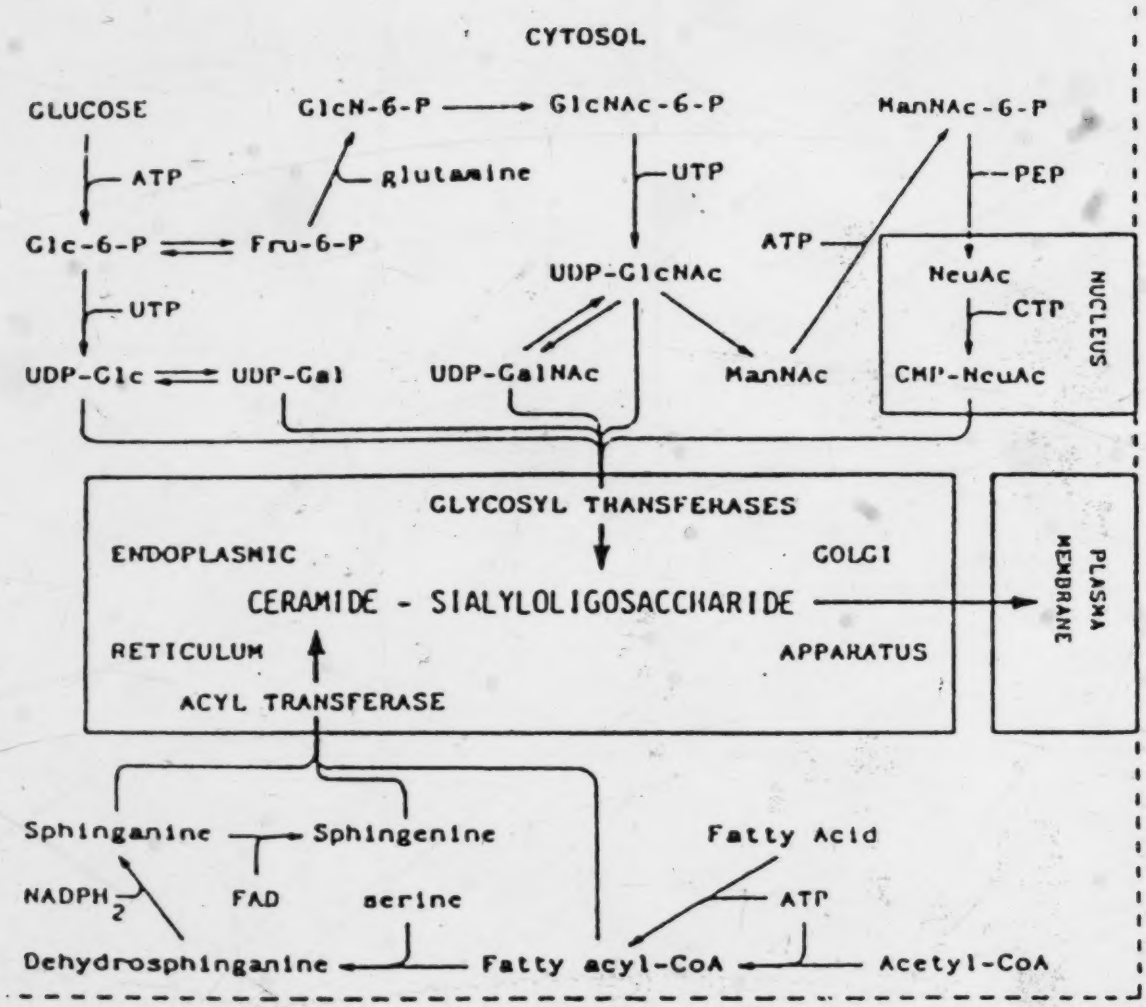

Figure I - 4. General Pathways involved in Ganglioside Biosynthesis. Adapted from Tettamanti et al. (ref. 356).

0-36-2.59 mmol sialic acid /g wet weight, whereas in mammals this level ranges from 1.29-4.53 mmol/g wet weight. In general, the higher the phylogenetic status of the animal, the lower the number of neuraminic acid residues and the lower the number of ganglioside factions isolated. Also the distribution of gangliosides within the brain of most vertebrates reveals a gradual decrease in their content when traversing from the forebrain regions to the medulla (codfish being exceptional in having a spinal cord ganglioside concentration twice that of forebrain cortex).

In adult human brain, the total concentration of gangliosides is much higher in grey than in white matter (964 vs 165 mg/g wet weight), higher in cerebral cortex than in cerebellar cortex or in the basal nuclei[332]. The most commonly found ganglioside in adult brain is GD1b (30% total content), followed by GT1 (28%), GD1a (21%) and GM1 (18%). This adult pattern is reached by age 30, and remains essentially the same for the duration of life[332]. There is a marked difference in pattern, however, between an adult and a neonate[359]. Neonatal ganglioside patterns reveal a preponderance of GD1a (48% total ganglioside content), followed by GM1 (21%), GD1b (11%) and GT1 (11%). There is a smooth upward transition of GT1 and GD1b (over 20 years) and a reciprocal downward transition in levels of GD1a and GM1 (over 30 years) between adults and neonates[332].

Human gliomas have a lower total ganglioside content than normal adult brain (grey or white matter)[360]. This ganglioside content is inversely proportional to tumour malignancy[361]. The pattern of ganglioside expression on the surface of these cells, with allowances made for phenotypic heterogneity, is markedly different from the pattern seen in adult glia, both in its complexity as well as in the proportions of each ganglioside component. In tumour biopsies, there are increases seen in the content of GM2, GD2 and GD3 with the suggestion that GD3 expression can

be correlated to the degree of malignancy[360-362]. These large shifts in ganglioside proportions are evident in the extreme case of glioblastoma multiforme, where GD3 predominates (20±6%), followed by GD1a (16±10%), GD1b (11±5%), GT1b (11±3%), GM1 (10±3%) and GM2 (8±5%), GD3 and GM2 normally accounting for less than 3% of brain ganglioside content[362]. In studies involving human glioma cell lines, with all the attendant confounding variables of clonal selection, alteration of extracellular microenvironment and lack of host tissue interaction, it was found that GM2 was found in 89% of the 19 cell lines tested. GD2 was found in 79% and GD3 in 68% of these cell lines. Moreover, in the positive cell lines tested, 8/10 expressed GM2 as 42-63% of total ganglioside content, with GD2 as 5-17% (5/6 lines) and GD3 as 4-45% of total content in 8/10 lines[363].

The D-54 MG human glioblastoma-derived cell line has also been found to express 3'-iso LM1 as its major ganglioside, when implanted subcutaneously in nude mice[364] (3'-isoLM1 being undetectable in D-54 MG cells grown in-vitro). Moreover 90% of the ganglioside in these subcutaneous mouse tumours was found to be present in the form containing N-glycolylneuraminic acid[365], altered perhaps from the human form by host-tissue interactions. Thus far, no equivalent studies have been done on intracerebrally-implanted D-54 MG tumours.

ANIMAL MODELS OF HUMAN GLIOMAS

The first experimental tumour used to model intracranial CNS tumours and screen potentially viable treatment modalities in any systematic fashion was the L1210 CNS leukemia cell line. This tumour, originally developed in the 1940's by the application of 0.2% methylcholanthrene to the skin of mice of the DBA strain[115], produced a disease similar to human leukemia, with tumour cells circulating in the blood forming widespread systemic metastases. CNS lesions were detectable 2-4 days after transplantation (10^6 cells, intraperitoneal route) as foci of tumour cells attached themselves to the leptomeninges at multiple sites along the neuraxis[116]. In a model developed by Schlabel et al.[117], using intracranial inoculation of L 1210 cells, a nitrosourea-derived compound - BCNU (1, 3 - bis - (2 - chloroethyl) - 1 - nitrosourea), was first tested with the view of applying this agent to clinical needs should encouraging results be obtained. Success of the therapy in the experimental model and its efficacy in subsequent clinical trials[118,119] lent strong support both for the use of BCNU and the continued use of CNS tumour models as experimental testbeds for novel chemotherapeutic regimes.

Realization that the cell kinetics of this and other non-neural intracranial tumours were substantially different from that of neurally-derived neoplasms[120-122] led to a shift in emphasis to tumour models whose lineage was CNS-based. A number of these models were generated, and can be divided into two broad classes :

1) Non-transplantable tumour models

2) Transplantable tumour models

Characteristics of an ideal intracranial model are multifaceted and include :

1) Glial tumour origin

2) Solely intraparenchymal growth

3) Fatal within a prescribed, replicable period of time

4) Autochthonous

5) Fidelity to therapeutic responsiveness of human CNS tumours

Characteristics desirable but whose inclusion is not mandatory, include :

1) Capability for in-vitro growth

2) Survival of transplantation into syngeneic or immunosuppressed xenogeneic hosts

3) Replicability of anatomic location

4) Safety of tumour handling.

No model to-date incorporates all the above requirements. However, transplantable tumour models appear more ideal than chemically or virally-induced tumours.These models will be discussed in greater detail in the following review.

Review of Transplantable Tumour Systems

The transplantable class of tumours consists of five major tumour system sub-types :

1) Murine ependymoblastoma

2) Avian Sarcoma Virus (ASV) - induced astrocytoma

3) Vm /dk murine astrocytoma

4) Nitrosourea - induced gliomas

5) Human xenograft models

Murine Ependymoblastoma Model

The murine ependymoblastoma model is the collective designation given to four separate tumour lines developed in the late 1930's and 1940's by the implantation of a pellet of polycyclic aromatic hydrocarbon - methylcholanthrene into young mice[124,125]. Implantation of a 20 - methylcholanthrene pellet by Seligman and Shear[125] into 5 month old C_3H mice resulted in ependymoblastoma production in 65% of twenty animals studied. Eleven of thirteen tumours were gliomas with considerable variation in both pathological appearance on light microscopic examination and latency of tumour expression, ranging from 227 to more than 500 days. One was found to be serially transplantable and was designated Glioma 26l.

The second of the four tumours was originally induced by Zimmerman and Arnold in 1941[124] by implanting 3 - methylcholanthrene pellets into the cerebral subcortices of mice. The original pathological description was "typical of an ependymoblastoma" and this designation has remained until today even though the tumour has been described by Rubinstein[126] as "poorly differentiated" and not demonstrating "ependymal differentiation". Bigner et al.[127] agrees that it "does not possess in its present state of passage distinctive cellular or cytoarchitectural features of ependymal differentiation, but rather consists of sheets of undifferentiated cells". One feature of this ependymoblastoma, hitherto unexplained, is the presence of Type B retrovirus particles as well as Type C retrovirus antigens consistent with the morphological description of components of mouse mammary tumour and Rauscher leukemia. Ependymoblastoma A (EpA), developed spontaneously while being cultured by Shapiro et al.[128] and acquired a more malignant character, producing death in 19 ± 1.2 days with 2% 60-day survivors compared to the original

tumour's survival of 29-30 days with 1% 60 day survival. The last of the four lines is Glioma 26, also induced by methylcholanthrene by Zimmerman (1948)[129], in this case, into C57 black mice.

Estimated cell generation times of the four tumours in vitro have been determined to be approximately 69 hrs for Ep, 45 hrs-EpA, 57 hrs-Glioma 261 and 55 hrs-Glioma 26[128].The advantages of this model are numerous - it is a glial origin tumour with well-defined and, with one exception (EpA), well-described kinetic and morphological characteristics[128].

The experimental animals are inexpensive and the technique simple enough to permit 100 animals to be inoculated in one hour[128]. This enables many different therapies to be tried using large sample sizes. Although pharmacokinetics of drugs administered in the mouse is at significant variance with that of humans, the majority of chemotherapeutic studies done on this tumour conform with human tumour results. BCNU[132],CCNU[133], ACNU[134] and procarbazine [133] have been effective in producing decreased growth in both systems. Mithramycin[132], cyclophosphamide[132], methotrexate[134], vincristine[135] and VM-26[136] (a podophyllotoxin) have not been effective in both tumour types. The one exception has been the discrepancy between the success of treatment of glioma 26 with dihydrogalactitol[137] and its disappointing performance against human anaplastic astrocytomas[138]. The main use, it seems, of this model would continue to be in the general screening of new drugs at moderate cost, though the exact fidelity of response to human tumours remains to be determined. Disadvantages of this model include the nature of the tumour itself, being a rare type of human tumour and due to the initial mandatory transplantation, not of spontaneous (autochthonous) type. Quantitation of inoculated tumour is, in fact, impossible because the transplantation technique uses a

solid fragment of tumour tissue. Moreover, the freehand inoculation through the skull does not give an anatomical locus as precisely replicable as inoculation using stereotactic instrumentation though the distribution of survival times is exceedingly small and does not seem to be affected by this imprecision in technique.

ASV - induced Astrocytoma Model

There are many viruses, both DNA and RNA type, that can be used to produce autochthonous CNS tumours in several different animal models, including mice[139],rats[140,141], Syrian hamsters[142], rabbits[143], guinea pigs[144], marmosets[145], cats[146], dogs[147,148], rhesus monkeys[149] and newborn cows[207]. However, in most cases, replicability of interanimal growth kinetics as well as the histological picture of the tumours produced is not attainable. One of the few exceptions to this rule has been the behaviour of the RNA Oncornavirus C - Avian Sarcoma Virus. This virus when intracerebrally inoculated into the cortical or subependymal cell plate region of neonatal Fischer 344 rats produces a 100% incidence of anaplastic astrocytomas, which in one study had a latency period of 29-119 days, producing a median survival of 69 days. Incidence of tumours is directly proportional to the size of the inoculum and inversely proportional to the age of the animal[150]. The type of tumour produced depends also on the site chosen for inoculation[151].

Forty-eight hours after the virus is inoculated, there is no detectable whole ASV virus present[152]. However, although tumours that result also contain no viral particles, they not only express ASV antigens on the cell surface but also fully express the viral genome when co-cultivated with susceptible avian cells[153]. The host animal develops a T cell-mediated antitumour immunity[154] though neither the

administration of most immunostimulants[155] nor immunosuppressants (Cyclosporin A has not been tried) has effected any change in survival times. Mahaley et al.[156], however, have significantly increased survival through a combination of levamisole, BCG and killed ASV tumour cells injected subcutaneously in an effort to effect an immune response.

There are numerous advantages to this model in that it is both autochthonous and transplantable; can grow in in-vitro culture, produces under the right conditions, a uniformly glial, parenchymal tumour with a latency that, though slightly more variable than the Ependymoblastoma tumour model is still within an acceptable range. Moreover, it also maintains a fairly good therapeutic fidelity to the human response to BCNU[157] and CCNU[158]. Procarbazine, however, produces a less significant response in the rat[159] than seen in clinical trials[160].

The disadvantages include the variability in tumour morphologies as well as the biohazard of working with ASV virus although there have been no reports of tumour induction in the human or nosocomial infections due to this oncogenic vector. Furthermore, the expense and difficulty of producing a standardized viral suspension limits large scale general screening studies.

The major uses for this model have been to investigate the immunological phenomenon associated with viral induction of CNS tumours and the efficacy of immunostimulant therapy. Due to the good correlation between rat and human chemotherapeutic trials, this model may provide accurate kinetic date on tumour chemotherapies tested in the future.

Vm/dk Murine Astrocytoma Model

During the course of research into scrapie sub-viral particles, Frazer in 1970 accidently discovered an unusually high incidence of spontaneously-occurring astrocytomas in a strain of mice (Vm/dk) inbred by sib-mating from random bred Moredun Institute Stock[161,162]. The tumour was identified in all but three of the fourteen inbreeding generations of the Vm/dk strain with a mean occurrence rate of 1.5% within the first 520 days of life. Histological examination revealed a moderately anaplastic astrocytoma present in various sites within the brain but with a strong predisposition to growth in white matter, spreading along fibre tracts sometimes as far as the dorsal columns of the spinal cord[161].

A concurrent feature of this inbred mouse strain was the occasional occurrence of developmental abnormalities including cleft palate and cranial meningocoele which parallels a human syndrome in which a rare familial tendency for astrocytoma development in the male members is seen along with an increased incidence of status dysraphicus[161]. Serano subsequently established transplantable tumourigenic cell lines from this strain in 1978[163], which could then be utilized in in-vivo models for chemotherapeutic study.

The advantages to this model include autochthonicity, as well as transplantability. A glial cell origin tumour producing solely intraparenchymal growth obviating the need for mechanical and therefore traumatic initiation is highly desirable. The fidelity to human tumour reponse is as yet unknown. However, this is the only tumour system that occurs spontaneously in experimental animals.

The disadvantages of this system include a low incidence rate, heterogeneous tumour position and as yet uncharacterized cell kinetics and chemotherapeutic response.

The major use of this model will probably be in the realm of carcinogenesis studies.However, methods of overcoming the low incidence seen in this model are needed to improve its potential.

Nitrosourea - induced Tumours

There are a number of tumours induced by the administration of two nitrosourea compounds N-methylnitrosourea and N-ethylnitrosourea, but only a few have been characterized well enough and are morphologically stable enough that meaningful therapeutic studies can be performed. They are the 9L rat gliosarcoma, C6 rat glioma, T9 rat glial tumour and RG2 rat glioma.

The 9L gliosarcoma was originally induced by repeated intravenous injections of N-methylnitrosourea into inbred CD Fischer rats. Three stable cell lines were produced by alternate tissue culture and animal transplantation, the 9L line being one of these three main cell line[164].

The morphological appearance on initial examination, was of a densely cellular tumour with a fine fibrillary background and evenly dispersed nuclear chromatin. After six months in cell culture, the tumour started exhibiting morphological changes and in 2.5 years of continuous culture, histological examination revealed glial cells that were interspersed among bundles of spindle cells with vesicular elongated nuclei and prominent nucleoli. The appearance of reticulin and collagen production was also noted. These new features resulted in a change in tumour designation from glioma to gliosarcoma[164]. Doubling time of the cell population during the exponential phase of in-vitro growth was estimated to be 18 hours and the cell cycle time to be 20 hours. The doubling time in-vivo was discovered to be 72 hours with a growth fraction of 0.35 - 0.46 and a labelling index of 0.15 - 0.20[164].

Due to its ability to withstand repeated freezing and thawing, experimental studies were performed on this tumour in many different centres. Its ability to be evaluated in-vitro after in-vivo growth, via the colony-formation assay[165] as well as cell kinetics comparable to those seen in human gliomas[166,167] also enhanced its reputation in comparison to other tumour models. Chemotherapeutic studies suggested a moderately good correlation with human studies using BCNU[168], CCNU[168] and PCNU[168]. The effectiveness of BCNU is dependant on the time of its administration with maximal effectiveness being achieved 16 days after implantation. Procarbazine was at variance with human results[118] showing little effect though, as Bigner has pointed out[122], this may be a species-specific phenomenon restricted to the ASV-induced rat model. Radiotherapeutic studies[170,171]showed that the 9L glioma was an adequate model for prediction of human radiotherapeutic responses. Combined treatment with radiotherapy and BCNU was also effective against these tumours[172], mimicking the clinical situation, though again the timing of the dose of BCNU was critical producing a maximal effect when BCNU was given 16 hours before irradiation.

The blood-brain barrier permeability characteristics of this tumour, however, differ from human gliomas[174]. The tumour also seems to travel along blood vessels[165], a phenomenon not commonly associated with human glioma growth. Its exceedingly fast growth, atypical of human tumours, calls into question many therapeutic results derived from studies of this model. The constant shift in cytological characteristics[164] decreases chances for strict replicability of studies and an insignificant hypoxic cell fraction[170], unlike that found in human glioma, decreases its credibility for use in radiotherapeutic studies.

The above evidence indicates that a substantial degree of concern has developed over the ability of this model to adequately reproduce human tumour growth and metabolic responses and thus further studies will be required.

The C6 rat glioma has been extensively studied in-vitro and is probably the tumour with the most detailed series of phenotypic characterizations performed to-date. This was done in an effort to evaluate changes in phenotypic expression as tumour cells passed from generation to generation.

This cell line was originally induced by i.v. injections of N-methylnitrosourea into randomly-bred Wistar rats, which resulted in a glioma that had a generation time of 40 hours and expressed S-100 protein[176]. However, a large variability in its in-vivo growth characteristics[177], largely due to the random-bred lineage of the cell line and an inherent instability in its in-vitro cytological characteristics and a strong tendency towards the development of sarcomatous features, has precluded development of an in-vivo model for use in chemotherapeutic studies. In-vitro studies however, may provide information beneficial to individual agent evaluation.

Similarly, the T9 cell line, originally induced by Benda et al. (1971)[163], by the administration of N-methylnitrosourea i.v. to CD Fischer rats, was diagnosed as a high-grade astrocytoma. On subsequent passages, however, it transformed into an undifferentiated tumour of CNS origin[178] with a doubling time in-vitro of 31.8 hours and a cell generation time of 31.5 hours[179]. It was utilized in a study which concluded that subcutaneous injections of tumour tissue immunized a host against subsequent intracranial inoculation of the same tissue[178]. T9 cells possess well-expressed tumour related transplantation antigens well suited for this

type of experimental approach but are of limited use, due to the aforementioned cell line instability.

The RG2 rat glioma was originally induced by administration of a single dose of N-ethylnitrosourea transplacentally, on the 20th day of gestation, to CDF-Fischer rat fetuses[179,180]. The malignant glioma appearing 7 months post-partum was transplanted subcutaneously into syngeneic rats.

The morphological appearance of the resultant tumors was characteristic of a differentiated glioma with a homogeneous appearance to the cells and an unusually high nuclear/cytoplasmic ratio with uniformly dispersed chromatin material and prominent nucleoli[181]. The cell doubling time was 26. 7 hours, with a cell generation time of 26.0 hours. The non proliferative population numbered 2.8% of all cells. The tumours also produced neuroglial markers such as S-100 protein[186] and 2', 3' - cAMP -3' phosphohydrolase enzyme[187]. This morphological appearance as well as the cell cycle kinetics did not change after 130 generations of in-vitro cell culture. Rats inoculated intracerebrally with 10^5 cells survived 20.0 ± 0.8 days indicating replicability of tumour growth in-vivo[179].

A colony formation assay was subsequently developed by Weizsacker et al.[182], and a multicellular tumour spheroid model has recently been constructed[183] making the RG2 tumour the only tumour, other than the 9L gliosarcoma, capable of having both in-vitro and in-vivo growth analyzed by an array of different experimental techniques including an in-vivo to in-vitro system. In addition, blood flow and blood-brain barrier permeability studies[184,185] have shown the intracerebral tumour to be 100% permeable to a large molecular weight molecule (horseradish peroxidase-HRP) making it an ideal model for the study of drug delivery and the methods that increase this delivery in intracranial tumours.Both these tumours, along with the T9 rat glioma line have been implanted into cat brain for

study using a variety of techniques including autoradiography[208], magnetic resonance imaging[209] and ^{31}P NMR spectroscopy[210].

Chemotherapeutic studies have only tested BCNU[182], to which the RG2 showed resistance until high concentrations were reached. This aspect of the tumour biology needs to be studied in greater detail before an assessment of fidelity to human tumour response can be determined.

The disadvantages of this tumour system include, as with all other nitrosourea-induced transplantable models, trauma to the brain on initial transplantation. Radiotherapeutic studies, have shown that the RG2 tumour[182], just like the 9L, seems to have no definable hypoxic fraction which may limit its usefulness in comparative analysis with clinical studies. A karyotypic analysis of the tumour has not yet been performed.

A major use for this tumour model appears to be in the analysis of drug delivery techniques. Although the effect of chemotherapeutic agents on this cell line remains unknown, its features of replicability, homogeneity and stability of this cell line, may provide valuable information on the sensitivity or resistance of the tumour to the various agents studied.

Human Tumour Xenografts

This group of tumour models holds the greatest promise in enhancing our knowledge of human brain tumour biology. At present however, the human brain tumour xenograft paradigm remain largely unexplored.

Three sub-types of the human xenograft model have been studied:

1) Xenotransplantation of human glioma cells into athymic nude mice
2) Xenotransplantation of human glioma cells into immune-deficient mice and rats

3) Xenotransplantation of human glioma cells into rats immunosuppressed with Cyclosporin A

Athymic Nude Mouse Model

The athymic nude mouse model has been the most extensively studied human tumour xenograft model to-date. After an unsuccessful attempt at glioma xenotransplantation in 1975[188], the first successful transplant of a human glioma into an athymic nude mouse was performed by Rana et al. in 1977[189]. The model was later refined by many workers, including Shapiro and Bigner, to the state where therapeutic regimes could be assessed[190-193].

Tumours used in the original studies were derived from brain tumour biopsies and were either implanted subcutaneously or intracerebrally. In one study[194], 94.1% of tumour explant types grew in subcutaneous locations with a time interval of between 24 and 364 days taken for tumours to reach 500mm^3. Though, initially the number of animals growing tumour was only 50% "take" rate increased to approximately 81% with serial passage. Doubling time varies from 3.0 - 19.1 days in the exponential phase of growth. The expression of glial fibrillary acidic protein (GFAP, expressed by glial cells and differentiated gliomas) was present in 89% of tumours prior to serial passage. This expression decreased with serial passage to 70% with 50% of these GFAP-expressing tumours producing decreased GFAP. The cells, in general, became more homogeneous with serial passage.

Established human glioma-derived cell lines were then transplanted subcutaneously into mice[195]. Only 4 of 15 lines produced tumours in this model.

The factors correlating best with tumourigenicity were percentage of colony formation in soft agar, saturation density and percentage of bizarre multinucleate giant cells. Growth of tumourigenic cell lines produced 1cc tumour volumes in 17 - 19 days.

There have been only scant reports of xenograft response to chemotherapy. Preliminary studies by Shapiro[196,197] show marked variability in tumour response depending on the patient of origin. One tumour was very responsive to the nitrosoureas tested (BCNU, CCNU, methyl-CCNU, PCNU) and resistant to procarbazine, the second tumour line showing greater resistance to nitrosoureas than to procarbazine.

Another study showed significant but variable decrease in tumour growth to a single i.p. dose of 25mg/kg BCNU[198] . Therapeutic synergism between radiation and BCNU has also been reported[199]. Mithramycin administration produced no effect, correlating with clinical experience[200]. The potential of this tumour model is still largely unexplored. Its major future use, with the high expense of maintaining cell and animal lines and the inherent difference in response to chemotherapy between tumours originating from different patients, remains as a pre-clinical screen, aiding in the individualization of chemotherapeutic protocols to the selected patients.

Although the change in growth rate in serial passage may indicate the selection of faster-growing cell sub-populations causing decreased reliability of trial results, the substantiation of this caveat still remains to be elucidated.

The following two models are still to be explored with respect to response patterns to chemotherapeutic stressors but may represent the future of such research.

Immunodeficient Mouse Xenotransplant Model

In 1978, Bradley et al.[201] artificially immunodeprived 6 week old CBA inbred mice by thymectomy followed by exposure to a lethal dose (900 rad) of radiation and reconstitution with injection of syngeneic marrow cells from normal sex-matched donors. A 44% "take" rate was achieved initially with subcutaneous implantation of human glioma cells with a 5 month delay before a palpable mass was observed. Similar experiments by Saris et al.[202], using anti-rat thymocyte serum with or without irradiation (sub-lethal) in neonatal and adult Fischer rats demonstrated an 86% intracranial tumour "take" with the combined treatment in adult rats and a 100% "take" in neonatal rats given ATS alone. However, the growth rate variability was so great as to preclude in-vivo treatment studies with this model.

Immunosuppressed Rat Xenograft Model

Only two studies have been performed to-date using an immunosuppressed animal as intracranial tumour host[203,211]. Immunosuppression was achieved through the use of Cyclosporin A (CyA), a fungal derivative[204] that selectively suppresses T cell function[96] thereby inhibiting cell-mediated immune response to tumour xenotransplantation.In a study performed by Adams et al.[203], treatment of the rats with 10mg/kg CyA commencing 3 days prior to tumour inoculation resulted in a 70 - 100% mortality within 20 - 44 days. Cytogenetic analysis revealed no difference between cultured tumour cells (D-54-MG human glioma cell line) pre-implantation and in-vivo tumour-derived cells. Doses of 10 - 50mg/kg/day CyA resulted in significant weight loss in all doses in females and at 15mg/kg/day or higher for males. 10% mortality was seen only in males given 30 and 50mg/kg/day CyA doses.

Conclusions

Human tumour xenografts appears to provide an advantage in assessing the effects of therapy on CNS tumour behaviour but the practical implications of this bright new prospect remain to be assessed.

A future goal of this form of research would be to institute a treatment for all CNS tumours regardless of individual variation. However, this objective will be fully realized only through the use of the diverse array of models and techniques that workers now have at their disposal. It is through this type of research that a more comprehensive understanding of the fundamental biological constructs essential in governing the spectrum of tumour response will be achieved.

THERAPY OF MALIGNANT GLIOMAS

Therapy of malignant gliomas can be grouped into two broad classes: surgical and adjuvant. Adjuvant therapies are considered to be of three main types : i) radiotherapy; ii) chemotherapy and iii) immunotherapy.

Surgical Treatment

After a presumptive diagnosis of a malignant intracranial mass lesion is made on the basis of clinical presentation and diagnostic tests such as CT, MRI and cerebral angiography, there are three surgical options which present themselves - 1) biopsy; 2) subtotal resection and 3) total resection of the tumour.

Stereotactic biopsy of the tumour is performed in debilitated patients or a tumour which is deep or in a particularly eloquent region of the brain[80]. This procedure is utilized to provide a pathological diagnosis or to aspirate a cystic area within the tumour[80].

A subtotal resection is the most commonly-performed surgical intervention in glioma patients, although it has been difficult to prove that this option offers significant improvement in survival over biopsy alone. Nevertheless, a logical argument can be made for debulking as a means of providing some intracranial space to perhaps delay the onset of mass effect and facilitate tolerance to radiotherapy. In most cases, a subtotal resection is the most that can be performed owing to the highly infiltrative nature of high-grade gliomas. If lesions are well-localized, surgically accessible and low-grade, total resection of the tumour can be attempted. There is some data showing improved survival in this subgroup of tumours[81].

Radiotherapy

Five basic strategies have been utilized to administer radiotherapy to glioma patients - 1) external-beam radiation - γ- or heavy-particle; 2) external-beam therapy in hyperfractionated doses; 3) external-beam therapy with radiosensitizers, including the use of neutron capture effects; 4) interstitial brachytherapy and 5) photoradiation therapy.

In 1969, a postoperative propective randomized clinical trial was performed by the United States Brain Tumour Study Group (BTSG) on 222 patients, 90% of whom harboured a glioblastoma multiforme, the rest having anaplastic astrocytomas[4,5]. This study was carried out to evaluate whole-brain radiotherapy (170-200 rads/day for 5 days/week to a total of 5000-6000 rads) versus i) chemotherapy (BCNU) alone; ii) radiotherapy plus chemotherapy and iii) supportive care. Patients receiving postoperative supportive care survived 14 weeks (median post-surgical survival); chemotherapy (BCNU) - 19 weeks; radiotherapy - 36 weeks and radiotherapy plus BCNU - 35 weeks. This data showed that radiotherapy was indeed an effective adjunct to surgery for malignant gliomas[4].

Subsequent studies, performed by Fulton et al.[82], have shown that increasing the number of doses per day (one versus three/day) and shortening the total treatment time (4 1/2 versus 6 weeks), again with a total dose of approximately 6000 rads, produced a significantly lengthened survival time (50 weeks for hyperfractionation versus 29 weeks for conventional (once/day) fractionation. Fulton et al.[82] also used misonidazole as a putative radiosensitizing agent in one arm of the same study. Misonidazole was found to be no more effective than radiation alone when median survival times were compared.

Interstitial brachytherapy, ie. the implantation, on a chronic basis, of high-activity radioactive sources within the resection cavity of a glioma, is usually restricted to tumour recurrences. Although a number of radionuclides have been tried eg. ^{198}Au, ^{192}Ir[83], it is ^{125}I with low-E γ-emissions that appears best suited for recurrent tumour therapy. ^{125}I permits a high tumour dose to be given with minimal irradiation to surrounding brain. Tumour doses of up to 12,000 rad have been well tolerated in the short-term[84]. Some patients, however, have experienced a sudden deterioration in neurological status after brachytherapy, due to radiation-induced necrosis with concomitant edema - a condition very difficult to distinguish from tumour growth using non-invasive techniques. In general, patients receiving brachytherapy tend to have longer survival times than non-treated patients (one study with 41 patients having a median survival of 35 weeks after recurrence of glioblastoma, compared to control - 27 weeks)[85]. One basic obstacle, however, to be overcome by any form of radiotherapy, is the radioresistance of glioma cells. Although no large-scale randomized, prospective trial of interstitial brachytherapy has been performed, results of preliminary studies look encouraging.

Photoradiation therapy has been attempted in a number of centres, the first trials being performed in 1980[86-88]. Photoradiation therapy relies on the instillation of a photoreactive compound which ideally is selectively taken up by brain tumours alone and effects cell kill. The light of the appropriate wavelength activates the compound within the cell, causing multiple destructive interactions with the cell membrane, cytoplasm and nucleus[89]. Although enough data has been collected to prove that this technique is capable of tumour cell destruction, in-vivo results have been equivocal[90]. Problems to overcome include lack of enough specificity to control destruction of normal tissue, penetration of light to the depths needed to eradicate tumour[91], suboptimal laser light sources which need to be adjusted to

maximize cell kill while minimizing tissue heating and development of photoreactive drugs activated at the longer wavelengths needed to achieve greater tissue penetration.

Chemotherapy

Chemotherapeutic intervention in malignant gliomas has involved trials of many different drugs including many members of the nitrosourea family of compounds (BCNU[92,93], MeCCNU[94], PCNU[95], ACNU[96]), procarbazine[95,97], hydroxyurea[98], dianhydrogalacticol[99], etoposide[100], VM-26[101], bleomycin[102] and cis-platin[103]. Results with these drugs, alone or in combination, have been, in general, disappointing. Most studies have produced equivocal results, due mainly to either their ineffectiveness or intolerance of patients to side effects.

Tumour cell defense mechanisms may play a decisive role in this resistance to drug therapy. One mechanism is the presence of enzymes which can repair damage to DNA produced by the various types of chemotherapeutic agents. An example of this type of repair is mediated through the methylreductase (Mer) enzyme, repairing nitrosourea-caused DNA methylations. Not all tumours have this enzyme[104]. One possible solution to this type of resistance is to screen tumours for the presence of this enzyme and to treat patients in whom the enzyme is found lacking.

Another mechanism for drug resistance is the presence of the P-glycoprotein molecular pump which ejects certain drugs eg. anthracyclines, from the cell as fast as they enter it. It has been shown that radiotherapy increases the proportion of cells producing P-glycoprotein[105]. One solution to this defense mechanism appears to be the administration of calcium channel-blockers such as verapamil, nifedipine, along with the chemotherapeutic agent. Calcium channel-blockers have been shown to block the action of this tumour drug pump[106]. Although major efforts in

chemotherapy research for malignant gliomas continues, it seems fair to conclude that more work is required to bring chemotherapy into the mainstream of glioma treatment.

Immunotherapy

Use of the patient's own immune system to combat tumours (immunotherapy) has been a concept that has intrigued investigators for several decades. Numerous attempts that have been made to achieve this goal have been replete with disappointments. This has been, at least in part, due to the nature of the host immune system in patients harbouring gliomas. Specifically, depressed B and T cell responses have been demonstrated in these patients[107], with decreased T-cell counts and lower IgM levels consistently seen. Anergy in glioma patients has been shown to be roughly proportional to the tumour grade[108]. In addition, glioma cells seem to have developed numerous mechanisms to enable escape from T-cell mediated damage. These mechanisms include : 1) defective tumour immunogenicity; 2) protection provided by an extracellular mucopolysaccharide coat and 3) production of immunosuppressive molecules[109].

Immunotherapy can be classified into: 1) active specific immunotherapy (vaccines); 2) cellular immunotherapy and 3) molecular immunotherapy (MAbs). Active specific immunotherapy was the first immunotherapeutic modality attempted[107]. However, all attempts to-date have not been successful, perhaps due to failure at disarming tumour-protective mechanisms.Cellular immunotherapy has also been considered as an immunotherapeutic option for many years. The latest attempt at cellular immunotherapy has been the intracavitary instillation of lymphokine-activated killer (LAK) cells along with recombinant interleukin-2 (rIL-2). In summary, autologous peripheral blood lymphocytes are exposed to rIL-2 (in-vitro)[110], then

re-infused or placed back into a surgical resection cavity where LAK-mediated killing is purported to take place[111-113]. Although some tumours do regress, most do so only temporarily. This form of immunotherapy is also dependent on a continuous maintenance supply of IL-2. Most studies have reported disappointing results.[111-113]

Tumour-infiltrating lymphocytes (TIL's) are also being studied for tumour kill efficacy. TIL's, which are harvested directly from the patient's tumours have been shown to produce more specific and more potent cell kill in-vitro[114]. However, one major drawback is the acquisition of sufficient numbers of TIL's to effect treatment. Research in this field continues, although it is still too early to predict the efficacy of this approach.

Successful treatment of human gliomas may ultimately necessitate a multimodal approach combining surgery, radio- and chemotherapy as well as immunotherapeutic modalities. However, more work is needed to understand the basic biology of these tumours and the defense mechanisms they utilize.

Application of Monoclonal Antibodies to the Management of Tumours.

Ability to produce large quantities of monoclonal antibodies, through a process developed by Kohler and Milstein in 1975[366], has made a tremendous impact on the feasibility of using immune-derived targetting molecules to localize and precisely deliver exogenous substances having the potential to detect or significantly alter the growth pattern of tumours. Numerous reviews have been performed[367,377] on strategies that could be employed and both the technical and tumour-derived obstacles that need to be overcome to achieve specific tumour targetting. Therefore, this overview will focus on constraints to which this

methodology must adhere, characteristics of both the tumour-associated antigen as well as the antibody-ligand complex, that could yield potential advantages or disadvantages in in-vivo efficacy.

Most tumour-associated antigens accessible to monoclonal antibodies are proteins, glycoproteins or glycolipids. There are many important characteristics that any tumour-associated antigen (TAA) must have to provide for in-vivo antibody binding in a high enough concentration to achieve adequate visualization or efficacious cell kill. These can be divided into three groups : 1) Level of Antigen Expression; 2) Degree of Antigen Movement and 3) Antigen Accessibility.

The level of expression of any chosen tumour-associated antigen must first be significantly greater on tumour cells than on surrounding normal cells. In addition, the absolute number of TAA molecules must be large enough such that the probability of antibody binding to any individual cell is maximized.

Studies by Schlom and others[367] have revealed that the level of TAA expression is remarkably heterogeneous. This heterogeneity can be temporally and/or spatially dependent. Specifically, only some tumours in a given category will express a particular TAA. Moreover, only some cells in a given tumour will express a particular TAA - in some instances, with a pattern that observers have noted to be reminiscent with that of a "patchwork quilt"[368]. In other cases patterns are determined by tumour depth, oxygenation states and a multitude of other anatomically-based variables. In many cases, these cells also express this particular TAA only some of the time, modulating their expression in accordance with cell cycle stages[369]. Prior treatment with standard radio-/chemotherapy or even surgery could modulate expression of these TAA's as well, although this potential complication has received minimal investigation so far.

Adaptations to these constraints on antigen expression levels include the selection of a TAA shown to be present at high concentrations as well as at levels higher than for normal tissue. Antigen selection can also be restricted to those TAA's shown to undergo limited modulation. The use of β– and γ-interferon has been shown to upregulate expression of selected TAA's[370,371]. Radiotherapy (low doses continuously over a long period of time) as well as the use of some drugs, e.g. adriamycin, in some tumours, have been shown to shift cells into cell cycle stages G2 and M[372], a point at which a TAA may be preferentially expressed.

The mobility of a TAA, due to phenomena such as internalization, capping or shedding can affect the target antigen. Internalization of antigen, especially when bound to antibody, can be beneficial and even essential in the case of some drug-linked antibodies that rely on this effect to achieve cell kill. On the other hand, a capped or shed antigen could prove to be a great liability if bound to antibody with the subsequent movement of the entire antigen-antibody complex into the bloodstream.

Degree of accessibility of a TAA depends on many factors, some of which are related to the structure of the TAA and some dependent on the architecture, both microscopic and macroscopic, of the tumour itself. TAA structural characteristics that may hinder accessibility include steric hindrance from neighbouring molecules on the cell surface or may be due to the molecule's own conformational changes while positioned within the membrane.

Tumour-related variables include size of the tumour (smaller tumours are easier to penetrate), necrotic areas, as well as size, distribution and concentration of vasculature. There can also be a blood-tumour barrier, formed as a result of the attachment of antibody to the periphery of the tumour, thus blocking the infiltration

routes for subsequent therapeutic molecules. Intensity of fibrotic reactions and, of particular importance to gliomas, tumour-mediated breakdown of naturally-occurring barriers such as the blood-brain barrier, can also influence accessibility of TAA's to targetting MAb's. Solutions proposed to increase antibody accessibility to TAA's include: 1) local instillation of antibodies; 2) use of lower-affinity antibodies to reduce the blood-tumour barrier ; 3) the use of hyperosmotic diuretics, such as mannitol to attempt to increase blood-brain barrier permeability; and 4) radiation pretreatment.

Constraints determined by the antibody-ligand complex can be grouped into : 1) monoclonal antibody pharmacokinetics; 2) antibody-ligand stability; 3) host responses and 4) antibody preparation.

To maximize visualization as well as potential therapeutic efficacy, the antibody has to be made in such a fashion as to maximize its on-site dwell time ie. penetration of natural and/or tumour-induced barriers. This is usually accomplished by adjusting the size of the antibody while maintaining antigen specificity or by the use of mechanical means to open up barriers. Use of MAb fragments such as F(ab) and $F(ab)_2$ has assisted investigators in this endeavour. In one study[373], human glioma xenografts in nude mice were treated with Mel-14 (anti-chondroitin) MAb in three different forms : whole IgG, $F(ab)_2$ and F(ab) fragments. MAb was administered intravenously. It was observed that antibody penetration of the blood-brain barrier was enhanced with the $F(ab)_2$ fragment. Although the F(ab) fragment produced better penetration, TAA specificity was markedly reduced.

Antibody-ligand stability is critical to immunoconjugate administration. The chelate must be as resistant as possible to: i) enzymatic degradation until bound or internalized within the cell; ii) degradation because of properties of the ligand itself

e.g. ligand radiolysis. The chelate must also not interfere with the ability of the MAb to bind to its target. The last two criteria can be screened prior to in-vivo administration while the first can only be eliminated using animal or clinical trials.

Most MAb's are produced from hybridomas derived in whole or in part from mouse cells. As a result, introduction of MAb's from such a source into humans produces a host immune response - a human anti-mouse antibody (HAMA), the MAb being treated as a foreign antigen[374,375]. This makes the likelihood of side effects with repeat MAb injections quite high. There have been two methodologies developed to try to minimize this response. The first approach, using immunosuppressants (eg. corticosteroids, cyclophosphamide) has met with only limited success[207]. The second approach has been to use genetic engineering to "humanize" the murine-derived MAb[376]. Humanization involves taking the genetic sequence of the murine MAb, determining the critical (antibody-binding) regions and linking this partial sequence with the gene sequence of a human MAb of the same isotype (minus the critical sequence). This gene fusion is then inserted into a recipient cell "factory", usually E. coli, where the fusion protein can be produced in large quantities. Murine variable regions have been transferred in this fashion into human antibodies, resulting in a TAA-specific murine-derived antibody that can be up to 98% human. This chimeric MAb minimizes the HAMA response because very few foreign antigenic epitopes are present to be recognized by host B or T lymphocytes.

Elimination of contaminants such as pyrogens, viruses, bacteria and extraneous protein must be performed with as much stringency as possible. The consequences include side effects of MAb administration resulted in increased morbidity and/or mortality.

The choice of ligand in immunoconjugate constraints depends on diagnostic

or therapeutic strategy. In immunolocalization, the choice is usually radionuclide well visualized using a γ-camera. Recent choices for such radioimmunoscintigraphic studies include ^{131}I, ^{111}In, ^{99m}Tc and ^{67}Ga. For immunotherapy, recent experiments have been performed[377-379] with β-emitters such as ^{131}I, ^{90}Y, ^{67}Cu, ^{186}Re and α-emitters such as ^{211}At and ^{212}Bi.

One advantage of radioimmunotherapy (RIT) over chemoimmunotherapy is the lack of having to bind to each cell - RIT being able to kill, in some cases, 50 or more cell diameters from the binding site of the immunoconjugate[377]. Unfortunately, however, gliomas are known to be notoriously radioresistant. Perhaps MAb "cocktails" of combined RIT and drug-linked MAb's may eventually be successful. Although specific immunotherapy is still in its infancy, the possibility of inducing a tumour-specific response from the host immune system, may make it the most promising therapeutic modality.

In-Vivo Localization of Monoclonal Antibodies to Antigens associated with Intracranial Tumours.

The first recorded attempt of in-vivo administration of radiolabelled antibody (heteroantiserum) to a brain tumour-associated antigen was performed by Day et al. in 1965[380], although ^{131}I-labelled human serum albumin had been successfully visualized after accumulation by a human glioma in a study done as early as 1951[381]. Since that time, a variety of studies have been performed on the biodistribution and pharmacokinetics of a number of putative glioma-specific MAb's, administered both intravenously[382] as well as intrathecally/intraventricularly[383]. Most in-vivo work has been performed on human glioma xenografts implanted into an animal model, such as the nude mouse. Studies have also been performed on monkeys to assess

normal brain permeability of MAb's[384].

The glioma-associated antigens targetted thus far with MAb's are either membrane-associated proteins (tenascin/81C6 MAb; ferritin/anti-ferritin MAb's (many); epidermal growth factor receptor/ α-EGFR MAb), glycoproteins (p97/ p96.5 MAb), proteoglycans (chondroitin sulfate/ Mel-14 MAb) fetal-brain antigens (UJ 13A antigen/ UJ 13A MAb) or as-yet uncharacterized tumour antigens (cervical CA antigen/ CLN-IgG MAb) (see review - pg.13). The 81C6, α-EGFR, p96.5 and Mel-14 MAb's have been shown to specifically localize to human glioma xenografts in nude mice. ^{131}I-labelled 81C6 and Mel-14 MAb's have also been shown to cause significant tumour growth delays in intracrebrally-implanted tumours grown in the nude mouse model using the D-54 MG human glioblastoma cell line[373,384]. Furthermore, tumour regression has been shown to occur following administration of ^{90}Y-labelled p96.5 MAb in subcutaneous xenografts of the U-251 glioma cell line with the intravenous administration route used above[372].

Lack of a large animal model thus far has precluded studies of the biodistribution, pharmacokinetics and efficacy of intrathecally-administered MAb's. Patients diagnosed with neoplastic meningitis were selected for treatment with one of a panel of MAb's by Coakham et al.[385] - these patients having previously failed on conventional therapy. Selection of the MAb treatment was performed by first screening CSF-borne tumour cells with a panel of MAb's. Each of the five patients in this study harboured a different primary tumour, only two of which were CNS-derived. After treatment with up to 45 mCi of ^{131}I, improvement was noted in all cases, excepting a patient with teratoma who died within 6 months of treatment. In fact, one patient harbouring a pineocytoma achieved a remission lasting at least 22 months.

At last report, 15 such patients had undergone intrathecal therapy using one of a panel of MAb's, with ^{131}I doses of up to 60mCi. Improvement was seen in 63% of patients, with three patients exhibiting myelosuppression and two patients developing seizures at the 60mCi dose[386]. The biological availability of specific intravenously- administered MAb was <0.005% of injected dose (UJ13A-glioma). Biological $t_{1/2}$ was biexponential with a rapid clearance ($t_{1/2}$ = 1.8 hrs) followed by a slower loss ($t_{1/2}$ = 53 hrs.) from blood[382]. Clearance of intrathecally-administered antibody ranged from 15 to 42 hrs from the CSF (4 patients), 70 to 92 hrs from the blood (5 patients)[385]. Tumour clearance for the UJ181.4 MAb for the pineblastoma has been measured to be between 150 to 250 hours (one patient)[383]. Recently, Brady et al.[387] has used a ^{131}I-labelled α-EGFR MAb in the treatment of 14 patients harbouring malignant gliomas. Of these patients, a response was seen in 8/14 cases.

More experience is needed with MAb's of a variety of different antigen-binding specificities, isotypes and ligands to substantiate the efficacy of this treament modality. However, the innate advantage of increased dose delivery to tumour when using the intrathecal route of administration for glioma-specific MAb's may result in enhanced survival rates.

REFERENCES

1) Wilkins, R.H., and Rengachary, S.S. Neurosurgery, vol.1, pp.586-590. Toronto: McGraw-Hill Publ., 1984.

2) Schwartz, S.I. (ed.-in-chief), Principles of Surgery, 3rd ed., p 1777. Toronto : McGraw-Hill Publ., 1979.

3) Seminars in Oncology. Vol.13, No 1 (March), pp 38-45, 1986.

4) Walker, M.D., Alexander, E. Jr., and Hunt, W.E. Evaluation of BCNU and/or radiotherapy in the treatment of anaplastic gliomas : A cooperative clinical trial. J . Neurosurg., *49:*333-343, 1978.

5) Walker, M.D., Green, S.B., and Byar, D.P. Randomized comparisons of radiotherapy and nitrosoureas for the treatment of malignant glioma after surgery. N Engl. J. Med., *303:*1323-1329, 1980.

6) Newbill, H.P., and Anderson, G.C. Racial and sexual incidence of primary intracranial tumours - Statistical study of 133 cases verified by autopsy. Arch. Neurol. Psychiatr. *51:* 564-567, 1944.

7) Odeku, E.L., and Janota, I. Intracranial masses - Ibadan. West Afr. Med. J. *16:* 31-42, 1967

8) Kurland, L.T. The frequency of intracranial and intraspinal neoplasms in the resident population of Rochester, Minnesota.. J. Neurosurg. *15:* 627-641, 1958.

9) Kurland, L.T., Elveback, L.R., Nobrega, F.T. Population studies in Rochester and Olmsted County, Minnesota, 1900-1968. *In :* Kessler, I., Levin, M.L. (Eds). The Community as an Epidemiologic Laboratory: A casebook of Community Studies, pp 47-70. Baltimore: Johns Hopkins Press, 1970.

10) Gudmundssen, K.R. A survey of tumors of the central nervous system in Iceland during the 10-year period 1954-1963. Acta Neurol. Scand., 1970, *46:* 538-552.

11) Mancuso et al. T. F. Epidemiological Study of Tumours of the Central Nervous System in Ohio. *In* : I.J. Selikoff, and E.C. Hammond (eds.), Brain Tumors in the Chemical Industry, pp. 17-39. Annals of the New York Academy of Sciences, *381* : 1982.

12) Walker,A.E., Robins, M., and Weinfeld, F.D. Epidemiology of brain tumors: The national survey of intracranial neoplasms. Neurology, *35:* 219-226, 1985.

13) Schoenberg, B.S., Christine, B.W., and Whisnant, J.P. The resolution of discrepancies in the reported incidence of primary brain tumors. Neurology, *28:* 817-823, 1978.

14) Zimmerman, H.M. Brain tumors: their incidence and classification in man and their experimental production. *In:* Albertson, P.D., Krauss,M., and Bielefeld, H.R.(eds.), Research in the Experimental and Clinical Aspects of Brain Tumors. Annals of the New York Academy of Sciences, *159:* 337-359, 1969.

15) Green, J.R., Waggener, J.D., and Kriegsfeld, B.A. Classification and incidence of neoplasms of the central nervous system. *In:* Advances in Neurology, vol.15, Neoplasia in the Central Nervous System, p.51. New York: Raven Press, 1976.

16) Peers, J.H. The occurrence of tumors of the central nervous system in routine autopsies. American Journal of Pathology, *12:* 911, 1936.

17) Weil, A. Textbook of Neuropathology, 2nd ed. London: Heinemann

18) Courville, C.B. Pathology of the Central Nervous System, 3rd ed. Mountain View, California: Pacific Press, 1950.

19) Heshmat, M.Y., Kovi, J., Simpson, C., Kennedy, J., and Fan, K.J. Neoplasms of the Central Nervous System. Incidence and Population Selectivity in the Washington, DC, Metropolitan Area. Cancer, *38:* 2135-2142, 1976.

20) Cohen, A., and Modan, B. Some epidemiologic aspects of neoplastic diseases in Israeli immigrant population. III. Brain Tumors. Cancer, *22:* 1323-1328, 1968.

21) Barker, D.J.P., Weller, R.O., and Garfield, J.S. Epidemiology of primary tumours of the brain and spinal cord: a regional survey in southern England. Journal of Neurology, Neurosurgery and Psychiatry, *39:* 290, 1976.

22) Sutherland, G.R., Florell, R., Louw, D., Choi, N.W., and Sima, A.A.F. Epidemiology of primary intracranial neoplasms in Manitoba, Canada Can. J. Neurol. Sci., *14:* 586-592, 1987.

23) Russell, D.S., and Rubinstein, L.J. Pathology of Tumours of the Nervous System, 5th edition. Baltimore: Williams & Wilkins Publ., 1989.

24) Percy, A.K., Elveback, L.R., Okazaki, H., and Kurland, L.T. Neoplasms of the central nervous system. Epidemiologic considerations. Neurology, *22:* 40, 1972.

25) Schoenberg, B.S. Epidemiology of primary nervous system neoplasms. *In:* Advances in Neurology, *19:* 475-495. Raven Press, 1978.

26) Codd, M.B., and Kurland, L.T. Descriptive epidemiology of primary intracranial neoplasms. *In:* Progress in experimental Tumor Research, *29:* 1, 1985.

27) Fogelholm, R., Uutela, T., and Murros, K. Epidemiology of central nervous system neoplasms. A regional survey in central Finland. Acta Neurologica Scandinavica, *69:* 129, 1984.

28) Wilkins, R.H., Rengachary, S.S., (eds.), Neurosurgery Vol. 1. p. 553. Toronto: McGraw-Hill Publ., 1985.

29) Kernohan, J.W., Mabon, R.F., Svien, H.J., and Adson, A.W. A simplified classification of the gliomas. Proc. Staff Mtg. Mayo Clin., *24* : 71-75, 1949.

30) Zulch, K.J. Histological Typing of Tumours of the Central Nervous System. Geneva: World Health Organization, 1979.

31) Russell, D.S., and Rubinstein, L.J. Tumours of Neuroglial Cells: Classification and histological types. *In:* Pathology of Tumours of the Nervous System, 5th edition., pp 97-99. Baltimore: Williams & Wilkins Publ., 1989.

32) Russell, D.S., and Rubinstein, L.J. Anaplastic Forms: Glioblastoma Multiforme. *In:* Pathology of Tumours of the Nervous System, 5th edition, pp 219-220. Baltimore: Williams & Wilkins Publ., 1989.

33) Russell, D.S., and Rubinstein, L.J. Anaplastic Forms: Glioblastoma Multiforme. *In:* Pathology of Tumours of the Nervous System, 5th edition, pp 221-232. Baltimore: Williams & Wilkins Publ., 1989.

34) Salcman, M. Survival in glioblastoma: Historical perspective. Neurosurgery, *7* : 435-439, 1980.

35) Rubinstein, L.J. Supplement to Tumors of the Central Nervous System. Atlas of Tumor Pathology, second series, fascicle 6. Armed Forces Institute of Pathology, Washington, DC., 1982.

36) Hesketh, J., and Baudier, J. Evidence that S100 proteins regulate microtubule assembly and stability in rat brain extracts. International Journal of Biochemistry, *18:* 691, 1986.

37) Loeffel, S.C., Gillespie, Y., Mirmiran, S.A., Miller, E.W., Golden, P., Askin, F.B., and Siegal, G.P. Cellular immunolocalization of S100 protein within fixed tissue sections by monoclonal antibodies. Archives of Pathology and Laboratory Medicine, *109:* 117, 1985.

38) Kahn, H.J., Marks, A., Thom, H., and Baumal, R. Role of antibody to S100 protein in diagnostic pathology. American Journal of Clinical Pathology, *79:* 341, 1983.

40) Dahl, D. The vimentin-GFA protein transition in rat neuroglia cytoskeleton occurs at the time of myelination. Journal of Neuroscience Research, *6:* 741, 1981.

41) Franke, W.W., Schmid, E., Osborn, M., and Weber, K. Different intermediate-sized filaments distinguished by immunofluorescence microscopy. Proc. Natl. Acad. Sci. USA, *75* : 503-538, 1978.

42) Paetau, A., and Virtanen, I. Cytoskeletal properties and endogenous degradation of glial fibrillary acidic protein and vimentin in cultured human glioma cells. Acta Neuropathologica, *69:* 73, 1986.

43) Thompson R.J., Graham, J.G., McQueen, I.N.F., Kynoch, P.A.M., and Brown, K.W. Radioimmunoassay of brain-type creatine kinase-BB isoenzyme in human tissue and in serum of patients with neurological disorders. J. Neurol. Sci., *47* : 241-254, 1980.

44) Norenber, M.D. The distribution of glutamine synthetase in the rat central nervous system. Journal of Histochemistry and Cytochemistry, *27:* 756, 1979.

45) Samuel, J., Dept. of Immunology, University of Alberta. Personal communication.

46) Kemshead, J.T., Jones, D.H., and Coakham, H.B. Markers for the identification of tumours arising from the neuroectoderm. Reviews in the Neurosciences, *1* : 127-144, 1987.

47) Russell, D.S., and Rubinstein, L.J. Specific Expression of Cell Lineage and Differentiation Markers. *In:* Pathology of Tumours of the Nervous System, 5th edition, pp36-37. Baltimore: Williams & Wilkins Publ., 1989.

48) Hoshino, T., Prados, M., Wilson, C.B., Cho, K.G., Lee, K.S., and Davis, R.L. Prognostic implications of the bromodeoxyuridine labeling index of human gliomas. J. Neurosurg., *71* : 335-341, 1989.

49) Giangaspero, F., Doglioni, C., Rivano, M.T., Pileri, S., Gerdes, J., and Stein, H. Growth fraction in human brain tumours defined by the monoclonal antibody Ki-67. Acta Neuropathologica, *74:* 179, 1987.

50) Fredman, P., von Holst, H., and Collins, V.P. Sialyllactotetraosylceramide, a gangliodide for human malignant gliomas. J. Neurochem., *50* : 912-919, 1988.

51) Shapiro, W.R., and Shapiro, J.R. Principles of Brain Tumor Chemotherapy. *In* : J.W. Yarbo, (ed.), Seminars in Oncology, pp. 56-70. Orlando: Grune & Stratton, Inc., 1986.

52) Becher, R., Gibas, Z., and Sandberg, A.A. Involvement of chromosomes 7 and 12 in large bowel cancer; trisomy 7 and 12q-. Cancer Genet. Cytogenet., *9* : 329-332, 1983.

53) Ochi, H., Takenchi, J., Holyoke, D., and Sandberg, A.A. Possible specific chromosome changes in large bowel cancer. Cancer Genet. Cytogenet., *10* : 121-122, 1984.

54) Balaban, G., Herlyn, M., Guerry, D., Bartolo, R., Koprowski, H., Clark, W.H., and Nowell, P.C. Cytogenetics of human malignant melanoma and premalignant lesions. Cancer Genet. Cytogenet., *11*: 429-439, 1984.

55) Seizinger, B.R., Rouleau, G., Orzelius, L.J., Lane, A.H., St. George-Hyslop, P., Huson, S., Gusella, J.F., and Martuza, R.L. Common pathogenetic mechanism for three tumor types of bilateral acoustic neurofibromatosis. Science, *236* : 317-319, 1987.

56) Seizinger, B.R., Martuza, R.L., and Gusella, J.F. Loss of genes of chromosome 22 in tumorigenesis of human acoustic neuroma. Nature (Lond.), *322* : 644-647, 1986.

57) Mark, J., Levan, G., and Mitelman, F. Identification by fluorescence of the G chromosome lost in human meningiomas. Hereditas, *71* : 163-168, 1972.

58) Zankl, H., and Zang, K.D. Cytological and cytogenetical studies on brain tumors. IV. Identification of the missing G chromosome in human meningiomas as number 22 by fluorescence technique. Humangenetik, *14* : 167-169,1972.

59) Bigner, S.H., Mark, J., Burger, P.C. Mahaley, M. S., Jr., Bullard, D.E., Muhlbaier, L.H., and Bigner D.D. Specific chromosomal abnormalities in malignant human gliomas. Cancer Research, *88* : 405-411,1988.

60) Cowell, J.K. Double minutes and homogeneously staining regions: Gene amplification in mammalian cells. Annu. Rev. Genet., *16* : 21-60, 1982.

61) Bigner, S.H., Wong, A.J., Mark, J., Muhlbaier, L.H., Kinzler, L.H., Vogelstein, K.W., B., and Bigner, D.D. Relationship between gene amplification and chromosomal deviations of malignant human gliomas. Cancer Genet. Cytogenet., *29* : 165-170, 1987.

62) Libermann, T.A., Nusbaum, H.R., Razon, N., Kris, R., Lax, I., Soreq, H., Whittle, N., Waterfield, M.D., Ullrich, A., and Schlesinger, J. Amplification, enhanced expression and possible rearrangement of the EGF receptor gene in primary human brain tumors of glial origin. Nature, *313* : 144-147, 1985.

63) Malden, L.T., Novak, U., and Burgess, A.W. Selective amplification of the cytoplasmic domain of the epidermal growth factor gene on glioblastoma multiforme. Cancer Res., *48* : 2711-2714,1988.

64) Bigner, S.H., Burger, P.C., Wong, A.J., Werner, M.H., Hamilton S.R., Muhlbaier, L.H., Vogelstein, B., and Bigner, D.D. Gene amplification in malignant human gliomas: Clinical and histopathological aspects. J. Neuropathol. Exp. Neurol., *47* : 191-205, 1988.

65) Grady, E.F., Schwab, M., and Rosenau, W. Expression of N-*myc* and *src* during the development of fetal human brain. Cancer Res., *43* : 2931-2936, 1987.

66) Friedman, B.A., and Rosner, M.R. Growth factors modify the EGF-receptor through multiple pathways. J. Cell. Biochem., *34* : 1-11, 1987.

67) Schlessinger, J. The epidermal growth factor receptor as a multifunctional allosteric protein. Biochemistry, *27* : 3119- 3123, 1988.

68) Massague, J. Epidermal growth factor-like transforming growth factor. II. Interaction with epidermal growth factor receptors in human placenta membranes and A431 cells. J. Biol. Chem., *258* : 13614-13620, 1983.

69) Davies, R.L., Grosse, V.A., Kucherlapati, R., and Bothwell, M. Genetic analysis of epidermal growth factor receptor gene to chromosome 7. Proc. Natl. Acad. Sci. USA., *77* : 4188-4192, 1980.

70) Downward, J., Yarden, Y., Mayes, E., Scarce, G., Totty, P., Stockwell, A., Ullrich, A., Schlessinger, J., and Waterfield, M.D. Close similarity of epidermal growth factor receptor and v-*erb* -B oncogene protein sequences. Nature, *307* : 521-527, 1984.

71) Goustin, A.S., Leof, E.B., Shipley, G.D., and Moses, H.L. Growth factors and cancer, Cancer Res., *46* : 1015-1029, 1986.

72) Antoniades, H.N. Human platelet-derived growth factor (PDGF): Purification of PDGF I and PDGF II and separation of their subunits. Proc. Natl. Acad. Sci. USA, *78* : 7314-7317, 1981.

73) Deuel, T.F. Polypeptide growth factors. Annu. Rev. Cell Biol., *3* : 443-492, 1987.

74) Stenman, G., Rorsman, F. and Betsholtz, C. Sublocalization of the human PDGF A-chain gene to chromosome 7, band q11.23, by in situ hybridization. Exp. Cell Res., *178* : 180-184, 1988.

75) Ross, R., Raines, E.R., and Bowen-Pope, D.F. The biology of platelet-derived growth factor. Cell, *46* : 155-169, 1986.

76) Richardson, W.D., Pringle, N., Mosley, M.J., Westermark, B., and Dubois-Dalcq, M. A role for platelet-derived growth factor in normal gliogenesis in the central nervous system. Cell, *53* : 309-319, 1988.

77) Gammeltoft, S., Ballotti, R., Kowalski, A., Westermark, B., and Van Obberghen, E. Expression of two types of receptor for insulin-like growth factors in human malignant glioma. Cancer Res., *48* : 1233-1237, 1988.

78) Nigro, J.M., Baker, S.J., Preisinger, A.C., Jessup, J.M., Hostetter, R., Cleary, K., Bigner, S.H., Davidson, N., Baylin, S., Devilee, P., Glover, T., Collins, F.S., Weston, A., Modali, R., Harris, C.C., and Vogelstein, B. Mutations on the *p53* gene occur on diverse human tumour types. Nature, *342* : 705-708,1989.

79) Baker, S.J., Fearon, E.R., Nigro, J.M., Hamilton, S.R., Preisinger, A.C., Jessup, J.M., vanTuinen, P., Ledbetter, D.H., Barker, D.F., and Nakamura, Y. Chromosome 17 deletions and p53 gene mutations in colorectal carcinomas. Science, 244 : 217-221, 1989

80) Piepmeier, J.M., and George, T.M. Surgical management of supratentorial gliomas. Contemporary Neurosurgery, *11* : no.21, 1989.

81) Ciric, I., Ammirati, M., Vick, N., and Mikhael, M. Supratentorial gliomas: Surgical considerations and immediate postoperative results. Gross total resection versus partial resection. Neurosurgery, *21* : 21, 1987.

82) Fulton, D.S., Urtasun, R.C., Shin, K.H., Geggie, P.H.S., Thomas, H., Muller, P.J., Moody, J., Tanasichuk, H., Mielke, B., Johnson, E., and Curry, B. Misonidazole combined with hyperfraction in the management of malignant glioma. Int. J. Radiat. Oncol. Biol. Phys., *10* : 1709-1712,1984.

83) Bernstein, M., and Gutin, P.H. Interstitial irradiation of brain tumors: A review. Neurosurgery, *9* : 741-750, 1981.

84) Apuzzo, M.L.J. Immunotherapy of human gliomas. *In* : Wilkins, R.H., Rengachary, S.S., (eds), Neurosurgery, Vol. 1. p 1139-1142. Toronto: McGraw-Hill Publ., 1985.

85) Leibel, S.A., and Sheline, G.E. Radiation therapy for neoplasms of the brain. J. Neurosurg., *66* :1-22, 1987.

86) Perria, C. Photodynamic therapy of human gliomas by hematoporphyrin and He-Ne laser. IRCS Med. Sci. (Cancer), *9* : 57-58, 1981.

87) Forbes, I.J., Cowled, P.A., Leong, A.S.-Y., Ward, A.D., Black, R.B., Blake, A.J., and Jacka, F.J. Phototherapy of human tumours using haematoporphyrin derivative. Med. J. Aust., *2* : 489-493, 1980.

88) Laws, E.R. Jr., Cortese D.A., Kinsey, J.H., Eagan, R.T., and Anderson, R.E. Photoradiation therapy on the treatment of malignant brain tumors: a phase I (feasibility) study. Neurosurgery, *9* : 672-678, 1981.

89) Dougherty, T.J. Photodynamic therapy (PDT) of malignant tumors. CRC Crit. Rev. Oncol. Hematol., *2* : 83-116,1984.

90) Perria, C., Carai, M., Falzoi, A., Orunesu, G., Rocca, A., Massarelli, G., Francaviglia, N., and Jori,G. Photodynamic therapy of malignant brain tumors: clinical results of, difficulties with, questions about, and future prospects for the neurosurgical applications. Neurosurgery, *23* : 557-563. 1988.

91) Cheng, M.-K., McKean, J., Boisvert, D., Tulip, J., and Mielke, B.W. Effects of photoradiation therapy on normal rat brain. Neurosurgery, *15* : 804-810, 1984.

92) Chang, C.H., Horton, J., Schoenfeld, D., Salazer, O., Perez-Tamayo, R., Kramer, S., Weinstein, A., Nelson, J.S. and Tsukada, Y. Comparison of postoperative radiotherapy and combined postoperative radiotherapy and chemotherapy on the multidisciplinary management of malignant gliomas. A joint Radiation Therapy Oncology Group and Eastern Cooperative Oncology Group study. Cancer, *52* :997-1107, 1983.

93) Levin, V.A., Wilson, C.B., Rubenstein, L., Bartyzel, L., and Vestnys, P. Adjuvant chemotherapy with BCNU or the combination of CCNU, procarbazine, and vincristine following irradiation and hydroxyurea for glioblastoma multiforme. Proc. Annu. Meet. Am. Assoc. Cancer Res., *21* :474, 1980 (Abstract).

94) Walker, M.D., Alexander, E., Jr., Hunt, W.E., MacCarty, C.S., Mahaley, M.S., Jr., Mealey, J., Jr., Norrell, H.A., Owens, G., Ransohoff, J., Wilson, C.B., Gehan, E.A., and Strike, T.A. Evaluation of BCNU and/or radiotherapy in the treatment of anaplastic gliomas. A cooperative clinical trial. J. Neurosurg., *49* : 333-343, 1978.

95) Green, S.B., Byar, D.P., Strike, T.A., Burger, P.C., Mahaley, M.S., Mealey, J., Pistenmaa, D.A., Ransohoff, J., Robertson, J.T., Selker, R.G., Shapiro, W.R , and Van Gilder, J.C. Randomized phase II comparison of PCNU and AZQ for the treatment of primary brain tumors (Study 8120). Proc. Annu. Meet. Am. Soc. Clin. Oncol., *4* : C-558, 1985 (Abstract)

96) Hara, T., Miyazaki, S., Ishii, E., Yoshida, N., Inaba, K., Ikeda, K., and Goya,N. High-dose 1-(4-amino-2-methyl-5-pyrimidinyl)-methyl-3-(2-chloroethyl)-3-nitrosurea hydrochloride (ACNU) with autologous bone marrow rescue for patients with brain stem tumors. Childs Brain, *11* : 369-374, 1984.

97) Green, S.B., Byar, D.P., Walker, M.D., Pistenmaa, D.A., Alexander, E.,Jr., Batzdorf, U., Brooks, W.H., Hunt, W.E., Mealey, J.,Jr., Odom, G,L., Paoletti, P., Ransohoff, J., Jr., Robertson, J.T., Selker, R.G., Shapiro, W.R., Smith, K.R., Jr., Wilson, C.B., and Strike, T.A. Comparisons of carmustine, procarbazine, and high-dose methylprednisolone as additions to surgery and radiotherapy for the treatment of malignant glioma. Cancer Treat. Rep., *67* : 121-132, 1983.

98) Levin, V.A., Wilson, C.B., Davies, R., Wara, W.M., Pischer, T.L., and Irwin, L. A Phase III comparison of BCNU, hydroxyurea, and radiation therapy to BCNU and radiation therapy for treatment of primary malignant gliomas. J. Neurosurg., *51* : 526-532, 1979.

99) Eagan, R.T., Childs, D.S., Jr., Layton, D.D., Jr., Laws, E.R., Jr., Bisel, H.F., Holbrook, M.A., and Fleming, T.R. Dianhydrogalactitol and radiation therapy. Treatment of supratentorial glioma. JAMA, *41* : 2046-2050, 1979.

100) Schold. S.C., Jr. Chemotherapy of primary central nervous system neoplasms. Semin. Neurol., *1* : 189-210, 1981.

101) Seiler, R.W., Zimmerman, A., and Markwalder, H. Adjuvant chemotherapy with VM 26 and CCNU after operation and radiotherapy of high-grade supratentorial astrocytomas. Surg. Neurol., *13* : 65-68, 1980.

102) Kristiansen, J., Hagen, S., and Kollevoid, T. Combined modality therapy of operated astrocytomas grade III and IV. Confirmation of the value of postoperative irradiation and lack of potentiation of bleomycin on survival time: a prospective multicenter trial of the Scandinavian Glioblastoma Study Group. Cancer, *47* : 649-652, 1981.

103) Feun, L.G., Stewart, D.J., Maor, M., Leavens, M., Savaraj, N., Burgess, M.A., Yung, W.K., and Benjamin, R.S. A pilot study of cis-diamminedichloroplatinum and radiation therapy in patients with high grade astrocytomas. J. Neurooncol., *1* : 109-113, 1983.

104) Day III, R., Ziolkowski, C.H.J., and Scudiero, D.A. Defective repair of alkylated DNA by human tumour and SV40-transformed human cell strains. Nature, *288* : 724-727, 1980.

105) Matsumoto, T., Tani, E., Kaba, K., Shindo, H., and Miyaji, K. Expression of P-glycoprotein in human glioma cell lines and surgical glioma specimens. J. Neurosurg. (submitted for publication), 1990.

106) Kartner, N., Riordan, J.R., and Ling, V. Cell surface P-glycoprotein associated with multidrug resistance in mammalian cell lines. Science, *221* : 1285-1288, 1983.

107) Young, H., Kaplan, A., and Regelson, W. Immunotherapy with autologous white cell infusions ("lymphocytes") in the treatment of recurrent glioblastoma multiforme: a preliminary report. Cancer, *40* : 1037, 1977.

108) Mahaley, M.S., Jr., Brooks, W.H., Roszman, T.L., Bigner, D.D., Dudka, L., and Richardson, S. Immunobiology of primary intracranial tumors. Part I: studies of the cellular and humoral general immune competence of brain-tumor patients. J. Neurosurg., *46* : 467, 1977.

109) Kornblith, P.L., and Sundstrom, D. LAK Cell/Interleukin-2 Treatment of Malignant Gliomas. Contemporary Neurosurgery, *11* : number 9, 1989.

110) Jacobs, S.K., Wilson, B.S., Kornblith, P.L., and Grimm, E.A. *In vitro* killing of human glioblastoma by interleukin-2-activated autologous lymphocytes. J.Neurosurg., *64* : 114, 1986.

111) Jacobs, S.K., Wilson, D.J., Kornblith, P.L., and Grimm, E.A. Interleukin-2 or autologous lymphokine-activated killer cell treatment of malignant glioma: phase I trial. Cancer Res., *46* : 2101, 1986.

112) Barba, D., Oldfield, E.H., Saris, S.C., Rosenburg, S.A., and Hamilton, J.M. Phase II immunotherapy of cystic primary brain tumors (PBT) with IL-2/LAK cells. Proceedings of ASCO, *7* : 313, 1988.

113) Merchant R.E., Merchant, L.H., Cook, S., McVicar, D., and Young, H. Intralesional infusion of lymphokine-activated killer (LAK) cells and recombinant interleukin-2 (rIL-2) for the treatment of patients with malignant brain tumor. Neurosurgery, *23* : 725, 1988.

114) Rosenberg, S.A., Packard, B.S., Aebersold, P.M., Solomon, D., Topalian, S.L., Lotze, M.T., Yang, J.C., Seipp, C.A., Simpson, C., Carter, C., Bock, S., Schwartzentruber, D., Wei, J.P., and White D.E. Special report. Use of tumor-infiltrating lymphocytes and interleukin-2 in the immunotherapy of patients with metastatic melanoma. A preliminary report. New Eng. J. Med., Dec. 22, 1988.

115) Law, L.W., Dunn, T.B., Boyle, P.J., and Miller, J.H. Observations on the effect of the effect of a folic-acid antagonist on transplantable lymphoid leukemias in mice. J. Natl Cancer Inst., *10* : 179-192, 1949.

116) Skipper, H.E., Schabel, F.M. Jr., and Wilcox, W.S. Experimental evaluation of potential anticancer agents. XXI. Scheduling of arabinosylcytosine to take advantage of its S-phase specificity against leukemia cells. Cancer Chemother. Rep., *51* : 125-165, 1967.

117) Schabel, F.M., Johnston, T.P., McCaleb, G.S., Montgomery, J.A., Laster, W.R., and Skipper, H.E. Experimental evaluation of potential anticancer agents. VIII. Effects of certain nitrosoureas on intracerebral L1210 leukemia . Cancer Res., *23* : 725, 1963.

118) Green, S.B., Byar, D.P., and Walker, M.D. Comparisons of carmustine, procarbazine, and high-dose methylprednisolone as additions to surgery and radiotherapy for the treatment of malignant glioma. Cancer Treat. Rep., *67* : 121-132, 1983.

119) Chang, C.H., Horton, J., Schoenfeld, D., Salazar, O., Perez-tamato, R., Kramer, S., Weinstein, A., Nelson, J.S., and Tsukada, Y. Comparison of postoperative radiotherapy and combined postoperative radiotherapy and chemotherapy in the multidisciplinary management of malignant gliomas. Cancer, *52* : 997-1007.

120) Steel, G.G. The Growth Kinetics of Tumours. Oxford University Press, Oxford, 1977.

121) Wodinsky, I., Kensler, C.J., and Venditti, J.M. Comparative kinetics and chemotherapy of the slow growing B16 melanoma and the fast growing L1210 leukemia. Proc. Am. Assoc. Cancer Res., *13* : 8, 1972.

122) O.D. Laerum, D.D. Bigner, and M.F. Rajewski (eds.), Biology of Brain Tumours, pp. 27-37. Geneva : UICC Technical Report Series 26, 1978.

123) O.D. Laerum, D.D. Bigner, and M.F. Rajewski (eds.), Biology of Brain Tumours, pp. 185-199. Geneva : UICC Technical Report Series 26, 1978.

124) Zimmerman, H.M., and Arnold, H. Experimental brain tumors. I. Tumors produced with methylcholanthrene. Cancer Res., *1* : 919-938, 1941.

125) Seligman, A.M., and Shear, M.J. Studies in Carcinogenesis. VIII. Experimental production of brain tumors in mice with methylcholanthrene. Am. J. Cancer, *37* : 364-395, 1939.

126) Rubinstein, L.J. Correlation of animal brain tumor models with human neuro-oncology. Nat. Cancer Inst. Monogr., *46* : 43-49, 1977.

127) Walker, M.D. Oncology of the Nervous System, p. 34. Boston: Martinus Nijhoff Publ., 1983.

128) Shapiro, W.R. Chemotherapy of brain tumors : results in an experimental murine glioma. *In* : Models of Human Neurological Diseases, H.L. Klawans (ed.), Excerpta Medica, Amsterdam, pp. 121-143, 1974.

129) Sugiura, K. Tumor transplantation. *In* : Gay Wi (ed.), Methods of Animal Experimentation , vol.2, pp. 171-222. New York: Academic Press, 1965.

130) Tator, C.H. Chemotherapy of brain tumors. Uptake of tritiated methotrexate by a transplantable intracerebral ependymoblastoma in mice. J. Neurosurg., *37* : 1., 1972.

131) Laerum, O.D., Bigner, D.D., and Rajeski, M.F. (eds.), Biology of Brain Tumours p. 196. Geneva : UICC Technical Report Series 26, 1978.

132) Shapiro, W.R., Ausman, J.I., and Rall, D.P. Studies on the chemotherapy of experimental brain tumors : evaluation of 1,3-bis(2-chloroethyl)-1-nitrosourea, cyclophosphamide, mithramycin, and methotrexate. Cancer Res., *30* : 2401-2413, 1970.

133) Geran, R.I., Congleton, G.F., Dudeck, L.E., Abbott, B.J., and Gargus, J.L. A mouse ependymoblastoma as an experimental model for screeningpotential antineoplastic drugs. Cancer Chemother. Rep. Part 2, *4* : 53-87, 1974.

134) Hasegawa, H., Shapiro, W.R., Posner, J.B., and Basler, G. Effect of 1-(4-amino-2-methyl-5-pyrimidinyl) methyl-3-(2-chloroethyl)-3-nitrosourea hydrochloride on experimental brain tumors. Cancer Res., *39* : 2687-2690, 1979.

135) Shapiro, W.R. Studies on the chemotherapy of experimental brain tumors : evaluation of 1-(2-chloroethyl)-3-cyclohexyl-1-nitrosourea, vincristine, and 5-fluorouracil. J. Natl Cancer Inst., *46* : 359-368, 1971.

136) Shapiro, W.R. The chemotherapy of intracerebral vs. subcutaneous murine gliomas : a comparative study of the effect of VM-26. Arch. Neurol., *30* : 222-226, 1974.

137) Levin, V.A., Freeman-Dove, M.A., and Maroten, C.E. Dianhydrogalactitol (NSC-13213) : pharmacokinetics in normal and tumor-bearing rat brain and antitumor activity against three intracerebral rodent tumors. J. Natl. Cancer Inst., *56* : 535, 1976.

138) Laerum, O.D., Bigner, D.D., and Rajewski, M.F. (eds.), Biology of Brain Tumours, p. 194. Geneva : UICC Technical Report , Series 26, 1978.

139) Kumanishi, T. Brain tumors induced with Rous sarcoma virus, Schmidt-Ruppin strain. I. Induction of brain tumors in adult mice with Rous chicken sarcoma cells. Jap. J. Exp. Med., *37* : 461, 1967.

140) Wilfgong, R.F., Bigner, D.D., and Wechsler, W. Susceptibility of inbred Fischer rats to brain tumor induction by Rous sarcoma virus. Naturwissen-schaften, *59* : 371, 1972.

141) Wilfgong, R.F., Bigner, D.D., Self, D.J., and Wechsler, W. Brain Tumor types induced by the Schmidt-Ruppin strain of Rous sarcoma virus in inbred Fischer rats. Acta. Neuropathol. Berl., *25* : 196, 1973.

142) Rabotti, G.F., and Raine, W.A. Brain tumors induced in hamsters inoculated intracerebrally at birth with Rous sarcoma virus. Nature, *204* : 898, 1964.

143) Rabotti, G.F., Sellers, R.L., and Anderson, W.R. Leptomeningeal sarcomata and gliomata induced in rabbits by Rous sarcoma virus. Nature, *209* : 524, 1966.

144) Ahlstrom, C.G., Olin, T., and Smitterberg, B. Intracranial tumors induced in guinea pigs with Rous sarcoma virus. Acta Path. Microbiol. Scand. Sect-A82, p. 326, 1974.

145) Deinhardt, F., Wolfe, L., Northrop, R., Marczynska, B., Ogden, J., McDonald, R., Falk, L., Sharmek, G., Smith, R., and Deinhardt, J. Induction of neoplasms by viruses in marmoset monkeys. J. Med. Primatol., *1* : 29, 1972.

146) Ikuta, F., and Kumanishi, T. Experimental virus-induced brain tumors. Prog. Neuropathol., *11* : 253, 1973.

147) Grove, A.S., di Chiro, G., and Rabotti, G.F. Experimental brain tumors with a report of those induced in dogs by Rous sarcoma virus. J. Neurosurg., *26* : 465, 1967.

148) Bigner, D.D., Odom, G.L., Mahaley, M.S., Jr. and Day E.D. Brain tumors induced in dogs by the Schmidt-Ruppin strain of Rous sarcoma virus. Neuropathological and immunological observations. J. Neuropathol. Exp. Neurol., *28* : 648, 1969.

149) Janisch, W., and Schreiber, D. Experimentelle Geschwulste des Zentral-Nervensystems. Fischer, Jena, 1968.

150) Copeland, D.D., Vogel, F.S., and Bigner, D.D. The induction of intracranial neoplasms by the inoculation of avian sarcoma virus in perinatal and adult rats. J. Neuropathol. Exp. Neurol., *34* : 340, 1975.

151) Bigner, D.D., Kvedar, J.P., Shaffer, T.C. Vick, N.A., Engel, W.K., and Day, E.D. Factors influencing the cell type of brain tumors induced in dogs by Schmidt Ruppin Rous sarcoma virus. J. Neuropath. Exp. Neurol., *31*: 583,595, 1972.

152) Bigner, D.D., Pegram, C.N., Vick, N.A., Copeland, D.D., and Swenberg, J.A. Characterization of the avian sarcoma virus induced mammalian brain tumors model for immunologic and chemotherapeutic studies. VIIth International Congress of Neuropathology. Excerpta Medica, Amsterdam, pp. 445-451, 1975.

153) Bigner, D.D., Vick, N.A., Kvedar, J.P., Mahaley, M.S. Jr., and Day, E.D. Virus-cell relationship in dog brain tumors induced with Schmidt-Ruppin Rous Sarcoma virus. Progr. Exp. Tumor Res., *17* : 40-58, 1972.

154) Roszman, T.L., Brooks, W.H., Markesbery, W.R., and Bigner, D.D. General immunocompetence of rats bearing avian sarcoma virus-induced intracranial tumors. Cancer Res., *38* : 74-77, 1978.

155) Mahaley, M.S.Jr., Gentry, R.E., and Bigner, D.D. Immunobiology of primary intracranial tumors. Part 2 : The evaluation of chemotherapy and immunotherapy protocols using the avian sarcoma virus glioma model. J. Neurosurg., *47* : 35-43, 1977.

156) Mahaley, M.S. Jr., Steinbok, P., Aronin, P. Dudka, L., and Zinn, D. Immunobiology of primary intracranial tumors. Part 4 : Levamisole as an immunostimulant in patients and in the ASV glioma model. J. Neurosurg., *54* : 220-227, 1981.

157) Steinbok, P., Mahaley, M.S. Jr., U.R., Zinn, D.C., Lipper, S., Mahaley, J.L., and Bigner, D.D. Synergism between BCNU and irradiation in the treatment of anaplastic gliomas : an in-vivo study using the avian sarcoma virus-induced glioma model. J. Neurosurg., *51* : 581-586, 1979.

158) Bigner, D.D., and Swenberg, J.A. (eds). Janish and Schreiber's Experimental Tumors of the Central Nervous System, p. 112. Kalamazoo: Upjohn, 1977.

159) Bigner, D.D., and Swenberg, J.A. (eds). Janish and Schreiber's Experimental Tumors of the Central Nervous System, p. 112. Kalamazoo: Upjohn, 1977.

160) Green, S.B., Byar, D.P., and Walker, M.D. Comparisons of carmustine, procarbazine, and radiotherapy for the treatment of malignant glioma. Cancer Treat. Rep., *67* : 121-132, 1983.

161) Fraser, H. Astrocytomas in an inbred mouse strain. J. Path., *102* : 266, 1971.

162) Fraser, H., and McConnell, I. Experimental brain tumors. Lancet *1* : 44, 1975.

163) Benda, P., Someda, K., Messer, J., and Sweet, W.H. Morphological and immunochemical studies of rat glial tumors and clonal strains propagated in culture. J. Neurosurg., *34* : 310, 1971.

164) Barker, M., Hoshino, T., Gurcay, O., Wilson, C.B., Nielsen, S.L., Downie, R., and Eliason, J. Development of a brain tumor animal model and its response to 1,2,bis-(2-chlorethyl)1-nitrosourea. Cancer Res., *33* : 976, 1973.

165) Wheeler, K.T., Barker, M., Wallen, C.A., Kimler, B.F., and Henderson, S.D. Evaluation of 9L as a brain tumor model. *In* : Sridner, R., Marcel Dekker, (eds.), Methods in Tumor Biology : Tissue Culture and Animal Tumor Models, New York (in press).

166) Laerum, O.D., Bigner, D.D., and Rajewski, M.F., (eds.), Biology of Brain Tumours, pp. 27-33. Geneva : UICC Technical Report Series 26, 1978.

167) Rosenblum, M.L., Knebel, K.D., Vasques, D.A., and Wilson, C.B. In-vivo clonogenic tumor cell kinetics following BCNU brain tumour therapy. Cancer Res., *36* : 3718, 1976.

168) Levin, V.A., and Kabra, P. Effectiveness of the nitrosoureas as a function of their lipid solubility in the chemotherapy of experimental rat brain tumors. Cancer Chemother. Rep., *58* : 787-792, 1974.

169) Tel, E., Barker, M., Levin, V.A., and Wilson, C.B. Effect of combined surgery and BCNU (NSC-409962) on an animal brain tumor model. Cancer Chemother. Rep., *58* : 627-631, 1974.

170) Leith, J.T., Schilling, W.A., and Wheeler, K.T. Cellular radiosensitivity of a rat brain tumor. Cancer, *35* : 545-1550, 1975.

171) Barker, M., Deen, D.F., and Baker, D.G. BCNU and x-ray therapy of intracerebral 9L rat tumors. Int. J. Radiat. Oncol. Biol. Phys., *5* : 1581-1583, 1979.

172) Wheeler, K.T., Kaufman, K., and Feldstein, M. Response of a rat brain tumor to fractionated therapy with low doses of BCNU and irradiation. Int. J. Radiat. Oncol. Biol. Phys., *5* : 1553-1557, 1979.

173) Wheeler, K.T., Deen, D.F., Wilson, C.B., Williams, M.E., and Sheppard, S. BCNU-modification of the in-vitro radiation response in 9L brain tumor cells of rats. Int. J. Radiat. Oncol. Biol. Phys., *2* : 79-88, 1977.

174) Vick, N., Khandekar, J.D., and Bigner, D.D. Chemotherapy of brain tumors - the blood brain barrier is not a factor. Arch. Neurol., *34* : 523, 1977.

175) Walker, M.D. Oncology of the Nervous System, p 39. Boston : Martinus Nijhoff Publ., 1983.

176) Benda, P., Lighbody, J., Sato, G., Levine, L., and Sweet, W. Differentiated rat glial cell strain in tissue culture. Science, *161*: 370, 1968.

177) Day, E.D., and Bigner, D.D. Specificity, cross-reactivity, and affinity of I-labelled antiglioma antibodies for monolayers of cultured glioma cells.Cancer Res., *33* : 2362, 1973.

178) Denlinger, R.H., Axler, D.A., and Koestner, A. Tumor-specific transplantation immunity to intracerebral challenge with cells from a methylnitrosourea induced brain tumour. J. Med., *6* : 249, 1975.

179) Ko, L., Koestner, A., and Wechsler, W. Characterization of cell cycle and biological parameters of transplantable glioma cell lines and clones. Acta Neuropath., *51* : 107-111, 1980.

180) Koestner, A., Swenberg, J.A., and Wechsler, W. Transplacental production of neoplasms of the nervous system in Sprague-Dawley rats with ethylnitrosourea. Am. J. Path., *63* : 37-56, 1971.

181) Ko, L., Koestner, A., and Wechsler, W. Morphological Characterization of Nitrosourea-induced Glioma Cell Lines and Clones. Acta Neuropath., *51* : 23-31, 1980.

182) Weizsacker, M. et al. Radiation and Drug Response of the Rat Glioma RG2.Eur. J. Cancer, *18* : 891-5, 1982.

183) Krajewski, S., Kiwit, J., and Wechsler, W. RG2 glioma growth in rat cerebellum after subdural implantation. J. Neurosurg., *65* : 222-9, 1986.

184) Groothuis, D.R. et al. Regional Measurements of Blood Flow in Experimental RG2 Rat Gliomas. Cancer Res., *43* : 3362-3367, 1983.

185) Groothuis, D.R. et al. Regional Measurements of Blood-to-Tissue Transport in Experimental RG2 Rat Gliomas. Cancer Res., *43* : 3368-3373, 1983.

186) Wechsler, W., Ramadan, M.A. and Giester, A. Isogenic transplantation of ethylnitrosourea-induced tumors of the central and peripheral nervous system in two different inbred rat strains. Naturwiss., *59* : 474, 1972.

187) Bigner, D.D. Proceedings of Neurologen (Abstract). Columbia, 1978.

188) Kuga, N., Seido, T., Oboshi, S., Yoshida, K., Koide, T., Shimasato, Y., and Nomura, T. Heterotransplantation of Cultured Human Cancer Cells and Human Cancer Tissues into Nude Mice. Gann, *66* : 547, 1975.

189) Rana, M.W., Pinkerton, H., Thornton, H., and Magy, D. Heterotransplantation of human glioblastoma multiforme and meningioma to 'nude' mice. Proc. Soc. exp. Biol. Med., *155* : 85, 1977.

190) Fogh, J., Fogh, J., and Orfeo, T. 127 cultured human tumor cell lines producing tumors in 'nude' mice. J. Natl Cancer Inst., *59* : 221, 1977.

191) Bullard, D.E., Kramer, R.S., and Bigner, D.D. Primary explantation of central nervous system tumors into the athymic 'nude' mouse model. Neurosurgery, *3* : 416, 1978.

192) Shapiro, W.R., Baster, G.A., Chernik, N.L., and Posner, J.B. Human brain tumor transplanted into 'nude' mice. J. Natl Cancer Inst., *62* : 447, 1979.

193) Reid, L.C.M., and Shin, S. Transplantation of heterologous endocrine tumor cells in 'nude' mice. *In* : Fogh, J., and Giovanella, B.C., (eds.), The Nude Mouse in Experimental and Clinical Research, p 313. New York : Academic Press, 1978.

194) Schold, S.C., Jr., Bullard, D.E., Bigner, S.H., Jones T.R., and Bigner, D.D. Growth, morphology, and serial transplantation of anaplastic human gliomas in athymic mice. J. Neuro-Oncology, *1*(1) : 5-14, 1983.

195) Bigner, S.H. et al. Relationship of in-vitro morphologic and growth characteristics of established human glioma - derived lines to their immunogenicity in athymic nude mice. J. Neuropath. and Ex. Neurol., *40* : 390-409, 1981.

196) Shapiro, W.R., Basler, G.A., Chernik, N.L., and Posner, J.B. Human brain tumor transplantation into nude mice. J. Natl Cancer Inst., *62* : 447-453, 1979.

197) Shapiro, W.R., and Basler, G.A. Chemotherapy of human brain tumors transplanted into nude mice. *In* : Paoletti, P., Walker, M.D., Butti, G., and Knerich, R. (eds.), Multidisciplinary Aspects of Brain Tumor Therapy, pp. 309-316. Elsevier: North Holland, Amsterdam, 1979.

198) Houchens, D.P., Ojevera, A.A., and Riblet, S.M. Human brain tumor xenografts in nude mice as a chemotherapy and/or immunotherapy model. Eur. J. Cancer. Clin. Onc., *19:* 799-805, 1983.

199) Slagel, D.E., Feola, J., Houchens, D.P., and Ovejera, A.A. Combined modality treatment using radiation and/or chemotherapy in an athymic (nude) mouse-human medulloblastoma and glioblastoma xenograft model. Cancer Research, *42* : 812-816, 1982.

200) Bullard, D.E., Schold, S.C. Jr., Bigner, S.H., and Bigner, D.D. Growth and chemotherapeutic response in athymic mice of tumors arising from glioma-derived cell lines. J. Neuropath. Exp. Neurol., *40* : 410-427, 1981.

201) Bradley, N.J., Bloom, H.J.G., Davies, A.J.A., and Swift, S.M. Growth of human gliomas in immune-deficient mice. Br. J. Cancer, *2* : 263, 1978.

202) Saris, S.C., Bigner, S.H., and Bigner, D.D. Intracerebral transplantation of a human glioma line in immunosuppressed rats. J. Neurosurg., *60* : 582-588, 1984.

203) Walker, M.D., Thomas, D.G.T. (eds.), Biology of Brain Tumors, pp. 97-105. Boston : Maretinus Nijhoff Publ., 1986.

204) Borel, J.F., Feurer, C., Gubler, H.U., and Stahelin, H. Biological effects of cyclosporin A : A new antilymphocytic agent. Agent Actions, *6* : 468-475, 1976.

205) Britton, S., and Palacios, R. Cyclosporin A - usefulness, risks and mechanism of action. Immunol. Rev., *65* : 5-22, 1982.

206) Serano, R.D., Pegram, C.N., Fraser, H., Dickerson, A.G., and Bigner, D.D.Established tumorigenic cell lines from a spontaneous murine (VM/Dk) astrocytoma (SMA). J. Neuropath. Exp. Neurol., *37* : 689, 1978.

207) Saris, S.C., and Bigner, D.D. Experimental neuro-oncology . *In* : A. Crockard, R. Hayward, and J.T.Hoff (eds.), Neurosurgery: The Scientific Basis of Clinical Practice, pp. 392-416. Oxford: Blackwell Scientific Publications, 1985.

208) Hossmann, K.A., Szymas, J., Seo, K., Assheuer, J., and Krajowski, S. Experimental transplantation gliomas in the adult cat brain. II: pathophysiology and magnetic resonance imaging. Acta Neurochir. (Wien), *98* : 189-200, 1989.

209) Linn, F., Seo, K., and Hossmann, K. A. Experimental transplantation gliomas in the adult cat brain. III: regional biochemistry. Acta Neurochir. (Wien), *99* : 85-93, 1989.

210) Lazareff, J.A., Boisvert, D.P.J., and Allen, P.S. Effect of Mannitol on In-vivo Transverse Relaxation Rates in Edematous Peritumor Brain Tissue. In : Society of Magnetic Resonance in Medicine (Book of Abstracts, Sixth Annual Meeeting and Exhibition), vol.1, p 48, 1987.

211) Mathiesen, T., Collins, V.P., Olson, L., and Granholm, L. Prolonged survival and vascularization of xenografted human glioblastoma cells in the central nervous system of Cyclosporin A treated rats. Cancer Letters, *44* :151-156, 1989.

212) Riccardi, V.M., Von Recklinghausen neurofibromatosis. N. Engl. J. Med., *305* : 1617-1627, 1981.

213) Riccardi, V.M., and Mulvihill, J.J. (eds.). Neurofibromatosis (von Recklinghausen disease): Genetics, Cell Biology, And Biochemistry. New York: Raven, 1981.

214) Todd, D.W., Christoferson, L.A., Leech, R.W., and Rudolf, L. A family affected with intestinal polyposis and gliomas. Ann. Neurol., *10* : 390-392, 1981.

215) Naguib, M.G., Sung, J.H., Erickson, D.L., Gold, L.H.A., and Seljeskog, E.L. Central nervous system involvement in the nevoid basal cell carcinoma syndrome: Case report and review of the literature. Neurosurgery, *11* :52-56, 1982.

216) Gomez. M.R. (ed.). Tuberous Sclerosis. New York: Raven, 1979.

217) Wallace, M.R., Marchuk, D. A., Andersen, L.B., Letcher, R., Odeh, H.M., Sauling, A.M., Fountain, J. W., Brereton, A., Nicholson, J., Mitchell, A.L., Brownstein, B.H., and Collins, F.S. Neurofibromatosis gene: identification of a large transcript disrupted in three NF1 patients. Science, *249* : 181-186, 1990.

218) Alberto, M.J., and Roses, A.D. Advances in molecular genetics in relation to neurogenetic diseases. *In* : R.H. Wilkins , and S.S. Rengachary (eds.), Neurosurgery Update I: Diagnosis, Operative Techniques and Neuro-Oncology, pp. 219-225. New York: McGraw-Hill, Inc., 1990.

219) I.R.Wanless, Dept. of Pathology, University of Toronto, personal communication, 1990.

220) Van der Wiel, H.J. Inheritance of Glioma. New York: Elsevier, 1960.

221) Modan, B., Baidatz, D., Mart, H., Steinitz, R., and Levin, S.G. Radiation-induced head and neck tumours. Lancet, *1* : 277-279, 1974.

222) Shore, R.E., Albert, R.E., and Pasternack, B.S. Follow-up study of patients treated by X-ray epilation for tinea capitis: Resurvey of post-treatment illness and mortality experience. Arch. Environ. Health, *31* : 21-28, 1976.

223) Schreier, H.A., Sherry, N., and Shaughnessy, E. Lead poisoning and brain tumors in children : a report of 2 cases. Ann. Neurol., *1* : 599-600, 1977.

224) Mancuso, T.F. Tumors of the central nervous system: Industrial considerations. Acta Unio. Internat. Contra. Cancrum., *19* : 488-489, 1963.

225) Gold, E., Gordis, L., Tanascia, J., and Szkio, M. Risk factors for brain tumors in children. Am. J. Epidemiol., *109* : 309-319, 1979.

226) Gold, E., Gordis, L., Tanascia, J., and Szklo, M. Increased risk of brain tumors in children exposed to barbituates. J. Natl. Cancer Inst., *61* : 1031-1034, 1978.

227) Reagan, T.J., and Freiman, I.S. Multiple cerebral gliomas in multiple sclerosis. J. Neurol. Neurosurg. Psychiatry, *36* : 523-528, 1973.

228) Aronson, S.M., and Aronson, B.E. Central nervous sustem in diabetes mellitus: Lowered frequency of certain intracranial neoplasms. Arch. Neurol., *12* : 390-398, 1965.

229) Buckwalter, J.A., Turner, J.H., Gamber, H.H., Raterman K., Soper, R.T., and Knowler, L.A. Psychoses, intracranial neoplasms, and genetics. Arch. Neurol. Psychiat., *81* : 480-485, 1959.

230) Band, P.R., Spinelli, J.J., Ng, Z.T.Y., Moody, J., and Gallagher, R.P. Mortality and cancer incidence in a cohort of commercial airline pilots. Aviat. Environ. Med., *61* : 299-302, 1990.

231) Waxweiler, R.J., Stringer, W., Wagoner, J.K., Jones, J., Falk, H., and Carter, C. Neoplastic risk among workers exposed to vinyl chloride. Ann. NY. Acad. Sci., *271* : 40-48, 1976.

232) Theriault, G., and Goulet, L. A mortality study of oil refinery workers. J. Occup. Med., *21* : 367-370, 1979.

233) Environmntal Protection Agency Preliminary Report. Due for release - August 1, 1990

234) Choi, N.W., Schuman, L.M., and Gullen, W.H. Epidemiology of primary central nervous system neoplasms: II. Case-control study. Am. J. Epidemiol., *91* : 467-485, 1970.

235) Preston-Martin, S. Abstract: A case-controlled study of intracranial meningiomas in women. Am. J. Epidemiol., *108* : 233-234, 1978.

236) Annegers, J.F., Coulam, C.B., Abboud, C.F., Laws, E.R., Jr., and Kurland, L.T. Pituitary adenoma in Olmsted County, Minnesota, 1935-1977; a report of an increasing incidence of diagnosis in women of childbearing age. Mayo Clin. Proc., *53* : 641-643, 1978.

237) Thomas. D.G.T., and Graham, D.I. (eds.), Brain Tumours: Scientific Basis, Clinical Investigation and Current Therapy, p. 146. London: Butterworths, 1980.

238) Allen N. Oxidative metabolism of brain tumors. *In* : Progr. Exp. Tumor Res., vol. 17, pp. 192-209. Basel: Karger, 1972.

239) Galarraga, J., Loreck, D.J., Graham, J.F., DeLaPaz, R.L., Smith, B.H., Hallgren, D., and Cummins, C.J. Glucose metabolism in human gliomas: Correspondence of *In Situ* and *In Vitro* metabolic rates and altered energy metabolism. Metabolic Brain Disease, *1* : 279-291, 1986.

240) Mc Ilwain, H. Biochemistry of the Central Nervous System, 2nd ed., p. 67. London: Churchill, 1959.

241) Heller, I., and Elliott, K.A.C. The metabolism of normal brain and human gliomas in relation to cell type and density. Canad. J. Biochem. Physiol., *33* : 395-403, 1955.

242) Victor, J.V., and Wolf, A. Metabolism of brain tumors. Res. Publ. Ass. Res. Nerv. and Ment. Dis., *16* : 44-58, 1937.

243) Warburg, O. The Metabolism of Tumors. London: Constable and Co., 1930.

244) Allen, N. Cytochrome oxidase in human brain tumors. J. Neurochem., *2* : 37, 1957.

245) Viale, F.L. Biochemical patterns in brain tumors, II. Enzymes of the tricarboxylic acid cycle, Acta Neurochir., *20* : 273-279, 1969.

246) Lowry, O.H., Berger, S.J., Carter, J.G., Chi, M.M.-Y., Manchester, J.K., Knor, J., and Pusateri, M.E. Diversity of metabolic patterns in human brain tumors: Enzymes of energy metabolism and related metabolites and cofactors. J. Neurochem., *41* : 994-1010, 1983.

247) Marzatico, F., Curti, D., Dagani, F., Silvani, V., Gaetani, P., Butti, G., and Knerich, R. Enzymes related to energy metabolism in human gliomas. J. Neurosurg. Sci., *30* : 129-132, 1986.

248) Mangiardi, J.R., and Yodice, P. Metabolism of the malignant astrocytoma. Neurosurgery, *26* : 1-19, 1990.

249) Viale, G.L., and Ibba, F. Histochemische Untersuchungen uber die Phosphorylasen in Hirngerschwulsten. Acta Neurochir. (Wien), *12* : 475, 1964.

250) Lowry, O.H., and Passonneau, J.V. The relationships between substrates and enzymes of glycolysis in brain. J. Bio. Chem., *239* : 31, 1964.

251) Lehrer, G.M. The quantitative histochemistry of human glial tumors. *In* : H. Jacob, (ed.), Proc. IV. International Congress of Neuropathology , vol. 1, p.66. Stuttgart: G. Thieme, Verlag, 1962.

252) Gonzalez, C., Ureta, T., Sanchez, R., and Niemeyer, H. Multiple molecular forms of ATP: hexose 6-phosphotranspherase from rat liver. Biochem. Biophys. Res. Commun., *16* : 347, 1964. _

253) Katzen, H.M. The multiple forms of mammalian hexokinase and their significance to the action of insulin. Adv. Enzyme Regul., *5* : 335, 1967.

254) Bennett, M.J., Timperley, W. R., Taylor, C.B., and Hill, A.S. Isoenzymes of hexokinase in the developing, normal and neoplastic human brain. Eur. J. Cancer, *14* : 189, 1978.

255) Scrutton, M.C., and Utter, M.F. Glycolysis and gluconeogenesis. Ann. Rev. Biochem., *37* : 249, 1968.

256) Bennett, M.J., Taylor, C.B., and Timperley, W.R. Electrophoretic study of phosphofructokinase isoenzymes from human tissues and tumours of the nervous system. Eur. J. Cancer, *11* : 359, 1975.

257) Wolleman, M. Biochemistry of brain tumours. *In* :Lajtha, A. (ed.), Handbook of Neurochemistry, vol.7, p. 515. New York: Plenum Press, 1971.

258) Tanaka, T., Imamura, K., Ann, T., and Taniuchi, K. Multimolecular forms of pyruvate kinase and phosphofructokinase in normal and cancer tissues. Gann Monogr. on Cancer Res., *13* : 219, 1972.

259) Lehninger, A.L. Biochemistry (2nd ed.). pp. 450-452. New York: Worth Publishers, Inc., 1975.

260) Yu, A.C.H., Drejer, J., Hertz, L., and Schousboe, A. Pyruvate carboxylase activity in primary cultures of astrocytes and neurons. J. Neurochem., *41*: 1484-1487, 1983.

261) Corridori, F., Cremona, T., and Tagliabue, G.J. Glutamicoxaloacetic transaminase and lactic dehydrogenase activities on brain tumour homogenates. J. Neurochem., *6* : 142, 1960.

262) Sherwin, A.L., Leblanc, F. E., and McCann, W.P. Altered LDH isoenzymes in brain tumours. Arch. Neurol., *18* : 311, 1968.

263) O'Connor, J.S., and Laws, E. R. Histochemical survey of brain tumor enzymes. Arch. Neurol., *9* : 91, 1963.

264) Paxton, H.D. Quantitatve histochemistry of brain tumors and analogous normal tissue. Neurol., *9* : 367, 1959.

265) Loreck, D.J., Cummings, C.J., Van der Freen, J., Galarraga, J., Phang, J.M., and Smith, B.H. Regulation of the pentose phosphate pathway on human astrocytes and gliomas. Metab. Brain Dis., *2* : 31-46, 1987.

266) Hertz, L., Murthy, Ch. R.K., and Schousboe, A. Metabolism of glutamate and related amino acids. *In* : Norenberg, M.D., Hertz, L., and Schousboe, A. (eds.), The Biochemical Pathology of Astrocytes : Neurology and Neurobiology, Vol. 39, Chan-Palay, V., and Palay, S.L., (eds.). pp. 395-406. New York: Alan R. Liss, Inc., 1988.

267) Schousboe, A., Larsson, O.M., Krogsgaard-Larsen, P., Drejer, J., and Hertz, L. Uptake and release processes for neurotransmitter amino acids in astrocytes. *In* : Norenberg, M.D., Hertz, L., and Schousboe, A. (eds.), The Biochemical Pathology of Astrocytes : Neurology and Neurobiology, Vol. 39, Chan-Palay, V., and Palay, S.L., (eds.). pp. 381-394. New York: Alan R. Liss, Inc., 1988.

268) Drejer, J., Larsson, O.M., and Schousboe, A. Characterization of uptake and release processes for D- and L-aspartate in primary cultures of astrocytes and cerebellar granule cells. Neurochem. Res., *8* : 231-243, 1983.

269) Drejer, J., Larsson, O.M., and Schousboe, A. Characteriztion of L-glutamate uptake into and release from astrocytes and neurons cultured from different brain regions. Exp. Brain Res., *47* : 259-269, 1982.

270) Schousboe, A., Svenneby, G., and Hertz, L. Uptake and metabolism of glutamate in astrocytes cultured from dissociated mouse brain hemispheres. J. Neurochem., *29* : 999-1005, 1977.

271) Balcar, V.J., Schousboe, A., Spoerri, P.E., Wolff, J.R. Differences between substrate specificities of L-glutamate uptake by neurons and glia, studied in cell lines and primary cultures. Neurochem. Int., *10* : 213-217,1987.

272) Hansson, E. Accumulation of putative amino acid neurotransmitter monoamines and d-Ala^2 -Met -enkephalinamide in primary astroglial cultures from various brain areas, visualized by autoradiography . Brain Res., *289* : 189-196, 1983.

273) Hansson, E. Co-cultivation of astroglial enriched cultures from striatum and neuronal containing cultures from substantia nigra. Life Sci., *39* : 269-277, 1986.

274) Snodgrass, S.R., and Iversen, L.L. Amino acid uptake into human tumors. Brain Res., *76* : 95-107, 1974.

275) Drejer, J., Benveniste, H., Diemer, N.H., and Schousboe, A. The cellular origin of ischemia-induced glutamate released from brain tissue in vivo and in vitro . J. Neurochem., *45* : 145-151,1985.

276) Yu, A.C.H., Schousboe, A., and Hertz, L. Influence of pathological concentrations of ammonia on metabolic fate of ^{14}C-labelled glutamate in astrocytes in primary cultures. J. Neurochem., *42* : 594-597, 1984.

277) Norenberg, M.D., and Martinez-Hernandez, A. Fine structural localization of glutamine synthetase in astrocytes of rat brain. Brain Res., 161 : 303-310, 1979.

278) Schousboe, A., Fosmark, H., and Hertz, L. High content of glutamate and of ATP in astrocytes cultured from rat brain hemispheres: Effect of serum withdrawal and cyclic AMP. J. Neurochem., *25* : 909-911, 1975.

279) Patel, A.J. and Hunt, A. Concentration of free amino acids in primary cultures of neurons and astrocytes. J. Neurochem., *44* : 1816-1821, 1985.

280) Saito, K., Barber, R., Wu, J.-Y., Matsuda, T., Roberts, E., and Vaughn, J.E. Immunohistochemical localization of glutamic acid decarboxylase in rat cerebellum. PNAS USA, *71* : 269, 1974.

281) Nicklas, W.J. Amino acid metabolism in glial cells: homeostatic regulation of intra- and extracellular milieu by C-6 glioma cells. J. Neurochem., *30* : 955-963, 1978.

282) Dranoff, G., Elion, G.B., Friedman, H.S., Campbell, G.L., and Bigner, D.D. Influence of glutamine on the growth of human glioma and medulloblastoma in culture. Cancer Res., *45* : 4077-4081, 1985.

283) Wollemann, M., and Devenyi, T. The GABA content and glutamate decarboxylase activity of brain tumors. J. Neurochem., *10* : 83, 1963.

284) Rubinstein, L.J., and Sutton, C.H. Histochemical observation on oxidative enzyme activity in tumors of the nervous system. J. Neuropath. Exper. Neurol., *23* : 196, 1964.

285) Hussain, M.M., and Vassilis, I.Z. Characterization of glutamate dehydrogenase isoproteins purified from the cerebellun of normal subjects and patients with degenerative neurological disorders, and from human neoplastic cell lines. J. Biol. Chem., *264* : 20730-20735, 1989.

286) MacIntosh, F.C., and Oborin, P.E. Release of acetylcholine from intact cerebral cortex (Abstr). *In* : Abstracts of the XIX International Physiology Congress, pp. 580-581, 1953.

287) Gaddum, J.H. Push-pull cannulae. J. Physiol. (Lond.), *155* : 1P, 1961.

288) Kessler, M., Clark, J.L., Lubbers, D.W., Silver, J.A., and Simon, W. Ion and Enzyme Electrodes in Biology and Medicine. Baltimore: University Park Press, 1976.

289) Buck, R.P. Ion selective electrodes. Anal. Chem., *50* : 17R-29R, 1978.

290) Marsden, C.A., Brazeli, M.P., and Maidment, N.T. In vivo voltammetry-direct monitoring, an introduction to in vivo electrochemistry. *In* : C.A. Marsden (ed.), Measurement of Neurotransmitter Release In Vivo, pp. 127-153. New York: Wiley and Sons, 1984.

291) Bito, L., Davson, H., Levin, E., Murray, M., and Snider, N. The concentrations of free amino acids and other electrolytes in cerebrospinal fluid, in vivo dialysate of brain, and blood plasma of the dog. J. Neurochem., *13* : 1057-1067, 1966.

292) Benveniste, H., and Diemer, N.H. Cellular reactions to implantation of a microdialysis tube in the rat hippocampus. Acta Neuropathol. (Berl.), 74 : 234-238, 1987.

293) Hamberger, A., Berthold, C.H., Karlsson, B., Lehmann, A., and Nystrom, B. Extracellular GABA, glutamate, and glutamine in vivo perfusion dialysis of the rabbit hippocampus. *In* : L. Hertz, E. Kvamme, E.G. McGeer, and A. Schousboe (eds.), Glutamine, Glutamate and GABA in the Central Nervous System, pp.473-492. New York: Alan R. Liss, 1983.

294) Sandberg, M. Manuscript in preparation, 1990.

295) Tossman, U., and Ungerstedt, U. Microdialysis in the study of extracellular levels of amino acids in the rat brain. ACTA Physiol. Scand., 128 : 9-14, 1986.

296) Benveniste, H., Drejer, J., Schousboe, A., and Diemer, N.H. Elevation of the extracellular concentrations of glutamate and aspartate in rat hippocampus during transient cerebral ischemia monitored by intracerebral microdialysis. J. Neurochem., 43 : 1369-1374, 1984.

297) Lazarewicz, J.W., Hagberg, H., and Hamberger, A. Extracellular calcium in the hippocampus of unanesthetized rabbits monitored with dialysis-perfusion. J. Neurosci. Methods, 15 : 317-328, 1986.

298) Ungerstedt, U., Herrera-Marchintz, M., Jungnelius, U., Stahle, L., Tossman, U., and Zetterstrom, T. Dopamine synaptic mechanisms reflected in studies conbining behavioural recordings and brain dialysis. *In* : M. Kotisaka (ed.), Advances in Dopamine Research, pp. 219-231. New York: Pergamon Press, 1982.

299) Zetterstrom, T., Vernet, L., Ungerstedt, U., Tossman, U., Jonzon, B., and Fredholm, B.B. Purine levels in the intact rat brain, studies with an implanted perfused hollow fibre. Neurosci. Lett., 29 : 111-115, 1982.

300) Benveniste, H., Drejer, J., Schousboe, A., and Diemer, N.H. Elevation of the extracellular concentrations of glutamate and aspartate in rat hippocampus during transient cerebral ischemia monitored by intracerebral microdialysis. J. Neurochem., *43* : 1369-1374, 1984.

301) Langlais, P.J., and Mair, R.G. Protective effects of the glutamate antagonist MK-801 on pyrithiamine-induced lesions and amino acid changes in rat brain. J. Neurosci., *10* : 1664-1674, 1990.

302) Hillered, L., Persson, L., Ponten, U., and Ungerstedt, U. Neurometabolic monitoring of the ischaemic human brain using microdialysis. Acta Neurochir. (Wien), *102* : 91-97, 1990.

303) Langen, K.J., Roosen, N., Herzog, H., Kuwert, T., Kiwit, J.C., Bock W.J., and Feinendegen, L.E. Investigations of brain tumours with 99Tcm-HMPAO SPECT. Nucl. Med. Commun., *10* : 325-332, 1989.

304) Black, K.L., Hawkins, R.A., Kim, K.T., Becker, D.P., Lerner, C., and Marciano, D. Use of thallium-201 SPECT to quantitate malignancy grade of gliomas. J. Neurosurg., *71* : 342-346, 1989.

305) Nishizawa, S., Tanada, S., Yonekura, Y., Fujita, T., Hukai, T., Saji, H., Fukuyama, H., Miyoshi, T., Harada, K., and Ishikawa, M.Regional dynamics of N-isopropyl-(^{123}I)p-iodoamphetamine in human brain. J. Nucl. Med., *30* : 150-156, 1989.

306) Araki, Y., and Yamada, H. Sequential study of glioblastoma with high uptake of N-isopropyl-p-(^{123}I)iodoamphetamine: a case report (Japanese). Kaku-Igaku., *26* : 523-527, 1989.

307) Cordes, M., Henkes, H., Eichstadt, H., Lefebre, C., Hosten, N., Langer, M., and Felix, R. Brain infarction: SPECT examination of regional cerebral blood flow (rCBF) and volume (rCBV) compared with gadolinium (Gd)-DTPA-enhanced MRI. *In* : M. Nadjmi (ed.), Imaging of Brain Metabolism Spine and Cord Intervention Neuroradiolgy Free Communications, pp. 27-30. Berlin: Springer-Verlag, 1989.

308) Watanabe, K., Hoshi, H., Jinnouchi, S., Yoshimura, H., and Nagamachi, S. Clinical cerebral perfusion scintigraphy with ^{123}I-IMP (Japanese). Rinsho-Hoshasen., *34* : 303-312, 1989.

309) Maier-Hauff, K., Gerlach, L., Baerwald, R., and Cordes, M. Cerebral blood flow measurements with HMPAO- and HIPDM-SPECT in brain tumors: basic rCBF studies. Psychiatry Res., *29* : 341-342,1989.

310) Biersack, H.J., Coenen, H.H., Stocklin, G., Reichmann, K., Bockisch, A., Oehr, P., Kashab, M., and Rollmann,O. Imaging of brain tumors with L-3-^{123}I-iodo-alpha-methyl tyrosine and SPECT. J. Nucl. Med., *30* : 110-112, 1989.

311) Front, D., Israel, O., Even-Sapir, E., Iosilevsky, G., Frenkel, A., Ben-Haim, S.. Ber, R., Robinson, E., and Kolodny, G.M. The concentration of bleomycin labeled with Co-57 in primary and metastatic tumors. Cancer, *64* : 988-993, 1989.

312) Behnke, J., Mach, J.P., Buchegger, F., Carrel, S., Delaloye, B., and de Tribolet, N. In-vivo localisation of radiolabelled monoclonal antibody in human gliomas. British J. Neurosurgery, *2*: 193-197, 1988.

313) Ordidge, R.J., Conelly, A., and Lohmann J.A.B. Image-selected In Vivo Spectroscopy (ISIS). A new technique for spatially selective NMR spectroscopy. J. Magn. Res., *66* : 283-294, 1986.

314) Frahm, J., Bruhn, H., Gyngell, M.L., Merboldt, K.D., Hanicke, W., and Sauter, R. Localized proton NMR spectroscopy in different regions of the human brain in vivo. Relaxation times and concentrations of cerebral metabolites. Mag. Res. Med., *11* : 47-63, 1989.

315) Felber, S., Sauter, R., and Loffler, W. Potentials of magnetic resonance spectroscopy in neuroradiology. *In* : M. Nadjmi (ed.), Imaging of Brain Metabolism Spine and Cord Intervention Neuroradiolgy Free Communications, pp. 19-25. Berlin: Springer-Verlag, 1989.

316) Frahm, J., Merboldt, K.D., Hanicke, W., and Villringer, A. Water-suppressed localized proton spectroscopy using stimulated echoes. *In* : Book of Abstracts, vol. 1, Society of Magnetic Resonance in Medicine (6th Annual Meeting and Exhibition), p.137. New York, 1987.

317) Barany, M., Venkatasubramanian, P.N., Dew, L.L., Glick, R.P., and Greenberg, I.M. Analysis of human brain tumors by proton magnetic resonance spectroscopy in vivo. *In* : Book of Abstracts, Society of Magnetic Resonance in Medicine, vol. 1, p. 429. Berkeley: Society of Magnetic Resonance in Medicine, 1989.

318) Heerschap, A., Luyten, P.R., Bernsen, H.J., van de Vlasakker, C., Prick, M.J.J., Meijer, E., Meyer, J., and den Hollander, J.A. Combined ^{1}H and ^{31}P NMR spectroscopic examination of human intracranial tumors at 1.5 tesla. *In* : Book of Abstracts, Society of Magnetic Resonance in Medicine, vol. 1, p. 430. Berkeley: Society of Magnetic Resonance in Medicine, 1989.

319) Felber, S., Sauter, R., and Aichner, F. Localized ^{1}H Spectroscopy applied to cerebral neoplasms and ischaemia at a clinical 1.5T MR-system. *In* : Book of Abstracts, Society of Magnetic Resonance in Medicine, vol. 1, p. 450. Berkeley: Society of Magnetic Resonance in Medicine, 1989.

320) Rothman, D.L., Howseman, A., Novotny, E.J., Hanstock, C.C., Lantos, G., Petroff, O.A.C., Prichard, J.W., and Shulman, R.G. Feasibility of proton-observe carbon-decouple editing of glutamate in the human brain. *In* : Book of Abstracts, Society of Magnetic Resonance in Medicine, vol. 1, p. 372. Berkeley: Society of Magnetic Resonance in Medicine, 1989.

321) Komoroski, R. A., Newton, J.E.O., Karson, C., Cardwell, D., Jagannathan, N.R., and Sprigg, J. Detection of psychoactive drugs in vivo in human brain using ^{19}F NMR spectroscopy. *In* : Book of Abstracts, Society of Magnetic Resonance in Medicine, vol. 1, p. 444. Berkeley: Society of Magnetic Resonance in Medicine, 1989.

322) Beaney, R.P. Positron emission tomography in the study of human tumors. Semin. Nucl. Med., *16* : 324-341, 1984.

323) Di Chiro, G. Positron emission tomography using (^{18}F)fluoro-deoxyglucose in brain tumors. Invest. Radiol., *22* : 360-371, 1987.

324) Tyler, J.L., Diksic, H., Villemure, J.-G., Evans, A.C., Meyer, E., Yamamoto, Y.L., and Feindel, W. Metabolic and hemodynamic evaluation of gliomas using positron emission tomography. J. Nucl. Med., *28* : 1123-1133, 1987.

325) Bergstrom, M., Ericson, K., Hagenfeldt, L., Mossken, M., von Holst, H., Norien, G., Ericksson, L., Ehrin, E., and Johnstriom, P. PET study of methionine accumulation in glioma and normal brain tissue: competition with branched chain amino acids . J. Assist. Tomogr., 11 : 208-213, 1987.

326) Lilja, A. PET in brain gliomas - biological and morphological aspects. *In* : M. Nadjmi (ed.), Imaging of Brain Metabolism Spine and Cord Intervention Neuroradiolgy Free Communications , pp. 35-38. Berlin: Springer-Verlag, 1989.

327) Lilja, A., Bergstrom, K., Hartvig, P., Spannare, B., Haldin, C., Lundqvist, H. and Langstrom, B. Dynamic study of supratentorial gliomas with L-methyl-^{11}C-methionine and positron emission tomography. AJNR, *6* : 505-514, 1985.

328) Rhodes, C.G., Wise, R.J.S., Gibbs, J.M., Frackowiak, R.S.J., Hatazawa, J., Palmer, A.J., Thomas, D.G.T., and Jones,T. In vivo disturbance of the oxidative metabolism of glucose in human cerebral gliomas. Ann. Neurol., *14* : 614-626, 1983.

329) Mosskin, M., von Holst, H., Bergstrom, M., Collins, V.P., Erikkson, L., Johnstrom, P., and Noren, G. Positron emission tomography with ^{11}C-methionine and computed tomography of intracranial tumours compared with histopathologic examination of multiple biopsies. Acta Radiol., *28* : 673-681, 1987.

330) Tovi, M., Tumour delineation with magnetic resonance imaging in gliomas. Acta Radiol. Suppl., *369* : 161-163,1986.

331) Hilbig, R., and Rahmann, H. Phylogeny of vertebrate brain gangliosides. Institute of Zoology, University of Stuttgart-Hohnenheim. *In:* Gangliosides and Modulation of Neuronal Functions, *H7:* 333-350. Berlin: Springer-Verlag, 1987.

326) Lilja, A. PET in brain gliomas - biological and morphological aspects. *In* : M. Nadjmi (ed.), Imaging of Brain Metabolism Spine and Cord Intervention Neuroradiolgy Free Communications , pp. 35-38. Berlin: Springer-Verlag, 1989.

327) Lilja, A., Bergstrom, K., Hartvig, P., Spannare, B., Haldin, C., Lundqvist, H. and Langstrom, B. Dynamic study of supratentorial gliomas with L-methyl-^{11}C-methionine and positron emission tomography. AJNR, *6* : 505-514, 1985.

328) Rhodes, C.G., Wise, R.J.S., Gibbs, J.M., Frackowiak, R.S.J., Hatazawa, J., Palmer, A.J., Thomas, D.G.T., and Jones,T. In vivo disturbance of the oxidative metabolism of glucose in human cerebral gliomas. Ann. Neurol., *14* : 614-626, 1983.

329) Mosskin, M., von Holst, H., Bergstrom, M., Collins, V.P., Erikkson, L., Johnstrom, P., and Noren, G. Positron emission tomography with ^{11}C-methionine and computed tomography of intracranial tumours compared with histopathologic examination of multiple biopsies. Acta Radiol., *28* : 673-681, 1987.

330) Tovi, M., Tumour delineation with magnetic resonance imaging in gliomas. Acta Radiol. Suppl., *369* : 161-163,1986.

331) Hilbig, R., and Rahmann, H. Phylogeny of vertebrate brain gangliosides. Institute of Zoology, University of Stuttgart-Hohnenheim. *In:* Gangliosides and Modulation of Neuronal Functions, *H7:* 333-350. Berlin: Springer-Verlag, 1987.

332) Suzuki, K. The pattern of mammalian brain gangliosides-III. Regional and developmental differences. J. Neurochem., *12:* 969-979, 1965.

333) Bremer, E.G., Hakomori, S.I. Gangliosides as receptor modulators. Adv. Exp. Med. Biol., *174:* 381-394, 1984.

334) Rahmann, H. Possible function of brain gangliosides in survival in the cold. Adv. Exp. Med. Biol., *152:* 307-314, 1982.

335) Hilbig, R., Lauke, G., and Rahmann, H. Brain gangliosides during life span (embryogenesis to senescence) of the rat. Develop. Neurosci., *6:* 260-270, 1984.

336) Klenk, E. Uber die Natur der Phosphatide und anderer Lipoide des Gehirns und der Leber bei der Niemann-Pickschen Krankheit. Z physiol. Chem., *235:* 24-36, 1935.

337) Klenk, E. Beitrage zur Chemie der Lipoidosen, 3. Mitt. Niemann-Picksche Krankheit und amaurotische Idiotie. Z physiol. Chem., *262:* 128-143, 1939.

338) Klenk, E. Neuraminsaure, das Spaltprodukt eines neuen Gehirn-lipoids. Z physiol. Chem., *258:* 50-58, 1941.

339) Klenk, E., and Langerbeins, H. Uber die Verteilung der Neuraminsaure im Gehirn. Z physiol. Chem., *270:* 185-193, 1941.

340) Klenk, E. Uber die Ganglioside, eine neue Gruppe von Zucker-haltigen Gehirnlipoiden. Z physiol. Chem., *273:* 76-86, 1942.

341) Blix, G., Svennerholm, L., and Werner, I. Chondrosamine as a component of gangliosides and of submaxillary mucin. Acta Chem. Scand., *4:* 717, 1950.

342) Svennerholm, L. Composition of gangliosides from human brain. Nature (London), *177:* 524-525, 1956.

343) Kuhn, R., and Wiegandt, H. Die Konstitution der Gangliotetraose und Gangliosides Gl. Chem. Berichte, *96:* 866-880, 1963.

344) Svennerholm, L. Ganglioside designation. Adv. Exptl. Med. Biol., *125:* 11, 1980.

345) Rapport, M.M. Introduction to the biochemistry of gangliosides. *In:* Rapport, M.M., and Gorio, A. (eds.), Gangliosides in neurological and neuromuscular function, development and repair. New York: Raven Press, 1981.

346) Svennerholm, L. Chromatographic separation of human brain gangliosides. J. Neurochem., *10:* 613-623, 1963.

347) IUPAC-IUB commission on Biochemical nomenclature. The nomenclature of lipids. Lipids, *12:* 455-468.

348) Schengrund, C.-L., and Garrigan, O.W. A comparative study of the gangliosides from the brains of various species, Lipids *4:* 488-495, 1969.

349) Wiegandt, H. Fundamentals of ganglioside structures. *In:* Rahmann, H. (ed.), Gangliosides and Modulation of Neuronal Functions, *H7:* 37-47. Berlin Heidelberg: Springer-Verlag, 1987.

350) Segler, K., Rahmann, H., and Rosner, H. Chemotaxonomical investigations on the occurrence of sialic acids in Protostomia and Deuterostomia. Biochem Systematics and Ecology, *6:* 87-93, 1978.

351) Dennis, R.D., Geyer, R., Egge, H., Peter-Katalinic, J., Keller, M., Menges, H., and Wiegandt, H. Insects: Animals without gangliosides - Preliminary data. *In:* Rahmann, H. (ed.), Gangliosides and Modulation of Neuronal Functions, *H7:* 351. Berlin: Springer-Verlag, 1987.

352) Makita, A., and Taniguchi, N. Glycosphingolipids. *In:* Wiegandt, H. (ed.), Glycolipids, *10:* 1-99. New comprehensive Biochem., 1985.

353) Wiegandt, H. Gangliosides. *In:* Neuberger,A., van Deenen, L.L.M (eds). New Comprehensive Biochemistry. *10:* 119-245. Amsterdam: Elsevier, 1985.

354) Schauer, R., and Corfield, A.P. Occurrence of Sialic Acids. *In:* Sialic Acids - Chemistry, Metabolism and Function, Schauer R. (ed.). Cell Biol. Monogr., *10:* 5-50, 1982.

355) Higashi, H., Hirabayashi, Y., Fukui, Y., Naiki, M., Matsumoto, M., Ueda, S., and Kato, S. Characterization of N-glycolylneuraminic acid-containing gangliosides as tumor-associated Hanganutziu-Deicher antigen in human colon cancer. Cancer Res., *45:* 3796-3802,

356) Tettamanti, G., Ghidoni, R., and Trinchera, M. Fundamentals of brain ganglioside biosynthesis. *In:* Rahmann, H. (ed.), Gangliosides and Modulation of neuronal functions, *H7:* 191-204. Berlin Heidelberg: Springer-Verlag, 1987.

357) Fredman, P., Noren, R., Mansson, J.E., and Svennerholm, L. Concentration, composition and structure of gangliosides from the CNS of dogfish Dqualus acanthias and cod Gadus callarias. Biochim et Biophys. Acta, *713:* 410-418, 1982.

358) Hilbig, R., and Rahmann, H. Variability in brain gangliosides of fishes. J. Neurochem., *34:* 236-240, 1980.

359) Svennerholm, L. The gangliosides. J. Lipid Research, *5* : 145-155, 1964.

360) Fredman, P., von Holst, H., Collins, V.P., Ammar, A., Dellheden, B., Wahren, B., Granholm, L., and Svennerholm, L. Potential ganglioside antigens associated with human gliomas. Neurological Res., *8:* 123-126, 1986.

361) Fredman, P., von Holst, H., Collins, V.P., Granholm, L., and Svennerholm, L. Sialyllactotetraosylceramide, a ganglioside marker for human malignant gliomas. J. Neurochemistry, *50:* 912-919, 1988.

362) Traylor, T.D., and Hogan, E.L. Gangliosides of human cerebral astrocytomas. J. Neurochem., *34:* 126-131, 1980.

363) The Eight International Conference on Brain Tumor Research and Therapy. J. of Neuro-Oncology, *7:* S33-S37.Abstract. Nertherlands: Kluwer Academic Publ., 1989.

364) Ledeen, R.W., Hogan, E.L., Tettamanti, G., Yates, A.J., and Yu, R.K. Comparison of the ganglioside pattern in the D-54MG cell line grown in culture or as a solid tumor in athymic nude mice. *In:* New Trends in Ganglioside Research, *14:* 157. Liviana Press, Springer Verlag, 1988.

365) Manssson, J.-E., Fredman, P., Bigner, D.D., Molin, K., Rosengren, B., Friedman, H.S., and Svennerholm, L. Characterization of new gangliosides of the lactotetraose series in murine xenografts of a human glioma cell line. FEBS Letters, *201:* 109-113, 1986.

366) Kohler, G., and Milstein, C. Continuous cultures of fused cells secreting antibody of predefined specificity. Nature, *256:* 495, 1975.

367) Schlom, J. Basic principles and applications of monoclonal antibodies in the management of carcinomas: The Richard and Hinda Rosenthal foundation award lecture. Cancer Research, *46:* 3225-3238, 1986.

368) Horan Hand, P., Nuti, M., Cocher, D., and Schlom, J. Definition of antigenic heterogeneity and modulation among human mammary carcinoma cell populations using monoclonal antibodies to tumor associated antigens. Cancer Res., *43:* 728-735, 1983.

369) Kufe, D.W., Nadler, L., Sargent, L., Shapiro, H., Hand, P., Austin, F., Colcher, D., and Schlom, J. Biological behavior of human breast carcinoma-associated antigens expressed during cellular proliferation. Cancer Res., *43:* 851-857, 1983.

370) Greiner, J.W., Horan Hand, P., Noguchi, P., Fisher, P., Pestka, S., and Schlom, J. Enhanced expression of surface tumor associated antigens on human breast and colon tumor cells after recombinant leukocyte α-interferon treatment. Cancer Res., *44:* 3208-3214, 1984.

371) Greiner, J.W., Tobi, M., Fisher, P.B., Langer, J.A., and Pestka, S. Differential responsiveness of cloned mammary carcinoma cell populations to the human recombinant leukocyte interferon enhancement of tumor antigen expression. Int. J. Cancer, 36 : 159-166, 1985.

372) Williams, J.A., Wessels, B.W., Edwards, J.A., Kopher, K.A., therapy of human glioma xenografts in-vivo utilizing radiolabeled antibodies. Cancer Res.(suppl.), *50:* 974s-979s, 1990.

373) Colapinto, E.V., Zalutsky, M.R., Archer, G.E., Noska, M.A., Friedman, H.S., Carrel, S., and Bigner, D.D. Radioimmunotherapy of intracerebral human glioma xenografts with ^{131}I-labeled F(ab')$_2$ fragments of monoclonal antibody Mel-14. Cancer Res., *50:* 1822-1827, 1990.

374) Bosslet, K., Madry, N., Kubel, R., Buchler, M., Muhrer, K.H., Klapdor, R., and Schulz, G. Human anti-idiotypic MAbs against the pancreatic carcinoma specific murine MAb BW494. Int. J. Cancer (in press).

375) Schulz, G., Buchler, M., Muhrer, K.H., Klapdor, R., Kubel, R., Harthus, H.P., Madry, N., and Bosslet, K. Immunotherapy of pancreatic cancer with monoclonal antibody BW494. Int. J. Cancer (in press).

376) Jones, P.T., Dear, P.H., Foote, J., Neuberger, M.S., and Winter, G. Replacing the complementarity-determining regions in a human antibody with those from a mouse. Nature, *321:* 522, 1986.

377) Larson, S.M., Carrasquillo, J.A., Reynolds, J.C., Hellstrom, I., Hellstrom, K.-E., Mulshine, J.C., and Mattis, L.E. Therapeutic applications of radiolabelled antibodies: current situation and prospects. Nucl. Med. Biol., *13:* 207, 1986.

378) Cheung, N.K., Saarinen, U.M., Neely, J.E., Landmeier, B., Donovan, D., and Coccia, P.F. Monoclonal antibodies to a glycolipid antigen on human neuroblastoma cells. Cancer Res., *45:* 2642, 1985.

379) Kurtzman, S.H., Russo, A., Mitchell, J.B., DeGraff, W., Sindelar, W.F., Brechbiel, M.W., Gansow, O.A., Friedman, A.M., Hines, J.J., Gamson, J., and Atcher, R.W. Bismuth linked to an anti-pancreatic carcinoma antibody: a model for alpha particle-emitter radioimmunotherapy. (in press).

380) Day, E.D., Lassiter, S., Woodhall, B., Mahaley, J.L., and Mahaley, M.S. The localisation of radioantibodies in human brain tumours.1. Preliminary exploration. Cancer Res., *25:* 773-8, 1965.

381) Chou, S.N., Aust, J.B., Moore, G.E., and Peyton, W.T. Radioactive iodinated human serum albumin as tracer agent for diagnosing and localising intracranial lesions. Proc. Soc. Exp. Biol. Med., *77:* 193-5, 1951.

382) Richardson, R.B., Davies, A.G., Bourne, S.P., Staddon, G.E., Jones, D.H., Kemshead, J.T., and Coakham, H.B. Radioimmunolocalisation of human brain tumours: biodistribution of radiolabelled monoclonal antibody UJ13A. Eur. J. Nucl. Med., *12:* 313-20, 1986.

383) Coakham, H.B., Richardson, R.B., Davies, A.G., Bourne, S.P., Eckert, H., and Kemshead, J.T. Neoplastic meningitis from a pineal tumour treated by antibody-guided irradiation via the intrathecal route. British J. Neurosurgery, *2:* 199-209, 1988.

384) Colapinto, E.V., Humphrey, P.A., Zalutsky, M.R., Groothuis, D.R., Friedman, H.S., de Tribolet, N., Carrel, S., and Bigner, D.D. Comparative localization of murine monoclonal antibody Mel-14 F $(ab')_2$ fragment and whole IgG2a in human glioma xenografts. Cancer Res., *48:* 5701-5707, 1988.

385) Coakham, H.B., Davies, A.G., Richardson, R.B., Bourne, S.P., Kemshead, J.T., Fabre, J., Mach, J.P., Carrel, S., Eckert, H., and Bullimore, J.A. Antibody-guided irradiation therapy for cases of neoplastic meningitis. *In:* Chatel, M., Darcel, F., and Pecker, J. (eds.), Brain oncology (Intro.), 349-352. Dordrecht: Martinus Nijhoff Publ., 1987.

386) Coakham, H.B. Section 82b.7, Imperial Cancer Research Fund - Annual Report, 1988.

387) Brady, L. Plenary lecture. 6th International Conference on Immuno-conjugates. San Diego, 1990.

CHAPTER II - DEVELOPMENT OF A LARGE-ANIMAL MODEL OF HUMAN GLIOMA IN IMMUNOSUPPRESED CATS

INTRODUCTION

Primary central nervous system neoplasms constitute approximately 10% of all cancer-related admissions to hospital and represent the cause for approximately 1% of all human mortality in North America[1]. Eighty percent of these primary tumours involve the brain and fully one-half of these tumours are gliomatous in nature. The more malignant types (malignant astrocytoma and glioblastoma multiforme) are clinically characterized by a rapidly progressive debilitating course with a uniformly fatal outcome. Current therapy consists of surgical biopsy and/or extirpation, followed by post-operative irradiation and chemotherapy[2]. Despite this combined therapeutic assault, median survival rates have only marginally increased[3].

It is the non-surgical (ie. chemo- or radiotherapy) modalities that hold greatest therapeutic promise; however, largely due to the lack of an intracranial CNS tumour model that faithfully reproduces human glioma behaviour, conclusive animal studies directed at specific glioma treatment strategies have not been possible. Furthermore, little intratreatment data on growth rate parameters has been acquired from experimental intracranially-placed tumours, further reducing the ability to adequately characterize existing tumour models.

In the experiments reported here, we have observed the reproducible intracerebral growth of the D-54MG human glioblastoma cell line as well as the TE671 rhabdomyosarcoma cell line using orally-administered CyA. In addition, we have grown both tumour types in subcutaneous locations allowing for studies comparing the effect of the peritumour environment on tumour growth characteristics.

MATERIALS AND METHODS

Karyotyping

Karyotyping was performed to substantiate the similarity of the genotypic characteristics of the D-54 MG cell line as compared to previously published reports[4,5]. 0.15ml Colcemid was added to a T-25 flask of D-54 MG cells - passage 66, and incubated x 3hrs at 37 C. 2ml of 0.25% trypsin in Hank's BSS was added. Suspension was placed, with washes from the flask and 2ml of DMEM with 10% FCS, into a centrifuge tube. After centrifugation (1000rpm x 10min.), hypotonic solution was added to supernatant which was then placed in a 37 C water bath x 17min. The mixture was fixed with methanol/acetic acid and left overnight at 4 C. The solution was spun and refixed thrice. 4-5 drops of fixed suspension were then dropped onto a cold, wet slide which was left overnight at 60 C. Slides were trypsinized for 15sec., rinsed in 70% and 100% ethanol then quickly dried. Giemsa stain (pH 6.8) was applied for 3min. and thereafter the slides were rinsed twice, dried, and made ready for examination.

Pharmacokinetic study

Three random-bred cats were sedated with Ketamine IM (Parke Davis, Morris Plains, New Jersey) (20mg/kg) and catheterized via the internal jugular vein. Cats were given 60mg CyA PO pre-sedation. Intravenous blood samples were taken at t = 0, 1, 2, 3, 5, 7, 10, 12, 24, 36 and 48 hours. An exponential curve -fitting analysis program was utilized to determine the $t_{1/2}$ of orally-administered CyA in cats.

Animals and CyA Treatment Protocol

Twenty random-bred male cats, weighing 3.5 - 5 kg. were quarantined for 21 days after receipt. All animals tested negative for Feline Leukemia virus and given no immunization. Animals were fed ad libitum. Cyclosporin A (courtesy Sandoz Canada Inc.) was administered as Sandimmune^{R} oral solution (Cyclosporin A 100mg/ml in Labrafil/olive oil.This solution was then transferred into commercially-available emptied cod-liver oil capsules (2 sizes-approx. 0.45 and 0.9ml) into which 0.4ml (40mg) and 0.8ml (80mg) of CyA solution was placed, respectively. After quarantine, cats were placed into one of four treatment groups : 1) 80mg CyA in 2 divided doses PO-starting 24 hours pre-implant (6 cats); 2) 120mg CyA in 2 divided doses (80mgqAM + 40mgqPM) PO-starting 24 hours pre-implant (5 cats); 3) 120mg CyA PO in 2 divided doses, starting ≥ 10 days pre-implant (6 cats); 4)120mg placebo solution (olive oil carrier solution for oral preparation - courtesy Sandoz Canada Inc.) in 2 divided doses, starting 10 days pre-implant) (3 cats). An additional 8 cats were split into the following three groups: 1) Intracerebrally implanted TE671 human rhabdomyosarcoma (80mg CyA in 2 divided doses PO-24 hours pre-implant) - 2 animals; 2) Subcutaneously implanted TE671 (80mg CyA in 2 divided doses PO-24 hours pre-implant) - 2 animals; 3) Subcutaneously implanted D-54 MG (same as above) - 4 cats. All animals receiving CyA underwent weekly blood tests to monitor liver function (SGOT, SGPT, Alk. Phos., Total Protein, Bilirubin, Calcium and Magnesium), kidney function (BUN, Creatinine), and hematological function (Hemoglobin, Hematocrit, Complete blood count with differential). In addition, the 6 cats receiving 120mg PO CyA/day starting 10 days pre-implant had CyA trough levels drawn at days 10 and 17.

Tumour Implantation

D-54 MG human glioblastoma-derived continuous cell line and TE671 human rhabdomyosarcoma (both cell lines - courtesy Dr. D. Bigner - Duke University) were used in all implants. Both were cultured in RPMI 1640 with 10% fetal calf serum and antibiotics (Penicillin/Streptomycin). Passages 66 through 70 of D-54 MG were used in intracerebral and subcutaneous implants. Passages 218 through 220 of TE671 were also used for implantation. After an overnight fast, animals were anaesthetized with Saffan (Alphaxalone-Alphadolone - courtesy Glaxo Ltd.) using an induction dose of 0.75ml/kg. (9mg. Alphaxalone and 3mg Alphadolone per ml. solution injected over a 1 minute period). The animals were intubated and the cephalic vein catheterized using a 20-gauge intravenous catheter. The animals were subsequently maintained on doses of 0.5ml titrated to respiratory rate and corneal reflex elicitation. Their heads were shaved, positioned in a stereotaxic head holder and cleansed with povodine-iodine solution. A 2.5cm. midline scalp incision was made. Two 5mm diameter burr holes were placed, one on each side of midline, 5mm. posterior to the coronal suture.

D-54 MG cells (1×10^7 cells), previously trypsinized and pelleted by gentle centrifugation (1000 rpm x 5 min.) and then mixed in equal volumes with 1% methyl cellulose in RPMI 1640, were inoculated in a 100 µl. volume, 5mm deep to dura, into each burr hole, through a Hamilton syringe fitted with a 22-gauge needle over a 3 min. period. Cells were implanted bilaterally to increase the tumour take rate/ animal. Delay time between inoculations was 5 min. Cells were allowed to spill out subpially over the cortical surface. Both burr holes were sealed with bone wax and the incision closed with interrupted sutures. Cats were then monitored twice daily for tumour- or CyA-related signs and sacrificed, after NMR imaging, when signs of neurologic

deterioration appeared. Animals not spontaneously presenting with signs were sacrificed 82 days post-implant.

Histopathological examination

Cat brains were removed within 2 hours after sacrifice and gross morphological characteristics were noted. Brains were fixed in 10% formaldehyde for ≥ 24 hours, then cut in coronal sections. The sections were paraffin-embedded and cut into 8μ serial slices which were then stained with hematoxylin and eosin. They were then examined for tumour presence and dimensions, cellular morphology as well as extent of lymphocytic infiltration. Statistical analysis was performed using the Chi-square test with the Yates continuity correction for small sample sizes. $P < 0.05$ was considered stastistically significant.

NMR Imaging

A single-slice, multi-echo experiment was performed on cats at least 21 days after implantation using a 2.35 T Bruker 40-cm bore magnet. An air-tight animal containment cylinder was constructed to prevent contamination of the surrounding area with allergens or pathogens (see Appendix I). Eight echoes in the spin-echo experiment were recorded with T_E = 26.5 ms. and T_R = 3 s., after centering on the position at which the greatest tumour diameter was observed. Furthermore, Gadolinium-DTPA (Gd-DTPA) (courtesy Berlex Canada, Inc - Lachine, Quebec) - 1 cc. IV over 2 min., was administered to several additional cats (4.4-5.0 kg.), implanted after the main studies were completed, in an attempt to increase delineation between tumour and surrounding tissue. T_E = 26.5 ms and T_R = 0.5 sec. for this small series.

RESULTS

Karyotyping

A determination of chromosome number was performed on 50 D-54 MG tumour cells in culture. 70% of these cells had chromosome counts of 70 - 73 chromosomes, however some cells had fewer than 68 chromosomes and others had a greater number, up to a maximum of 76 chromosomes (see Fig. 1). Five of these cells taken from the mid-range of chromosome number were karyotyped and a representative set of marker chromosomes is shown in Fig. 2. This set contains 15 of 18 marker chromosomes previously described for this tumour cell line and both the karyotype as well as the distribution of chromosomal markers compare favourably to previously published reports[5,6].

Pharmacokinetic study

This study was performed to ascertain the appropriate dosing schedule for oral Cyclosporin A. The time-to-peak concentration for a 60 mg oral dose in all 3 cats was 3 hours. A representative study is shown (Figure 3). The average half-life of CyA in blood was determined to be 13.6 ± 2.5 hrs.

Tumour implantation

Thirty-three percent (2/6) of D-54 MG tumours implanted intracerebrally with a preparatory regime of 80 mg PO CyA/day, commencing 24 hours pre-implant, grew into macroscopic tumours. In Group 2, with an increased dose (120 mg/day) for an equivalent length of time (24 hours), the take rate was 60% (3/5 animals). Group 3 animals, exposed to a high-dose (120mg) regime for an increased length of time ($\geq$ 10 days), grew tumours in 100% cases (6/6 animals) although the actual tumour take rate is only 75% (9/12 inoculations - $P \leq 0.05$). All cats in this last

group achieved growth of right-sided implants. However, cells implanted into the left hemisphere invariably grew into smaller tumours and in 50% (3/6) of cases did not establish tumour nidi. A case-by-case synopsis of this last series can be found in Table 1. None of the 3 placebo-fed cats developed tumours, on a macroscopic or microscopic level (0/6 inoculations). The cat sacrificed earliest (due to the appearance of signs of increased intracranial pressure), on coronal sectioning, revealed a cystic tumour with a necrotic centre (B-1; 15 days); all other tumours had no such necrotic focus. The 2 cats implanted intracerebrally with TE 671 rhabdomyosarcoma grew tumours - both dying of mass effect 13 and 17 days after implantation. A low-power H&E section of brain revealed the necrotic centre of the tumour, which, on gross examination, was filled with a viscous red-tinged fluid.

All animals received CyA dosing from initiation of treatment until sacrifice or death. Two cats implanted into the right flank with TE671 cells grew tumours, which, after 28 days, averaged 1.5 - 2.0 cm. in diameter. On sectioning, these tumours invaded underlying muscle, but not overlying skin. Of the 4 cats implanted subcutaneously with D-54 MG cells, only 1 developed a macroscopic tumour (2 cm diam.), at 28 days post-implantation. All 4 initially developed macroscopic tumours which had a peak diameter of approximately 3cm. at 2 weeks post-implant, but underwent progressive diminution in size until at 4 weeks there was neither macroscopic nor microscopic evidence of tumour tissue. All biochemical parameters tested were within normal limits, although 2/20 (10%) and 1/20 (5%) of the animals developed gingival hyperplasia and intussusception, respectively. The minimum CyA 12-hour trough level in Group 3 was 640 ng/ml.

NMR Imaging

There was considerable difficulty resolving tumour tissue on the 1st echo of a multi-echo NMR Image (Figure 4), but by the 2nd and especially the 3rd echo, even with the general disappearance of signal, one could clearly delineate tumour/edema from normal brain, although differentiation of tumour from surrounding edema still remained a matter for speculation. Gd-DTPA markedly increased the contrast (cf. pre- and post-injection - Figure 5) in the area in which blood-brain barrier (BBB) breakdown occurred, which, according to previous studies[7,8], represents the main body of the tumour

Histopathological examination

On gross examination the tumours resulting from the D-54 MG implants were pale yellow, firm and distinguishable in texture from surrounding parenchyma. Histologically, the neoplasms extended from the cerebrum into the subarachnoid and subdural spaces. In some cases there was invasion into the overlying subcutis, as well. The subdural extension was in most cases greater in the anterior-posterior plane from the implant site, than in the lateral direction. Extensive invasion was present into the surrounding brain. The histomorphology of the tumours was characterized by solid sheets of polygonal cells interspersed with occasional giant cells. Mitoses were frequent throughout (Figures 6 and 7). Some perivascular lymphocytic cuffing was present and was associated with minimal penetration into the tumour tissue in some cases, but was completely absent in most.

It was interesting to note that in an animal that expired 3 days after implantation (prior to the commencement of the study) no tumour cells were present within the injection track but there was an extensive infiltration of lymphocytes and

fibroblasts at the site of injury. There were, however, numerous, viable D-54 MG cells in the subarachnoid region surrounding this site, many with mitotic figures. Differences were also seen between D-54 MG tumours grown in subcutaneous and intracerebral sites. Whereas sheets of closely cohesive polygonal cells were observed in intracerebrally implanted tumours, the subcutaneously implanted tumours had a more sarcomatous appearance with whorls and haphazard arrangements of fusiform cells as well as striated organization of cell sheets.

One cat was also implanted (pre-study) with both D-54 MG as well as TE671 cells, both of which grew into macroscopic tumours. On microscopic examination these neoplasms showed distinct differences, with the TE 671 lesion being much more densely populated with anaplastic, pleomorphic cells, as well as containing multifocal areas of necrosis (Figure 8).

DISCUSSION

Numerous attempts have been made to establish a replicable model of a human tumour in an immunocompetent large animal, going as far back as 1951[10]. Various methods have been utilized to overcome the response of the host immune system to the insertion of a nidus of foreign tissue, including the use of: 1) immune-protected areas for implantation such as cheek pouch (hamster[11]) and the anterior chamber of the eye (rabbit[12,13], among others[14-16]); 2) exogenous immunosuppression - including total body irradiation[9], antithymocyte serum[9], cyclophosphamide[17] and steroids[9,18]; 3) implantation of a fast-growing tumour into a partially immunoprotected area - human choriocarcinoma in brain (monkey[19]). However, the great majority of these attempts were not successful and the remainder proved to have limitations with respect to the size of tumour produced or

incongruity of the host implant tissue type when compared with the site of origin of the implanted human tumour.

The advent of Cyclosporin A[20] has radically altered both the survival of organ transplant recipient as well as the scope of studies on the rejection of grafts of various tissue types. Cyclosporin A is a fungal metabolite which binds to peptidyl-prolyl cis-trans isomerase (PPIase),which in turn inhibits isomerase-dependent refolding of proteins[21]. This may be one mechanism necessary for the activation of transcriptional activators including those involved in the activation of lymphokine genes such as interleukin-2 (IL-2) and gamma-interferon. Inhibition of the activation of these genes would therefore block production of these lymphokines, necessary for T-cell activation. Use of Cyclosporin A in xenografting human neural tissue into mammalian CNS began with Stromberg et al.[22] who grafted fetal human (6.5-8 wk) neural tissue into rat brain, achieving 100% survival of grafted tissue at 140 days. Adams et al.[4] grafted D-54 MG glioblastoma into rat brains with a 70-100% tumour-related mortality in 20-44 days. Our results have shown the presence of viable D-54 MG tumours 2 - 20mm. in diameter in cat brain, 27-44 days after implantation in 100% cases. In addition, these tumours as well as TE 671 human rhabdomyosarcoma can be grown in both subcutaneous as well as intracerebral locations.

The D-54 MG cell line was utilized because of previous work showing it to be the most tumourigenic glioma cell line out of 15 cell lines tested[23]. Male cats were used because of the appearance of a consistent gender discrepancy in weight loss when CyA was used in xenografted rats[4]. Oral administration of CyA was chosen because of the ease with which it could be administered and the avoidance of problems associated with the intravenous vehicle - Cremophor EL, namely

vasoconstriction and histamine release (cf. Albrechtsen et al.[24]). One possible explanation of the uneven outgrowth distribution of bilaterally-implanted tumour cells may be methodological i.e. the time delay (approx. 5 min.) between cells implanted first into the right hemisphere, followed by the left-sided implant. Pelleting, as well as the addition of Methocel may decrease access to the nutrients present in the surrounding medium, perhaps contributing to cell death in-vitro pre-implantation.

The observation that tumour cells remain viable and initially grew only in the subarachnoid space with subsequent invasion into the cerebral hemispheres (unpublished observations) has led us to believe there may be trophic factors conducive to tumour growth present in the cerebrospinal fluid (CSF).From these studies,we suggest there may be three major prerequisites for successful growth of human tumours in the mammalian CNS (cf. Bjorklund et al[25]):

1) Adequate number of viable tumourigenic cells;

2) Adequate level of immunosuppression present for a long enough period of time prior to transplantation;

3) Immediate access to a nutrient supply (eg. CSF), pending the establishment of a permanent blood supply.

Whether or not xenografted tumours are capable of withstanding host cell mediated immune responses after withdrawal of exogenous immunosuppression also awaits studies in progress.

The large animal human glioma model presents several potential advantages over the currently used athymic mouse/rat model. These include: 1) larger cranial vault volume allowing for increased initial tumour cell implant volume and increased size of resultant tumour; 2) high tolerance of oral Cyclosporin A and relative paucity of significant side effects; 3) facilitated visualization of a) in-vivo serial NMR images

monitoring tumour growth and b) in-vivo radioimmunoscintigraphic studies utilizing tumour-specific monoclonal antibodies. To summarize, the use of a large animal model of human glioma confers the ability to test an augmented range of administration routes (eg. intrathecal/intratumoural vs. parenteral) and in vivo testing modalities, both invasive and non-invasive, that can be brought to bear in a study of brain tumour therapy. This may facilitate the development and ease the subsequent evaluation of innovative and efficacious approaches to this as yet incurable condition.

REFERENCES

1) Schwartz, S. Principles of Surgery, p 1777. Toronto: McGraw-Hill Publ., 1979.

2) Wilkins, R.H., Rengachary, S.S., (eds), Neurosurgery. pp 586-590. Toronto: McGraw-Hill Publ., 1985.

3) Sutherland, G.R., Florell, R., Lown, D., et al. Epidemiology of primary intracranial neoplasms in Manitoba, Canada. Can. J. Neurol. Sci., *14*: 586-592, 1987.

4) Adams, C., Bullard, D.E., Bigner, S.H. et al. Intracerebral transplantation of D-54 MG human glioma line in immunosuppressed rats. *In:* M.D. Walker, D.G.T. Thomas (eds.), Biology of Brain Tumours, pp 97-105. Boston: Martinus Nijhoff Publ., 1986.

5) Bigner, S.H., Mark, J., and Bigner, D.D. Chromosomal composition of four permanent cultured cell lines derived from human gliomas. Cancer Gen. and Cytogen., *10:* 335-349, 1983.

6) Wikstrand, C.J., Bigner, S.H., and Bigner, D.D. Demonstration of complex antigenic heterogeneity in a human glioma cell line and eight derived clones by specific monoclonal antibodies. Cancer Res., *43:* 3327-3334, 1983.

7) Yoshida, K., Furuse, M., Kaneoke, Y. et al. Assessment of T_1 time course changes and tissue-blood ratios after Gd-DTPA administration in brain tumours. Mag. Res. Imaging, *7:* 9-15, 1989

8) Claussen, C., Lanaido, M., Schörner, W. et al. Gadolinium-DTPA in MR imaging of glioblastomas and intracranial metastases. A.J.N.R., *6:* 669-674, 1985.

9) Saris, S.C., Bigner, S.H., and Bigner, D.D. Intracranial transplantation of a human glioma line in immunosuppressed rats. J. Neurosurg., *60:* 582-588, 1984.

10) Greene, H.S.N. The transplantation of tumours to the brains of heterologous species. Cancer Res., *11:* 529-534, 1951.

11) Shcheglovitova, O.N., Voskoboinik, A.D., Solov'eva, M.N., Fan'kovskaia, M.K., and Ezepchuk, I.V. Protoopukholevaia espetsificheskaia aktivnost' stafilokokkovykh enterotoksinov. Eksp. Onkol., *9:* 28-30, 1987.

12) Kan-Mitchell, J., Mitchell, M.S., Rao, N., and Liggett, P.E. Characterization of uveal melanoma cell lines that grow as xenografts in rabbit eyes. Invest. Opth. Vis. Sci., *30:* 829-834, 1989.

13) Rand, R.W., Khonsay, A., Brown, W.J., Winter, J., and Snow, H.D. Leksell stereotactic radiosurgery in the treatment of eye melanoma. Neurol. Res., *9:* 142-146, 1987

14) McFall, R.C., Sery, T.W., and Makadon, M. Characterization of a new continuous cell line derived from a human retinoblastoma. Cancer Res., *37:* 1003-1010, 1977.

15) Manuelidis, E.E. The fate of serially heterologously transplanted glioblastoma multiforme in the eye of the Guinea pig. Am. J. Pathol., *48:* 65-89, 1966.

16) Burns, R.P., and Tidwell, M. Experimental ocular malignant melanoma in Sinclair swine. Curr. Eye Res., *5:* 257-262, 1986

17) Amsten, P., Taylor, D.O., Nelson-Rees, W.A., Huebner, R.J. et al. Propogation of human tumours in antithymocyte serum-treated mice. J. Nat. Cancer Inst., *52:* 71-84, 1974.

18) Manuelidis, E.E. Experiments with tissue culture and heterologous transplantation of tumours. Ann. NY Acad. Sci., *159:* 409-431, 1969.

19) Yamada, K., Bremer, A.M., and West, C.R. Effects of dexamethasone on tumour-induced brain edema and its distribution in the brain of monkeys. J. Neurosurg., *50:* 361-367, 1979.

20) Borel, J., Feurer, C., Gubler, H., and Stahelin, H. Biological effects of Cyclosporin A: A new antilymphocytic agent. Agents Actions, *6:* 468-9, 1976.

21) Takahashi, N., Hayano, T., and Suzuki, M. Peptidyl-prolyl cis-trans isomerase is the Cyclosporin A-binding protein cyclophilin. Nature, *337:* 473-475, 1989.

22) Stromberg, I., Bygdeman, M., Goldstein, M., Seiger, A., and Olson,L. Human fetal substantia nigra grafted to the dopamine-denervated striatum of immunosuppressed rats; evidence for functional reinnervation. Neurosci. Lett., *71:* 271-276, 1986.

23) Bigner, D.D., Bigner, S.H., Ponten, J. et al. Heterogeneity of genotypic and phenotypic characteristics of fifteen permanent cell lines derived from human gliomas. J. Neuropath Exp. Neurol., *40:* 201-209, 1981.

24) Albrechtsen, D., Helgerud, P., Jakobsen, A., and Rugstad, H.E. Blood and interstitial lymph Cyclosporin levels in the rat after oral and intravenous medication. Transplant. Proc., *18*: 42-43, 1986.

25) Bjorklund, A., and Stenevi, U. Intracerebral Neural Implants: Neuronal replacement and reconstruction of damaged circuitries. Annu. Rev. Neurosci., *7*: 279-308, 1984.

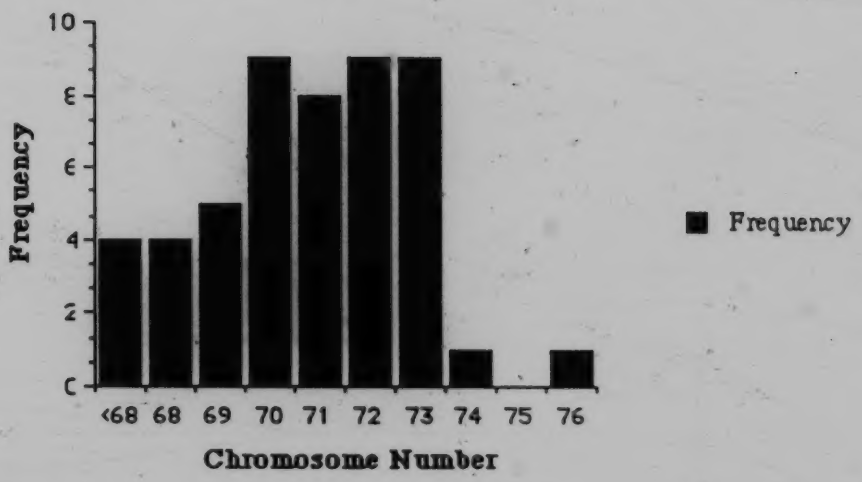

Figure II - 1. Karyotype Distribution of 50 metaphases from the D-54 MG cell line (passage 66).

Cat Number	Time until Sacrifice	CyA Dose	B.W.	Trough [CyA] (mg/l) @ 10,17d	Tumour Dimensions (A/P x lat. x depth)
A-143	38 days	120mg/d	4.6kg	2.24; 3.10	R - 2x2x2 mm L - no growth
A-162	27 days	120mg/d	4.3kg	2.95; 2.42	R - 5x3x2 mm L - no growth
B-1	15 days	120mg/d	4.8kg	0.75; 0.64	R - 12x8x8 mm L - no growth
B-14	44 days	120 mg/d	3.8kg	0.93; 2.91	R - 20x10x5 mm(cystic) L - 20x10x5 mm
B-2	38 days	120 mg/d	4.1kg	2.93; 4.60	R - 20x10x5 mm L - 20x10x1 mm
B-30	41 days	120 mg/d	4.1 kg	0.94; 1.45	R - 20x10x12 mm L - 3x5x2 mm

Table II - 1. An analysis of the 6 cats receiving 120 mg/d CyA, starting ≥ 10 days pre-implant (i.c. and s.c. indicate intracerebral and subcutaneous, respectively)

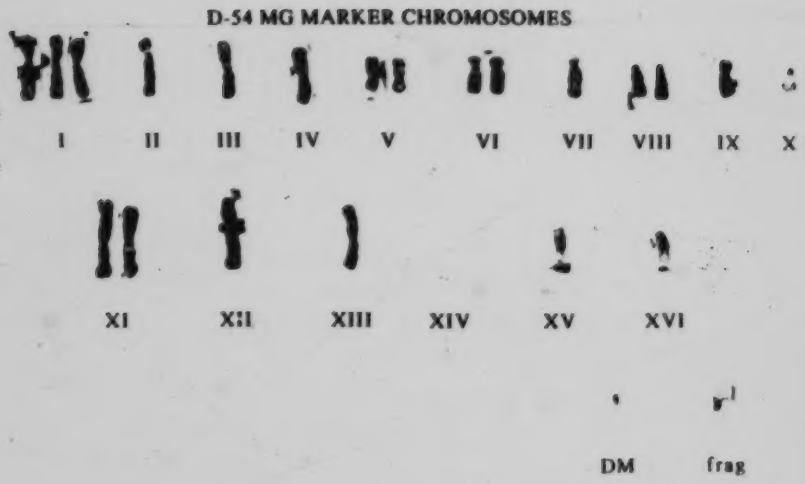

Figure II - 2. Marker chromosomes found in a representative D-54 MG cell (grown in tissue culture). Roman numerals indicate chromosomes previously assigned (ref. 4). DM indicates double minute. 'frag' indicates unassigned chromosomal fragment.

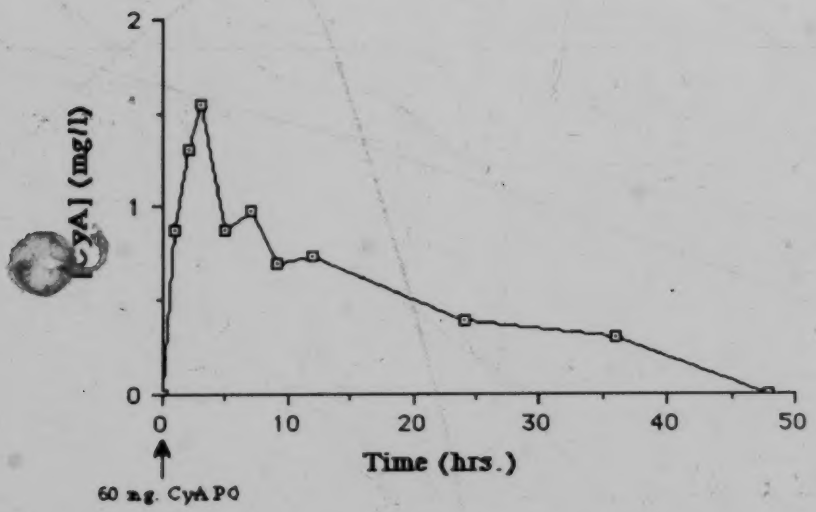

Figure II - 3. Representative time course of blood [CyA] values after administration of 60 mg. of CyA dissolved in olive-oil carrier solution. Analysis performed using HPLC on samples of whole blood.

Figure II - 4. Six coronal NMR images of cat brain (B-116). Images a) - f) represent echoes 1, 2, 3, 5, 7, 8 of a multi-spin-echo T2-weighted (TE = 26.5 ms., TR = 3 sec) sequence.

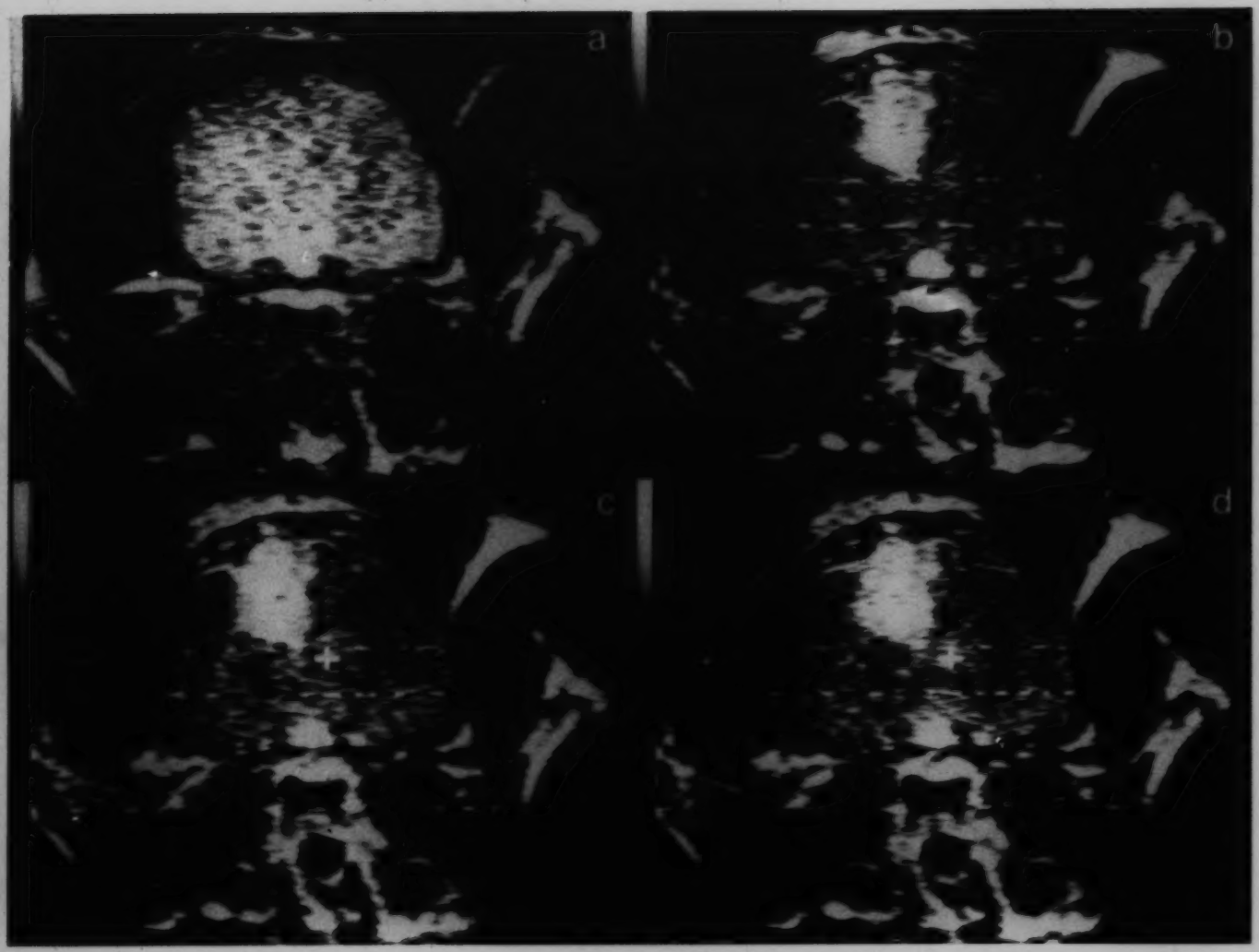

Figure II - 5. Four coronal NMR images of cat brain (B-116) with a single right-sided D-54 MG implant taken pre- (Image a)) and 2, 5 and 10 minutes post-Gd-DTPA contrast enhancement (Images b) - d)). Imaging parameters include: TE = 26.5 ms., TR = 0.6 sec. (1st echo shown in each case).

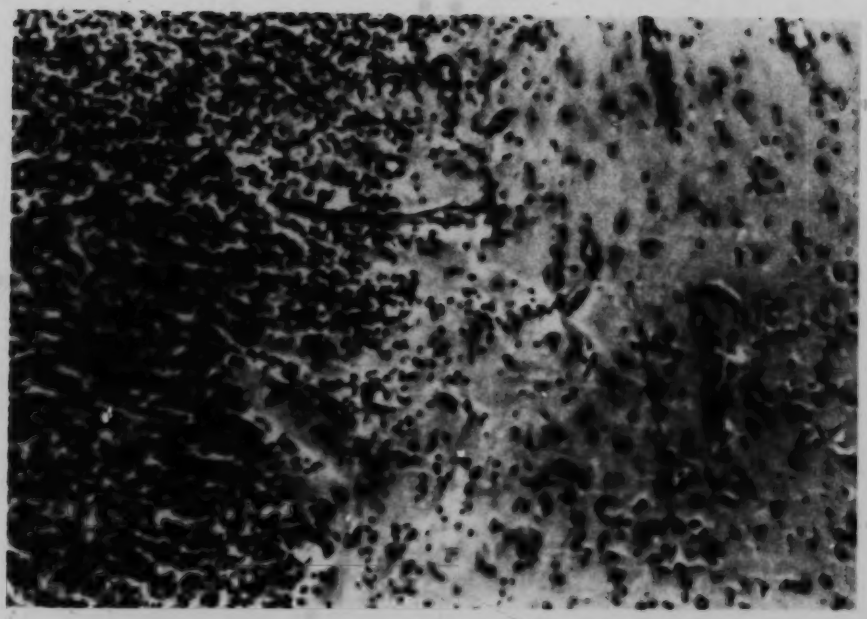

Figure II - 6. Photomicrograph of D-54 MG glioblastoma multiforme implanted into cat brain showing interface between tumour and brain. H&E stain (X 115).

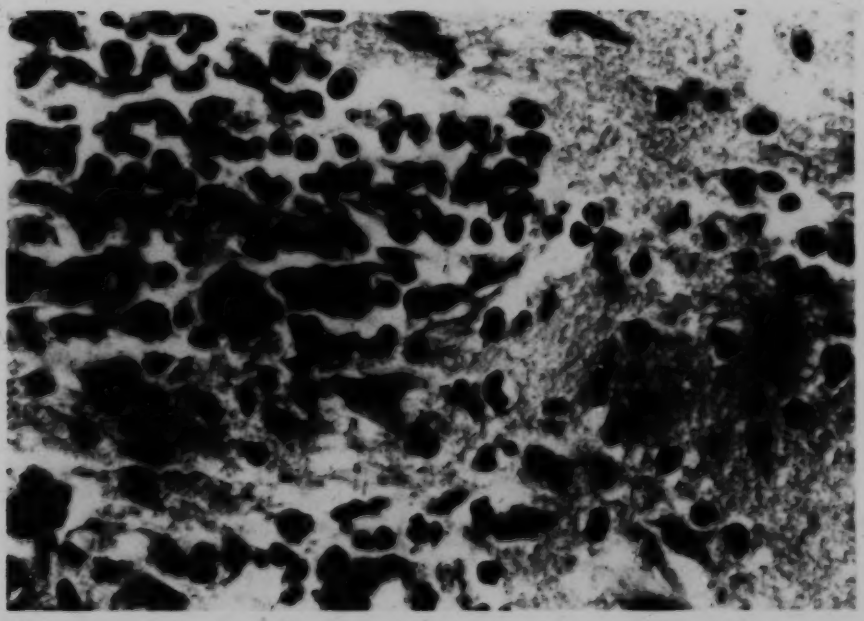

Figure II - 7. High-power photomicrograph of Figure II - 6. H&E stain (X 620).

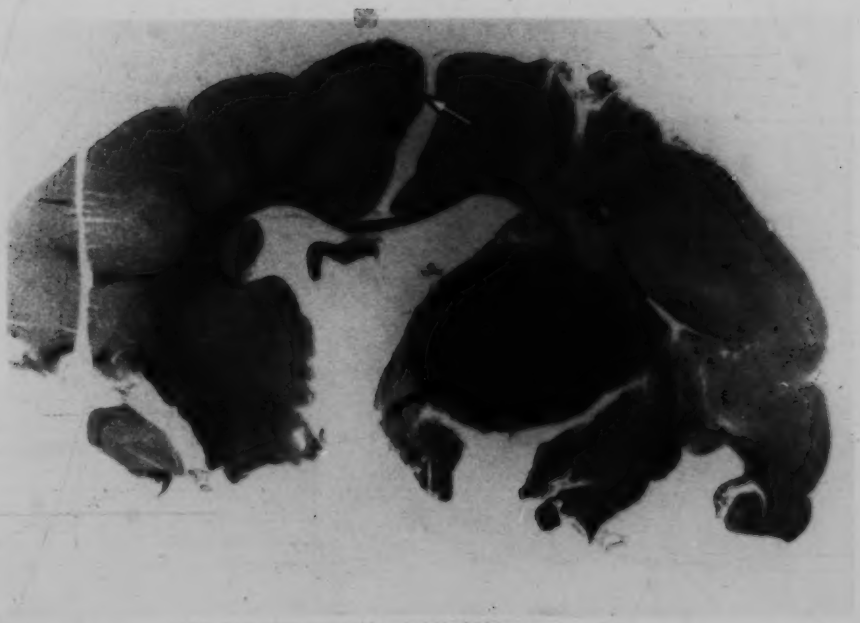

Figure II - 8. Whole-mount coronal section of cat brain taken 70 days after being implanted with D-54 MG (solid arrow) and 13 days after TE671 implantation (open arrow). Preparatory regime of 80 mg/d CyA PO, commenced 24 hrs. pre-implant. H&E stain.

CHAPTER III - REGULATION OF EXTRACELLULAR SUBSTRATE LEVELS BY D-54 MG HUMAN GLIOBLASTOMA CELL LINE

INTRODUCTION

Glucose and glutamine represent the two main substrates used by the central nervous system to drive the metabolic pathways used in energy production and neurotransmitter synthesis. Glucose is metabolized through four pathways upon entering a neuron or glial cell - 1) Glycolysis, producing pyruvate and lactate with concomitant controlled energy release; 2) Kreb's cycle/Cytochrome chain, pyruvate undergoing degradation to $C0_2$ and H_20; 3) Hexose monophosphate shunt, producing purines and pyrimidines for nucleic acid synthesis (minor); and 4) Glycogenesis, producing glycogen (minor). For its part, glutamine takes part in energy substrate synthesis through its conversion to glutamate, which enters the Kreb's cycle after its metabolism, both through deamination (glutamine dehydrogenase - GDH) and transamination (aspartate aminotransferase - AAT) to α-ketoglutarate. Glutamate also serves as a precursor for neurotransmitter synthesis as well as itself being the major amino acid neurotransmitter found in the CNS.

Human glioma cells in-vitro have been shown to exhibit activity along most of these metabolic pathways. However, a major difference with respect to normal glial metabolism is the different priorities assigned to and therefore the altered flux of substrate input through these routes. Malignant gliomas, for the most part seem to subscribe to the energy production strategy of "aerobic glycolysis" , first proposed by O. Warburg in 1930[1], who described an increased flux through the glycolytic

pathways, with accompanying high lactate levels, even in the presence of an adequate supply of oxygen. It has also been demonstrated that glutamine uptake and metabolism is substantially different from that observed in normal glia[2].

^{1}H-NMR spectroscopy possesses the ability to determine the concentrations of various metabolically-active substances, both in-vitro[3] and more recently, in-vivo[4,5]. However, the precision with which estimates of those concentrations are made in complex biological solutions eg. blood, cell culture medium, has not been well studied.

Therefore, the purpose of the present study is three-fold:

1) A comparative analysis of the chemosensitivity of the D-54 MG human glioblastoma-derived cell line to three drugs - a) Methyl prednisolone; b) BCNU- a nitrosourea derivative widely used in the chemotherapy of malignant glioma and c) Daunomycin - an anthracycline derivative.

2) A determination of the relative fluxes of a variety of metabolically -active substrates, including such NMR-visible ones as lactate, glutamine, glutamate and alanine, between D-54 MG cells and the surrounding culture medium.

3) A comparison of the errors that accrue in the determination of concentration, in in-vitro ^{1}H-NMR spectroscopy and other more commonly used techniques such as high-pressure liquid chromatography (HPLC) and analyses done with enzymatic techniques.

METHODS AND MATERIALS

Colony-Formation Assay

D-54MG human glioblastoma-derived continuous cell line (passage number 70 - courtesy Dr. D. Bigner, Duke University) was grown to approximately 80% confluence in monolayer culture using 60 mm. diameter Falcon culture-plates (optimal medium volume - 5ml) containing RPMI 1640 (Grand Island Biological Co., Grand Island, NY) supplemented with 10% heat-inactivated fetal calf serum, 20mM N-2-hydroxyethyl- piperazine-N'-2-ethanesulfonic acid buffer (HEPES), 100IU/ml Penicillin, 100 mg/ml Streptomycin, 2.5 mg/ml Fungizone, 1mM sodium pyruvate and 2mM L-glutamine. Plates were incubated in 5% CO_2 at 37°C. For chemosensitivity experiments, D-54 MG cells were mechanically harvested with a Pasteur pipette, washed with PBS, and resuspended in the same medium at a concentration of 5×10^5 cells/ml (as counted by hemocytometer). Cells were then plated in quadruplicate at concentrations of 100, 500 and 1,000 cells/plate and left to equilibrate overnight before addition of drug. All drug solutions were freshly prepared on the day of their administration. 1,3 - bis (2-chlorethyl)-1-nitrosourea (BCNU) was dissolved in 3 ml sterile absolute ethanol and 27ml of sterile PBS, providing a stock solution at 3.33 mg/ml. Dilutions were made and the drug was administered in doses of 20, 40, 60, 80 and 100 mM, resulting in 12 plates/dose. Methylprednisolone was similarly administered in doses of 20, 40, 60, 80, 100 mM after dilution of 40mg/ml stock solution (Mix-o-Vial). 10mg Daunomycin HCl crystalline solid (Sigma) was mixed in a glass volumetric flask with 100ml sterile PBS, providing a 100µg/ml stock solution, from which final doses of 1,5,10,15 and 20 µg/ml were administered to the cells in-vitro upon mixing with culture medium. All cells underwent drug treatment for 2 hours. Solutions were then gently

removed, plates rinsed twice with PBS, then incubated for 7 days in the original medium. Subsequently the number of colonies (>50 cells) on each plate was counted using an inverted microscope (Bausch and Lomb - Rochester, NY) after fixing and staining with 70% isopropyl alcohol and methylene blue.

Cell Culture Procedures for Metabolic Assays

D-54 MG cells were grown to confluence (approx. $1x10^7$ cells/plate) in 150mm diameter Petri plates in culture medium described above. At confluence, medium was replaced with 43.0 ml fresh medium. BCNU and Daunomycin stock solutions were made up as previously described, on the day of their administration. There were 4 experimental groups : 1) Media control (no cells, no treatment; 2) Cell control (confluent cells, no treatment); 3) BCNU and 4) Daunomycin, each done in triplicate. 1.5ml of media was removed from each plate at time 0, 0.5, 1, 2, 3, 4.5, 6, 7.5, 9,12, 24 and 36 hrs. Immediately after t = 1hr., 1ml of drug solution was added to the 38.5ml. medium remaining to attain a final drug concentration of 100 mM - BCNU and 50 µg/ml - Daunomycin, which was left for the remainder of the experiment.

After the 1.5ml sample was removed, it was split 3 ways - 450µl from 2 of the 3 plates for t = 0, 1, 3, 6, 12 and 24 hours was placed in an Eppendorf tube to which 15mg of sulfosalicylic acid was added to lower pH. This solution was centrifuged at 16,000g in an Eppendorf centrifuge (model #5145) x 10min. The supernatant was removed, filtered through a 0.22µm syringe filter, pH determined to be less than or equal to 2.0, and stored at -70°C awaiting amino acid analysis. 200µl was taken from each of the 3 plates sampled at all time points in the experiment and stored in glass tubes containing sodium fluoride and potassium oxalate at -70°C to undergo

enzymatic analysis for lactate. 500µl was taken from 2 of the 3 plates at all time points (t = 0, 0.5, 1, 2, 3, 4.5, 6, 7.5, 9, 12, 24, 36 hours), placed in an Eppendorf tube and stored at -70°C for NMR analysis.

Preliminary experiments done with standard solutions of lactate and amino acids ensured that no loss of metabolites occurred during processing and storage.

HPLC Analysis - Amino Acids

25µl of filtrate was diluted with lithium citrate buffer (0.27M, pH 2.2). The equivalent of 2µl of sample was injected in a 10ml total volume into a Perkin-Elmer HPLC fitted with a Series 10 HPLC Isocratic Pump for continuous delivery of o-phthaldehyde (0.20ml/min) used as the pre-column derivatizing agent and a 4-solvent Titanium Biopump, delivering a separation gradient of lithium citrate, 0.24 to 0.64M with a pH change of 2.75 to 7.50. The separation lasted 96 minutes and was itself performed using a 5µ High Speed Lithium Cation Exchange column (Pickering Cat. #0373150). 1-alkylthio-2 alkylsubstituted amino acid derivatives were detected by measuring fluorescence using an LS-5 Luminescence Spectrometer at excitation and emission optima of 340 and 455nm, respectively. Each sample set was calibrated using both a control sample and a concentration standard of known precision.

Enzymatic Assay Lactate Determination

Enzymatic assays were performed with a Du Pont Automatic Clinical Analyzer, using a modification of a method developed by Marbach and Weil, employing the oxidation of lactate to pyruvate. 40µl of sample was analyzed within 24 hours of collection, injected into the sampler along with 4.960ml of Tris buffer.

Reaction then occurred within a proprietary (Du Pont®) chamber containing 120U lactate dehydrogenase, 27 mmoles NAD, 60 mg dihydrazine sulfate (trapping agent) and NaOH (pH adjustment). The formation of NADH (proportional to lactate concentration) was measured with a dual-beam spectrophotometer, set at 340 and 383nm. Determination of protein concentration was performed using D-54 MG cells grown in 35mm plates to confluence (1.5×10^6 cells/plate) using the aforementioned medium. Confluent cells were rinsed twice with DMEM, then extracted with 3 ml of 3M perchloric acid (4°C) which was neutralized, after protein precipitation with 1M NaOH. The partially soluble protein was heated to 40°C for 30 min. to increase solubility. Mixture of cell debris and solubilized protein was then centrifuged and supernatant filtered (0.45µm syringe filter) to remove debris. Protein concentration was assessed using the Bio-Rad® protein assay. Statistical analysis was performed with a one-way ANOVA, using the Scheffe multiple comparison procedure. $P < .05$ was considered to be statistically significant.

NMR Analysis - Amino Acids

Eppendorf tubes were taken directly from storage at -70°C and lyophilized. Samples were reconstituted in 99.6% D_2O and lyophilized again. A second reconstitution was performed with 490ml of 99.996% D_2O and 10ml of 12.5mM disodium-2.2-dimethyl(-2-silapentane-5-sulfonate) (DSS; chemical shift standard). ^1H NMR spectroscopic determination was performed using a 90°-ACQ pulse sequence on a 7.05T (Nicolet Instruments) narrow-bore analytical spectrometer Model NMC-1280 with a $t_{90°} = 9.9ms$ and $t_{ACQ} = 10sec$ ($T_1 = 2.17sec.$). 32 scans were needed to achieve a S/N ratio ≥ 50. Integration of glutamine, glutamate and alanine peaks was performed using the NMC Software Package (Oxford Instruments).

RESULTS

Colony-Formation Assay

The colony-forming ability of D-54 MG cells was determined after exposure to three different drugs - Methylprednisolone, BCNU and Daunomycin. Figures III - 1 and III - 2 provide a comparative analysis for the first two and the third drugs, respectively. There was a considerable difference between all 3 drugs. Methylprednisolone had no effect on the clonogenic ability of D-54 MG cells. BCNU however, had some effect on colony formation. Exponential curve-fitting revealed that the IC_{50} = 11.7 mM, with even a dose of 100 mM not achieving 2-log cell kill. This is at variance with the sensitivity to nitrosoureas predicted by the Mer⁻ phenotype of the D-54 MG cell line (R. Day III, personal communication). Daunomycin achieved a high degree of cell kill using very low drug concentrations. Curve-fit analysis revealed that an IC_{50} = 0.5mM was achieved for this drug, a 20-fold improvement in cell kill efficacy over BCNU.

Lactate Determination

Preliminary experiments on the effect of preparation and storage of lactate samples showed a 3% decrease in lactate concentration over a storage period of 96 hours, but no loss after 24 hours. Media control plates maintained a steady lactate level of 2.62 ± 0.33 mmoles/l throughout the 36 hour course of the experiment. However, untreated D-54 MG cells showed a linear rise in lactate concentration over 24 hours, with some evidence of plateauing from 24 to 36 hours. The linear rate of rise over the first 24 hours was 0.36mM/hr. plate. Assuming that 1) the only source of lactate was the D-54 MG cell line in monolayer culture; 2) 1×10^7 D-54 MG

cells/plate at confluence; 3) a steady-state volume approximation of 34.75ml/plate, and 4) no lactate was degraded or utilized by the cell line, then one can calculate that, on average, a single D-54 MG cell at confluence with adequate nutrition, produced 36×10^{-12} moles/*l*·hr·cell x *l*/1000m*l* x 34.75m*l*. = 1.25 pmoles of lactate per hour per cell.

BCNU produced no change in this rate of rise of lactate levels at a dose of 100μM. However, 50μg/ml (89mM) of daunomycin produced a statistically-significant ($p \leq .01$) decrease in lactate production into the media, with an 18% lower concentration in media after 24 hours relative to untreated cells. Figure III - 3 gives a graphical representation of the aforementioned data. Figure III - 4 gives a similar representation of the effect of the 2 drugs on protein levels with time, which is a direct measure of cell detachment, presumably prior to cell death. This reveals a similar drop in protein levels (25.4% - $p < .05$) as measured by the Bio-Rad protein assay.

Amino Acid Analysis - HPLC

In control experiments, there was a net increase in concentration of only two amino acids - glutamate, which changed from 311 ± 11 mM at $t = 0$ to 1142 ± 18 mM at $t = 24$ hrs and alanine which rose from 132 ± 9mM at $t = 0$ hr to 355 ± 12mM at $t = 24$ hrs. Figures III - 5, III - 6 and III - 7 show the pattern of alteration in levels of a variety of amino acids over a 24 hour period in plates containing untreated D-54 MG cells. As can be observed from these graphs, the remainder of the amino acid levels decrease with time.

Treatment of D-54 MG cells with BCNU did not produce any significant differences in amino acid uptake in most amino acids studied. The only

possible exception is aspartate, although this increase was not statistically significant at 24 hours. (Figure III - 8).

Treatment of D-54 MG cells with daunomycin produced significant changes in most amino acids studied. The most profound change is again seen in glutamate levels which are significantly elevated over control at 12 hours ($p \leq .05$), with the 24 hour value being 234% higher than control values taken at the same point, a value which would be significant if not for the uncharacteristic 70-fold increase in standard deviation for the value at 24 hours. Other amino acid values are not only elevated with respect to control values but are also elevated from initial conditions. These include phenylalanine, tyrosine, threonine, aspartate, alanine, taurine and glycine with the latter two changing 250% ($p = .02$) and 60% ($p > .05$ - NS) over control values at 24 hours.

Table III - 1 summarizes the amino acid levels seen at 24 hour in control, BCNU and Daunomycin treated cells. There seem to be 3 different patterns of change seen in the time courses of amino acid levels. The first, exemplified in Figure III - 9 with glutamate but also seen with taurine and glycine, shows a large difference between daunomycin-treated cells and those in the other 3 groups. The second pattern (Figure III - 10) shows a net uptake of amino acid from the media in both untreated and BCNU-treated cells but daunomycin-treated cells reflecting values approaching those seen in media. This pattern is seen with valine, leucine, isoleucine, phenylalanine, tyrosine and threonine. The last pattern (Figure III - 11), seen with glutamine and asparagine produced little change in levels of these amino acids in daunomycin-treated cells over the duration of the experiment, although not only the control and BCNU values but the media values also decrease with time. GABA was not seen in any of the amino acid determinations.

Amino Acid Determinations - NMR.

Figure III -13 shows a typical ^{1}H NMR Spectrum taken of media surrounding D-54 MG cells. Although showing trends in relative values of alanine, glutamine and glutamate similar to those results obtained with HPLC, the standard deviation in values, sometimes exceeding 50%, prevented any differences from attaining statistical significance. Table III - 1 also records the increase, relative to control values for the three amino acids that could be adequately identified and separated from neighbouring peaks. Figure III - 12 shows the glutamate values in media, as determined by NMR spectroscopic techniques (cf. Figure III - 9), with untreated, BCNU and daunomycin-treated D-54 MG cells. Neither GABA nor N-acetylaspartate were observed in any NMR Spectra.

DISCUSSION

There are a number of results presented in the preceeding section that require closer examination. The Mer phenotype has been extensively studied as a predictor of tumour sensitivity to the nitrosourea class of chemotherapeutic agents[7,8]. Importance of this potential predictive ability is manifest in the status of nitrosoureas as the most commonly-used chemotherapy for gliomas with the mechanism of nitrosourea resistance postulated to be the repair of nitrosourea-mediated DNA damage by a methyl-reductase enzyme (Mer). The parent cell line of the D-54 MG tumour cell line, A-172, is Mer negative[9]. The results of the chemosensitivity studies on the D-54 MG cell line in this study however, are inconclusive, with a flattening of the cell survival curve at high drug doses. This flattening may be artifactual in nature owing to BCNU degradation between its administration to low-dose plates and high-dose plates.

The preliminary finding that daunomycin produced a cell kill comparable to that seen with BCNU at one-twentieth the dose confirms the findings of other recent, preliminary efficacy studies of this drug on in-vitro glioma cell lines[10,11]. A study by Matsumoto et al.[11] has shown that the IC_{50} of 5 glioma cell lines for adriamycin varies between 5 and 34 mM, with the A-172 line having an IC_{50} = 15.0±1.5 mM - one order of magnitude below our findings with daunomycin. Nevertheless, anthracycline derivatives have been shown to be more efficacious than BCNU in, albeit, a small number of glioma cell lines in-vitro. A more extensive, formal in-vitro comparison between these two treatment modalities remains to be performed. Anthracycline derivatives are used extensively in the treatment of other tumour types such as leukemias and lymphomas. Clinical studies have observed that even daunomycin concentrations below 100μg/ml in CSF can cause substantial morbidity (seizures) and mortality[12,13]. For this reason, neurochemotherapists have refrained from the use of this class of drugs in-vivo due to direct toxicity to normal brain. This remains a substantial problem to be overcome once in-vitro testing is completed. There are three mechanisms through which daunomycin (daunorubicin) is postulated to affect cells : 1) DNA intercalation; 2) inhibition of DNA topoisomerase II, preventing proper unwinding of DNA and 3) free radical formation. Since the first two mechanisms take one or more cell cycles to achieve a substantial effect, one can hypothesize that the majority of the early effects (within a few hours) of daunomycin seen on cell metabolism should be through the mechanism of free radical formation, producing reactive molecules interacting with cell membranes.

The preliminary finding of a substantial rise in glutamate and taurine as a result of daunomycin treatment and the accompanying decrease in lactate production, relative to control or BCNU-treated cells, may be an important external manifestation of the effect of environmental stresses on intracellular metabolic processes.

In studies on human glioma biopsies, there was a net uptake of glutamine, glutamate, alanine, valine, glycine, taurine, GABA and phenylalanine into the cell[14]. Neuroblastoma clones have shown uptake of tyrosine, tryptophan, phenylalanine and glycine that is concentration- dependent[15]. C6 rat glioma cells have been observed to avidly produce lactate, glycine and GABA and to take up glutamate, aspartate and glutamine[16].

Normal glia, when immersed in normal extracellular concentrations of amino acids, reveal a net intake of glutamine into the cell, but no net flux (ie. dynamic equilibrium) of either glutamate or taurine[17]. There is also no production of GABA in astrocytes because of absent glutamate decarboxylase (GAD) activity, although uptake from extracellular sources does occur[17]. C6 rat glioma cells therefore have at least one metabolic pathway substantially different from those present in human glia or glioma cells[16] (in-vivo ^{1}H NMR Spectroscopy has also been unable to observe GABA in human gliomas).

In control cells in this study, a net uptake of all studied amino acids (cf. Table 1), except glutamate and alanine, was observed. It has been shown that glutamine is metabolized principally to glutamate, which itself enters the Kreb's cycle (through alanine and α-ketoglutarate)[18]. There is also a decreased flux of all substrates through both this cycle and the cytochrome chain, due to decreased activity of some TCA enzymes as well as cytochrome oxidase, in systems such as glioma cells that have a relative dependence on aerobic glycolysis for energy production[19-22]. It is

therefore possible to hypothesize that in the event of an extracellular excess of glutamine, a condition not observed in other studies, that an excess of glutamate may arise if the rate of glutamate synthesis from glutamine exceeds the rate of entry of glutamate into the Kreb's cycle. In such a case, a net efflux of glutamate may occur.

Although the total rate (including deamination) may possibly be slower than that of glutamine synthesis, the rate of transamination of glutamate alone (aspartate aminotransferase) may still be fast enough to produce an excess of alanine, which may then be excreted and therefore account for the net increase in alanine concentration seen in this study. Recent data does point to an alteration in GDH isoenzyme type present in a human glioma cell line[23]. This may produce a decreased rate of deamination, leaving additional glutamate for transamination. In any event, many further studies would need to be performed, including the use of radioactive tracers, to lend credence to this hypothesis.

It was also observed in this study that, under stress, the release of glutamate markedly increased and that taurine levels were also elevated (as compared to a slight decrease in control cells). Work with normal glial cells suggests that hypoxic, hypoglycemic or ischemic stress does not produce an efflux of glutamate[24]. However, the application of hypoosmotic stress does elicit a significant efflux of both glutamate and taurine[25]. Taurine is postulated to act as an inhibitory neuromodulating substance, antioxidant and osmoregulator. Its release is slower in onset and in its time to peak values than the stimulated release of glutamate under the same conditions[26]. In addition, taurine release is dependent on both K^{+}[27] and glutamate levels[25] in the extracellular space. Therefore, it may be possible that the action of daunomycin at the cell membrane level may induce a release of both glutamate and taurine into the surrounding medium.

^{1}H NMR Spectroscopy could potentially provide useful data on metabolite concentrations in-vivo but it is hampered by its inherent lack of sensitivity, and decreased precision relative to commonly-used in-vitro techniques such as HPLC and enzymatic assays. Results from this study lend strong credence to these assertions, especially with data obtained under controlled in-vitro conditions. If one adds the confounding variables of tissue inhomogeneity, hidden peak components, decreased S/N in whole-body systems (resulting in longer scan times and lower absolute S/N) as well as increased peak broadening and localization error, it may be difficult to accurately determine in-vivo metabolite levels. Solutions to these conundrums await further technical advances.

In summary, the metabolism of glucose and glutamine in glioma cells and their relationship to the metabolic pathways in normal glia is complex. The preliminary findings of this study reveal that under conditions of excess glutamine, there is a net efflux of glutamate and alanine, of unknown origin, from untreated D-54 cells. Furthermore, daunomycin was found to be more efficacious than BCNU in preventing D-54 MG colony formation and its application resulted in a net increase in efflux of both glutamate and taurine from these glioma cells. ^{1}H NMR spectroscopy incurred greater errors than HPLC or enzymatic techniques in determining metabolite concentrations in complex solutions of biological origin in-vitro. Metabolic pathways underlying these metabolite fluxes and the observation of these fluxes in-vivo remain to be observed.

REFERENCES

1) Warburg, O. The Metabolism of Tumors. London: Constable and Co., 1930.

2) Nicklas, W.J. Amino acid metabolism in glial cells: homeostatic regulation of intra- and extracellular milieu by C-6 glioma cells. J. Neurochem., 30 : 955-963, 1978.

3) Petroff, O.A., Ogino, T., and Alger, J.R. High-resolution proton magnetic resonance spectroscopy of rabbit brain: regional metabolite levels and postmortem changes. J. Neurochem., *51* : 163-171, 1988.

4) Felber, S., Sauter, R., and Aichner, F. Localized ^{1}H Spectroscopy applied to cerebral neoplasms and ischaemia at a clinical 1.5T MR-system. *In* : Book of Abstracts, Society of Magnetic Resonance in Medicine, vol. 1, p. 450. Berkeley: Society of Magnetic Resonance in Medicine, 1989.

5) Barany, M., Venkatasubramanian, P.N., Dew, L.L., Glick, R.P., and Greenberg, I.M. Analysis of human brain tumors by proton magnetic resonance spectroscopy in vivo. *In* : Book of Abstracts, Society of Magnetic Resonance in Medicine, vol. 1, p. 429. Berkeley: Society of Magnetic Resonance in Medicine, 1989.

6) Marbach, E.P., and Weil, M.H. Rapid enzymatic measurment of blood lactate and pyruvate. Clin. Chem., *13* : 314-325, 1967.

7) Scudiero, D.A., Meyer, S.A., Clatterbuck, B.E., Mattern, M.R., Ziolkowski, C.H.J., and Day III, R. Relationship of DNA repair phenotypes of human fibroblasts and tumour strains to killing by N-methyl-N'-nitro-N-nitrosoguanidine. Cancer Res., *44* : 961-969, 1984.

8) Scudiero, D.A., Meyer, S.A., Clatterbuck, B.E., Mattern, M.R., Ziolkowski, C.H.J., and Day III, R. Sensitivity of human cell strains having different abilities to repair O^{6}-methylguanine in DNA to inactivation by alkylating agents including chloroethylnitrosourea. Cancer Res., *44* : 2467-2474, 1984.

9) R. Day III, Ph.D., Cross Cancer Institute, University of Alberta (personal communication).

10) Stewart, D.J., Maroun, J., and Verma, S. Phase I study of once-weekly IV Menogaril. Proc. Amer. Assoc. Cancer Res., *28* : 189, 1987.

11) Matsumoto, T., Tani, E., Kaba, K., Shindo, H., and Miyaji, K. Expression of P-glycoprotein in human glioma cell lines and surgical glioma specimens. J. Neurosurg. (submitted for publication), 1990.

12) Pittrova, H., Koza, V., Vozobulova, V., and Cetkovsky, P. Treatment of medium and highly malignant non-Hodgkin's lymphoma with combined chemotherapy using methotrexate, adriamycin, cyclophosphamide, vincristine, prednisone and bleomycin (protocol MACOP-B). (Czech.). Vnitr.-Lek. 35 : 1177-1182, 1989.

13) Silber, R., Potmesil, M., and Bank, B.B. Studies on drug resistance in chronic lymphocytic leukemia. Adv. Enzyme Regul., 29 : 219-228,1989.

14) Snodgrass, S.R., and Iversen, L.L. Amino acid uptake into human tumors. Brain Res., 76 : 95-107, 1974.

15) Archer, E.G., Breakefield, X.O., and Sharata, M.N. Transport of tyrosine, phenylalanine, tryptophan and glycine in neuroblastoma clones. J. Neurochem., *28* : 127-135, 1977.

16) Nicklas, W.J. Amino acid metabolism in glial cells: homeostatic regulation of intra- and extracellular milieu by C-6 glioma cells. J. Neurochem., 30 : 955-963, 1978.

17) Schousboe, A., Larsson, O.M., Krogsgaard-Larsen, P., Drejer, J., and Hertz, L. Uptake and release processes for neurotransmitter amino acids in astrocytes. *In* : Norenberg, M.D., Hertz, L., and Schousboe, A. (eds.), The Biochemical Pathology of Astrocytes : Neurology and Neurobiology, Vol. 39, Chan-Palay, V., and Palay, S.L., (eds.). pp. 381-394. New York: Alan R. Liss, Inc., 1988.

18) Hertz, L., Murthy, Ch. R.K., and Schousboe, A. Metabolism of glutamate and related amino acids. *In* : Norenberg, M.D., Hertz, L., and Schousboe, A. (eds.), The Biochemical Pathology of Astrocytes : Neurology and Neurobiology, Vol. 39, Chan-Palay, V., and Palay, S.L., (eds.). pp. 395-406. New York: Alan R. Liss, Inc., 1988.

19) Allen, N. Cytochrome oxidase in human brain tumors. J. Neurochem., *2* : 37, 1957.

20) Viale, F.L. Biochemical patterns in brain tumors, II. Enzymes of the tricarboxylic acid cycle, Acta Neurochir., *20* : 273-279, 1969.

21) Lowry, O.H., Berger, S.J., Carter, J.G., Chi, M.M.-Y., Manchester, J.K., Knor, J., and Pusateri, M.E. Diversity of metabolic patterns in human brain tumors: Enzymes of energy metabolism and related metabolites and cofactors. J. Neurochem., *41* : 994-1010, 1983.

22) Marzatico, F., Curti, D., Dagani, F., Silvani, V., Gaetani, P., Butti, G., and Knerich, R. Enzymes related to energy metabolism in human gliomas. J. Neurosurg. Sci., *30* : 129-132, 1986.

23) Hussain, M.M., and Vassilis, I.Z. Characterization of glutamate dehydrogenase isoproteins purified from the cerebellun of normal subjects and patients with degenerative neurological disorders, and from human neoplastic cell lines. J. Biol. Chem., *264* : 20730-20735, 1989.

24) Drejer, J., Benveniste, H., Diemer, N.H., and Schousboe, A. The cellular origin of ischemia-induced glutamate released from brain tissue in vivo and in vitro. J. Neurochem., *45* : 145-151, 1985.

25) Dutton, G.R., and Philibert, R.A. Taurine release from cultured astrocytes. *In* : G. Levi, (ed.), Differentation and Function of Glial Cells, pp. 235-241. New York: Wiley-Liss, 1990

26) Philibert, R.A., Rogers, K.L., Allen, A.J., and Duton, G.R. Dose-dependent, K+-stimulated efflux of endogenous taurine from primary astrocyte cultures is Ca^{2+}-dependent. J. Neurochem., *51* : 122-126, 1988.

27) Walz, W., Swelling and potassium uptake in cultured astrocytes. Can. J. Physiol. Pharmcol., *65* : 1051-1057, 1987.

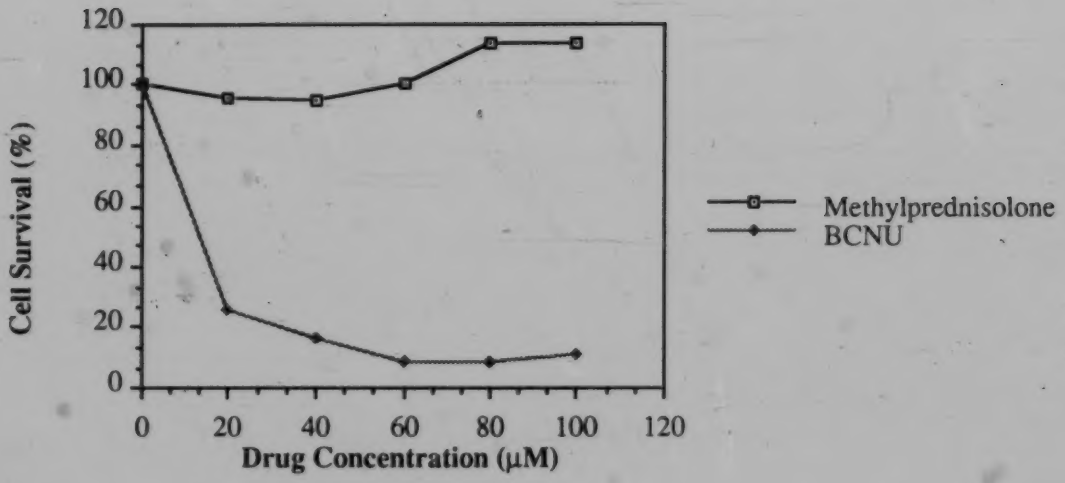

Figure III - 1. Colony-formation chemosensitivity assay of D-54 MG human glioma-derived cells after treatment with Methylprednisolone (control) and BCNU (experimental).

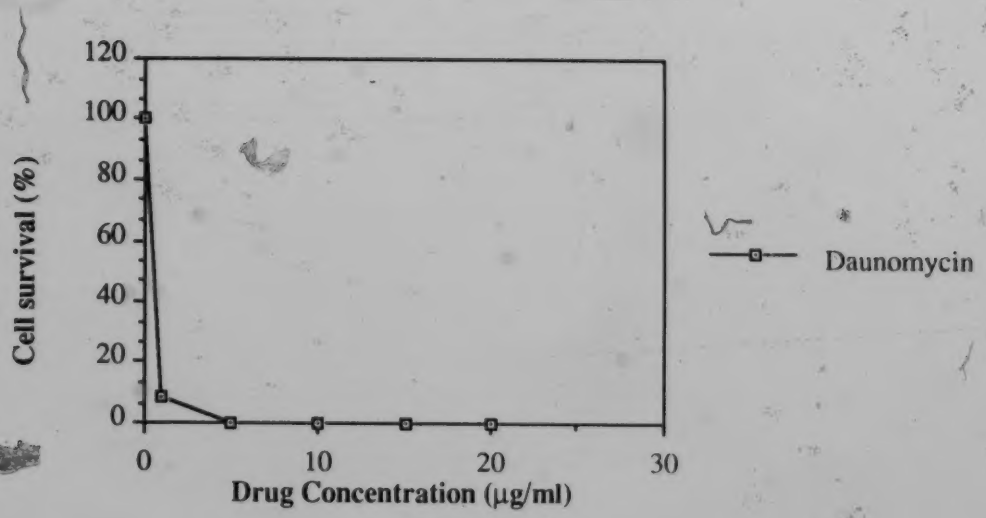

Figure III- 2. Colony-formation chemosensitivity assay of D-54 MG human glioma-derived cells after treatment with Daunomycin (experimental).

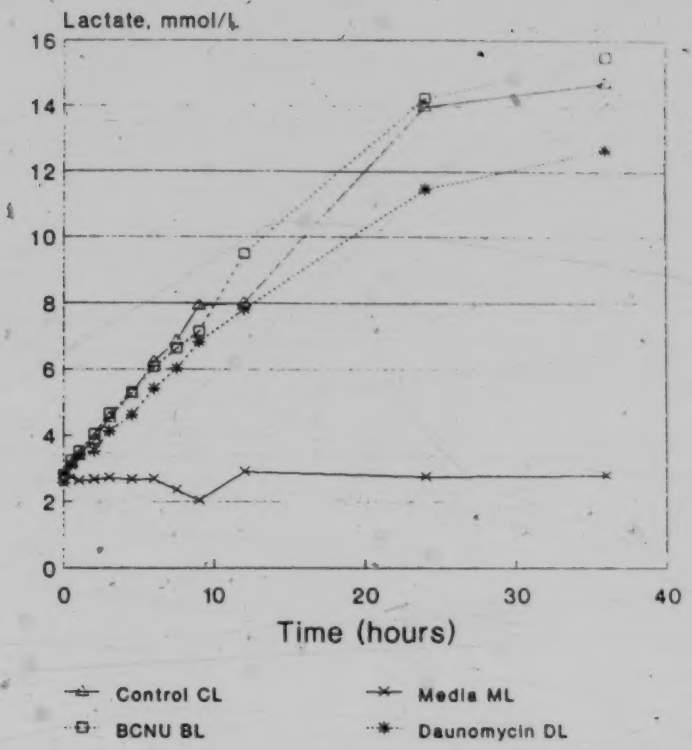

Figure III - 3. Representation of Media Concentration of lactate (mM) vs. time (hrs.). Incubation with D-54 MG cells.

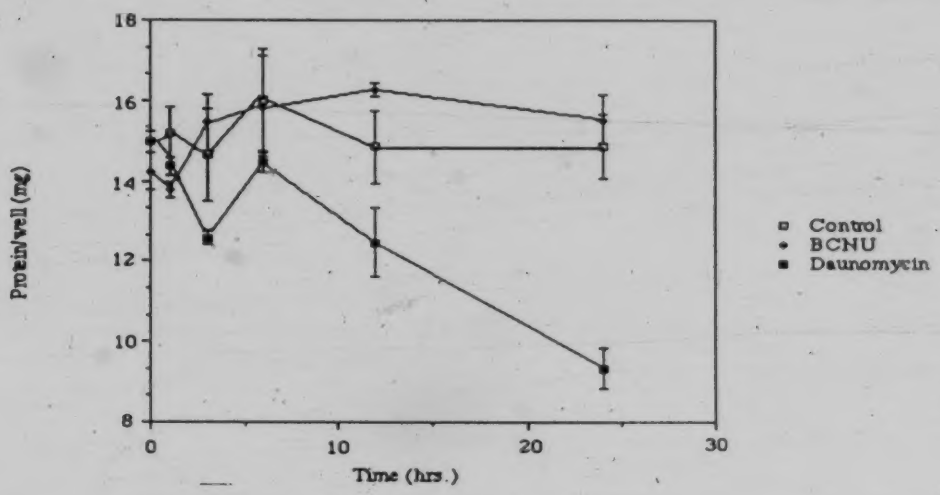

Figure III - 4. Representation of Protein levels (mg/plate) vs. time. Incubation with D-54 MG cells.

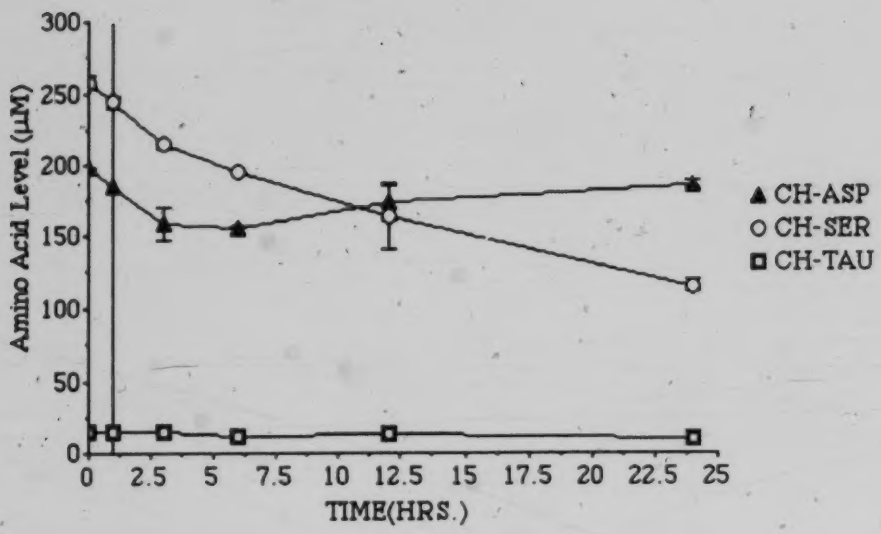

Figure III - 5. Aspartate (CH-ASP), serine (CH-SER) and taurine (CH-TAU) levels in the incubation medium of untreated D-54 MG cells with time.

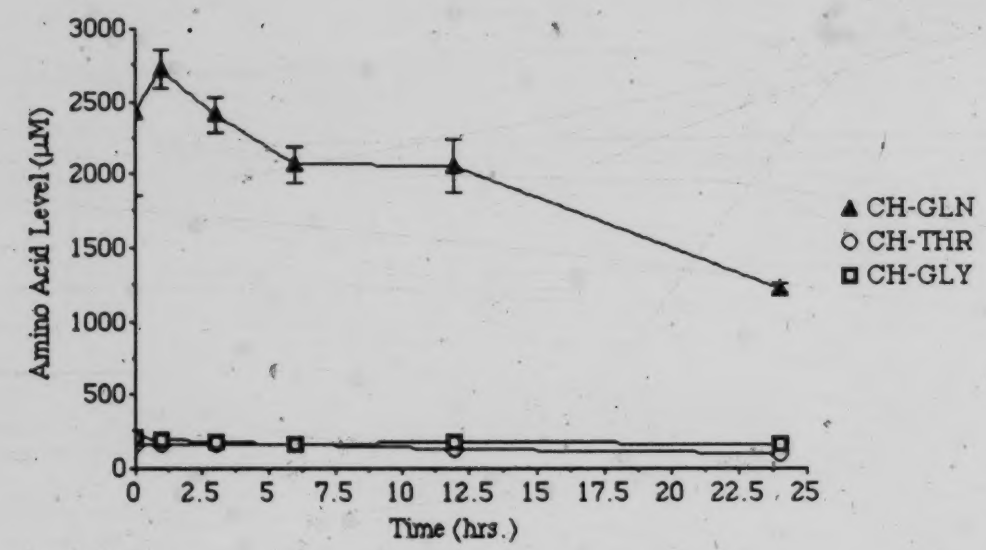

Figure III - 6. Threonine (CH-THR), glycine (CH-GLY) and glutamine (CH-GLN) levels in the incubation medium of untreated D-54 MG cells with time.

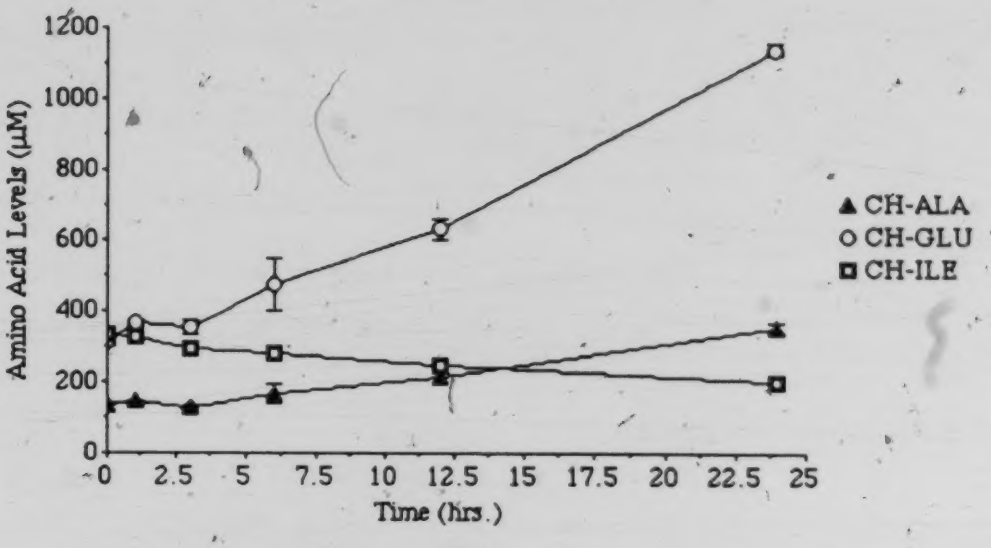

Figure III - 7. Glutamate (CH-GLU), alanine (CH-ALA) and isoleucine (CH-ILE) levels in the incubation medium of untreated D-54 MG cells with time.

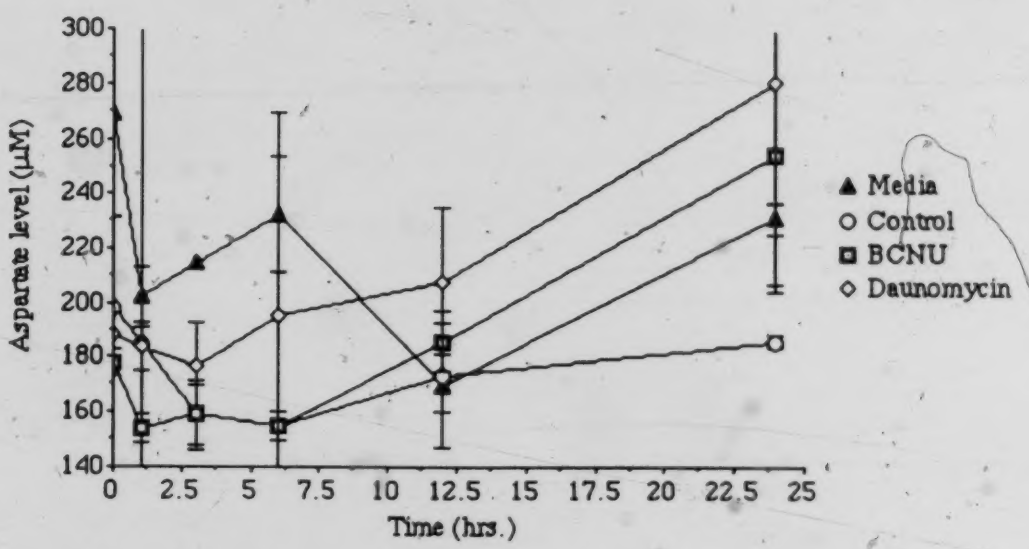

Figure III - 8. Aspartate levels in incubation medium of untreated (control), BCNU- and Daunomycin-treated D-54 MG cells with time.

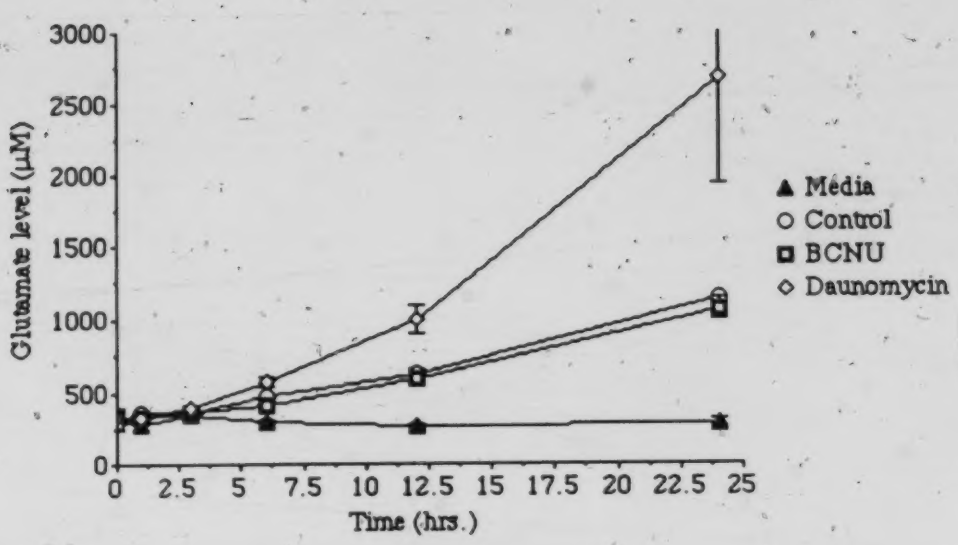

Figure III - 9. Glutamate levels in incubation medium of untreated, BCNU- and Daunomycin-treated D-54 MG cells with time, as determined by HPLC.

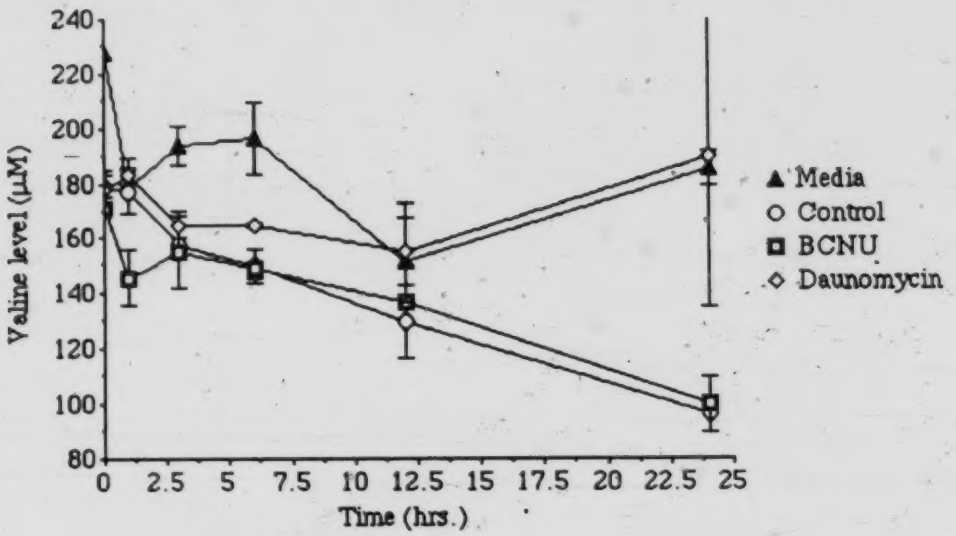

Figure III - 10. Valine levels in incubation medium of untreated, BCNU- and Daunomycin-treated D-54 MG cells with time, as determined by HPLC.

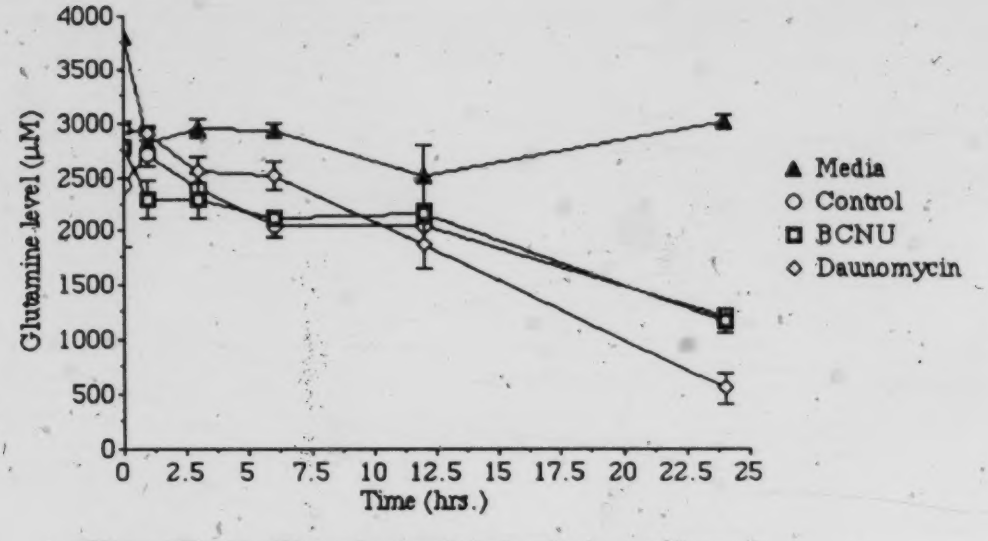

Figure III - 11. Glutamine levels in incubation medium of untreated, BCNU- and Daunomycin-treated D-54 MG cells with time, as determined by HPLC.

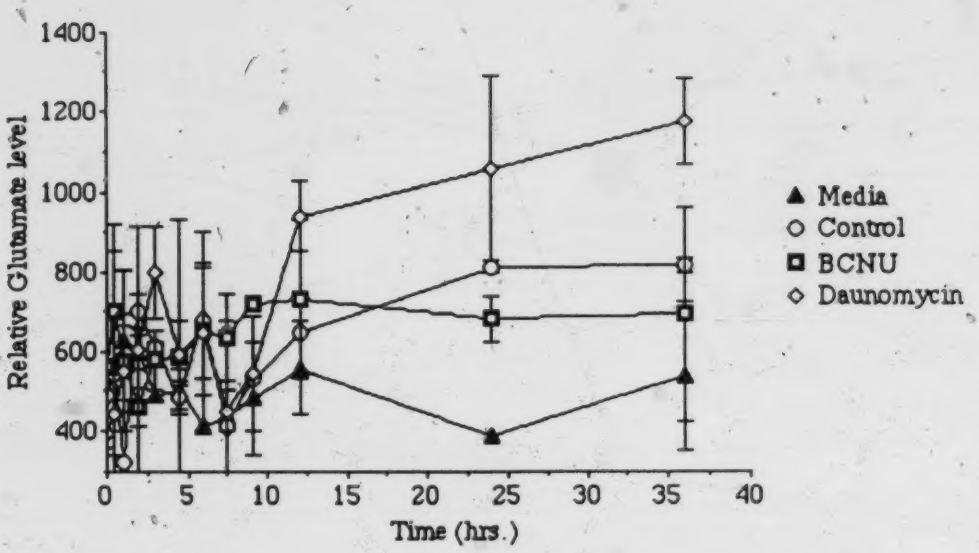

Figure III-12. Glutamate levels in incubation medium of untreated, BCNU- and Daunomycin-treated D-54 MG cells with time, as determined by integration of peak areas in 1H-NMR spectra. Reference is glutamate level from the most accurately determined peak area (t = 9 hrs.).

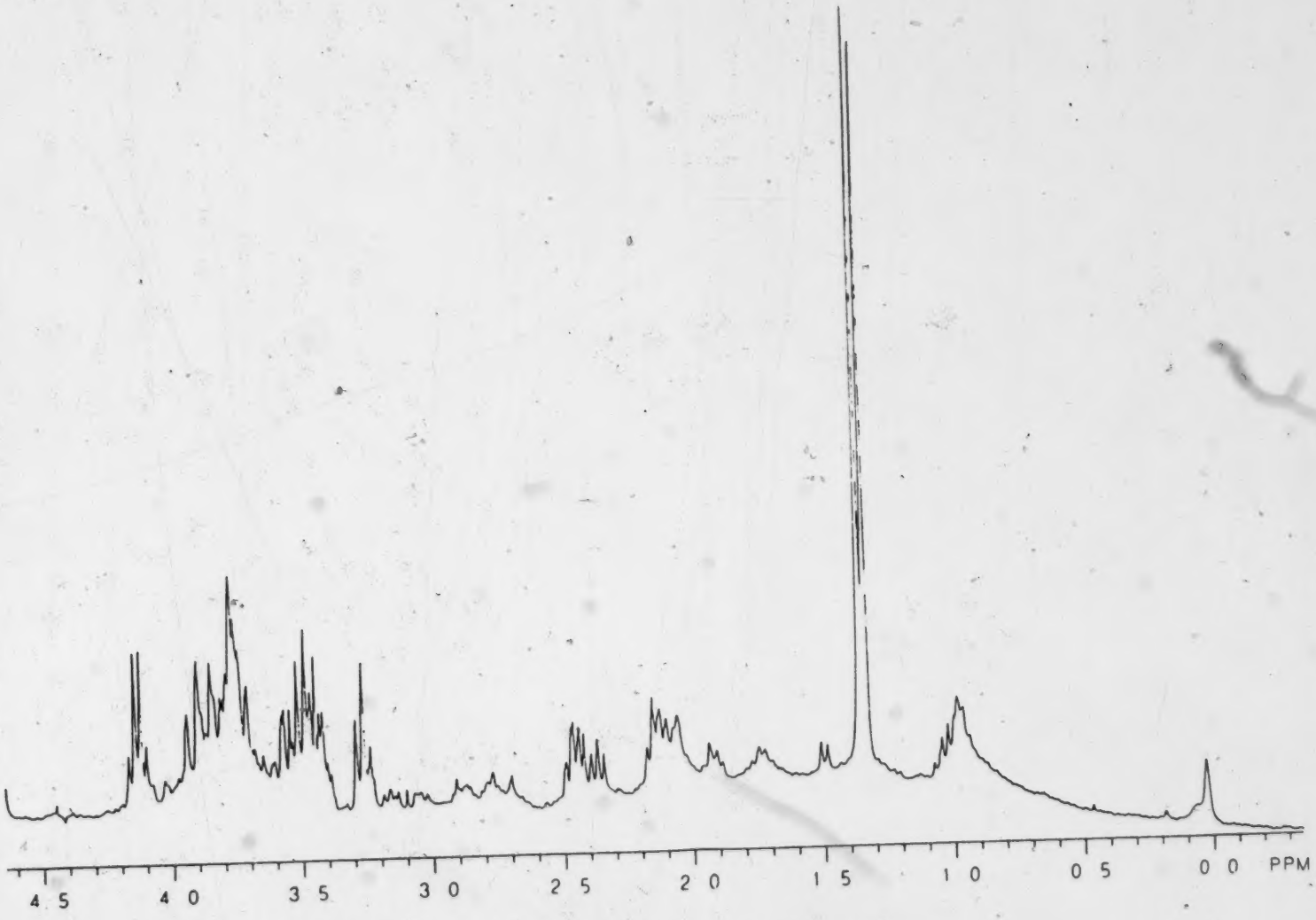

Figure III - 13. Typical representation of 1H-NMR Spectrum taken of medium incubating untreated D-54 MG cells.

Amino Acid	HPLC Analysis			1H - NMR Analysis		
	C - 24	B - 24	D - 24	C - 24	B - 24	D - 24
Taurine	10±0	7±1	39±6	-------	---------	-------
Threonine	104±0	89±2	208±83	-------	---------	-------
Asparigine	205±1	198±6	284±0	-------	---------	-------
Glycine	166±1	147±4	333±103	-------	---------	-------
Valine	97±1	123±5	189±54	-------	---------	-------
Methionine	125±105	47±4	98±27	-------	---------	-------
Leucine	127±98	207±4	346±94	-------	---------	-------
Phenylalanine	58±0	51±4	118±37	-------	---------	-------
Aspartate	186±2	254±47	281±77	-------	---------	-------
Serine	115±4	85±11	250±82	-------	---------	-------
Glutamate	1142±18	1072±80	2673±741	808±9	682±57	1059±232
Glutamine	1225±32	1183±102	562±147	769±99	647±97	557±153
Alanine	355±12	269±29	425±127	520±109	309±38	552±211
Isoleucine	198±5	216±2	300±80	-------	---------	-------
Tyrosine	62±1	58±6	109±33	-------	---------	-------

Table III - 1. Amino acid levels seen at t = 24 hours, in medium incubating D-54 MG cells, as determined by HPLC and 1H-NMR.
* indicates significance level of $p < .05$.

CHAPTER IV - IN-VITRO AND IN-VIVO LOCALIZATION OF GM2 GANGLIOSIDE TO D-54 MG HUMAN GLIOBLASTOMA-DERIVED CELLS USING IMMUNOHISTOCHEMICAL TECHNIQUE

INTRODUCTION

Gangliosides are integral components of cellular plasma membranes. Previous studies have noted that species with higher levels of CNS organization tend also to contain higher levels of gangliosides[1]. Humans have been observed to harbour the highest ganglioside content among 150 species studied, with human brain tissue having the highest levels of any human organ - gangliosides representing 15% of the total lipid content of neuronal plasma membranes[1]. The function of gangliosides remains unclear although their expression seems to correlate with differentiation of embryonic and tumour cells in-vitro[2]. These molecules may also be involved in cell-cell communication[3], as well as synaptogenesis[4].

Ganglio- series gangliosides (GalNacβ- Galβ) - Glc-Cer) predominate within membranes of CNS cells, with both levels of particular gangliosides and their anatomical distribution adhering to a prescribed pattern of expression. This expression pattern is itself modulated in accordance with the different stages of CNS development. The level of gangliosides is highest in grey matter, substantially lower in white matter and decreased even further in glial-derived tumours[5]. Analysis of ganglioside content in human gliomas reveals a pattern that is substantially altered with respect to both the total number of gangliosides found as well as the quantity of selected ganglioside components. Specifically, the ganglioside most abundantly expressed in adult brain is GD1b, followed by GT1, GD1a and GM1[6]. The major brain ganglioside in human glioma biopsies is GD3, followed by GD1a, GD1b and

GT1b[7,8]. Although not as prevalent overall, major relative increases have been noted in the expression of both GM2 and GD2 in these tumours[8]. Moreover, in-vitro cell culture of glioma cell lines has revealed that although GM2 is present in small quantities in normal brain, it was found to be a major glioma-associated ganglioside, expressed in 17/19 cell lines tested and representing 42-63% of total ganglioside content in eight of these cell lines[9].This makes the GM2 ganglioside potentially useful in techniques utilized to discriminate between normal and gliomatous tissue.

The D-54 MG human glioblastoma-derived cell line in particular has been shown by gel electrophoresis to contain GM2, when grown in-vitro. This tumour cell line has also been intracerebrally implanted as a xenograft in a large-animal tumour model, using cats immunosuppressed with Cyclosporin A.

The 10-11 monoclonal antibody has been found to bind specifically to the GM2 ganglioside in tumour tissues of various types. The purpose of this study, therefore, is two-fold :

1) To determine the presence of GM2 ganglioside within intracerebrally-implanted D-54 MG xenografted tumours;

2) To present preliminary radioimmunoscintigraphic data obtained after the administration of ^{131}I-labelled 10-11 MAb into the intrathecal space of D-54 MG tumour-bearing cats.

METHODS AND MATERIALS

Immunohistochemical Staining of Cultured Cells

D-54 MG cells (passage number 70) were maintained in Nunc LabTek 8-chamber slides using RPMI 1640 culture medium supplemented with 10% heat-sterilized fetal calf serum and antibiotics (Penicillin/Streptomycin). Cells were quickly rinsed with PBS three times at 22°C (RT), then fixed with 2% glutaraldehyde in PBS for 3 minutes. Reduction of nonspecific background staining was performed with 10% horse serum in PBS for 30 minutes. Cells were rinsed then incubated with primary antibody, which was left for 24 hours at room temperature (22°C). Cells were then rinsed three times with PBS. Secondary antibody was then applied for 1 hour at RT. After three PBS washes in 30 minutes, avidin-biotin complex (Vector) was applied for 1 hour at RT. Cells were then rinsed with PBS and chromogen applied for approximately 5 minutes (until deep brown staining observed in positive wells). Counterstaining was then performed with hematoxylin and Scott's tap water after rinsing with 0.1M Tris buffer and distilled water. Primary antisera used were purified monoclonal IgM mouse antibody to GM2 ganglioside 10-11 (courtesy of Dr. P. Livingston, Memorial Sloan-Kettering Institute) at 5mg/ml concentration; purified mouse IgG monoclonal antibody MOPC-21 (Sigma) at 1:100 dilution; purified IgM monoclonal antibody to CA50 antigen C-50 (Pharmacia, Sweden) at 1:4 dilution. Secondary antisera used were biotinylated anti-mouse IgM (γ chain-specific) (Vectorlabs) at 1:100 dilution and biotinylated anti-mouse IgG (μ chain-specific) at 1:200 dilution (Zymed; California, U.S.A.). Chromogen was made up just before application - 0.01g diaminobenzidine tetrachloride (DAB) dissolved in 20ml 0.1M Tris buffer at 4 °C. 70µl of 3% hydrogen peroxide was added, the pH adjusted to 7.68 and solution filtered through a 0.45µm filter.

Immunohistochemical Staining of Tissue Sections

D-54 MG cells were implanted into cat cerebral cortex, 10 days after cats had been initiated on an immunosuppressive regimen of Cyclosporin A (120 mg PO/day). NMR Imaging was performed to assess tumour size at 3 weeks post-implantation . Tumour-bearing cats were sacrificed after evidence of mass effect had been noted. Brains were removed after intracardiac perfusion with 2% glutaraldehyde at 4 ^{o}C. Whole brains were further fixed with 2% glutaraldehyde for 24 hours, followed by 20% sucrose for a further 24 hours to cryoprotect tissue. Brain tissue was then sectioned and tumour-bearing blocks were covered with Tissue-Tek OCT Compound. Blocks were then immersed in isopentane maintained at 77 ^{o}K. After flash freezing, 6 µm. thick frozen sections were cut at -20 ^{o}C and sections placed on individual glass slides. Immunohistochemical staining was then performed as described above. Stained sections were coverslipped with glycerol-gelatin (Sigma). Sections were also stained with hematoxylin and eosin to further delineate tumour.

Radioimmunoscintigraphic Studies

Two cats (1 bearing D-54 MG intracranial tumour; 1 control cat) were utilized in this preliminary experimental series. D-54 MG human-glioma bearing cat was imaged using a 2.35T 40cm-bore Bruker NMR Spectrometer, 21 days after tumour implantation. During imaging, tumour size was more accurately delineated using IV administration of Gadolinium-DTPA (0.2 ml/kg over 2 minutes) coupled with the use of a spin-echo sequence - T_R = 600 ms and T_E = 26 ms. 24 hours after tumour visualization, a 4-French Silastic® catheter was implanted into the intrathecal space with its tip situated 3 mm inferior to the inferior margin of the fourth ventricle. The

non-tumour bearing cat was catheterized in the same fashion. Cyanoacrylate adhesive and fascial sutures were utilized to fix the catheter in place. The distal end was connected to a small (0.1cc) reservoir above the skin surface and the 3 cm. incision (at the level of the upper cervical vertebrae) was closed in layers with 3-0 Dexon.

Anti-GM2 monoclonal antibody 10-11 (IgM) and anti-myeloma protein MOPC-21 (IgG) were labelled using the iodogen method, with ^{131}I and ^{125}I, respectively. The resultant immuno-reactivities were then compared to those of unlabelled antibodies using an ELISA assay - absorption being determined by a Titertek Multiscan Plate Reader with filters set at 405 and 540nm. 4,8-diaza-3,6,6,9-tetramethylundecane-2,10-dione-bisoxime (HMPAO) was also labelled with ^{99m}Tc 10 minutes before administration. Both cats were anaesthetized with IV Saffan (Alphaxolone - alphadolone; Glaxovet, U.K.) (1ml/kg induction dose with 0.5 ml maintenance doses titrated to respiratory rate and corneal reflex) and injected IV with 40MBq ^{99m}Tc-labelled HMPAO. A series of radio-immunoscintographic scans were then taken at 10, 30 and 60 minutes post injection using a Searle PHo/gamma IV Camera coupled to a low-energy (^{99m}Tc) parallel-hole collimator. Data acquisition was performed using an on-line ADAC CAM II clinical acquisition processing unit. After the 99mTc study was complete, both cats were given a bolus of (37MBq of ^{131}I-labelled 10-11 + 17MBq ^{125}I-labelled MOPC-21) in a total volume of 0.5ml. into the intrathecal space. Radioimmunoscintigraphic scans were then performed of both head and body gamma emissions at t = 0.1, 1 and 24 hours (control cat) and at t = 0.1, 1, 20 and 24 hours (D-54 MG tumour-bearing cat). Cats were then sacrified and appropriate organs removed, weighed and samples placed in scintillation vials for a differential (^{131}I vs ^{125}I) count using a Beckman

gamma counter. Before sectioning, the removed D-54 MG-bearing brain was placed on the gamma-camera in an attempt to visually distinguish tumour from surrounding brain. Thereafter, percentage dose/gm tissue values were then determined for both ^{131}I and ^{125}I-labelled MAb's using a calculated injected dose of 1.0×10^9 cpm for ^{125}I and 1.15×10^9 cpm for ^{131}I.

RESULTS

In-Vitro Immunohistochemical Studies

The specificity of anti-GM2 ganglioside immunostaining of D-54 MG human glioblastoma-derived cells is illustrated in Figure IV - 1. D-54 MG cells in culture show marked reactivity to the 10-11 monoclonal antibody, indicating the presence of GM2 antigen. At higher magnification , it can be discerned that most of this staining is observed to be forming a ring at the cell membrane. An irrelevant antibody, C-50, of the same isotype (IgM) showed essentially no staining of D-54 MG cells. Both C-50 (IgM) and MOPC-21 (IgG) were used as negative antibody controls for this experiment, both of which remained unstained. Negative controls for technique included incubation without primary antibody followed by either anti-IgG or anti-IgM secondary antibodies. These two wells also showed no reactivity.

In-Vivo Immunohistochemical Determinations

The relative specifity of 10-11 monoclonal antibody for intracerebrally xenotransplanted D-54 MG cells in cat brain can be seen in Figures IV - 2 to IV - 5. The distribution of staining is determined by the location of the tumour. The ring-like distribution in immunostaining of cells (Fig. IV - 3) provides additional evidence of

the cell surface location of GM2. Staining with a non-specific antibody (MOPC-21) is negative (Figure IV - 5) as is immunostaining (of tissue sections) without the use of primary antibody.

Preliminary tests compared three different methods of fixation. Perfusion and immersion of brain for 24 hours was performed in : 1) 4% formalin; 2) 4% paraformaldehyde and 3) 2% glutaraldehyde. It was found that the intensity of staining with 10-11 MAb was most marked with the 2% glutaraldehyde, although the brain was only lightly fixed for distances greater than 5mm deep to the cortical surface.

Radioimmunoscintigraphic Studies (Preliminary Results)

Gamma-camera images obtained from the heads of both the control and tumour-bearing cats are shown in Figures IV - 6, 7 and 8. There is no visible difference in the distribution of ^{131}I-10-11 antibody at t = 0.1 and 1 hours between the control and D-54 MG bearing cat, which was implanted 5mm posterior to the coronal suture and 2mm to the right of midline. At 20 hours, there is a suggestion of increased uptake anterior to the main antibody depot, present also on a lateral image, in the head of the tumour-bearing cat. This phenomenon disappears, however, at 24 hours with both control and experimental head scans showing no visible difference in appearance. An extrathecal depot of ^{131}-labelled MAb, formed possibly due to inadequate sealing of the CSF entry point of the intrathecal catheter. This depot was found to contain approximately 90% of the injected dose of ^{131}I and therefore reduced the total intrathecal dose to this degree.

Body scans done at t = 0.1, 1 and 24 hours revealed a progressively increasing degree of antibody uptake in the spleen with time (Figure IV - 9 and 10). This,

however,may be influenced in part by slow leakage of antibody from extrathecal depot into the circulation. Distribution of the antibody inferiorly into the spinal intrathecal space was also noted, especially in the D-54 MG-bearing cat.

An autopsy performed on the D-54 MG cat at 24 hours post-MAb administration revealed a superficially-growing intracerebral tumour, yellowish-white in colour, measuring 5mm (L) x 3mm (W) x 2mm (D). This correlated well with a Gd-DPTA enhanced NMR image performed at 21 days post-implantation, which showed blood-brain barrier disruption extending 2-3mm. deep to the cortical surface on the right side, near the midline (Fig. IV - 12). A gamma camera image performed on the dissected brain, however showed no asymmetries in the count distribution.

Analysis of ^{131}I and ^{125}I-MAb uptake (Table IV - 1) in different organs, revealed that the tumour uptake/gm tissue of ^{131}I - 10-11 was 2.77 times greater than uptake of the surrounding tissue in the ipsilateral parietal lobe. However, it was also noted that uptake of the control MAb (MOPC-21), relative to surrounding brain, was elevated to the same degree. Splenic uptake was shown to be the highest of any extracerebral organ, confirming the in-vivo results but ^{125}I counts more than doubled those from ^{131}I. On an organ-by-organ basis, the whole liver uptake however, exceeded that of the spleen. Total body counts were low, again possibly because of the effect of an extrathecal depot of ^{131}I and ^{125}I-labelled MAb's.

DISCUSSION

The antigen specificity of the monoclonal antibody 10-11 has been well characterized by Natoli et al.[10] 10-11 MAb has been found to be non-reactive to a variety of gangliosides including GM1, GD1a, GT1, GD2, asialo-GM2, GM3, GD3 and GD4. Competitive inhibition assays using GM2 also produced specific inhibition

of immunoreactivity of the 10-11 monoclonal antibody. The use of the C-50 antibody as negative control was predicated on the absence of reactivity of this MAb in previous ELISA studies on the D-54 MG cell line (data not shown) as well as a finding by Svennerholm et al.[11], based on an electrophoretic analysis.This data showed that the CA-50 antigen could not be detected in extracts of D-54 MG grown in tissue culture, which was surprising in light of the fact that CA50 (3'-iso-LM1) antigen is the major monosialyted ganglioside in D-54 MG cells when grown as a solid tumour subcutaneously in nude mice[12]. The in-vitro studies performed in this paper provide preliminary confirmation the previous studies[12,13] showing the presence of GM2 as well the absence of CA50 antigen in D-54 MG cells grown in-vitro.

The normal distribution of GM2 ganglioside in humans is restricted to CNS tissues in adults but is also present on the surface of many embryonic cells. This is in contrast to the mouse where GM2 has also been found in liver[14]. In malignant tissue, GM2 has been isolated in tumours of neuroctodermal origin, including melanomas and neuroblastomas[15]. Glioma tissue, in the form of fresh biopsy material or grown in monolayer culture, has been shown to contain GM2 (as well as GD2 and GD3) in far higher concentrations than normally found in adult CNS tissue[7,8]. In fact, 17 of 19 human glioblastoma-derived cell lines were found to contain GM2, with the GM2 content in 8 of these lines representing 42-63% of the total ganglioside content of these cells[9]. The D-54 MG cell line when grown in tissue culture, produced GM2 more than any other monosialyted ganglioside (with GD1a being the major oligosialyted ganglioside component)[13]. Serious consideration however, was given to antigenic modulation of this ganglioside, in light of the presence of this phenomenon with the CA50 antigen in the same cell line. The results of the in-vivo immunohistochemical studies in this study show that considerable amounts of GM2

are produced by these cells, despite a marked environmental transition from cell culture medium to immunosuppressed xenogeneic cerebral tissue. In addition, although the majority of the tumour cells stained positively, there was a considerable degree of heterogeneity in antigen expression within the tumour mass.

Radioimmunoscintigraphic studies have been performed on patients harbouring malignant gliomas as early as 1951[16]. The earliest use of a radioactively-labelled monoclonal antibody as a putative targetting agent for glioma localization in humans was recorded by Phillips et al. in 1983[17]. Since that time, a number of studies of this type have been performed using both intravenous and intrathecal administration routes. In a preliminary study, Kemshead et al.[18] could not demonstrate specific uptake of ^{131}I-labelled UJ13A MAb injected intravenously, but showed up to 20:1 specificity ratio after intrathecal administration of ^{131}I-UJ 181.4 (specific) and ^{125}I-HMFG2 (nonspecific) into a pineoblastoma-bearing patient. In 1986, Richardson et al.[19] showed that intravenous administration of MAb (UJ-13A) in glioma patients resulted in a biological t 1/2 = 179 hrs. in tumour compared with 130 hrs. from normal brain. The disappearance of this antibody from blood was found to be biexponential with average $t_{1/2}$'s of the fast and slow components, being 1.8 and 53 hrs., respectively. Sequestration of the injected dose in those studies was found to take place in the liver. Further study of the intrathecally-dosed pineoblastoma patient revealed a biological $t_{1/2}$ (UJ 181.4) of between 150 and 250 hours whereas CSF concentrations of both specific and irrelevant antibodies decreased with a t 1/2 of 12.7 - 16.9 hrs[20]. Moreover, intrathecally-injected MAb was found to be present in greatest amounts in the periventricular white matter and in the leptomeninges (caudate nucleus did not show MAb accumulation)[21]. In contrast to intravenous studies,

neither liver nor splenic uptake could be demonstrated with this administration route.

Any definitive interpretations derived from the preliminary radioimmumoscintigraphic data presented in this paper would be premature. One can delineate some data trends, that may be borne out with study of a large sample size. In the single animal from which data was obtained, intrathecal administration of pair-labelled MAb's did not produce any MAb uptake that could be designated as specific.In addition, non-specific enhanced MAb uptake by the tumour was observed.

This lack of specificity may be artefactual due to confounding variables such as a difference in isotype between control and glioma specific MAb's, the presence of an extradural MAb depot and even the possible presence in the CSF of halogenases capable of cleaving iodide-MAb linkages must be accounted for. Uptake by the spleen was also observed, with ^{125}I-IgG concentration more than twice that of ^{131}I-IgM MAb. This could possibly be explained by a slow absorption of MAb into the blood from the extrathecal depot with the lower molecular weight MAb diffusing faster than the heavier MAb. A direct comparison of this data with previously-performed studies cannot be made because of the absence of published data on intrathecally- injected MAb uptake by human gliomas.

In summary, the presence of GM2 ganglioside and the absence of 3'iso LM1 (CA50) ganglioside antigen on the cell surface of the D-54 MG human glioblastoma cell line has been confirmed in-vitro. Moreover, the maintenance of the expression of GM2 antigen in D-54 MG cells grown intracerebrally in immunosuppressed cat brain tissue has been shown. As well, the specificity of 10-11 MAb localization to tumour tissue, prepared in tissue section was demonstrated. Finally, preliminary trends reveal an increase in tumour uptake of MAb's relative to surrounding brain, although specificity of this phenomenon to a putative glioma-specific MAb could not be seen in a single experimental subject.

Further research to ascertain the veracity of these preliminary trends is required.Because of a critical lack of effective treatments, a similar sense of urgency exists with regards to establishing the intrathecal glioma-specific MAb approach as a viable and efficacious alternative in the treatment of malignant glioma.These projects are now feasible with the development of a human glioma in a large animal xenograft model.

REFERENCES

1) Hilbig, R., and Rahmann, H. Phylogeny of vertebrate brain gangliosides. Institute of Zoology, University of Stuttgart-Hohnenheim. *In:* Gangliosides and Modulation of Neuronal Functions, *H7:* 333-350, 1987.
2) Hilbig, R., Lauke, G., and Rahmann, H. Brain gangliosides during life span (embryogenesis to senescence) of the rat. Develop, Neurosci., *6:* 260-270, 1984.
3) Bremer, E.G., Hakomori, S.I. Gangliosides as receptor modulators. Adv. Exp. Med. Biol., *174:* 381-394, 1984.
4) Rahmann, H. Possible function of brain gangliosides in survival in the cold. Adv. Exp. Med. Biol., *152:* 307-314, 1982.
5) Fredman, P., von Holst, H., Collins, V.P., Ammar, A., Dellheden, B., Wahren, B., Granholm, L., and Svennerholm, L. Potential ganglioside antigens associated with human gliomas. Neurological Res., *8:* 123-126, 1986.
6) Suzuki, K. The pattern of mammalian brain gangliosides-III. Regional and developmental differences. J. Neurochem., *12:* 969-979, 1965.

7) Fredman, P., von Holst, H., Collins, V.P., Granholm, L., and Svennerholm, L. Sialyllactotetraosylceramide, a ganglioside marker for human malignant gliomas. J. Neurochemistry, *50:* 912-919, 1988.

8) Traylor, T.D., and Hogan, E.L. Gangliosides of human cerebral astrocytomas. J. Neurochem., *34:* 126-131, 1980.

9) The Eighth International Conference on Brain Tumor Research and Therapy. J. Neuro-Oncology,*7:* S33-S37. Abstract. Netherlands: Kluwer Academic Publ., 1989.

10) Natoli, E.J., Jr., Livingston, P.O., Pukel, C.S., Lloyd, K.O., Wiegandt, H., Szalay, J., Oettgen, H.F., and Old, L.J. A murine monoclonal antibody detecting N-acetyl- and N-glycolyl-GM2: Characterization of cell surface reactivity. Cancer Res., *46* : 4116-4120, 1986.

11) Mansson, J.-E., Fredman, P., Bigner, D.D., Molin, K., Rosengren, B., Friedman, H.S., and Svennerholm, L. Characterization of new gangliosides of the lactotetraose series in murine xenografts of a human glioma cell line. FEBS Letters, *201:* 109-113, 1986.

12) Fredman, P., von Holst, H., Collins, V.P., Granholm, L., and Svennerholm, L. Sialyllactotetraosylceramide, a ganglioside marker for human malignant gliomas. J. Neurochemistry, *50:* 912-919, 1988.

13) Fredman, P. Gangliosides in human malignant gliomas. *In:* Ledeen, R.W., Hogan, E.L., Tettamanti, G., Yates, A.J., and Yu, R.K. (eds.), New Trends in Ganglioside Research: Neurochemical and Neuroregenerative Aspects, *14:* 151-161. Padova: Liviana Press, 1988.

14) Ledeen, R.W., Hogan, E.L., Tettamanti, G., Yates, A.J., and Yu, R.K. (eds.), New Trends in Ganglioside Research: Neurochemical and Neuroregenerative Aspects, *14:* 634. Padova: Liviana Press, 1988.

15) Tai, T., Paulson, J.C., Cahan, L.D., and Irie, R.F. Ganglioside GM2 as a human tumor antigen (OFAI-1). Proc. Natl. Acad. Sci. USA, *80:* 5392-5396, 1983.

16) Chou, S.N., Aust, J.B., Moore, G.E., and Peyton, W.T. Radioactive iodinated human serum albumin as tracer agent for diagnosing and localising intracranial lesions. Proc. Soc. Exp. Biol. Med., *77:* 193-5, 1951.

17) Phillips, J., Alderson, T., Sikora, K., and Watson, J. Localisation of malignant glioma by a radiolabelled human monoclonal antibody. J. Neurol.Neurosurg. Psychiatry, *46:* 388-92, 1983.

18) Kemshead, J.T., Jones, D.H., Lashford, L., Prichard, J., Gordon, I., Breatnach, F., and Coakham, H.B. 131-I Coupled to monoclonal antibodies as therapeutic agents for neuroectodermally derived tumors: Fact or fiction? Cancer Drug Delivery, *3:* #1, 25-43. Liebert, M.A.,Inc., Publ., 1986.

19) Richardson, R.B., Davies, A.G., Bourne, S.P., Staddon, G.E., Jones, D.H., Kemshead, J.T., and Coakham, H.B. Radioimmunolocalisation of human brain tumours: biodistribution of radiolabelled monoclonal antibody UJ13A. Eur. J. Nucl. Med., *12:* 313-20, 1986.

20) Coakham, H.B., Richardson, R.B., Davies, A.G., Bourne, S.P., Eckert, H., and Kemshead, J.T. Neoplastic meningitis from a pineal tumour treated by antibody-guided irradiation via the intrathecal route. British J. Neurosurgery, *2:* 199-209, 1988.

21) Benjamin, J.C., Moss, T., Path, M.R.C., Moseley, R.P., Maxwell,R., and Coakham, H.B. Cerebral distribution of immunoconjugate after treatment for neoplastic meningitis using an intrathecal radiolabeled monoclonal antibody. Neurosurgery, *25:* 253-258, 1989.

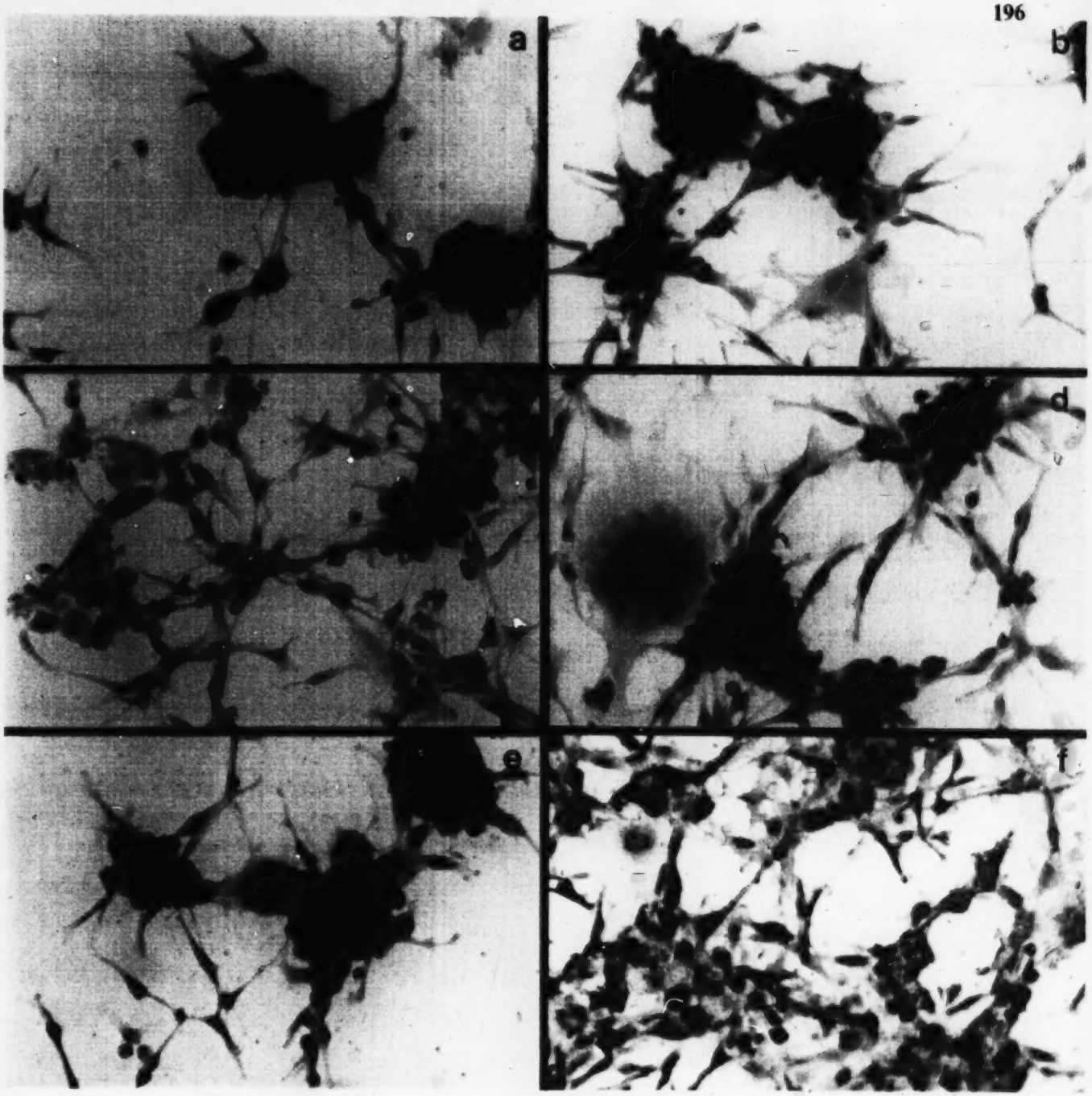

Figure IV - 1. Composite images of in-vitro immunoreactivity of 10-11 (anti-GM2) MAb to D-54 MG cells. Image a: C50 (IgM) MAb; b: MOPC-21 (IgG) MAb (negative controls for primary antibody); c: no primary antibody with IgM secondary MAb; d: no primary antibody with IgG secondary MAb; e: 10-11 (IgM) MAb with IgG secondary MAb; f: 10-11 MAb with IgM secondary MAb. ABC methodology (X 115).

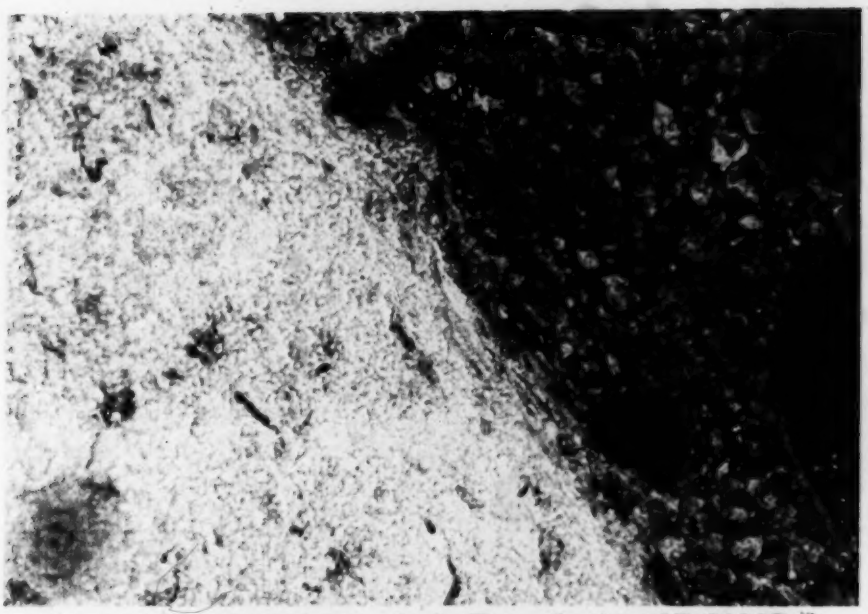

Figure IV - 2. Photomicrograph of a Tissue Section of D-54 MG human glioma cells grown as a xenograft in cat brain. This section is stained immunohistochemically with 10-11 MAb for GM2 surface antigen. This representation shows the tumour-normal brain interface. ABC methodology (X 115).

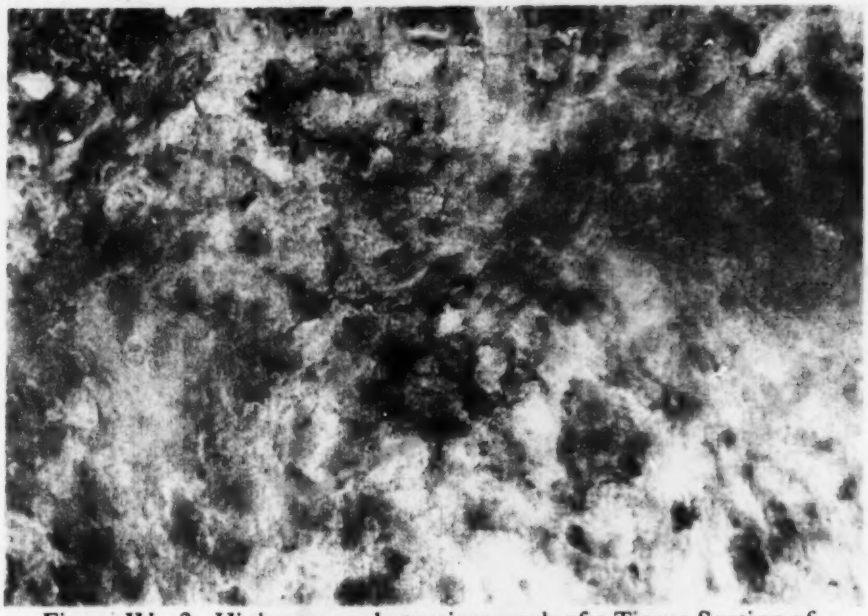

Figure IV - 3. High-power photomicrograph of a Tissue Section of D-54 MG human glioma cells grown as a xenograft in cat brain. This section is stained immunohistochemically with 10-11 MAb for GM2 surface antigen. This representation shows ring-like staining of cell membranes within the tumour. ABC methodology (X 390).

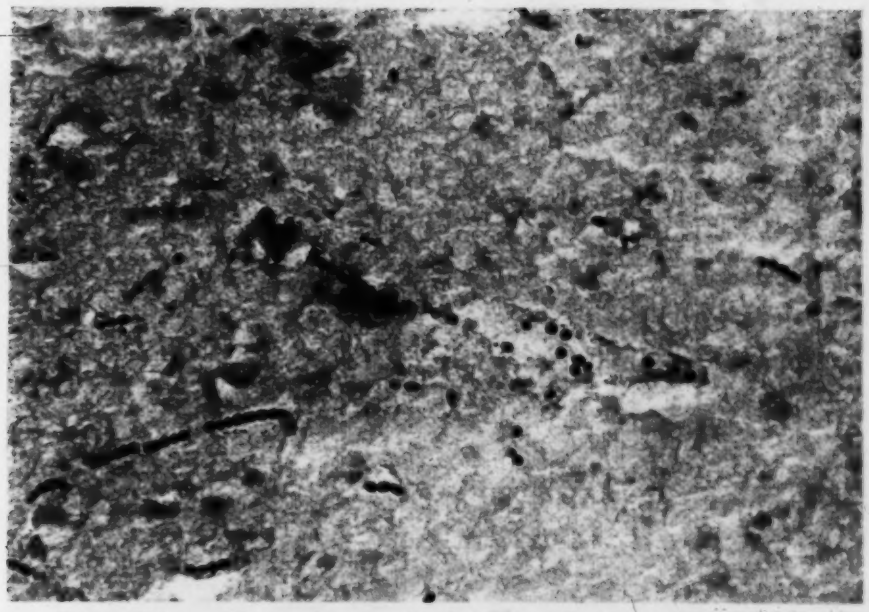

Figure IV - 4. Photomicrograph of a Tissue Section of D-54 MG human glioma cells grown as a xenograft in cat brain. This section is stained immunohistochemically with 10-11 MAb for GM2 surface antigen. This representaion shows absence of staining in brain tissue surrounding the D-54 MG tumour. Artefactual staining of biotin-containing erthrocytes is seen. ABC methodology (X 115).

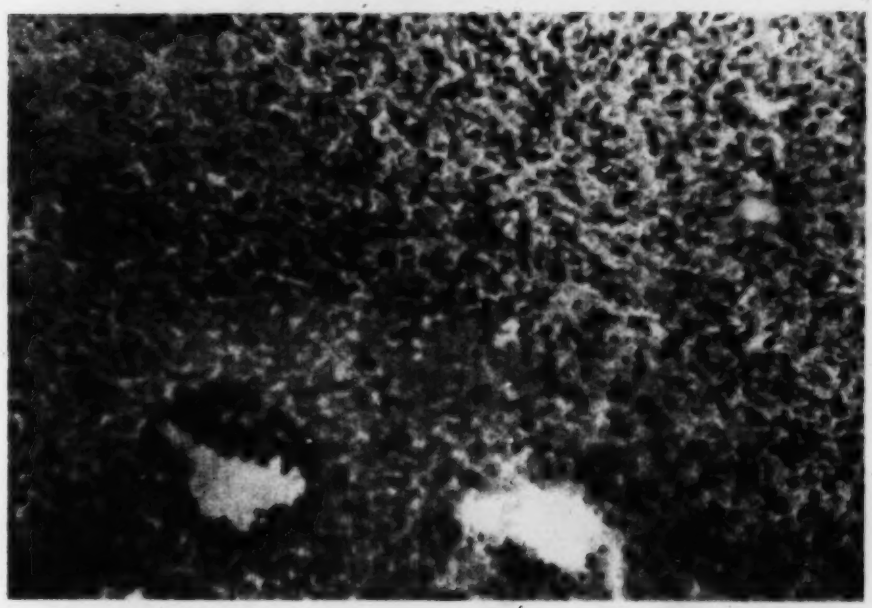

Figure IV - 5. Photomicrograph of a Tissue Section of D-54MG human glioma cells grown as a xenograft in cat brain. This section is stained immunohistochemically (ABC) with MOPC-21 MAb (control). This representation shows absence of MAb-linked staining within the tumour i.e. no contrast between tumour and normal brain regions. ABC methodology (X 115).

Figure IV - 6. Radioimmunoscintigraphic image obtained by injection of 131I-10-11 (anti-GM2) MAb into the intrathecal space of a D-54 MG human glioma-bearing cat (intracerebral tumour). Head image taken at 1 hour post-injection of an anteroposterior view.

Figure IV - 7. Radioimmunoscintigraphic image obtained by injection of 131I-10-11 (anti-GM2) MAb into the intrathecal space of a D-54 MG human glioma-bearing cat (intracerebral tumour). Head image taken at 20 hours of a right lateral view.

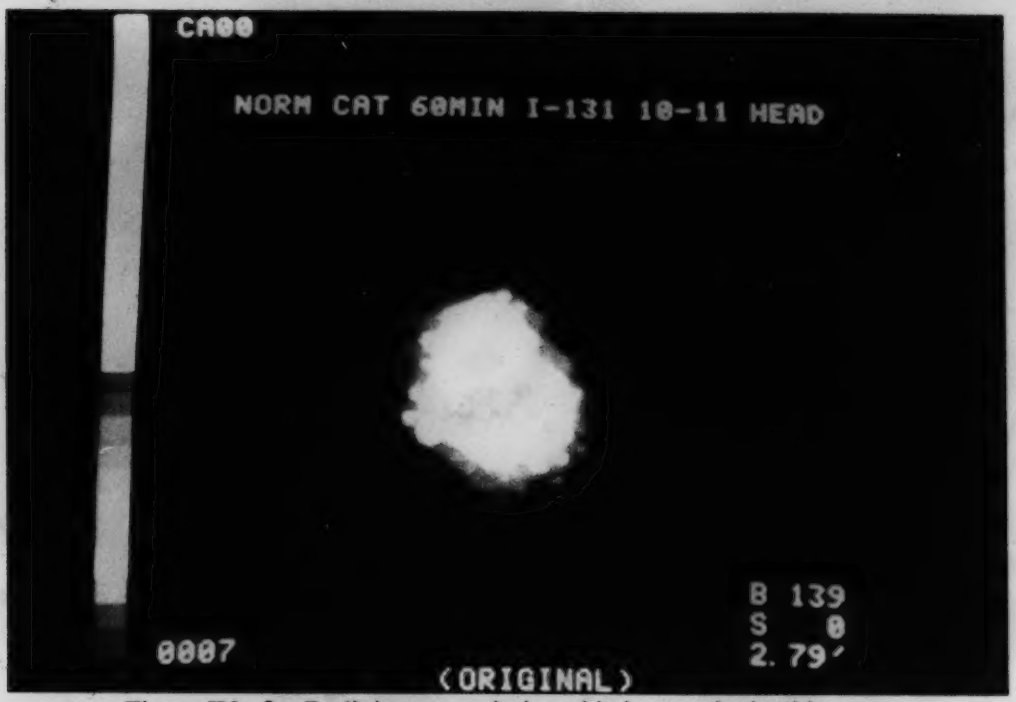

Figure IV - 8. Radioimmunoscintigraphic image obtained by injection of 131I-10-11 (anti-GM2) MAb into the intrathecal space of a non-tumour bearing cat. Head image taken at 1 hour of an anteroposterior view.

Figure IV - 9. Radioimmunoscintigraphic image obtained by injection of 131I-10-11 (anti-GM2) MAb into the intrathecal space of a non-tumour bearing cat. Head image taken at 22 hours of a left lateral view.

Figure IV - 10. Radioimmunoscintigraphic image obtained by injection of 131I-10-11 (anti-GM2) MAb into the intrathecal space of a D-54 MG human glioma-bearing cat (intracerebral tumour). Body image taken at 1 hour of an anteroposterior view.

Figure IV - 11. Radioimmunoscintigraphic image obtained by injection of 131I-10-11 (anti-GM2) MAb into the intrathecal space of a D-54 MG human glioma-bearing cat (intracerebral tumour). Body image taken at 23 hours of an anteroposterior view.

Figure IV - 12. Gd-EDTA enhanced coronal NMR image of the D-54 MG tumour- bearing cat 21 days post-tumour implantation. Note small area of hyperintensity in superficial region of right parietal lobe corresponding to the tumour implantation site.

Anatomical Structure	125-I % dose / organ	125-I % dose / gram	131-I % dose / organ	131-I % dose / gram
Heart	0.210	0.019	0.105	0.009
Lung	0.549	0.031	0.458	0.026
Spleen	0.810	0.074	0.330	0.030
Liver	2.30	0.035	1.10	0.016
Kidney	0.402	0.034	0.192	0.016
Cerebellum	0.110	0.019	0.150	0.025
R occipital lobe	0.052	0.025	0.018	0.009
L occipital lobe	0.118	0.039	0.054	0.018
R parietal lobe	0.080	0.018	0.046	0.010
L parietal lobe	0.098	0.025	0.044	0.011
R frontal lobe	0.095	0.034	0.035	0.009
L frontal lobe	0.110	0.024	0.029	0.009
Tumour	0.003	0.063	0.0012	0.025

Table IV - 1. Comparative tissue uptakes of 131I-10-11 and 125I-MOPC-21 labelled MAbs 24 hours after intrathecal injection.

CHAPTER V - CONCLUSIONS AND RECOMMENDATIONS FOR FUTURE RESEARCH

This thesis has endeavoured to present three novel facets to the study of brain tumours. The first study presented data which documented the development of a new class of brain tumour model - the human-large animal glioma xenograft. The second study presented evidence of flux differences in specific metabolites of both glucose and glutamine in D-54 MG cells as a result of exposure to chemotherapy. It also suggested that daunomycin is more efficacious in killing D-54 MG cells than BCNU. The third study identified the GM2 ganglioside as being a component of D-54 MG cell membranes in a host tissue environment that may be similar to that found in naturally-occurring tumours.

Each one of these three threads can be interwoven to produce an integrated investigational approach that may provide new insights into both the biology of brain tumours and clinical approaches to their management that any one thread alone could not achieve.

Taking the large number of possible variations on each theme in turn :

1) Large animal human glioma xenograft -

a) Expansion of the model - this can be achieved by implantation of any number of different tumour cell lines, both glioma-derived and non-glioma derived (for study of metastatic disease) to see if growth occurs, in one or multiple locations. In addition, models of neoplastic meningitis could be established using a number of cell lines. This cat model could also serve as a testbed for the growth of other tumours, including those of non - CNS origin, implanted into various body cavities, i.e. pleural and peritoneal spaces.

b) The role of Cyclosporin A in tumour formation - this could be investigated by varying the dose, the timing of administration and cessation of the drug at different times pre-and post-implantation.Novel immunosuppressants, eg. FK 506 and rapamycin, could be assessed for efficacy of action as well. Combinations of immunosuppressants should also be investigated.

c) The action of host immune response - this could be assessed by examination of the origin of cellular immune response (T_H, T_S, T_D) to xenografts. Furthermore, investigation of T cell receptor subtypes can be initiated. Similar studies can be performed with B cells as well as antigen-presenting cells. The effect of the tumour on surrounding brain as well as the effect of different host tissues on the morphology, antigen expression and ultimately transcription and translation of genes can also be examined. The presence of any tumour-derived immunosuppressive factors could be studied as well as the secretion of growth factors into the extracellular space.

d) The effect of various therapeutic modalities - these can be studied using both invasive and non-invasive methodologies, after single or multiple doses or in combination with other chemo- or radiotherapeutic regimes (some restriction may be necessary due to the presence of Cyclosporin A).

2) Metabolite flux rates -

a) Study of the mechanisms of abnormal metabolite production - studies of kinetics in both normal glia and glioma cells, of enzymes such as GDH, AAT and phosphate-activated glutaminase in an attempt to understand increased glutamate production levels. Similar studies could be performed focussing on pyruvate carboxylase and the pyruvate dehydrogenase complex to elucidate evidence for the cause for switching from an oxidative system of energy production to that dominated by aerobic glycolysis.

b) The role of the cell membrane in metabolite flux control - this can be studied using electrophysiological techniques along with monoclonal antibodies or inhibitors of ionic and/or molecular groups to ascertain the normal controlling mechanisms of substrate flux through the glioma cell membrane under the stress of radio - or chemotherapy.

c) In-vivo metabolite assessment - the in-vitro results may replicate in-vivo studies using both invasive and non-invasive techniques. In-vivo microdialysis would be a natural first choice as it is one of the few methodologies capable of measuring solute concentrations in the extracellular space. This methodology is useful both in animal studies as well as in patients. Non-invasive techniques such as NMR Spectroscopy of various nuclear species as well as PET imaging, in concert with the probes for glutamate, taurine and other potentially treatment-sensitive molecules may ultimately provide a modality useful in non-invasively providing a fast, accurate and sensitive prediction of the efficacy of new therapeutic modalities.

3) Ganglioside Antigen Expression -

a) Determination of Glioma-specific gangliosides - some putative candidates (3'-iso-LM1) have been discovered but may not be optimal due to antigenic modulation. GM2 as well as GD2 and GD3, although present in minimal quantities in normal brain may not be as transiently expressed. Tissue section determination of expression of all four of the above antigens using immunohistochemical methods, not only on sections of D-54 MG tumour in cat brain, but of a variety of glioma cell lines in-vivo as well as human tumour biopsies should establish the expression of these antigens and their proclivity for modulation.

b) Augmentation of Ganglioside Expression - studies using β -and γ-interferon have been shown to augment a variety of ganglioside or glycoprotein antigens in human tumours. In-vivo administration prior to MAb-directed therapy presents an inviting route of study.

c) Localization and Therapeutic MAb studies - these studies would use techniques such as radioimmunoscintigraphy and single photon emission computerized tomography (SPECT) imaging to study the biodistribution and pharmacokinetics of MAb's of many different types (IgM/IgG isotype, targetting to gangliosides and non-ganglioside antigens), administered intrathecally or into a tumour cavity immediately after resection, using a variety of different radionuclides for diagnostic as well as therapeutic studies. Non-radionuclide studies can be performed, an example of which could be the intrathecal administration of daunomycin linked to the anti-GM2 monoclonal antibody with observation of glutamate or taurine concentrations in the extracellular space of intracerebrally-implanted D-54 MG tumours using in-vivo microdialysis in cats.

Once the boundary conditions of these three entities, the model, the tumour targetting mechanism and the predictive assay of tumour response are more fully delineated and the methods refined, a powerful new set of tools could be created, the use of which together may provide information that could not only be important in basic studies in neuro-oncology but could also produce a novel set of diagnostic and therapeutic approaches that may assist in the eradication of this devastating disease.

APPENDIX I - IN-VIVO NMR SPECTROSCOPY

INTRODUCTION

Magnetic resonance spectroscopy has been utilized in the elucidation of chemical interactions in solids and liquids - both pure and in the form of solutions, since the seminal experiments on this methodology performed by Bloch and Purcell in 1946[1,2]. The field upon which it had and is still having its greatest impact is the investigation of the 3-dimensional structural configuration of molecules and binding characteristics of their ligands. This work was and is currently being performed using extremely high field magnets (up to 16.2T) that are equipped with central bores sometimes not more than a few millimetres in diameter. The resolution of biological compounds and their structure, especially in purified, simple solutions containing a small number of molecular species, is truly impressive.

In the mid-1970's, the first practical experiments were performed using magnetic resonance spectroscopy on living systems. Pioneers such as R. Richards, G. Radda among others, created the field of in-vivo NMR spectroscopy by placing first living tissue, then whole animals in instruments that of necessity had wider bores and far higher energy requirements, due to the design constraint of maintaining a high-strength magnetic field over a greater spatial volume. The first such spectra were acquired using the ^{31}P nucleus in muscle tissue.

Similar acquisition parameters were used on human brains in-vivo with resultant ^{31}P spectra in these relatively low-field systems (approx. 2T) being of simple form, providing relative concentrations of ATP, ADP, Phosphocreatine (PCr), inorganic phosphate (P_i), phosphodiesters and phosphomonoesters. In addition, the chemical shift of P_i from PCr provided a measure of pH within the volume from which signal was acquired.

Human brain tumours, noted for tissue heterogeneity on a gross as well as microscopic level, were studied using ^{31}P acquisition techniques.These studies did not reveal any overriding "tumour signature" in the metabolite pattern, as compared to surrounding brain or the brains of normal volunteers[3]. pH changes were also considered to be variable in degree and consistency.

In general, the obvious first choice of nucleus for spectroscopists to study was ^{1}H due to its high concentration and ubiquity in biological systems. However, most of the ^{1}H was bound in H_2O, forming a peak so massive that other ^{1}H peaks representing biochemically-important metabolites such as lactate, creatine/phosphocreatine and neurotransmitters were obliterated. The solution to this problem, ^{1}H spectra acquired using H_2O-suppression techniques[4], has only been widely available in the last four years. Another problem that has been almost completely brought under control has
been in the acquisition of spectra from accurately localized in-vivo volumes. Various localization routines have been developed in the last three years, with stimulated-echo acquisition mode (STEAM[5]) and image-selected in-vivo spectroscopy (ISIS[6]) being the two most commonly-used software packages. Hardware improvements that also assisted in selectivity include the use of surface coils of various configurations.

Although the volume of interest (VOI) could be significantly reduced in ^{1}H spectroscopy by virtue of its higher concentration, the first human brain tumours studied were analyzed with VOI's of approximately 64cc. The findings in gliomas included higher lactate levels, little or no N-acetylaspartate, little or no creatine/phosphocreatinine and no GABA[7-10]. However, these data could not be considered conclusive due to the significant degree of tissue heterogeneity that would exist in a 64cc VOI taken from cerebral tissue, normal or abnormal. The purpose of

the present study was therefore two-fold :

1) To acquire a ^{1}H spectrum of potentially-high homogeneity from a human glioma, in the form of intracerebrally-implanted D-54 MG human glioma-derived cells forming a 1-2cc tumour in immunosuppressed cat brain.

2) To correlate the relative concentrations of these metabolites with perchloric acid (PCA) extracts of D-54 MG tumour tissue removed immediately after ^{1}H spectroscopy.

METHODS AND MATERIALS

Animal Preparation

D-54 MG human glioma cells were implanted into animals as discussed previously. At three weeks, an NMR multi-spin-echo image was acquired to determine the presence of tumour growth as determined previously. At four weeks, the animal was prepared for NMR spectroscopic analysis in the following manner :

1) A pre-anaesthetic preparatory dose of 0.1ml/kg
Atropine IM was given to prevent excessive salivation;

2) With the animal under human restraint, 1ml/kg Saffan (see Chapter II) was administered into the cephalic vein. Anaesthesia was achieved within 30 seconds of Saffan administration;

3) A 3 French cuffed endotracheal tube was positioned in the trachea and cuff blown up with 5 c.c. air;

4) A #20 intravenous catheter was inserted into the cephalic vein and flushed with saline;

5) A 60cm plastic extension was connected to a 3-way stopcock, which was connected to the IV catheter. This entire arrangement was then flushed with saline to remove trapped air;

6) 0.5cc Saffan doses were administered as needed for maintenance of

anaesthesia.These doses were titrated to corneal reflex, toe-pinch response, respiratory rate and cat movement;

7) A respiratory rate monitor with rubber bellows sensor attached by 10m. plastic tubing to an amplifier system with LED readout (M.Sc. thesis: Karim Al - Daoudi - U.of Alberta, 1989) was then fastened with Velcro straps around the abdomen of the animal and the operational status of the device was checked;

8) Cat was then placed in an acrylic animal-constraint device designed to fit in both wide-bore and medium-bore NMR instruments (see Figures 1-3). String was placed around the paw with the IV line and fastened to a hole drilled into a flange on the side of the chamber to prevent accidental IV line disengagement. The IV line was brought out through the front of the chamber and the respiratory rate monitoring line was brought through a hole in the back of the chamber. The head of the animal was positioned between two foam pads and the lower jaw fastened to a ramp running from the floor of the chamber. The NMR surface coil was then positioned such that it lay horizontal with respect to both the top of the head and the floor. The 6cm copper coil, tuned to the resonance frequency for ^{1}H @ 1.5T (67.63 MHz.) was also positioned such that the coil's anterior-posterior diameter lay along the midline of the head. In this way, signals from both cerebral hemispheres could be acquired with equal ease;

9) Cat was then transported within the closed chamber to the Philips wide-bore 1.5T magnet;

10) The animal constraint device was placed inside the magnet and connected to an airflow system (two 10m hoses connected to a Filter

Queen vacuum cleaner) which maintained the inside of the chamber under negative pressure relative to room air;

11) A standard multi-slice multi-echo sequence with 3mm cuts established the location of the tumour in coronal section;

12) Individual multi-echo scans were acquired to precisely determine the maximal diameter of the tumour in the coronal plane;

13) The software package was then switched from imaging to spectroscopy. This necessitated rebooting the computer as the two programs were incompatible with each other;

14) A spectroscopy sequence was designed as in Figure 6, using ISIS as its basic localization sequence, overlaid with DEPTH pulses to narrow the transmission volume of the surface coil, binomial pulses as well as inversion-recovery pulse timed to suppress the H_2O peak by a factor of 5,000. Lastly, surface suppression pulses were used to suppress unwanted signal from superficial regions of the head;

15) A volume of 1cc was selected such that the edges of the VOI were all within the tumour in the coronal plane;

16) ^1H spectrum acquisition lasted for approximately 20 minutes for the full 128-scan cycle;

17) A similar spectrum was obtained from the contra-lateral hemisphere with the VOI at the same relative position within the coronal plane.

RESULTS

The results of a phantom study documenting ISIS localization ability are shown in Figure 7. The outer phantom is filled with 50cc 5mM N-Acetyl aspartate and the inner phantom with 1.3cc 50mM lactate, both being instilled just prior to spectral acquisition. As one can discern, the NAA peak decreases and the lactate peak remains approximately the same height as the ISIS VOI's decrease in size. At 1cc VOI, one can still visualize a small NAA peak. This is due mostly to slightly off-center positioning of the VOI on the small phantom. However, one can also, from this spectral series, determine that the signal-to-noise ratio is low. Figure 6 presents a representative spectrum acquired from the tumour hemisphere (VOI - 2.25cc). Lack of spectral resolution does not permit identification of individual peaks. Use of an acquisition volume size of 1cc did not permit resolution of any peaks above the background level of noise.

DISCUSSION

Further efforts to acquire a ^{1}H NMR spectrum from a 1cc VOI in a D-54 MG glioma-bearing cat were halted for three principal reasons :

1) The signal-to-noise ratio produced by the hardware/ software combination on the Philips system did not permit identification of any peaks from a 1cc volume. This loss of signal (or increase in noise) could be due to losses incurred by: a) hardware component including the surface coil (due to low Q in construction), the preamplifier, the coaxial cables transmitting the signal back to the data analysis module; b) Software routines such as surface suppression pulses and binomial pulses that may take out a small portion of relevant signal along with irrelevant signal. In addition, the putative concentration of even the most abundant of the NMR- visible metabolites that may change with treatment eg. lactate, are in the 1-5 mM range which

is at, or slightly below the limit of detection for the hardware and software utilized with the Philips magnet. The relatively low field strength of the Philips magnet (1.9T), not designed for animal use, also contributed to the low signal intensities seen. This difficulty with signal-to-noise leads to the second constraint;

2) Inadequate spatial resolution - not only did the VOI have to be increased significantly (8cc) to acquire signals with S/N = 5-10:1 but the exact position of the VOI could not be ascertained within the brain. The reason for this was the inability, at the time, for a transfer of data to be completed using Phillips system software, between imaging and spectroscopy. Consequently, even if a signal of high-enough intensity were to be acquired, one, at the time, could never be confident whether or not the signal came from the implanted tumour;

3) Inadequate spectral resolution - cat studies were being done concurrently with in-vitro studies on both PCA cell extracts and media. Both correlative approaches are inherently flawed - PCA cell extracts measuring only intracellular metabolite and media analysis measuring only extracellular metabolites (in an artificial environment) whereas, in-vivo ^{1}H spectroscopy, in theory, detects metabolites in both spaces. Nevertheless, the ^{1}H spectra of the PCA cellular extracts had two major technical problems associated with them - firstly, the presence of a very complex set of peaks, many of which overlapped each other, making it almost impossible to determine relative concentrations without major errors being introduced during data analysis. Secondly, the concentration of metabolites when extracted from even 10^{7} cells grown in monolayer culture was frequently in the low mM range. From data presented in chapter III, one can discern that this range was at the low range of accurate detectability even for a 7.05T magnet.

Media experiments, therefore produced spectra of sufficient spectral resolution and simplicity to be able to produce the data shown in chapter III.

Applicability of these findings to in-vivo work however, is fraught with problems. Unfortunately, the peaks that may potentially be of predictive value (glutamate, taurine) are found in the midst of a multitude of other peaks, making them extremely difficult to adequately resolve and quantitate with the current spectral resolution of the Philips system.

There is much progress being made to increase the S/N ratio and to maximize both the spatial and spectral resolution. The first change, made by C. Hanstock et al. was to initiate ^{1}H spectroscopy experiments on the higher-field (2.35T) Bruker magnet in addition to continuing work to improve the resolution of the Philips magnet. A preliminary test result (C. Hanstock, personal communication) has produced a ^{1}H spectrum from 9L rat gliosarcoma in cat brain resolving a much greater number of peaks with a S/N ratio of at least 20, from a 1cc. volume. This is more typical of what has already been achieved in brain tissue in other laboratories[10,11]. To further increase S/N for selected metabolites, ^{13}C-decoupled ^{1}H spectroscopy can be utilized[12]. This involves the administration of ^{13}C-glucose (or any other important substrate) in a quantity large enough such that a major portion of the substrate concentration (and therefore that of its metabolites) is labelled, over a short period of time (usually a few hours), with ^{13}C. Sophisticated editing techniques can then be used to edit out individual metabolites from amongst a number of non-labelled peaks, taking advantage of the difference in homonuclear J-coupling constants between ^{13}C and ^{1}H and ^{12}C and ^{1}H in labelled versus non-labelled metabolites, respectively, This technique has already been used by Rothman et al.[13] to visualize lactate (using C3) and glutamate[14] (using C4) and would be admirably suited to acquire data on at least these two metabolites from small VOI within brain tumours.

In summary, work on this study did not progress due to lack of sufficient spatial and spectral resolution on the Phillips magnet to perceive potentially important metabolites present in concentrations inherently too low to be seen at present. Major adjustments in both hardware and software, performed after postponement of the study, will enable increases in spatial, spectral as well as temporal resolution sufficient to accurately determine concentrations, and in the future, fluxes of these potentially-relevant indicators of the metabolic activity in tumour cells.

REFERENCES

1) Purcell, E.M., Torrey, H.C., and Pound, R.V. Resonance absorption by nuclear magnetic moments in a solid. Phys. Rev., *69* : 37, 1946.

2) Bloch, F., Hansen, W.W., and Packard, M.E. Nuclear induction. Phys. Rev., *69* : 127,1946.

3) Felber, S., Sauter, R., and Loffler, W. Potentials of magnetic resonance spectroscopy in neuroradiology. *In* : M. Nadjmi (ed.), Imaging of Brain Metabolism Spine and Cord Intervention Neuroradiolgy Free Communications, pp. 19-25. Berlin: Springer-Verlag, 1989.

4) Tanaka, C., Naruse, S., Horikawa, Y., Hirakawa, K., Yoshizaki, K., Nishikawa, H. Proton nuclear magnetic resonance spectra of brain tumors. Magn. Reson. Imaging, *4* : 503-508, 1986.

5) Frahm, J., Bruhn, H., Gyngell, M.L., Merboldt, K.D., Hanicke, W., and Sauter, R. Localized proton NMR spectroscopy in different regions of the human brain in vivo. Relaxation times and concentrations of cerebral metabolites. Mag. Res. Med., *11* : 47-63, 1989.

6) Ordidge, R.J., Conelly, A., and Lohmann J.A.B. Image-selected In Vivo Spectroscopy (ISIS). A new technique for spatially selective NMR spectroscopy. J. Magn. Res., *66* : 283-294, 1986.

7) Frahm, J., Merboldt, K.D., Hanicke, W., and Villringer, A. Water-suppressed localized proton spectroscopy using stimulated echoes. *In* : Book of Abstracts, vol. 1, Society of Magnetic Resonance in Medicine (6th Annual Meeting and Exhibition), p.137. New York, 1987.

8) Barany, M., Venkatasubramanian, P.N., Dew, L.L., Glick, R.P., and Greenberg, I.M. Analysis of human brain tumors by proton magnetic resonance spectroscopy in vivo. *In* : Book of Abstracts, Society of Magnetic Resonance in Medicine, vol. 1, p. 429. Berkeley: Society of Magnetic Resonance in Medicine, 1989.

9) Heerschap, A., Luyten, P.R., Bernsen, H.J., van de Vlasakker, C., Prick, M.J.J., Meijer, E., Meyer, J., and den Hollander, J.A. Combined ^{1}H and ^{31}P NMR spectroscopic examination of human intracranial tumors at 1.5 tesla. *In* : Book of Abstracts, Society of Magnetic Resonance in Medicine, vol. 1, p. 430. Berkeley: Society of Magnetic Resonance in Medicine, 1989.

10) Felber, S., Sauter, R., and Aichner, F. Localized ^{1}H Spectroscopy applied to cerebral neoplasms and ischaemia at a clinical 1.5T MR-system. *In* : Book of Abstracts, Society of Magnetic Resonance in Medicine, vol. 1, p. 450. Berkeley: Society of Magnetic Resonance in Medicine, 1989.

11) Lenz, M., Sauter, R.S., Konig, H., and Requardt, H. MRI of the head and neck region. *In* : Book of Abstracts, Society of Magnetic Resonance in Medicine, vol. 1. p. 373, 1985 (London, U.K.).

12) Luyton, P.R. Proton Spectroscopy of the Human Brain. *In* : Book of Abstracts, Society of Magnetic Resonance in Medicine, vol. 1, p. 79. Berkeley: Society of Magnetic Resonance in Medicine, 1989.

13) Rothman, D.L., Behar, K.L., Hetherington, H.P., denHollander, J.A., Bendall, M.R., Petroff, O.A.C., Prichard, J.W., and Schulman, R.G. ^{1}H-observe/^{13}C-decouple spectroscopic measurements of lactate and glutamate in the rat brain in vivo. PNAS, *82* : 1633, 1985.

14) Prichard, J., Rothman, D., Novotny, E., Petroff, O., Avison, M., Howseman, A., Hanstock, C., and Shulman, R. Photic stimulation raises lactate in human visual cortex. *In* : Works in Progress, Society of Magnetic Resonance in Medicine, p. 1071. Berkeley: Society of Magnetic Resonance in Medicine, 1989.

15) Rothman, D.L., Novotny, E.J., Howseman, A., Lantos, G., Petroff, O.A.C., Hanstock, C.C., Prichard, J.W., Shulman, G.I., and Shulman, R.G. 1H NMR measurement of 4-13C glutamate turnover in the human brain. *In* : Works in Progress, Society of Magnetic Resonance in Medicine, p. 1060. Berkeley: Society of Magnetic Resonance in Medicine, 1989.

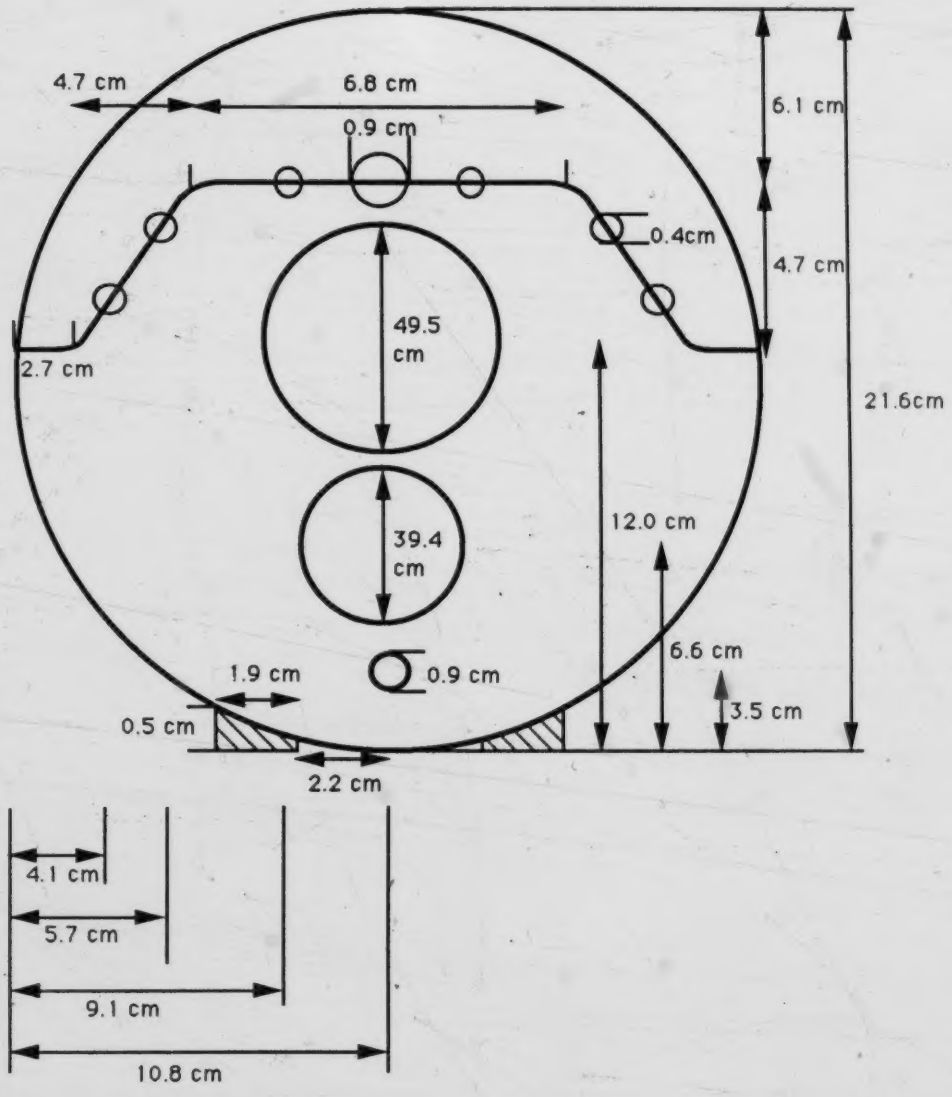

Figure 1. Animal constraint device, front plate.

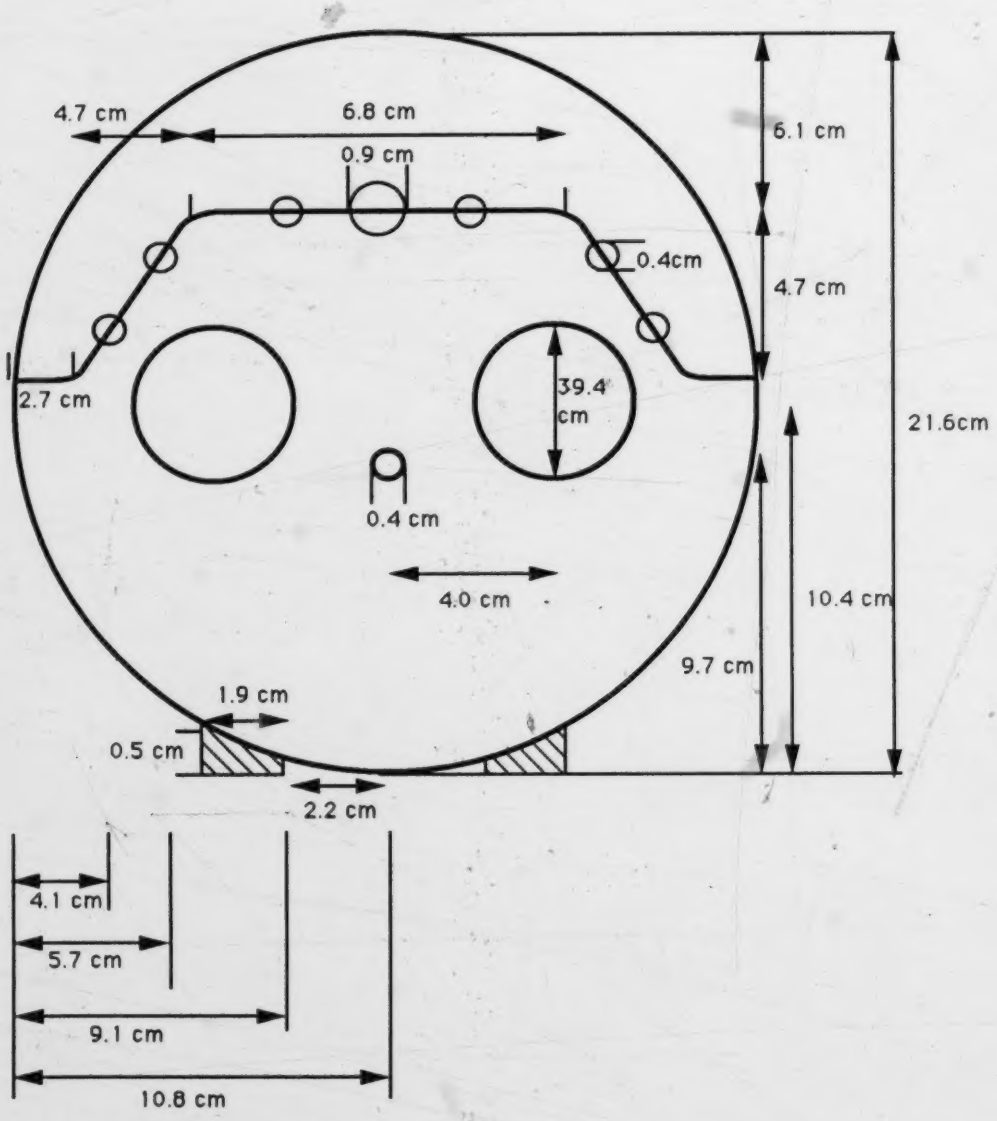

Figure 2. Animal constraint device, rear plate.

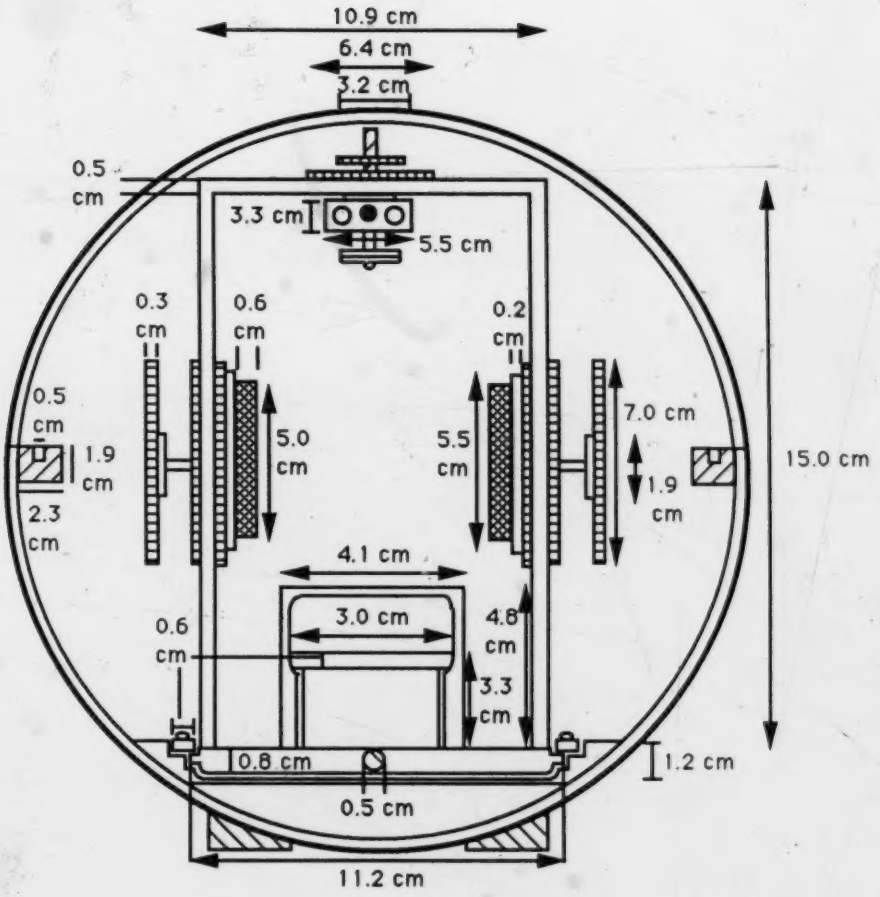

Figure 3. Animal constraint device, cross-section through head restraint.

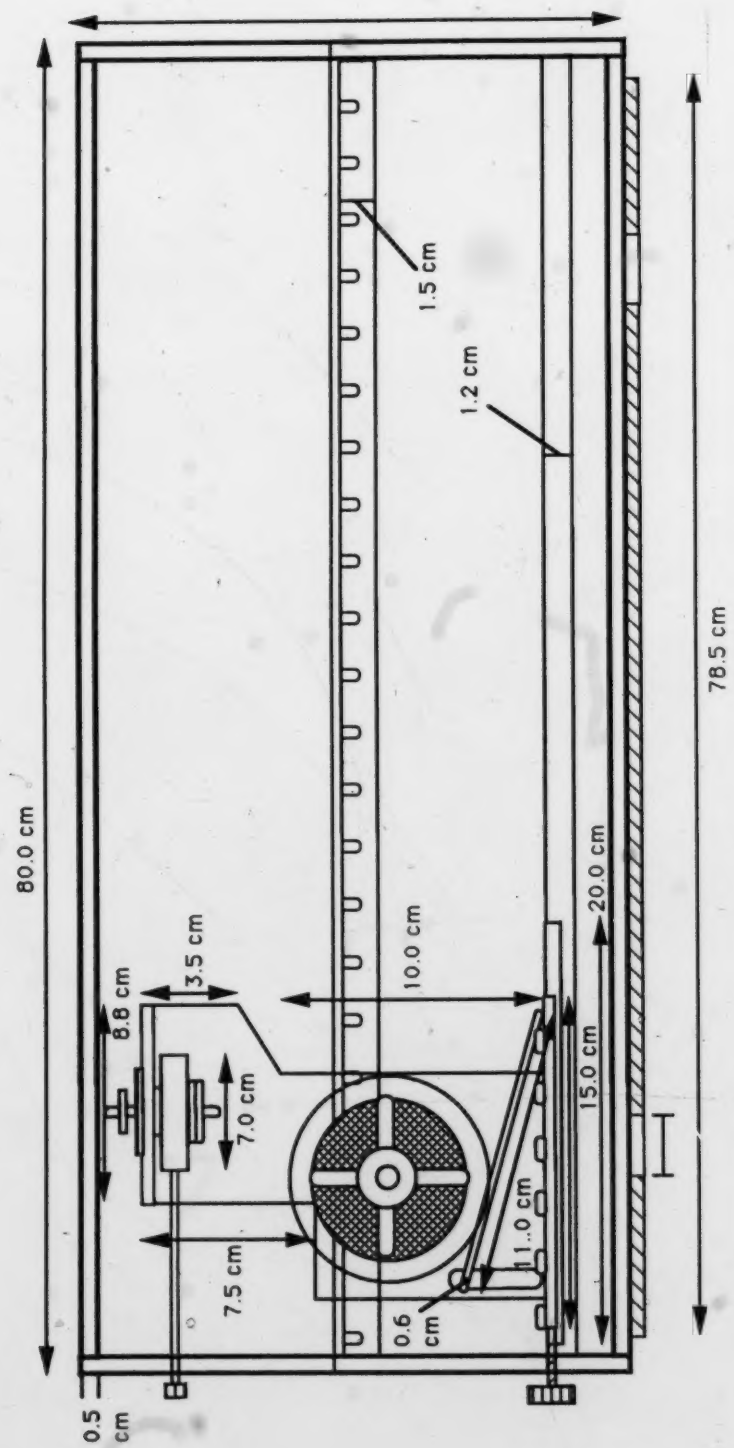

Figure 4. Animal constraint device, lateral view.

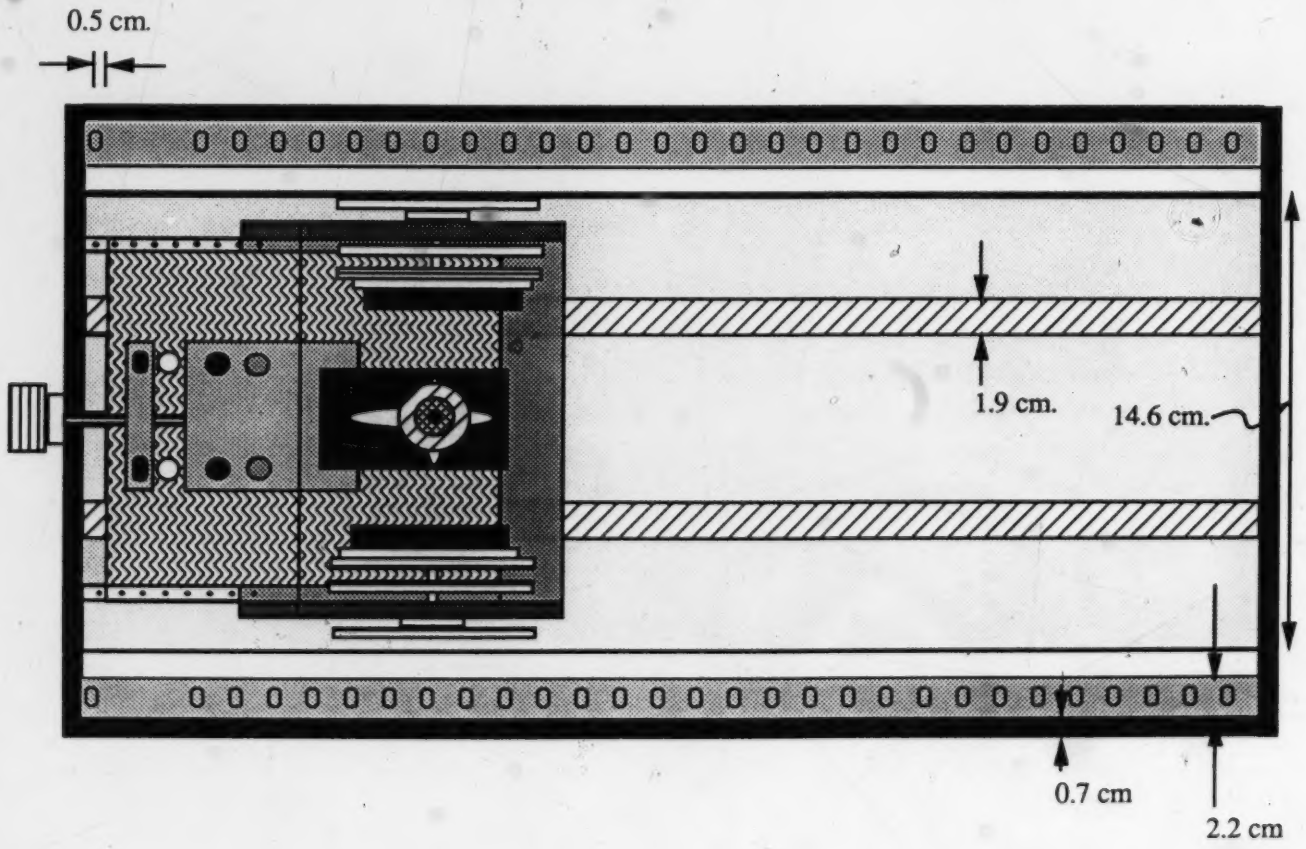

Figure 5. Animal constraint device, top view.

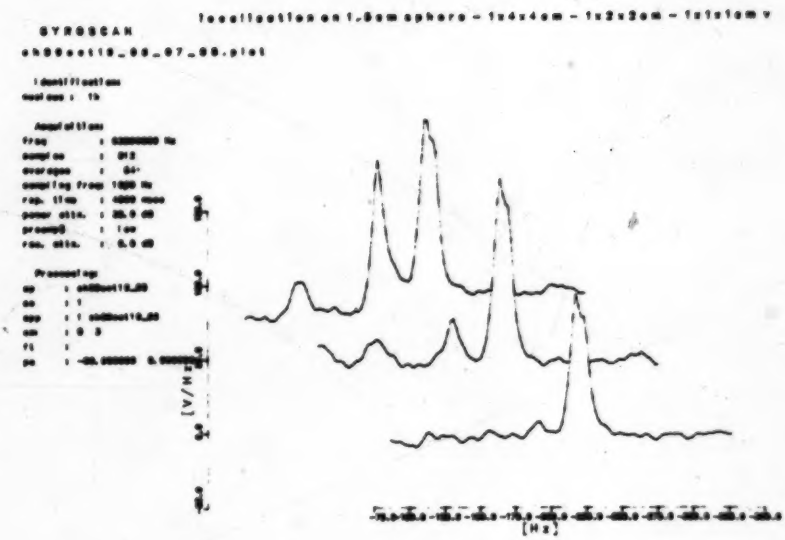

Figure 7. Three overlapping spectra (1H) of a glass phantom containing 1.3cc of 50mM lactate within a larger glass phantom containing 50cc of 5mM N-acetyl aspartate.

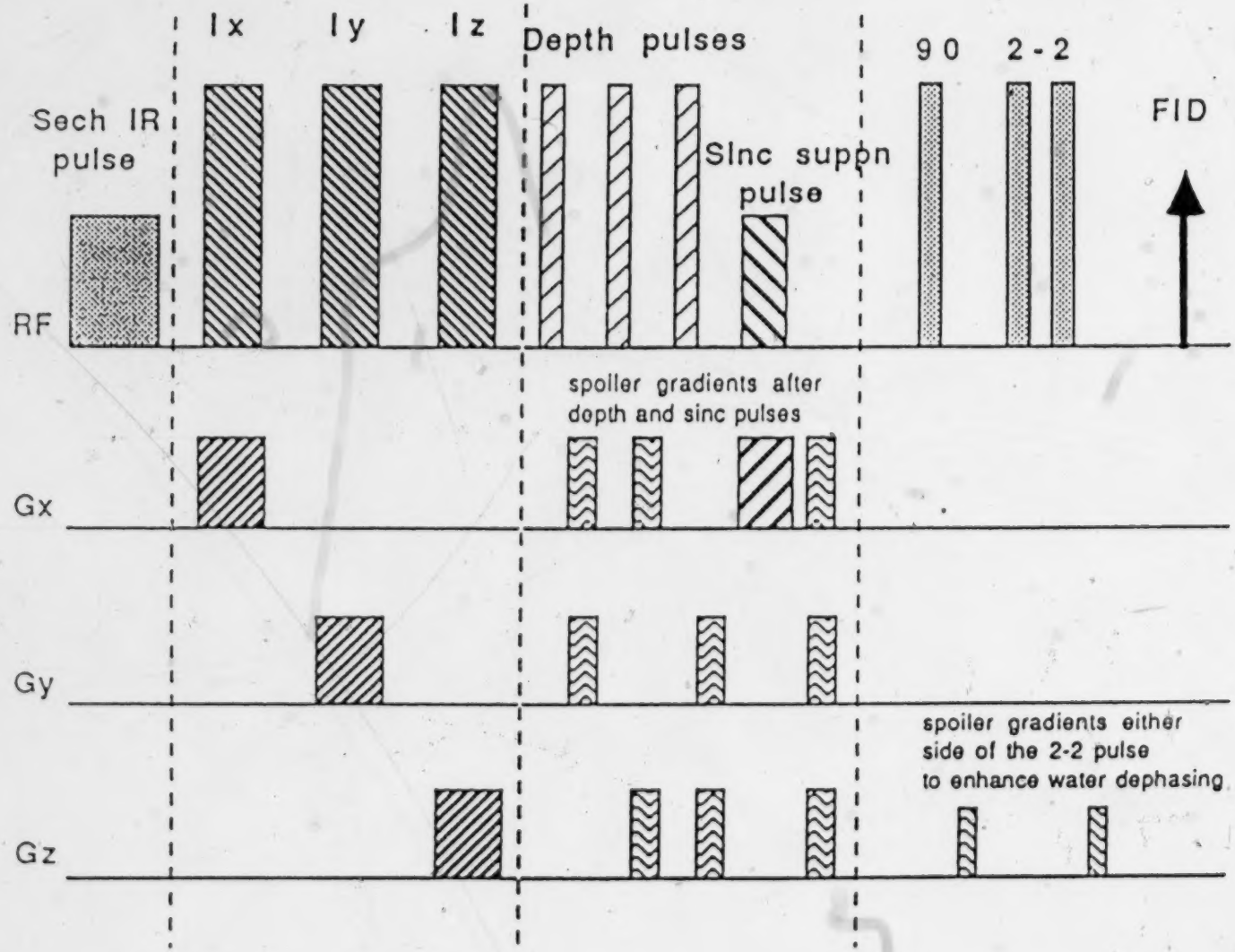

Figure 6. 1H-NMR localized spectrum acquisition sequence.

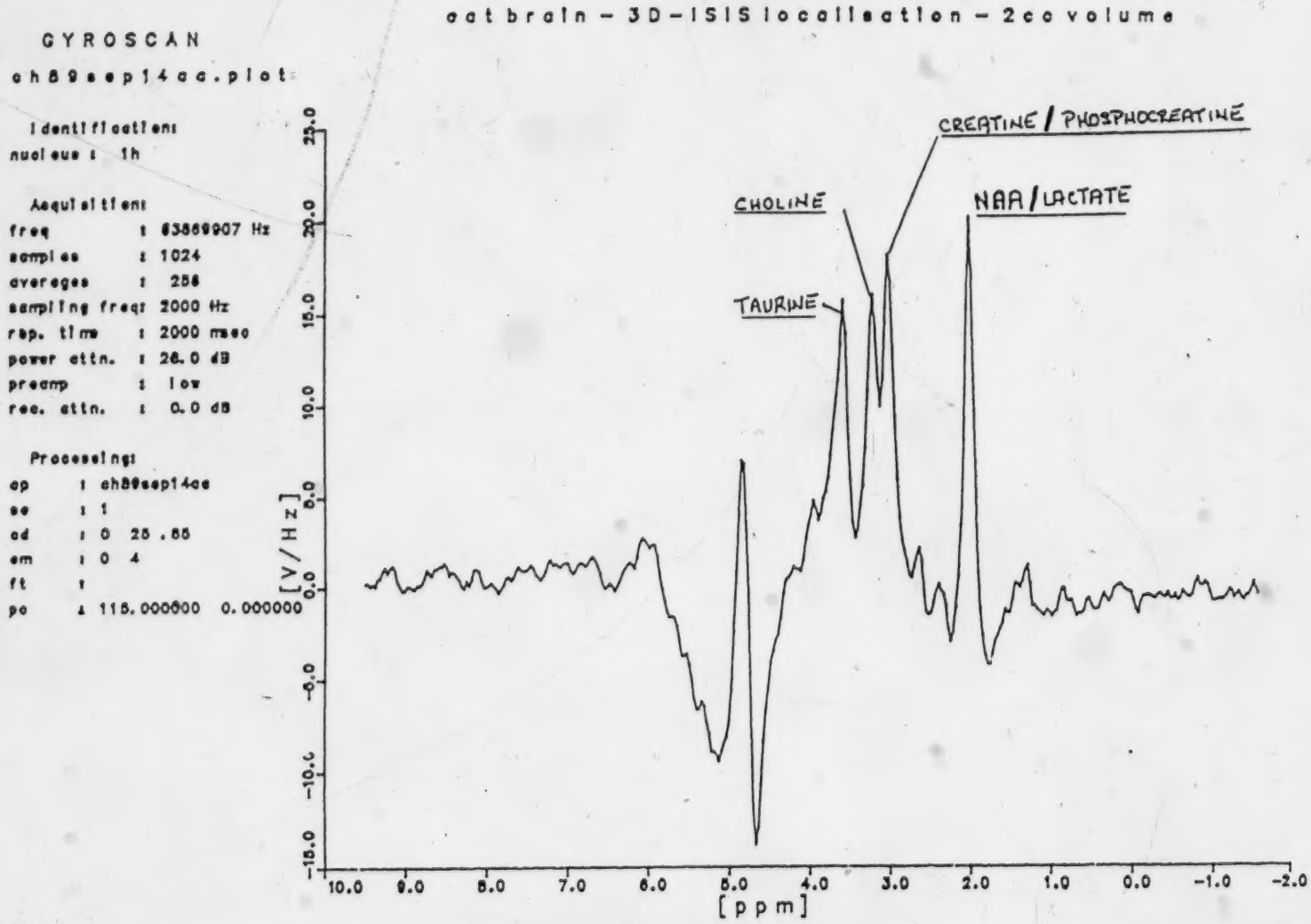

Figure 8. Representative 1H-NMR spectrum from a 2.25cc volume of interest enclosing a 1cc D-54 MG human glioma grown in cat brain.

APPENDIX II - AUXILIARY METHODS

METHOD 1 - MONOCLONAL ANTIBODY RADIOIODINATION

5 µg of Iodogen® was dissolved in 50 µl. chloroform and pipetted into a 12 x 75 mm. glass test tube. The solution was allowed to evaporate under N_2 onto the test tube walls. 10-11 (IgM) and MOPC-21 (IgG) MAbs were centrifuged in a Centricon® tube containing a filter permeable to solutes of < 20kD molecular weight, thereby producing a MAb solution concentrated to approx. 3mg/ml. 100µl of this concentrated solution was mixed with 2 mCi ^{131}I or ^{125}I (NaI) and 30µl of 0.5 M phosphate buffer (pH 7.2) @ 20°C. After removal of 2 µl. of this solution, the rest of the mixture was transferred to the Iodogen® coated test tube, where the iodination reaction was allowed to proceed with gentle agitation for 2 minutes. After the 2 minute incubation period, the reaction mixture was transferred to a microcentrifuge tube containing 20 µl. of 1.0 M $Na^{127}I$ (cold). 2 µl.of this solution was removed and added to 10 ml. of PBS/ 1% BSA containing 50 µl. of 1.0 M $Na^{127}I$ (cold) to undergo TCA precipitation.

The rest of the reaction mixture was then added to the top of a minicolumn prepared in the following manner - 6 gm. of Biogel P-100 size exclusion gel was mixed with 200 ml. PBS/Azide in a 500 ml. beaker @ 90°C. The mixture was allowed to settle and cool to room temperature and was then decanted to remove fines. Three washes of 100 ml. PBS/Azide at room temperature were then used to remove remaining fines by settling and decanting. The washed solution was then diluted with buffer to make a 75% slurry. 0.5 ml. PBS/Azide was pepitted into a minicolumn, to which 3.0 ml. of the thoroughly mixed 75% slurry was then

added. After this column packing was allowed to settle, the column was washed with 10 ml. PBS/Azide before use.

After the reaction mixture was added to the top of the minicolumn, the column was spun at 1000 rpm in a Dynac® centrifuge or equivalent for 2.5 minutes. Two 100 µl. PBS washes were then added to the top of the column and the centrifugation repeated in a clean 15 ml. centrifuge tube containing a new 5 µl. microcentrifuge tube for each centrifugation.

2 µl. of each microcentrifuge tube solution (containing purified labelled MAb) was then withdrawn and added to 10 ml. of PBS/1% BSA containing 50 µl. of 1.0M $Na^{127}I$ (cold) for labelling efficiency testing using TCA precipitation. Aliquots (microcentrifuge tubes solutions) showing greater than 97% of ^{125}I or ^{131}I precipitated (ie. > 97% of ^{131}I or ^{125}I bound to the MAb) by the TCA method were then pooled and used in subsequent studies.

The TCA (trichloroacetic acid) precipitation method of testing labelling efficiencies consisted of taking 2 µl. of reaction mixture and adding it to 10 ml. 1% BSA (bovine serum albumin). 0.5 ml. of this solution was reacted with 0.5 ml. 20% TCA. The precipitate was centrifuged in an Eppendorf table-top centrifuge @ 14,000 rpm x 1 minute. After 2 more washes of 1 ml. 20% TCA (with subsequent centrifugations), the precipitate was counted using a Beckman gamma counter. The following determinations could then be made :

% protein bound activity = precipitate count / counts in precipitate + washes (i.e. total counts).

% radiolabelling efficiency = MAb-bound Activity / Total Activity added

Specific Activity = MAb-bound Activity (Ci) / Amount MAb (M)

Standards for this procedure include :

1) Unreacted MAb and ^{125}I or ^{131}I (2µl);

2) Reacted MAb with cold (^{127}I) added (2µl);

3) Purified, reacted MAb (2µl from each purification fraction).

METHOD 2 - CYCLOSPORIN TROUGH LEVEL ASSAY (HPLC METHOD)

Whole blood samples were mixed continuously in heparinized or EDTA-coated blood tubes for 20 min.at 20°C. 1.0 ml. of whole blood was pipetted into a 15 ml. culture tube. An internal standard (Cyclosporin D - 750 ng. in 750 µl. of 10 mg/l methanolic solution) was added, followed by 2.0 ml. 180mM HCl solution. A 10 second vortex treatment was used to lyse the cell. 10 ml. HPLC-grade diethyl ether was added to the lysate after which the tubes were mixed (after being tightly capped) for 20 minutes. Solution was then centrifuged at 3000 rpm for 10 min. The ether layer was pipetted into a second 15 ml. culture tube to which 2 ml. 95mM NaOH had been added. The organic phase was washed by inversion 15 - 20 times. A final centrifugation (3000 rpm x 5 min.) was performed, after which the ether layer was transferred into a clean 16 x 100 mm. etest tube to dry under N_2 at 45°C. Extracts were reconstituted with 0.2 ml. solvent (70% CH_3CN) and 100 µl. was injected onto a reverse-phase C_{18} (1.5 cm. x 4.6 mm.) column, kept at 80°C. Solvent flow = 1.0 ml./ min., using a Hewlett - Packard HPLC isocratic pump system.

APPENDIX III - DATA

EXPERIMENT 1 - HPLC AMINO ACID ANALYSIS - D-54 MG

MH - Media HPLC; CH - Control HPLC; BH - BCNU-treated cells (HPLC); DH - Daunomycin-treated cells (HPLC). Amino Acid Abbreviations - see Table III - 1 (p. 180 in text).

	TIME	MH-TAURINE	MH-THREONINE	MH-ASN	MH-GLY	MH-CIT
1	TIME 0	20.0	232.0	421.0	270.0	121.0
2	TIME 0	16.0	178.0	315.0	204.0	85.0
3	TIME 1	14.0	161.0	303.0	180.0	84.0
4	TIME 1	12.0	168.0	304.0	172.0	76.0
5	TIME 3	14.0	185.0	314.0	193.0	87.0
6	TIME 3	15.0	187.0	324.0	201.0	89.0
7	TIME 6	14.0	170.0	313.0	201.0	100.0
8	TIME 6	15.0	171.0	309.0	193.0	96.0
9	TIME 12	14.0	147.0	211.0	182.0	108.0
10	TIME 12	12.0	128.0	184.0	154.0	96.0
11	TIME 24	16.0	175.0	228.0	209.0	156.0
12	TIME 24	17.0	160.0	223.0	207.0	150.0

	MH-ASP	MH-SER	MH-GLU	MH-GLN	MH-ALA	MH-AAB
1	296.0	350.0	382.0	4366.0	149.0	•
2	242.0	261.0	308.0	3244.0	92.0	•
3	210.0	232.0	250.0	2934.0	90.0	•
4	194.0	233.0	309.0	2713.0	83.0	•
5	215.0	247.0	335.0	2886.0	94.0	•
6	215.0	260.0	347.0	3006.0	98.0	•
7	247.0	248.0	307.0	2971.0	101.0	•
8	217.0	250.0	279.0	2899.0	95.0	•
9	186.0	226.0	276.0	2720.0	117.0	•
10	154.0	193.0	246.0	2326.0	101.0	•
11	236.0	260.0	301.0	2973.0	136.0	•
12	227.0	253.0	267.0	3064.0	128.0	•
13	•	•	•	•	•	•
14	•	•	•	•	•	•
15	•	•	•	•	•	•
16	•	•	•	•	•	•
17	•	•	•	•	•	•
18	•	•	•	•	•	•

	MH-VAL	MH-MET	MH-LEU	MH-PHE	MH-ORN	MH-HIS
1	266.0	119.0	486.0	133.0	•	•
2	191.0	89.0	371.0	99.0	•	•
3	186.0	78.0	336.0	91.0	•	•
4	172.0	77.0	318.0	85.0	•	•
5	189.0	85.0	348.0	94.0	•	•
6	199.0	88.0	365.0	98.0	•	•
7	205.0	90.0	359.0	100.0	•	•
8	187.0	82.0	345.0	94.0	•	•
9	163.0	77.0	322.0	81.0	•	•
10	142.0	65.0	277.0	72.0	•	•
11	190.0	90.0	374.0	95.0	•	•
12	181.0	89.0	368.0	97.0	•	•
13	•	•	•	•	•	•
14	•	•	•	•	•	•
15	•	•	•	•	•	•
16	•	•	•	•	•	•
17	•	•	•	•	•	•

	MH-CYS	MH-ILE	MH-TYR	MH-TRP	MH-LYS	MH-ARG	CH-TAU
1	187.0	482.0	129.0	•	•	•	16.0
2	149.0	362.0	95.0	•	•	•	14.0
3	122.0	339.0	86.0	•	•	•	15.0
4	127.0	321.0	83.0	•	•	•	15.0
5	141.0	351.0	91.0	•	•	•	14.0
6	144.0	371.0	93.0	•	•	•	15.0
7	142.0	367.0	92.0	•	•	•	12.0
8	133.0	350.0	89.0	•	•	•	13.0
9	136.0	295.0	78.0	•	•	•	14.0
10	125.0	260.0	71.0	•	•	•	13.0
11	157.0	355.0	95.0	•	•	•	10.0
12	153.0	347.0	95.0	•	•	•	10.0
13	•	•	•	•	•	•	•
14	•	•	•	•	•	•	•
15	•	•	•	•	•	•	•
16	•	•	•	•	•	•	•
17	•	•	•	•	•	•	•
18	•	•	•	•	•	•	•

	CH-THR	CH-ASN	CH-GLY	CH-CIT	CH-VAL	CH-MET	CH-LEU
1	166.0	250.0	209.0	173.0	175.0	86.0	360.0
2	162.0	282.0	203.0	108.0	183.0	91.0	359.0
3	170.0	287.0	191.0	93.0	171.0	82.0	333.0
4	165.0	313.0	199.0	96.0	183.0	83.0	352.0
5	149.0	272.0	178.0	94.0	159.0	76.0	305.0
6	166.0	282.0	172.0	82.0	157.0	73.0	299.0
7	167.0	276.0	172.0	103.0	154.0	70.0	283.0
8	157.0	263.0	167.0	92.0	146.0	68.0	274.0
9	141.0	270.0	180.0	96.0	139.0	68.0	263.0
10	119.0	247.0	165.0	86.0	121.0	59.0	239.0
11	104.0	204.0	166.0	116.0	98.0	200.0	58.0
12	104.0	206.0	167.0	113.0	96.0	51.0	197.0
13	•	•	•	•	•	•	•
14	•	•	•	•	•	•	•
15	•	•	•	•	•	•	•
16	•	•	•	•	•	•	•
17	•	•	•	•	•	•	•

	CH-PHE	CH-ORN	CH-HIS	CH-ASP	CH-SER	CH-GLU	CH-GLN
1	92.0	•	•	199.0	261.0	321.0	2829.0
2	100.0	•	•	197.0	256.0	306.0	2019.0
3	89.0	•	•	188.0	242.0	359.0	2631.0
4	93.0	•	•	183.0	247.0	372.0	2810.0
5	81.0	•	•	167.0	216.0	337.0	2492.0
6	79.0	•	•	151.0	213.0	370.0	2319.0
7	77.0	•	•	157.0	197.0	420.0	2155.0
8	77.0	•	•	154.0	194.0	526.0	1976.0
9	69.0	•	•	182.0	181.0	651.0	2174.0
10	63.0	•	•	164.0	148.0	611.0	1924.0
11	•	•	•	188.0	118.0	1130.0	1248.0
12	58.0	•	•	185.0	112.0	1155.0	1203.0
13	•	•	•	•	•	•	•
14	•	•	•	•	•	•	•
15	•	•	•	•	•	•	•
16	•	•	•	•	•	•	•
17	•	•	•	•	•	•	•
18	•	•	•	•	•	•	•

	CH-ALA	CH-AAB	CH-CYS	CH-ILE	CH-TYR	CH-TRY	CH-LYS
1	126.0	•	93.0	335.0	92.0	•	•
2	139.0	•	100.0	333.0	93.0	•	•
3	149.0	•	141.0	321.0	87.0	•	•
4	150.0	•	145.0	335.0	91.0	•	•
5	134.0	•	121.0	297.0	80.0	•	•
6	124.0	•	117.0	295.0	79.0	•	•
7	188.0	•	105.0	282.0	74.0	•	•
8	149.0	•	122.0	272.0	74.0	•	•
9	224.0	•	108.0	262.0	73.0	•	•
10	202.0	•	96.0	231.0	67.0	•	•
11	364.0	•	92.0	202.0	62.0	•	•
12	347.0	•	93.0	195.0	63.0	•	•
13	•	•	•	•	•	•	•
14	•	•	•	•	•	•	•
15	•	•	•	•	•	•	•
16	•	•	•	•	•	•	•
17	•	•	•	•	•	•	•

	CH-ARG	BH-TAU	BH-THR	BH-ASN	BH-GLY	BH-CIT	BH-VAL
1	•	16.0	153.0	269.0	195.0	84.0	172.0
2	•	16.0	152.0	272.0	192.0	80.0	170.0
3	•	15.0	132.0	233.0	162.0	65.0	139.0
4	•	16.0	136.0	249.0	183.0	74.0	153.0
5	•	18.0	150.0	262.0	198.0	89.0	164.0
6	•	15.0	129.0	231.0	173.0	80.0	146.0
7	•	15.0	120.0	233.0	174.0	87.0	147.0
8	•	16.0	132.0	263.0	169.0	89.0	151.0
9	•	13.0	126.0	229.0	161.0	102.0	137.0
10	•	14.0	124.0	238.0	159.0	107.0	137.0
11	•	8.0	91.0	194.0	150.0	127.0	107.0
12	•	7.0	88.0	202.0	144.0	120.0	93.0
13	•	•	•	•	•	•	•
14	•	•	•	•	•	•	•
15	•	•	•	•	•	•	•
16	•	•	•	•	•	•	•
17	•	•	•	•	•	•	•
18	•	•	•	•	•	•	•

	BH-MET	BH-LEU	BH-PHE	BH-ORN	BH-HIS	BH-ASP	BH-SER
1	84.0	340.0	87.0	•	•	182.0	244.0
2	82.0	339.0	86.0	•	•	175.0	247.0
3	70.0	288.0	74.0	•	•	151.0	207.0
4	76.0	314.0	79.0	•	•	158.0	221.0
5	78.0	333.0	83.0	•	•	169.0	230.0
6	70.0	287.0	70.0	•	•	150.0	200.0
7	69.0	272.0	68.0	•	•	159.0	185.0
8	69.0	274.0	75.0	•	•	152.0	194.0
9	65.0	269.0	73.0	•	•	178.0	162.0
10	65.0	261.0	68.0	•	•	194.0	168.0
11	50.0	210.0	54.0	•	•	287.0	93.0
12	45.0	204.0	49.0	•	•	221.0	78.0
13	•	•	•	•	•	•	•
14	•	•	•	•	•	•	•
15	•	•	•	•	•	•	•
16	•	•	•	•	•	•	•
17	•	•	•	•	•	•	•
18	•	•	•	•	•	•	•

	BH-TRP	BH-LYS	BH-ARG	DH-TAU	DH-THR	DH-ASN	DH-GLY
1	•	•	•	14.0	165.0	249.0	200.0
2	•	•	•	16.0	150.0	237.0	192.0
3	•	•	•	21.0	166.0	261.0	207.0
4	•	•	•	20.0	151.0	240.0	199.0
5	•	•	•	20.0	168.0	244.0	194.0
6	•	•	•	19.0	157.0	277.0	188.0
7	•	•	•	21.0	168.0	285.0	196.0
8	•	•	•	21.0	152.0	277.0	203.0
9	•	•	•	23.0	153.0	227.0	203.0
10	•	•	•	27.0	170.0	269.0	228.0
11	•	•	•	35.0	149.0	284.0	260.0
12	•	•	•	44.0	267.0	•	406.0
13	•	•	•	•	•	•	•
14	•	•	•	•	•	•	•
15	•	•	•	•	•	•	•
16	•	•	•	•	•	•	•
17	•	•	•	•	•	•	•
18	•	•	•	•	•	•	•

	DH-CIT	DH-VAL	DH-MET	DH-LEU	DH-PHE	DH-ORN	DH-HIS
1	111.0	182.0	88.0	360.0	91.0	•	•
2	102.0	175.0	83.0	345.0	90.0	•	•
3	100.0	185.0	90.0	369.0	92.0	•	•
4	111.0	181.0	85.0	352.0	91.0	•	•
5	104.0	169.0	83.0	356.0	84.0	•	•
6	100.0	162.0	76.0	314.0	85.0	•	•
7	110.0	165.0	81.0	311.0	92.0	•	•
8	119.0	166.0	81.0	319.0	83.0	•	•
9	116.0	142.0	71.0	264.0	72.0	•	•
10	132.0	168.0	88.0	319.0	97.0	•	•
11	115.0	151.0	79.0	280.0	92.0	•	•
12	173.0	227.0	118.0	413.0	145.0	•	•
13	•	•	•	•	•	•	•
14	•	•	•	•	•	•	•
15	•	•	•	•	•	•	•
16	•	•	•	•	•	•	•
17	•	•	•	•	•	•	•
18	•	•	•	•	•	•	•

	DH-ASP	DH-SER	DH-GLU	DH-GLN	DH-ALA	DH-AAB	DH-CYS
1	194.0	249	305	2980	124	•	163
2	182.0	237	250	2924	121	•	157
3	190.0	250	356	2936	144	•	167
4	178.0	234	308	2898	146	•	156
5	166.0	231	396	2475	151	•	144
6	189.0	230	396	2648	146	•	125
7	193.0	227	595	2430	184	•	127
8	196.0	224	544	2617	190	•	128
9	189.0	202	936	1719	231	•	116
10	227.0	225	1073	2020	260	•	127
11	227.0	192	2149	458	335	•	104
12	336.0	308	3197	666	515	•	157
13	•	•	•	•	•	•	•
14	•	•	•	•	•	•	•
15	•	•	•	•	•	•	•
16	•	•	•	•	•	•	•
17	•	•	•	•	•	•	•
18	•	•	•	•	•	•	•

	DH-ILE	DH-TYR	DH-TRP	DH-LYS	DH-ARG	TIME(HRS.)
1	334	91	•	•	•	0
2	322	88	•	•	•	0
3	350	95	•	•	•	1
4	333	88	•	•	•	1
5	311	84	•	•	•	3
6	294	81	•	•	•	3
7	288	85	•	•	•	6
8	294	82	•	•	•	6
9	237	79	•	•	•	12
10	285	93	•	•	•	12
11	244	86	•	•	•	24
12	357	133	•	•	•	24
13	•	•	•	•	•	•
14	•	•	•	•	•	•
15	•	•	•	•	•	•
16	•	•	•	•	•	•
17	•	•	•	•	•	•
18	•	•	•	•	•	•

EXPERIMENT 2 - NMR AMINO ACID ANALYSIS - D-54 MG

M - media; C - control; B - BCNU-treated cells; D - Daunomycin-treated cells

ALA -alanine; LAC - lactate; GLU - glutamate; GLN - glutamine.

	Time(hrs.)	M-LAC	M-ALA	M-GLN	M-GLU	C-LAC	C-ALA
1	0	•	•	•	•	395.15	358.20
2	0	•	•	•	•	284.51	308.00
3	.500	410.51	502.03	1414.86	659.44	485.68	571.23
4	.500	349.38	341.92	1291.22	445.61	286.66	272.72
5	1.000	447.51	591.58	1492.26	504.44	254.32	192.67
6	1.000	430.76	419.26	1424.14	755.41	294.06	253.57
7	2.000	384.61	449.11	1173.37	569.65	419.77	333.78
8	2.000	339.58	438.26	1074.30	628.48	540.21	652.64
9	3.000	334.37	468.11	1120.74	492.26	545.47	523.74
10	3.000	292.69	299.86	1021.67	492.26	582.47	609.22
11	4.500	314.31	394.84	1201.23	541.79	442.84	350.06
12	4.500	323.58	283.58	1129.82	470.17	492.51	286.29
13	6.000	•	•	•	•	917.42	620.08
14	6.000	309.25	299.86	1092.87	411.76	680.26	359.56
15	7.500	•	•	•	•	793.38	280.86
16	7.500	215.08	192.67	828.07	287.71	253.74	153.32
17	9.000	355.20	443.69	1247.67	585.13	895.72	335.14
18	9.000	312.95	249.66	1000.00	382.45	•	•
19	12.000	435.16	377.20	1449.12	645.61	1044.63	370.42
20	12.000	410.91	355.49	1386.99	476.78	462.41	461.32
21	24.000	213.82	191.31	708.97	•	617.33	597.01
22	24.000	292.03	257.80	1070.17	392.68	1598.30	442.33
23	36.000	408.61	362.27	1396.49	670.17	775.68	519.67
24	36.000	269.71	251.01	1056.14	407.01	1712.19	510.47

	C-GLN	C-GLU	B-LAC	B-ALA	B-GLN	B-GLU	D-LAC	D-ALA
1	1207.01	585.96	318.19	331.07	1084.21	477.19	259.20	233.27
2	1046.43	399.78	403.51	526.45	1164.08	656.34	396.48	318.36
3	1362.22	808.04	409.38	301.22	1242.10	596.49	348.58	282.22
4	907.12	281.73	525.99	534.59	1493.62	811.14	344.30	274.08
5	747.36	326.31	498.53	605.15	1167.18	640.86	453.35	401.62
6	851.39	321.18	359.10	364.99	959.75	507.73	463.48	533.24
7	1171.92	733.73	581.69	512.89	1476.78	498.45	386.36	312.07
8	1368.42	671.82	468.93	377.20	829.32	427.26	545.08	645.86
9	1250.77	619.19	547.03	470.82	1185.75	634.67	347.22	226.59
10	1114.55	600.61	554.04	310.71	1074.30	526.31	531.84	514.24
11	885.44	517.02	684.90	568.52	1585.13	829.72	436.02	426.05
12	940.00	455.10	384.61	200.81	696.59	343.65	487.04	510.17
13	1455.10	783.28	777.40	540.02	1337.46	826.62	691.33	512.89
14	1024.56	578.94	772.73	390.77	814.24	476.78	625.22	370.42
15	1161.40	600.00	717.62	434.19	1207.43	712.07	374.29	313.43
16	402.47	229.10	799.53	344.64	1101.75	561.40	726.19	420.62
17	1143.85	536.84	918.98	526.45	1241.48	727.55	537.09	233.37
18	•	•	829.16	345.99	1178.94	715.78	764.90	375.84
19	1091.22	578.94	1191.43	546.81	1352.94	873.06	1000.00	578.00
20	1068.11	721.36	1108.50	359.56	785.96	592.98	969.62	576.66
21	839.00	801.85	1411.31	336.49	715.78	722.80	1362.80	701.49
22	698.24	814.03	1398.61	282.22	578.94	642.10	1190.26	402.98
23	592.98	803.50	891.13	379.91	421.05	504.64	1477.49	522.38
24	519.29	831.57	1747.59	451.83	610.52	880.70	1509.05	515.60

	D-GLN	D-GLU	Column 18
1	869.96	303.40	•
2	1142.41	486.06	•
3	1046.43	520.12	•
4	944.27	374.61	•
5	1000.00	448.91	•
6	1346.74	656.34	•
7	972.13	390.09	•
8	1433.43	823.52	•
9	944.27	882.35	•
10	1241.48	718.26	•
11	981.42	541.79	•
12	1043.34	653.25	•
13	1176.47	764.70	•
14	1171.92	536.84	•
15	814.24	414.86	•
16	863.77	489.16	•
17	699.69	442.72	•
18	807.01	649.12	•
19	1083.62	1000.00	•
20	1027.86	876.16	•
21	665.63	1222.91	•
22	448.91	894.73	•
23	554.38	1256.14	•
24	557.27	1102.16	•

EXPERIMENT 3 - ENZYMATIC LACTATE DETERMINATION

	Time (hrs.)	Media	Control	BCNU	daunomycin	Column 6
1	Time 0	2.03	2.67	2.79	2.850	0
2	Time 0	2.38	2.66	2.86	2.930	0
3	Time 0	2.41	2.68	2.72	2.730	0
4	Time 0	3.27	2.66	2.76	2.780	0
5	Time 0	1.90	2.69	2.72	2.855	0
6	Time 0	3.26	2.60	2.82	2.850	0
7	Time 0.5	2.76	3.20	3.26	3.280	.500
8	Time 0.5	2.62	3.12	3.26	3.390	.500
9	Time 0.5	2.74	3.18	3.16	3.310	.500
10	Time 0.5	2.66	3.01	3.22	2.680	.500
11	Time 0.5	2.72	3.19	3.29	3.230	.500
12	Time 0.5	2.81	3.09	3.20	2.600	.500
13	Time 1	2.53	3.26	3.56	3.090	1.000
14	Time 1	2.69	3.50	3.51	3.450	1.000
15	Time 1	2.66	3.41	3.47	3.080	1.000
16	Time 1	2.67	3.44	3.42	3.350	1.000
17	Time 1	2.62	3.33	3.52	3.640	1.000
18	Time 1	2.54	3.28	3.46	3.690	1.000
19	Time 2	2.57	3.86	4.06	2.830	2.000
20	Time 2	2.57	3.90	4.10	4.020	2.000
21	Time 2	2.66	3.85	3.98	3.680	2.000
22	Time 2	2.67	3.86	4.06	3.970	2.000
23	Time 2	2.71	3.83	4.05	2.850	2.000
24	Time 2	2.71	3.74	3.92	3.700	2.000
25	Time 3	2.69	4.44	4.80	3.870	3.000
26	Time 3	2.70	4.62	4.63	4.230	3.000
27	Time 3	2.68	4.57	4.68	4.130	3.000
28	Time 3	2.76	4.56	4.54	4.380	3.000
29	Time 3	2.68	4.44	4.60	4.200	3.000
30	Time 3	2.74	4.52	4.72	3.940	3.000
31	Time 4.5	2.68	5.28	5.29	4.810	4.500
32	Time 4.5	2.63	5.25	5.54	4.290	4.500
33	Time 4.5	2.63	5.38	5.35	4.710	4.500
34	Time 4.5	2.64	5.04	5.18	4.760	4.500
35	Time 4.5	2.70	5.29	5.28	4.220	4.500
36	Time 4.5	2.70	5.30	5.09	4.910	4.500
37	Time 6	1.98	6.33	6.29	4.690	6.000
38	Time 6	2.00	6.44	6.22	4.760	6.000
39	Time 6	3.33	6.12	5.89	5.830	6.000
40	Time 6	3.20	6.16	6.18	6.080	6.000

	Time (hrs.)	Media	Control	BCNU	daunomycin	Column 6
41	Time 6	2.81	6.17	6.01	5.560	6.000
42	Time 6	2.68	6.10	5.83	5.500	6.000
43	Time 7.5	2.57	6.98	6.53	6.160	7.500
44	Time 7.5	2.58	6.80	6.57	6.050	7.500
45	Time 7.5	2.51	6.88	6.92	6.100	7.500
46	Time 7.5	2.42	6.80	6.96	6.000	7.500
47	Time 7.5	1.99	6.81	6.47	6.010	7.500
48	Time 7.5	2.03	6.96	6.37	5.860	7.500
49	Time 9	1.87	8.25	6.78	6.640	9.000
50	Time 9	2.26	7.69	7.51	6.880	9.000
51	Time 9	1.98	7.86	7.09	6.780	9.000
52	Time 9	1.95	8.05	6.81	7.000	9.000
53	Time 9	1.94	7.85	7.13	6.860	9.000
54	Time 9	2.23	7.94	7.50	6.810	9.000
55	Time 12	3.13	9.35	8.80	8.020	12.000
56	Time 12	2.39	7.19	•	7.610	12.000
57	Time 12	2.98	7.49	9.97	7.740	12.000
58	Time 12	3.13	7.57	10.24	7.930	12.000
59	Time 12	3.14	9.34	8.94	8.060	12.000
60	Time 12	2.55	7.05	•	7.620	12.000
61	Time 24	2.71	13.91	•	11.360	24.000
62	Time 24	2.75	14.02	14.34	11.460	24.000
63	Time 24	2.71	13.92	•	11.730	24.000
64	Time 24	2.89	14.17	14.12	11.390	24.000
65	Time 24	2.67	13.96	•	11.680	24.000
66	Time 24	2.79	13.87	•	11.180	24.000
67	Time 36	2.76	14.67	15.67	12.940	36.000
68	Time 36	2.76	14.77	15.40	12.910	36.000
69	Time 36	2.73	14.84	15.10	12.010	36.000
70	Time 36	2.90	14.76	15.66	13.000	36.000
71	Time 36	2.80	14.80	15.50	12.470	36.000
72	Time 36	2.78	14.49	15.59	12.730	36.000

EXPERIMENT 4 - PROTEIN DETERMINATION - D-54 MG

Abs. - Absorbance

	Group	Time	Abs. 1	Abs.2	Abs. 3	Avg. Abs.	Column 7
1	C-1	0	.695	.644	•	.670	.604
2	C-2	0	.700	.677	.710	.696	.630
3	C-3	0	.689	.705	.687	.694	.628
4	C-4	0	.695	.692	.682	.690	.624
5	C-1	1	.643	.705	.699	.682	.617
6	C-2	1	.689	.673	.645	.669	.603
7	C-3	1	.697	.710	.682	.696	.631
8	C-4	1	.740	.740	.737	.739	.673
9	C-1	3	.719	.755	.754	.743	.677
10	C-2	3	.695	.690	.675	.687	.621
11	C-3	3	.680	.656	.635	.657	.592
12	C-4	3	.615	.631	.590	.612	.546
13	C-1	6	.758	.760	.730	.749	.684
14	C-2	6	.705	.705	.700	.703	.638
15	C-3	6	.642	.674	.647	.654	.589
16	C-4	6	.775	.804	.805	.795	.729
17	C-1	12	.744	.770	.743	.752	.687
18	C-2	12	.756	.727	.727	.737	.671
19	C-3	12	.730	.734	.743	.736	.670
20	C-4	12	.721	.764	.740	.742	.676
21	C-1	24	.650	.680	.670	.667	.601
22	C-2	24	.720	.745	.740	.735	.669
23	C-3	24	.720	.695	.710	.708	.643
24	C-4	24	.730	.730	.725	.728	.663
25	B-1	0	.690	.680	•	.685	.619
26	B-2	0	.630	.630	.655	.638	.573
27	B-3	0	.650	.650	.620	.640	.575
28	B-4	0	.650	.680	.650	.660	.595
29	B-1	1	.640	.640	.625	.635	.570
30	B-2	1	.620	.640	.615	.625	.559
31	B-3	1	.610	.650	.670	.643	.578
32	B-4	1	.625	.650	.665	.647	.581
33	B-1	3	.747	.729	.705	.727	.662
34	B-2	3	.720	.765	.715	.733	.668
35	B-3	3	.710	.720	.697	.709	.644
36	B-4	3	.650	.630	.700	.660	.595
37	B-1	6	.664	.650	.626	.647	.581
38	B-2	6	.744	.770	.841	.785	.720
39	B-3	6	.775	.760	.750	.762	.696
40	B-4	6	.745	.730	.715	.730	.664

	Group	Time	Abs. 1	Abs.2	Abs. 3	Avg. Abs.	Column 7
41	B-1	12	.630	.640	.640	.637	.571
42	B-2	12	•	•	•	•	•
43	B-3	12	.660	.690	.690	.680	.614
44	B-4	12	.745	.730	.715	.730	.664
45	B-1	24	.680	.710	.690	.693	.628
46	B-2	24	.670	.705	.705	.693	.628
47	B-3	24	.610	.650	.620	.627	.561
48	B-4	24	.690	.740	.720	.717	.651
49	D-1	0	.680	.705	.715	.700	.634
50	D-2	0	.685	.695	.690	.690	.624
51	D-3	0	.660	.650	.685	.665	.600
52	D-4	0	.715	.780	.750	.748	.683
53	D-1	1	.680	.685	.660	.675	.610
54	D-2	1	.650	.683	.665	.666	.600
55	D-3	1	.640	.660	.675	.658	.593
56	D-4	1	.640	.670	.635	.648	.583
57	D-1	3	.595	.590	.600	.595	.529
58	D-2	3	.540	.610	.610	.587	.521
59	D-3	3	.590	.594	.597	.594	.528
60	D-4	3	.560	.580	.590	.577	.511
61	D-1	6	.652	.700	.682	.678	.613
62	D-2	6	.650	.670	.650	.657	.591
63	D-3	6	.670	.670	.680	.673	.608
64	D-4	6	.660	.645	.660	.655	.590
65	D-1	12	.540	.530	.540	.537	.471
66	D-2	12	.585	.600	.600	.595	.529
67	D-3	12	.575	.570	.560	.568	.503
68	D-4	12	.620	.630	.650	.633	.568
69	D-1	24	.480	.480	.490	.483	.418
70	D-2	24	.460	.450	.460	.457	.391
71	D-3	24	.440	.460	.450	.450	.385
72	D-4	24	.420	.440	.410	.423	.358

	[Protein] (mg/sample)	[Protein] (mg/1.5 X 10E6 cells)
1	.727	14.549
2	.759	15.179
3	.757	15.131
4	.752	15.035
5	.743	14.858
6	.727	14.537
7	.760	15.195
8	.811	16.223
9	.816	16.311
10	.748	14.962
11	.712	14.248
12	.658	13.164
13	.824	16.472
14	.768	15.364
15	.709	14.184
16	.878	17.564
17	.827	16.544
18	.808	16.167
19	.807	16.143
20	.814	16.287
21	.724	14.481
22	.806	16.127
23	.774	15.484
24	.798	15.966
25	.746	14.922
26	.690	13.798
27	.692	13.838
28	.716	14.320
29	.686	13.718
30	.674	13.477
31	.696	13.919
32	.700	13.999
33	.797	15.934
34	.804	16.087
35	.775	15.500
36	.716	14.320
37	.700	13.999
38	.867	17.331
39	.838	16.769
40	.800	16.006

	[Protein] (mg/sample)	[Protein] (mg/1.5 X 10E6 cells)
41	.688	13.758
42	•	•
43	.740	14.802
44	.800	16.006
45	.756	15.123
46	.756	15.123
47	.676	13.517
48	.784	15.685
49	.764	15.284
50	.752	15.043
51	.722	14.441
52	.822	16.448
53	.734	14.681
54	.723	14.465
55	.714	14.280
56	.702	14.039
57	.638	12.754
58	.628	12.554
59	.636	12.722
60	.616	12.313
61	.738	14.754
62	.712	14.240
63	.732	14.641
64	.710	14.200
65	.567	11.349
66	.638	12.754
67	.606	12.112
68	.684	13.678
69	.503	10.065
70	.471	9.422
71	.463	9.262
72	.431	8.619

EXPERIMENT 5 - IMMUNOREACTIVITY EXPERIMENTS

MONOCLONAL REACTIVITY TO D-54 MG HUMAN GLIOBLASTOMA CELL LINE IN-VITRO (ELISA)

MONOCLONAL ANTIBODY	D-54 MG REACTIVITY
MEDIA CONTROL	0
B37.43R352 (IgM)	++++
320H.14 (IgG)	+++ - ++++
184H.3 (IgG)	+++ - ++++
320H.22 (IgG)	+++
B67.30R11 (IgM)	+++
B32.2R20 (IgM)	++ - +++
49H.8 (IgM)	++ - +++
B45.1R31 (IgM)	++
318H.1(IgM)	+ - ++
B67.24R11 (IgM)	+ - ++

MONOCLONAL ANTIBODY	D-54 MG REACTIVITY
B27.1R10 (IgG)	+
B28.2R1 (IgM)	+
B45.1R31 (IgM)	+
B45.3R2 (IgM)	+
B45.7R1 (IgM)	+
50H.9 (IgG)	+
B25.10R30 (IgM)	0 - +
B45.24R1 (IgM)	0 - +
C50 (IgM)	0
C242 (IgG)	0
28 other MAb's	0